Mechanistic studies of the synthesis and decomposition of some amine-carbonyl condensation products

Hamid, Javid

MECHANISTIC STUDIES OF THE SYNTHESIS AND DECOMPOSITION OF SOME AMINE-CARBONYL CONDENSATION PRODUCTS

by

Javid Hamid, G.R.S.C. Hons. (Teesside), Graduate Society

A thesis submitted for the degree of Doctor of Philosophy in the Department of Chemistry, University of Durham, 1992.

MECHANISTIC STUDIES OF THE SYNTHESIS AND DECOMPOSITION OF SOME AMINE-CARBONYL COMPOUNDS

by Javid Hamid.

A thesis submitted for the degree of Doctor of Philosophy in the Department of Chemistry, University of Durham, 1992.

ABSTRACT

Condensation of benzylamine and glyoxal in a 2:1 molar ratio in acetonitrile containing a catalytic amount of acid is found to give the cage compound 2,4,6,8,10,12-hexabenzyl-2,4,6,8,10,12-hexaazatetracyclo [5.5.0.$0^{5,9}$.$0^{3,11}$] dodecane (hexabenzylhexaazaisowurtzitane). The yield of the isowurtzitane cage compound was optimised by varying the temperature and the acid catalyst. Eight phenyl ring substituted benzylamines were also found to give the isowurtzitane cage structure. Yields were found to be lower for benzylamines carrying electron-withdrawing ring substituents. A tetra-acetylated isowurtzitane derivative was also prepared and the NMR spectra were examined showing it to consist of a mixture of isomers due to restricted rotation about the N-acetyl bonds.

^{1}H and ^{13}C spectral assignments were aided by the use of deuteriated isowurtzitane cage compounds in which all the benzyl methylene hydrogens had been replaced by deuterium. N,N'-dibenzyl-1,2-ethane diimine and 1,2-bis(benzylamino)-1,2-ethanediol which are thought to be intermediates in the formation of the cage compounds were prepared and the mechanism of formation of the hexabenzylhexa-azaisowurtzitanes is discussed.

The reaction mixture left after the precipitation of the cage compounds was examined by HPLC and ^{1}H NMR to ascertain if any other products could be isolated. Results indicated a complex mixture from which the diimine, protonated benzylamine and the diol could be identified.

In acidic solution the cages are found to exist in either the monoprotonated or diprotonated forms. The monoprotonated species is found to be fairly stable whereas the diprotonated species is found to decompose fairly rapidly. ^{1}H and ^{13}C NMR show that the proton is held strongly in a position between the two nitrogen atoms in the two five-membered rings on one side of the molecule. The diprotonated species has two protons, one incorporated on each side of the molecule.

Kinetic results show that decomposition of the isowurtzitane cages in acidic media occurs via an acid or water catalysed pathway. An approximate value of the K_a for hexabenzylhexaazaisowurtzitane of ≥ 4 has been calculated.

The decomposition of some 3,7 di-substituted bicyclononanes in acidic media has been investigated. Kinetic results indicated two decomposition pathways involving reaction of the monoprotonated forms of DPT, DNPT and DAPT with either water or acid. In the case of DNPT there was also evidence for reaction via a diprotonated species.

The reaction of 2-aminobenzylamine with glyoxal is found not to give the expected cage structure but a novel cyclisation product 2,2'-bis(1,2,3,4-tetrahydro-quinoxaline). Formation is thought to involve intramolecular cyclisation of the diimine intermediate. Reaction of 4-aminobenzylamine with glyoxal gave an unidentified solid which does not possess an isowurtzitane cage structure.

ACKNOWLEDGEMENTS

I would like to thank my supervisor Dr. M.R. Crampton, for his invaluable help and encouragement during this work. I would also like to thank Hanif, Shirlene, Alan, Tim, John, Simon, Jonathan, Paula, Rachel, Maureen, Alex, and Simon for their encouragement and friendship throughout my period of study, and particularly Dr. R.S. Matthews for help with NMR spectra and Mr. C. Greenhalgh for maintenance of all the spectrophotometers and technical assistance. My thanks also extend to G. Ferguson at Guelph, Canada, André, Jason and Prof. J. A. K. Howard at Durham University for x-ray crystal determinations.

Thanks are also due to my industrial supervisor, Dr. R. Millar of R.A.R.D.E., Fort Halstead, for advice on synthetic methods, and to the Procurement Executive, Ministry of Defence for funding the project.

DECLARATION

The material in this thesis is the result of research carried out in the Department of Chemistry, University of Durham, between October 1989 and October 1992. It has not been submitted for any other degree, and is the author's own work, except where acknowledged by reference.

For my wife Farida,
and my family who made it all possible.

CONTENTS

Chapter 1

Introduction

Amine Condensation Reactions

1.1. General Considerations

Condensation of amines with carbonyl compounds may lead to the formation of Schiff bases (also known as imines, aldimines and azomethines) (1.2). The reactions as shown in eqn. 1.1 involve nucleophilic attack by the amine to give tetrahedral carbinolamine intermediates (1.1) which may eliminate water to give the product.[1]

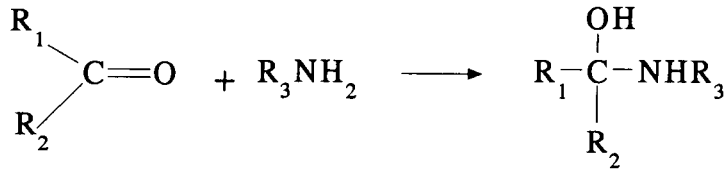

1.1

eqn.1.1

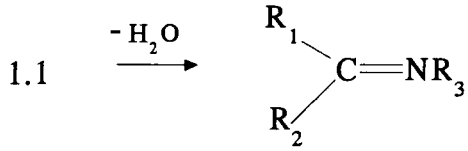

1.2

This type of reaction involving formation of carbinolamines and Schiff bases is thought to play a major part in a number of important biochemical processes[2] such as those involving pyridoxal phosphate (Vitamin B6) which is an important co-factor in a number of enzymatic systems.

Many important chemical[3] reactions involve initial condensation of amines with carbonyl functions. One such reaction is the formation of "aldehyde-ammonias" from ammonia and aldehydes.[4,5,6] Reaction with ethanal (acetaldehyde) gives[7] the hydrated carbinolamine, 1-amino-ethanol, (1-amino-1-alkanol) as shown in eqn. 1.2.

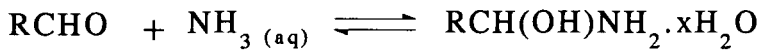

eqn. 1.2

$R = CH_3$

However, due to its unstable nature this undergoes further dehydration to initially give the Schiff base (1.3). This dimerises to give the acyclic dimer (1.4) (Scheme 1.1).

Scheme 1.1

$$RCH(OH)NH_2 \longrightarrow RCH{=}NH + H_2O$$

1.3

$$RCH{=}NH \xrightarrow{1.3} RCH{=}NCH(NH_2)R$$

1.4

$$\xrightarrow{1.3} [RCH(NH_2)NHCH(R)N{=}CHR]$$

1.5

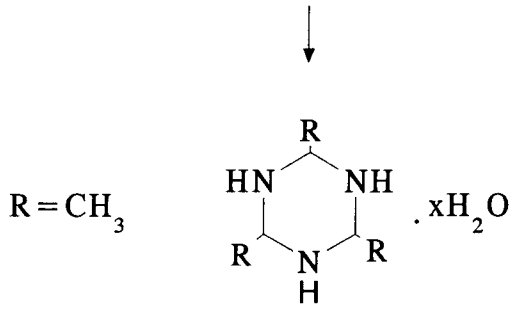

1.6

which can react further with (1.3) to give a trimer (1.5). Cyclisation of (1.5) gives the 2,4,6-trialkyl-1,3,5-hexahydrotriazine (1.6).[8] Other intermediates are thought to exist such as covalent hydrates of (1.4) and (1.5) e.g. $RCH(OH)NHCH(NH_2)R$.

In the reaction of aldehydes with ammonia, Ogata and Kawasaki[9] showed that electron-releasing groups decrease the rate of the forward reaction and increased the rate of the reverse reaction (the reaction is much slower with n-heptanal than with acetaldehyde, and the n-heptanal derived triazine product is less stable than that derived from acetaldehyde).

For convenience amine condensation reactions may be divided into three categories :-

(a) Primary amines

(b) Secondary amines

(c) Tertiary amines

1.2. Addition Of Primary Amines

1.2.1 Carbinolamine Formation

Addition of primary amines to a carbonyl group results in the formation of a carbinolamine (1.1).[10,11] The compounds are usually unstable and tend to undergo elimination to give the imine (1.2), this stage being analogous to the elimination of water in the second stage of acetal formation. The imine is isoelectronic with oxygen stabilised carbocations.

Kinetic evidence for the existence of a carbinolamine intermediate was obtained by French and Bruice.[12] However they could only infer its presence from evidence of a rapid pre-equilibrium prior to the rate determining dehydration step to give the Schiff base.

More recently Sander and Jencks[13], have confirmed the existence of carbinolamine intermediates using stopped-flow spectrophotometry and have measured equilibrium constants for their formation for a series of primary and secondary amines.

Poziomek and co-workers[14] isolated carbinolamines as unstable salts from reactions of 2-formyl-1-methylpyridinium iodide with hydroxylamine, hydrazine or phenylhydrazine. A carbinolamine adduct with acetamide corresponding to 2-(acetomidohydroxymethyl)-1-methylpyridinium iodide (1.7) was also isolated as a very stable salt.

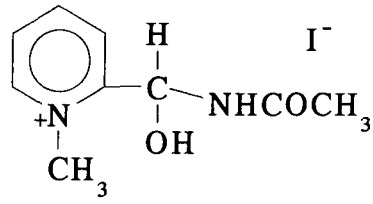

1.7

Another possible reaction of the carbinolamine , observed in the addition of amides or urea is substitution of the hydroxyl group by a second molecule of the nucleophile[15] (eqn. 1.3).

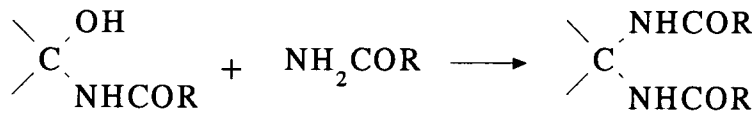

eqn. 1.3

1.2.2 Imine Formation

Usually the reaction does not stop at the carbinolamine stage but tends to go through to give the imine.[16,17,18] The imines formed are usually too reactive to isolate if the substituents on carbon and nitrogen are all alkyl or hydrogen.

Unsubstituted imines are often described as reaction intermediates, e.g. in photolysis of azides and primary amines, and in reduction of oximes.[19,20,21] Accounts of the synthesis of unsubstituted imines (RCH=NH) from aldehydes and ammonia are found in the literature.[22-25] However, recent re-examination of some of these reports has established that unsubstituted imines of this type cannot be isolated as stable free bases.[26,27,28] Rather, their self-reaction occurs extremely rapidly leading to other products such as 2,4,6-trisubstituted-1,3,5-hexahydrotriazines (1.6)[29] (eqn. 1.4) and diimines (1.10).[30]

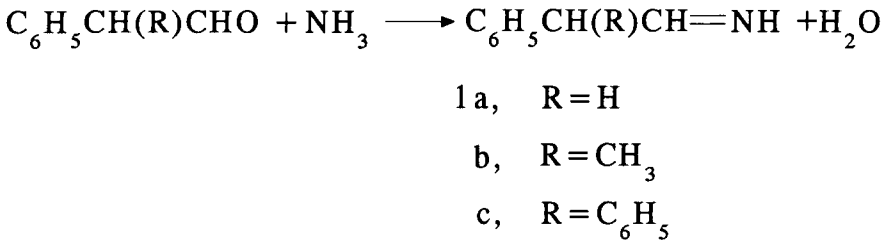

eqn. 1.4

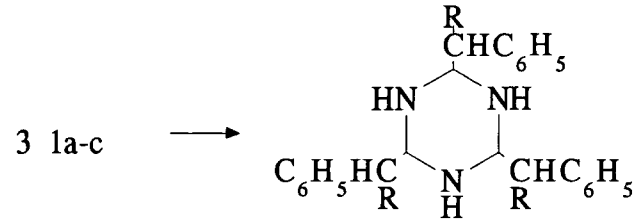

1.6

Stabilisation of imines can be achieved by attachment of one or more aryl groups to carbon or nitrogen in which case the compounds are easily isolated.[31,32]

Addition of a hydroxyl group or second nitrogen attached to the imine nitrogen also enhances stability. N-substituted imines have been shown to be more stable than those bearing a NH group.[33,34] Thus some of the most common structures formed are oximes (1.7), semicarbazones (1.8) and hydrazones (1.9).

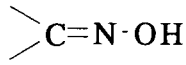

1.7

1.8

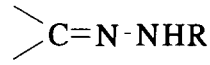

1.9

Stability of diimines (1.10) also varies with the substituent R. The trimethyl compound (1.10a) is a liquid which readily polymerises.[35] Diimines with small n-alkyl groups polymerise extremely rapidly on heating. Those containing alkyl groups with alpha-branching (1.10 c,d) are rather stable.

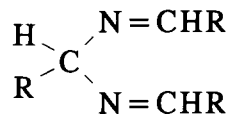

1.10

a, $R = CH_3$

b, $R = C_2H_5$

c, $R = i\text{-}C_3H_7$

d, $R = t\text{-}C_4H_9$

1.3 Addition Of Secondary Amines

Addition of secondary amines to a carbonyl group leads to a carbinolamine which cannot form an imine of neutral structure. An iminium ion (1.11) is produced. However, if there is a hydrogen on the alpha-carbon, elimination of a proton can occur to give a species with a carbon-carbon double bond, referred to as an enamine (1.12) (eqn. 1.5); a process similar to that seen in aldol type condensations.

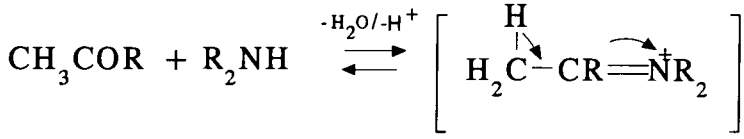

1.11

eqn. 1.5

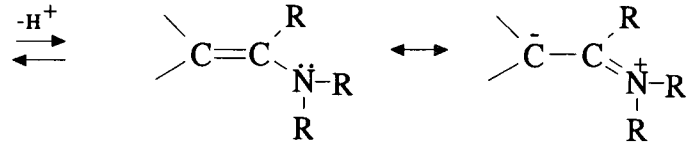

1.12

Much of the pioneering work on the synthetic applications of enamines has been carried out by Stork and co-workers.[36] Enamines are useful as synthetic intermediates for the formation of a variety of carbocyclic and heterocyclic ring systems.[37] They serve as carbanion equivalents in many of their reactions.

Like many of the other carbonyl addition reactions, enamine formation is readily reversible and the carbonyl compound can be recovered by hydrolysis with aqueous acid.

1.4 Addition Of Tertiary Amines

Addition of tertiary amines to the carbonyl group results in the formation of an ionic carbinolamine. As there is no possibility of forming a neutral addition compound the carbinolamine reverts to reactants.[38]

1.5 Mechanism Of Addition By Primary Amines

The mechanism of addition by primary amines has been the subject of extensive study. The most striking feature of these reactions seems to be the characteristic maximum in the graph of rate constant as a function of pH [39] (fig.1.1).

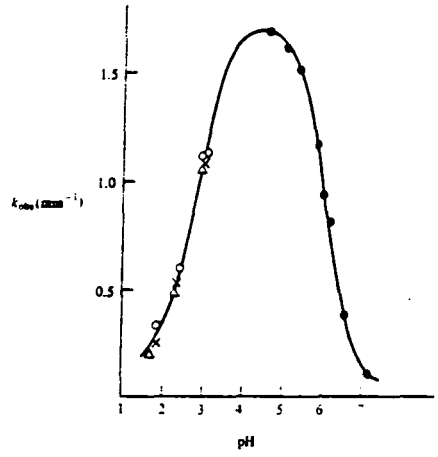

Dependence of rate constant on pH for reaction of :-

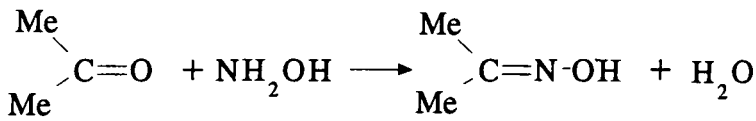

It has been shown that sensitivity of the rate constant of reaction to acid catalysis and substituent effects is different on either side of the maximum in the pH-rate curve.[40] These phenomena may be understood in terms of the two step nature of the reaction. Either the addition or the dehydration step may be rate determining.

For strongly basic amines such as aliphatic amines and hydroxylamine, there is strong evidence to suggest that in media more basic than pH=5 dehydration is rate determining (scheme 1.2) and the overall reaction is subject to general acid catalysis.[41]

Scheme 1.2

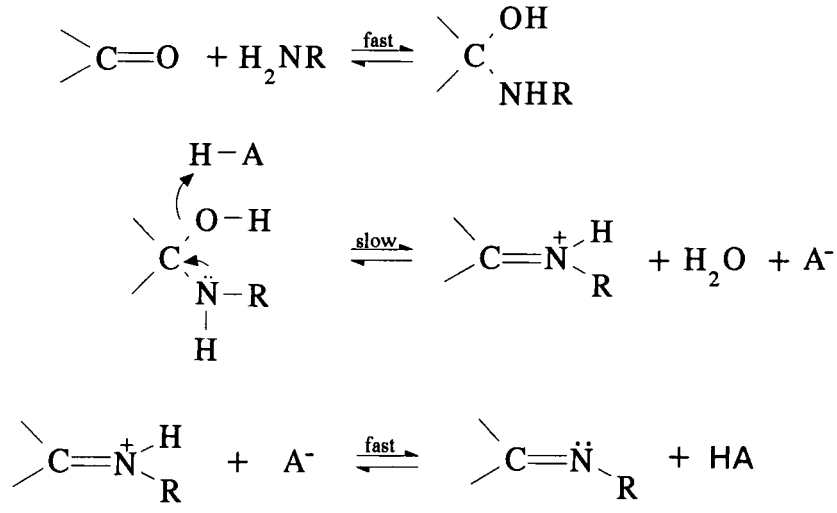

The decrease in rate constant that occurs on decreasing the pH below 5 is due to protonation of the amine. While greater acidity facilitates the dehydration step, it also inhibits the addition step as only the unprotonated amine is reactive, and therefore the addition step becomes rate determining.

The more strongly basic amines do not require assistance from general acids when nucleophilic (eqn. 1.6) addition is rate determining. The overall process is shown in scheme 1.3 with the first step rate-determining in acidic solution and the catalysed dehydration rate-determining at higher pH.

Scheme 1.3

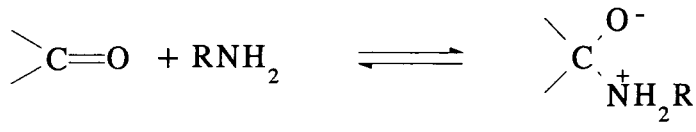

eqn. 1.6

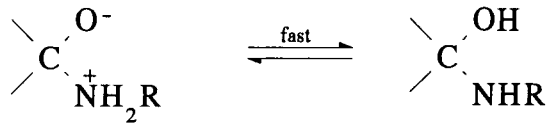

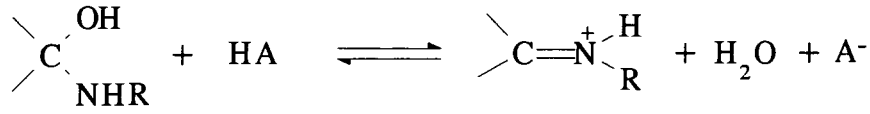

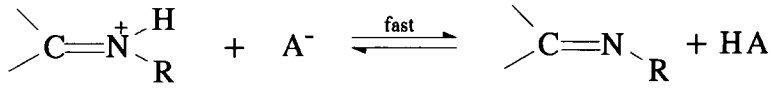

A generally similar pattern holds true also for weakly basic nitrogen nucleophiles such as aryl amines and semicarbazides.

In this instance the electron withdrawing groups retard the addition step in which the nitrogen lone pair attacks carbon but they also retard the dehydration step, where again the lone pair on nitrogen assists the expulsion of the hydroxyl group. The change from rate-determining dehydration to rate-determining addition is observed at roughly the same pH as with the more basic amines. However, the weaker bases require more help from acid catalysts (scheme 1.4) so that both the addition and dehydration step show general acid catalysis.

Scheme 1.4

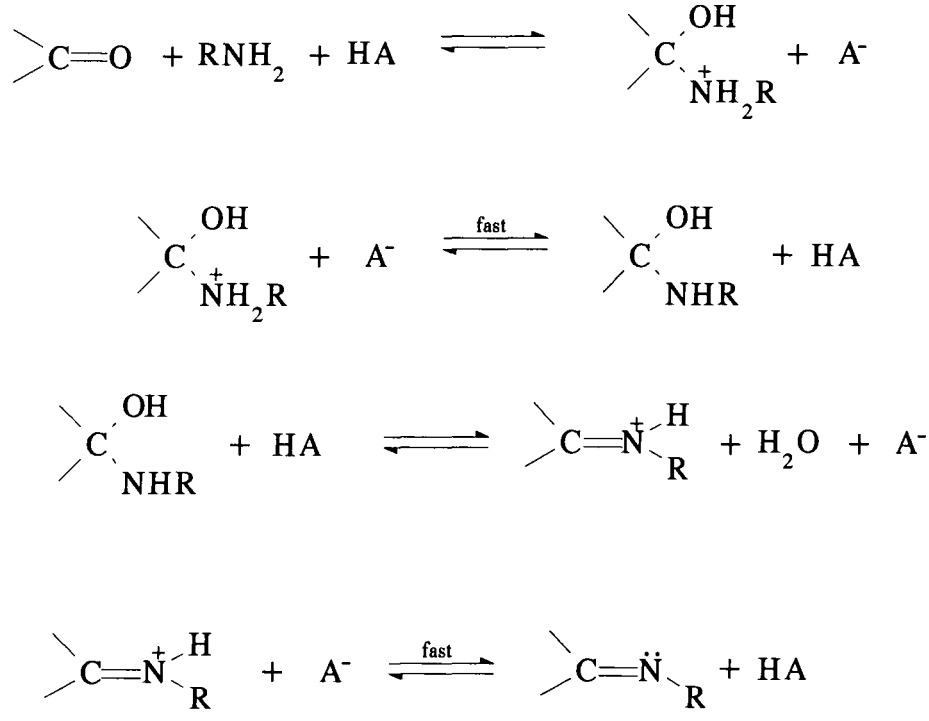

1.6 Glyoxal

Glyoxal (1.14) (biformyl, oxaldehyde or ethanedial) has a wide range of synthetic applications, which usually fall into two general classes :-

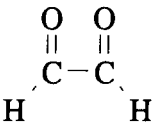

1.14

(a) Those using glyoxal as a reactive intermediate in preparation of materials such as pharmaceuticals,[42] photographic hardeners[43] and textile[44] additives for crease-proofing.

(b) Those using glyoxal alone in its reactions especially in this case with primary and secondary amines.

Monomeric glyoxal is a yellow solid (M.P. 15°C[45]) which polymerises readily on standing. The rate of polymerisation is accelerated when trace amounts of water are present. In the presence of mineral acids an inert hexaglycol hydrate is formed[46] Glyoxal can be obtained commercially as a 40% solution in water.

The major drawback of aqueous glyoxal is its immiscibility with various organic solvents which results in poor reactions for those compounds which are insoluble in aqueous media.

2,3-Dihydroxy-1,4-dioxane (1.15)[47,48] is a more stable synthetic equivalent of anhydrous glyoxal which can easily be prepared and has the advantages that it can be used in organic solvent systems and with ethylene glycol as the sole by-product.

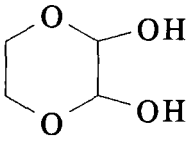

1.15

1.6.1 Reactions Of Glyoxal With Primary Amines

Condensation of aqueous glyoxal with primary aliphatic and aromatic amines gives 1,2-diimines (1.16)[49-52] (eqn 1.7).

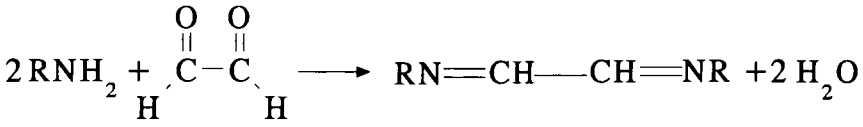

1.16 **eqn 1.7**

a, $R = C_6H_{11}$ (cyclohexyl)

b, $R = n\text{-}C_4H_9$

c, $R = p\text{-}CH_3C_6H_4$

d, $R = i\text{-}C_3H_7$

Most of the aliphatic diimines tend to be either high boiling liquids or high melting solids while all the aromatic homologues are high melting. A few aliphatic members , however,have been found surprisingly to be extremely volatile and show a very high degree of physiological activity characterised by lachrymation and stomach cramps.[53]

Glyoxal reacts with anilines and certain substituted anilines to give 1,2-diimines (1.16). Other derivatives which may be formed[54] are 1,2-dihydroxy-1,2-diamino-ethanes (1.17), alkoxytri-aminoethanes (1.18) and tetra-aminoethanes (1.19). The compounds formed are dependent on the stoichiometry of reactants and solvent composition (scheme 1.5).

Scheme 1.5

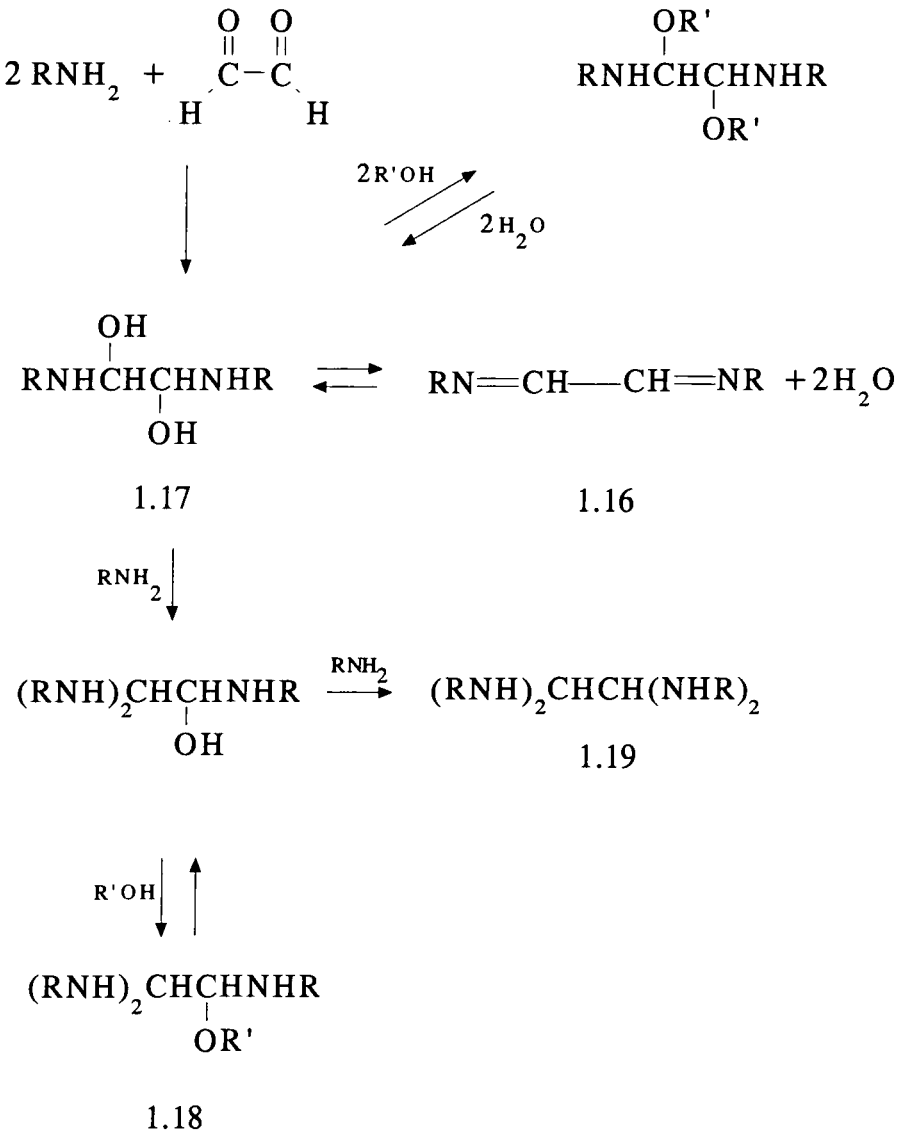

Recently a novel cage compound has been obtained from the reaction of glyoxal and benzylamine in a 2:1 molar ratio by the author and this has been subsequently investigated. The name isowurtzitane has been ascribed to the new cage system due to its close resemblance to the hydrocarbon wurtzitane (1.20).[55,56]

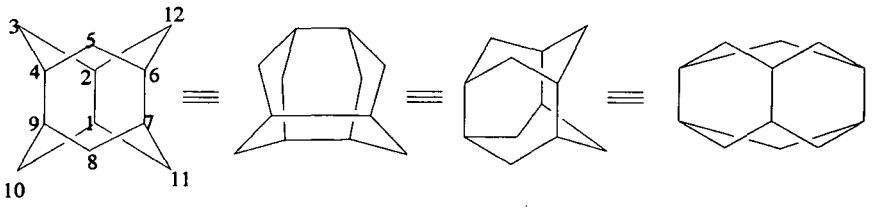

1.20

The new compound is known as 2,4,6,8,10,12-hexabenzyl-2,4,6,8,10,12-hexaazatetracyclo[5.5.0.$0^{5,9}$.$0^{3,11}$]dodecane or more trivially as hexabenzylhexaazaisowurtzitane (HBIW) (1.21). Nielsen and co-workers[57] working independently have also recently synthesised (1.21).

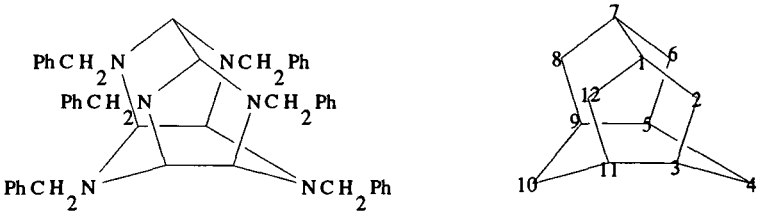

1.21

Wurtzitane (1.20) has been known since 1974. This highly symmetrical and rigid molecule has a carbon skeleton consisting of two chair cyclohexane rings connected to each other by three axial bonds and the periphery of the molecule consists of three boat cyclohexanes.

The trivial name iceane has been proposed for this molecule[58] as it is geometrically the hydrocarbon analogue of crystalline water (hexagonal diamond structure).

Ganter and co-workers prepared the first wurtzitanes incorporating a ring hetero atom such as 3-oxawurtzitane (1.22)[59] and 3-azawurtzitane (1.23).[60] Working independently Hammon and co-workers also prepared (1.22).[61]

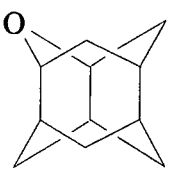

1.22

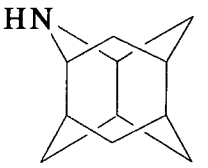

1.23

More recently wurtzitanes incorporating more than one ring hetero atom have been synthesised.[62] These 3,5,12-trisubstituted-3,5,12-triazawurtzitanes (3,5,12-triazatetracyclo [$5.3.1.1^{2,6}0^{4,9}$] dodecanes (1.26) have been obtained by condensation of 1,3,5-triformylcyclohexane (1.24) with selected primary amines (eqn. 1.8)

eqn. 1.8

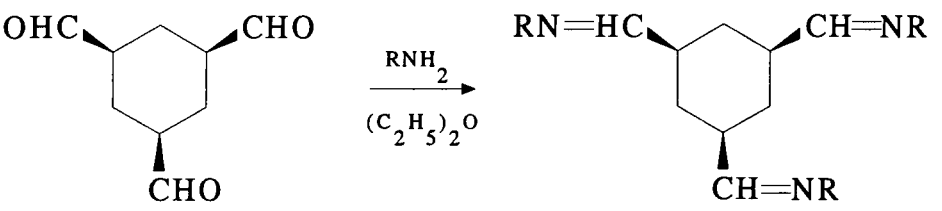

1.24 1.25

a, R = CH_3

b, R = C_2H_5

c, R = $C_6H_5CH_2$

d, R = 4-$CH_3OC_6H_4CH_2$

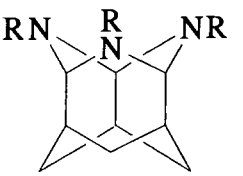

1.26

In solution in various solvents 1.26a-d are seen to exist in equilibrium with their corresponding triimines (1.25a-d).

12,17-Dimethyl-1,9,12-tetraazabicyclo [7.5.5] nona-decane (1.27) a new aza cage compound, has also been recently reported in the literature[63] and its basicity behaviour and solution equilibria have been investigated.

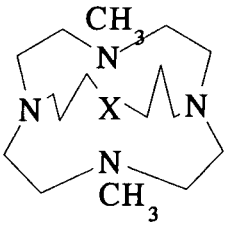

1.27 a, X = CH_2

b, X = N-CH_3

c, X = NH

d, X = S

e, X = O

In one report condensation of ethylene diamine in 2:3 molar ratio with glyoxal gave a tetraazadioxa caged compound (1.28), also an isowurtzitane derivative.[64,65] Condensation of certain ortho-diamino compounds with glyoxal gave pyrazines.[66,67]

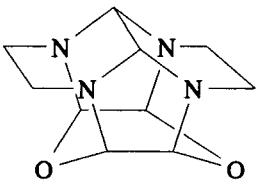

1.28

1.6.2 Reactions Of Glyoxal With Secondary Amines

Reaction of glyoxal with secondary amines leads to 1,1,2,2-tetra-amino-ethanes and also 1,1,2-tri-aminoethanes.[68,69] The different products obtained can be explained by proposing equilibria similar to those already seen for primary aromatic amines.

Reactions of N,N-disubstituted ethylene diamines gives trans-1,4,5,8-tetra-azadecalins (1.29), cis-1,4,5,8-tetra-azadecalins (1.30), 2,2'-bi-imidazolidines (1.31) and cis-trans 1,4,6,9-tetra-alkyl-tetra-aza-5,10-dioxa-perhydroanthracenes (1.32).[70,71] The products obtained are found to be dependent on both amine substituent and reaction conditions.

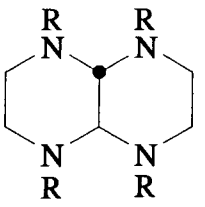

1.29

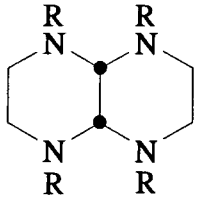

1.30

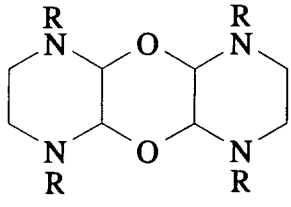

1.32

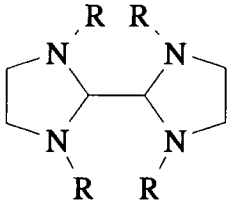

1.31

a, R = H

b, $R = CH_3$

c, $R = CH_2Ph$

1.7 Hexamethylenetetramine

1,3,5,7-Tetra-aza-tricyclo [3.3.1.$1^{3,7}$] decane, 1,3,5,7-tetra-azaadamantane (1.33), known also as hexamine, methanimine, urotropine and formin amongst other names is readily formed from the condensation of formaldehyde and ammonia.[72,73] Hexamine is widely used as a source of anhydrous formaldehyde.

Formation of hexamine is an important example of an amine condensation reaction. The reaction is thought to go through a 1,3,5-hexa-hydrotriazine (cyclotrimethylene-triamine) (1.34)[74] intermediate as shown in scheme 1.6.

Scheme 1.6

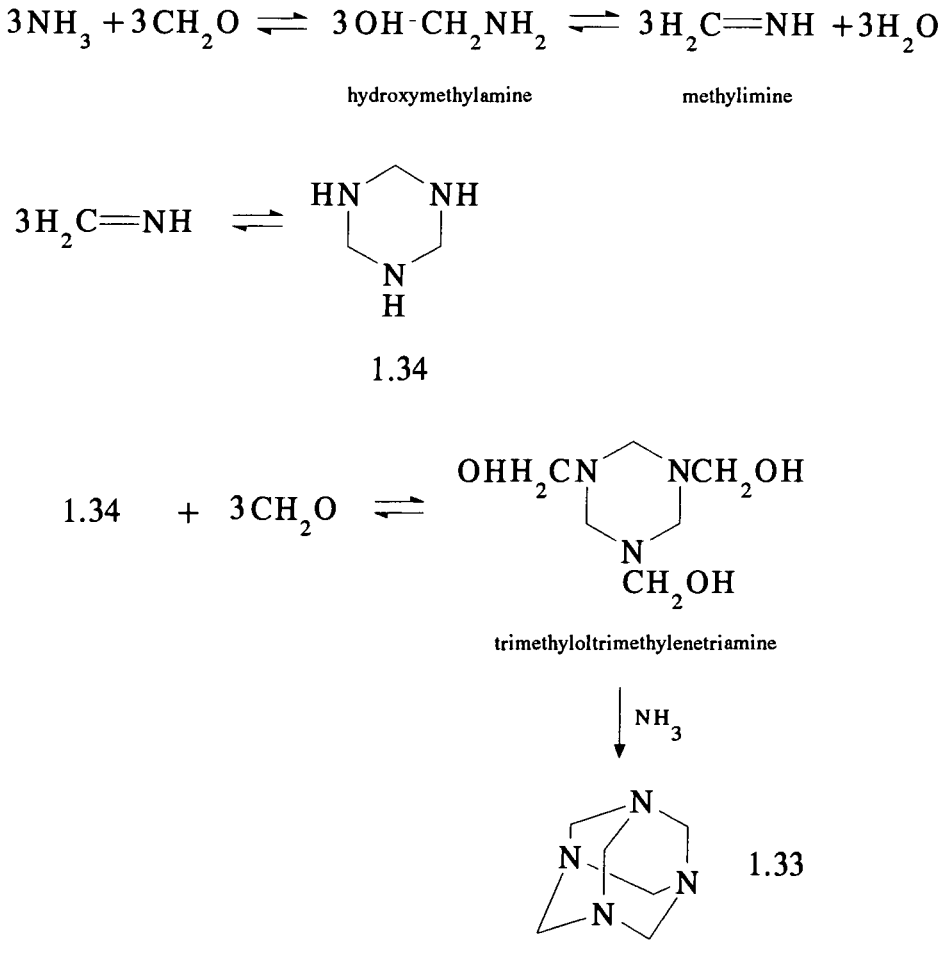

Hexamine being a tertiary amine shows characteristic properties of such amines forming innumerable salts[75], addition compounds and complexes.[76]

Some important reactions of hexamine are nitration, acetylation and nitrosation to give the corresponding 3,7-dinitro- (1.37), 3,7-diacetyl- (1.41) and 3,7-dinitroso- (1.39) 1,3,5,7-tetra-azabicyclo [3.3.1] nonanes respectively. These compounds are of military interest as intermediates in the preparation of a number of important explosives.

1.7.1 Nitration Of Hexamine

One of the products of nitration of hexamine is the high explosive cyclotrimethylene-trinitramine , also called hexogen, cyclonite and more recently designated as RDX (Research Department Explosive) (1.35).[77,78,79]

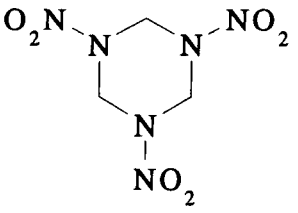

1.35

RDX (1.35) is a white crystalline substance having a melting point 202-207°C[80] and was first prepared by Henning[81] in 1879 by the action of nitric acid on hexamine dinitrate but was later produced by improved methods.[82]

A by-product from the production of RDX (1.35) studied by Bachmann and Sheehan[83] is 1,3,5,7-tetranitro-1,3,5,7-tetra-azacyclooctane, also known as octogen and HMX (High Melting Explosive) (1.36). The relative yields of HMX and RDX can be varied by changing the nitrating conditions.

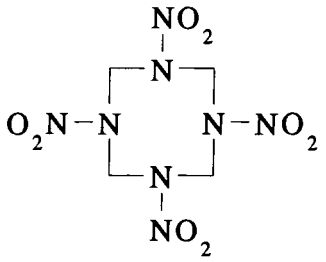

1.36

HMX (1.36) is also a white crystalline substance with a melting point of 276-277°C.[84] HMX (1.36) is a powerful high explosive, being far superior to RDX (1.35) in having a higher ignition temperature, and being chemically more stable.[85]

If the RDX (1.35) formed during nitration is removed and the mother liquor neutralised with ammonia or an alkali in the cold to about pH 5 precipitation of DPT (1.37).(Dinitropentamethylenetetramine) occurs.[82,86,87,88] Nitration of DPT (1.37) can also lead to the formation of HMX (1.36).

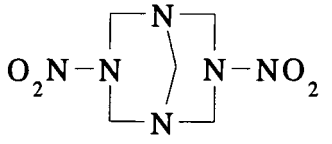

1.37

Wright and co-workers[86] also synthesised DPT (1.37) by the reaction of methylenediamine with dimethylol nitramide (1.38) (scheme 1.7). It has been suggested that 1.38 is a direct precursor to DPT (1.37) in this process.

Scheme 1.7

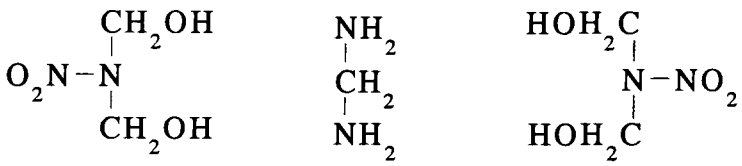

1.38

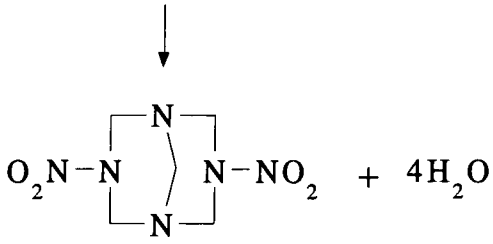

1.37

1.7.2 Nitrosation Of Hexamine

Degradative nitrosation of hexamine in aqueous solution occurs by simultaneous addition of dilute hydrochloric acid and sodium nitrite[89] to give trimethylene-trinitrosamine (TMTN) (1.38) and dinitrosopentamethylenetetramine (DNPT) (1.39).

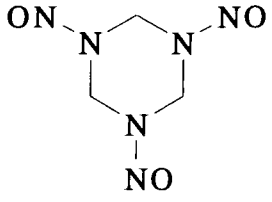

1.38

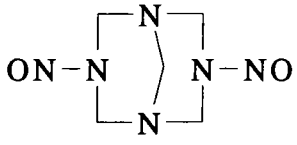

1.39

Several workers[90,91,92] found that depending on the rate of addition sodium nitrite they obtained either TMTN (1.38), DNPT (1.39) or a mixture of both. Reinvestigation by Bachmann and Deno[89] showed that the pH of the solution determined which product was produced irrespective of the rate of addition of sodium nitrite to the mixture. At pH 1-2 TMTN (1.38) is formed exclusively, whereas at pH 3-6 DNPT (1.39) is formed.

TMTN (1.38) is a powerful explosive. Oxidation of 1.38 with a mixture of nitric acid and hydrogen peroxide gives RDX (1.35), the reaction proceeding via the partially oxidised intermediate (1.40) (scheme 1.8).[92]

Scheme 1.8

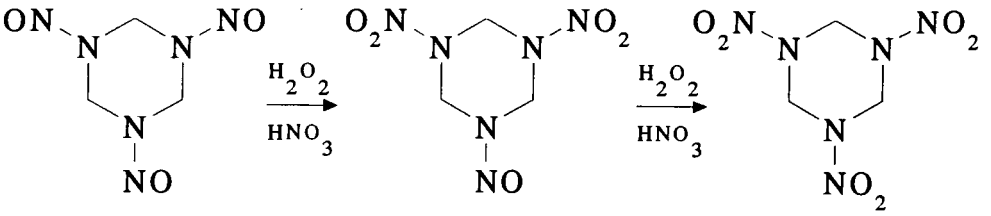

1.38 1.40 1.35

DNPT (1.39) was originally prepared by Greiss and Harrow.[93] Formulae for DNPT (1.39) and TMTN (1.38) were proposed by Duden and Scharff[94], and Cambier and Brochet.[95]

1.7.3 Acetylation Of Hexamine

The products of acetolysis of hexamine (1.33) are very much dependent on the conditions employed. Hexamine and acetic anhydride yield DAPT (diacetyl-pentamethylenetetramine) (1.41) at low temperatures, whereas the six-membered TRAT (1,3,5-triacetyl-1,3,5-triazacyclohexane), triacetyltrimethylenetriamine is formed at elevated temperatures (1.42) (scheme 1.9).[96]

Scheme 1.9

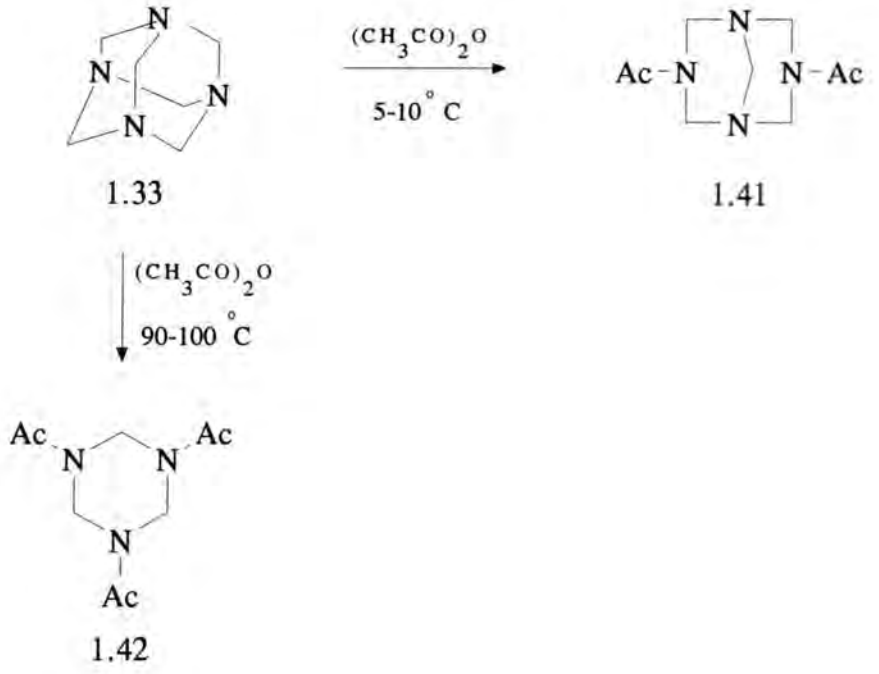

1.33 1.41

1.42

Earlier attempts to prepare DAPT (1.41) under anhydrous conditions gave poor yields[97]. Far greater yields were obtained by conducting the reaction in the presence of water[98]. Ogata and Kawasaki[99] suggested the effectiveness of water in promoting the formation of DAPT (1.41) was due to the equilibrium shown in scheme 1.10, species (1.43) probably being the actual species undergoing acylation when water is present.

Scheme 1.10

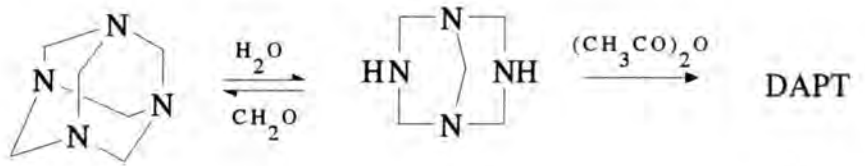

1.33 1.43 1.41

DAPT (1.41) has aroused recent interest[100] due to its potential usefulness as a synthetic route to HMX (1.37).

Further acetylation of DAPT (1.41) gives TAT (1,3,5,7-tetraacetyl-1,3,5,7-tetraazacyclooctane) (1.44).[100] TAT (1.44) can be converted to HMX by heating with a mixture of nitric acid and phosphorus pentoxide.[101]

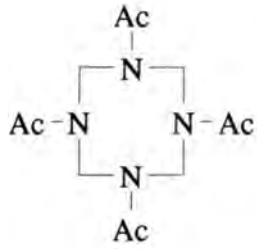

1.44

1.8 Present Work

The main thrust of the present work has been to examine the reaction of benzylamine with glyoxal. It was of interest to examine the yields of HBIW (1.21) obtainable from this reaction and to study, if possible the mechanism of the reaction. The effect of substituents in the benzylamine ring have been investigated in terms of the efficiency of the process. There was particular importance in finding out whether other cage structures, apart from HBIW (1.21), could be produced from this reaction.

Since synthetic reactions require acidic conditions there was also interest in examining the stability of HBIW (1.21) and some of its substituted derivatives in the presence of acid. Thus the protonation equilibria have been examined by ^{1}H NMR spectroscopy and the decomposition followed by U.V. spectroscopy.

It has been reported previously[102] that the acid-catalysed decomposition of 3,7-bis (arylazo)-1,3,5,7-tetra-azabicyclo [3.3.1] nonanes (1.45) in aqueous acetonitrile occurs in two stages via an observable intermediate which may be an iminium ion.

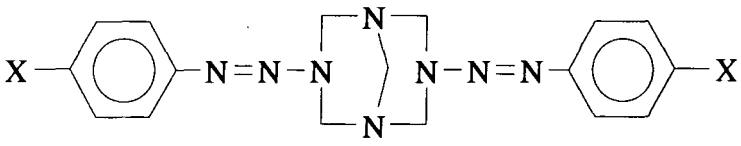

1.45

It was therefore thought of interest to examine the acid catalysed decomposition of DPT (1.37), DNPT (1.39) and DAPT (1.41) in aqueous acetonitrile to compare their behaviour with that of (1.45).

1.9 References

1. W. P. Jencks, "Catalysis in Chemistry and Enzymology", McGraw-Hill, New York, N. Y., 1969, p. 490.
2. W. P. Jencks, *ibid.*
3. R. L. Reeves, "The Chemistry Of The Carbonyl Group", Vol.1, S. Patai, Edition, Wiley London, 1966, p. 567.
4. J. Liebig, *Justus Liebigs Ann. Chem.*, 1874, 14, 133.
5. N. N. Ljubavin, *J. Russ. Phys. Chem. Soc.*, 1874, 6, 34.
6. C. F. Winans and H. Adkins, *J. Am. Chem. Soc.*, 1933, 55, 2051.
7. C. M. Caserio, "Basic Principles In Organic Chemistry", 2nd. Edition, 1977, p.700.
8. H. H. Richmond, G. S. Meyers and G. F. Wright, *J. Am. Chem. Soc.*, 1948, 70, 3659.
9. Y. Ogata and A. Kawasaki, *Tetrahedron,* 1964, 20, 855, 1573.
10. P. K. Chang P. K. Ulbricht, TLV, *J. Am. Chem. Soc.*, 1958, 80, 976.
11. H. Diebler and H. Thorneley, R. N. F., *J. Am. Chem. Soc.*, 1973, 95, 896.
12. T. C. French and T. C. Bruice, Biochemistry, 1964, 3, 1589.
13. E. G. Sander and W. P. Jencks, *J. Am. Chem. Soc.*, 1968, 90, 6154.
14. Poziomek, E. J. D., N. Kramer, B. W. Fromm, and W. A. Mosher and *J. Org. Chem.*, 1961, 26, 423.
15. T. H. Lowry and K. S. Richardson, "Mechanism And Theory In Organic Chemistry", 2nd. Edition, 1981, p.636.
16. M. M. Sprung, *Chem. Rev.*, 1940, 26, 297.
17. D. Y. Curtin, J. A. Kampmeier and B. R. O'Connor, *J. Am. Chem. Soc.*, 1965, 87, 863.
18. B. Witkop, *J. Am. Chem. Soc.*, 1956, 78, 2873.
19. V. I. Steinberg, N. Kulevesky and C. H. Niu, *J. Org. Chem.*, 1973, 38, 1227.
20. J. V. Michael and W. A. Noyes Jr., *J. Am. Chem. Soc* 1963, 85, 1228.
21. C. F. Winans and H. Adkins, *J. Am. Chem. Soc.*, 1933, 55, 2051.
22. L. Claisen and R. Feyerband, *Chem. Ber.*, 1905, 37, 699.

23. (a) M. Delepine, *Acad. Sci.*, 1897, 125, 297; (b) *Bull. Soc. Chim. Fr.*, 1898, 19, 15; (c) *Bull. Soc. Chim. Fr.*, 1907, 4, 590.

24. P. A. S. Smith, "The Chemistry Of Open-Chain Nitrogen Compounds", Vol.1, W. A. Benjamin, New York, N. Y. , 1965, p.326.

25. S. Coffey, Ed., "Rodds Chemistry Of Carbon Compounds", Vol. 1c, 2nd Edition, Elsevier, Amsterdam, 1965, pp.41-43.

26. J. Meier, F. Akermann and H. H. Gunthard, *Helv. Chim. Acta,* 1968, 51, 1686.

27. P. Sachs and P. Steinert, *Chem. Ber.*, 1904, 37, 1733.

28. R. K. McLeod and T. I. Crowell, *J. Org. Chem.*,1961, 26, 1094.

29. A. T. Nielson, R. L. Atkins, A. T. Moore, R. Scott, D. Mallory and J. M. La Berge, *J. Org. Chem.*, 1973, 38, 3288.

30. R. H. Hasek, E. U. Elam and J. C. Martin, *J. Org. Chem.*, 1961, 26, 1822.

31. J. J. Cornejo K. D. Larson and G. D. Mendenhall, *J. Org. Chem.*, 1985, 50, 5382

32. M. F. Aly and R. Grigg, *J. Chem. Commun.*,1985, 21, 1523.

33. D. H. R. Barton and L. R. Morgan Jr., *J. Chem. Soc.*, 1962, 622.

34. J. Hine and F. A. Via, *J. Am. Chem. Soc.*, 1972, 94, 190.

35. V. Capprio, A. Dilorenzo and G. Russo, *Chem. Ind. (Milan)*, 1968, 50, 898; *Chem. Abstr.* 1969, 70, 4070.

36. G. Stork, R. Terell and J. Szmuszkovicz, *J. Am. Chem. Soc.*, 1954, 76, 2029.

37. P. W. Hickmott, *Tetrahedron,* 1982, 38, 3363.

38. T. H. Lowry and K. S. Richardson, "Mechanism And Theory In Organic Chemistry", 2nd. Edition, 1981, p.637.

39. W. P. Jencks, *J. Am. Chem. Soc.*, 1959, 81, 475.

40. E. H. Cordes and W. P. Jencks, *J. Am. Chem. Soc.*, 1962, 84, 832.

41. E. H. Cordes and W. P. Jencks, *J. Am. Chem. Soc.*, 1963, 85, 2843.

42. J. B. Wright and R. B. Moffet, *J. Am. Chem. Soc.*, 1957, 79, 1682.

43. Matsui, Mitsuo Kanebo Co. Ltd. Japanese Patent 73,61,795 29th August 1973.

44. Ilford Ltd. British Patent 1,587,278 1st Nov. 1967.

45. R. C. Weast and M. J. Astle "CRC Handbook Of Chemistry And Physics" 63rd. Edition, 1981, CRC Press Inc. Boca Raton, Florida

46. Schiff *Annalen.*, 1874, 1, 172.

47. M. C. Venuti, *Synthesis,* 1982, 61.

48. F. S. H. Head, *J. Am. Chem. Soc.*, 1955, 1036.

49. J. M. Kliegman and R. K. Barnes, *Tetrahedron,* 1970, 26, 255.

50. H. tom Dieck and J. Dietrich, *Chem. Ber.*, 1984, 117, 694.

51. J. M. Kliegman and R. K. Barnes, *Tetrahedron Letters,* 1969, 24, 1953.

52. J. M. Kliegman and R. K. Barnes, *Tetrahedron Letters,* 1970, 22, 1859.

53. J. M. Kliegman and R. K. Barnes, United States Patent no. 3,652,672 1972.

54. J. M. Kliegman and R. K. Barnes, *J. Org. Chem.*, 1970,35, 3140.

55. H. Tobler, R. O. Klaus and C. Ganter, *Helv. Chim. Acta,* 1975, 58.

56. C. A. Cupas; L. Hodakowski, *J. Am. Chem. Soc.*, 1974, 96, 4668.

57. A. T. Nielsen, R. A. Nissan and D. J. Venderah, *J. Org. Chem.*, 1990, 55, 1459.

58. L. F. Fieser, *J. Chem. Educ.*, 1965, 42, 408.

59. R. O. Klaus, H. Tobler and C. Ganter, *Helv. Chim. Acta,* 1974, 57, 2517.

60. R. O. Klaus; C. Ganter, *Helv. Chim. Acta,* 1980, 63, 2559.

61. D. P. G. Hammon, G. F. Taylor and R. N. Young, *Aust. J. Chem.*,1977, 03, 589.

62. A. T. Nielsen , S. L. Christian and W. D. Moore, *J. Org. Chem.*, 1987, 52, 1656.

63. A. Bencini, A. Bianchi, A. Borselli, M. Ciampolini, M. Micheloni, P. Paoli and B. Valtancoli, *J. Chem. Soc. Perkin Trans. 2.*, 1990, 209.

64. J. M. Edwards, U. Weiss, R. D. Gilardi and I. L. Karle, *Chem. Commun.*, 1968, 1649.

65. R. D. Gilardi, *Acta Crystallogr.*, 1972, B28, 742.

66. J. K. Landquist, *J. Am. Chem. Soc.*, 1953, 2186.

67. V. Petrow and J. Saper, *J. Am. Chem. Soc.*, 1948, 1389.

68. M. Kliegman and R. K. Barnes, *J. Heterocyclic Chem.*, 1970, 7, 1153.

69. B. Fuchs; A. Ellencweig, *Recl. Trav. Chim.*, 1979, 98, 326.

70. R. L. Willer and D. W. Moore, *J. Org. Chem.*, 1985, 50, 2365.

71. R. L. Willer, D. W. Moore, and C. K. Lowe-Ma, *J. Org. Chem.*, 1985, 50, 2368.

72. A. T. Nielson, D. W. Moore, M. D. Ogan and R. L. Atkins, *J. Org. Chem.*, 1979, 44, 1678.

73. N. Blazevic, N. Kolbah, D. Belin, V. Sunjic and F. Kajfez, *Synthesis,* 1973, 3, 161.

74. J. F. Walker; "Fomaldehyde", Chapter 19. 3rd edition, Reinhold, New York, 1964.

75. F. K. Bieistein; "Handbuch de Organischen Chemie", Vol.1, 4th edition, B. Prager and P. Jacobsen (Eds.), Verlag von Julius Springer, Berlin, 1918, p.586.

76. Butlerov, *Ann.*, 1860, 115, 323.

77. G. C. Hale, *J. Am. Chem. Soc.*, 1925, 47, 2754.

78. E. von Herz, Swiss Patent 1920, 88, 759.

79. G. F. Wright, E. Aristoff, J. A. Graham, R. H. Meen and G. S. Meyers, *Can. J. Res.*, 1949, 27B, 520.

80. T. Urbanski, "Chemistry and Technology Of Explosives", Vol.3, Pergammon Press, Oxford, 1983, p.78.

81. G. F. Henning, German Patent 104,280 1899.

82. M. Delepine, *Bull. Soc. Chimi France,* 1911, 9, 1025.

83. W. E. Bachmann and J. C. Sheehan, *J. Am. Chem. Soc.*, 1949, 71, 1842.

84. T. Urbanski, "Chemistry and Technology Of Explosives", Vol.3, Pergammon Press, Oxford, 1983, p.117.

85. T. Urbanski, "Chemistry and Technology Of Explosives", Vol.3, Pergammon Press, Oxford, 1983, p.118.

86. G. F. Wright, W. J. Chute, D. C. Downing, A. F. McKay and G. S. Meyers, *Can. J. Res.*, 1949, 27B, 218.

87. P. Golding, Ministry Of Defense, private communication.

88. G. F. Wright and W. J. Chute, U. S. Patent 1954, 2,678,927.

89. W. E. Bachmann and N. C. Deno, *J. Am. Chem. Soc.*, 1951, 73, 2777.

90. F. Mayer, *Ber.*, 1888, 21, 2883.

91. D. C. Downing, private communication.

92. F. J. Brockman, D. C. Downing and J. F.Wright, *Can. J. Res.*, 1949, 27B, 469.

93. P. Griess and G. Harrow, *Ber.*, 1888, 21, 2737.

94. P. Duden and M. Scharff, *Ann.*, 1895, 288, 18.

95. R. Cambier and A. Brochet, *Compt. Rend.*, 1895, 120, 105.

96. V. I. Seale, M. Warman and E. E. Gilbert, *J. Heterocyclic Chem.*, 1973, 10, 97.

97. M. Dominikiewiez, *Arch. Chemi.*, Farm., (Warsaw), 1935, 2, 78.

98. V. I. Seale, M. Warman and E. E. Gilbert, *J. Heterocyclic Chem.*, 1974, 11, 237.

99. Y. Ogata and A. Kawasaki, "Chemistry of The Carbonyl Group", Interscience, New York, Vol.21, 51.

100. V. I. Seale, M. Warmann, J. Leccavorvi, R. W. Hutchinson, R. Moho, E. E. Gilbert, T. M. Benzinger, M. D. Corburn, R. K. Rohwer and R. K. Davey, *Propellants and Explosives,* 1981, 6, 67.

101. Chen Ju and Wang Shaofung, *Propellants, Explosives and Pyrotechnics,* 1984, 9, 58.

102. M. R. Crampton J. K. Scranage and Peter Golding *J. Chem. Res.*, 1990, 182-183.

Chapter 2

Kinetic And Equilibrium Studies On The Formation And Decomposition Of HBIW In Acidic/Aqueous Media

2.1 Formation Of HBIW

It is known that on a preparative scale the reaction of benzylamine with glyoxal in a 2:1 molar ratio in either acetonitrile or methanol, containing a catalytic amount of acid produces HBIW[1] (eqn. 2.1)

eqn. 2.1

$$6PhCH_2NH_2 + 3(CHO)_2 \xrightarrow[CH_3CN]{H^+} HBIW + 6H_2O$$

It was thought of interest from a mechanistic point of view to attempt to follow the reaction using U.V. spectroscopy in order to identify any other species or intermediates produced.

Reactions were monitored in acetonitrile as opposed to methanol, the former solvent having the advantage of producing HBIW in far greater yields. This would help to minimise production of by-products which may also absorb in the U.V. region. Acetonitrile also has the added advantage of having a much lower extinction coefficient in the U.V. range where measurements were made (210-320nm).

2.1.1 Reactions Of N-N'-Dibenzyl-1,2-ethane-diimine

N-N'-Dibenzyl-1,2-ethanediimine (2.1) is thought to be an intermediate in the formation of HBIW. Formation of HBIW is thought to involve trimerisation of 2.1 in the presence of catalytic amounts of acid. The reaction is analogous to the trimerisation of acyclic aldimines ($CH_2=NR$ or $RCH=NH$) leading to 1,3,5- or 2,4,6-trisubstituted-1,3,5-hexahydrotriazines[2-4] (2.2 and 2.3 respectively). Reactions of diimine 2.1 in the presence of acid were investigated.

$PhCH_2N=CHCH=NCH_2Ph$

2.1

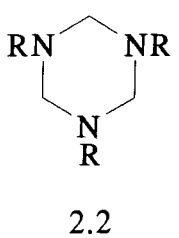

2.2

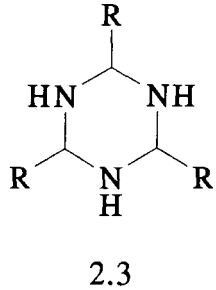

2.3

2.2 Stability of HBIW

The effects of acid and water on the stability of HBIW in acetonitrile and acetonitrile containing varying amounts of water were investigated. k_{obs}, the first order rate coefficient for the decomposition of HBIW was determined by following an increase in U.V. absorbance at 240nm. Results are given in tables 2.4-2.6 with infinity values given in parentheses.

2.3 Extent Of Protonation Of HBIW

HBIW contains six nitrogen atoms and therefore one would expect several possibilities of protonation on the molecule, although it will be seen later that in practice only two sites are utilised. The degree of protonation on addition of perchloric acid was measured by following the decrease in U.V. absorbance at 240nm and at 280nm (tables 2.1-2.3).

2.4 Formation Of HBIW

HBIW is very sparingly soluble in acetonitrile. A solution of HBIW shows an inflection λ_{max} at 207nm $\varepsilon=6x10^4$ mol^{-1} dm^3 cm^{-1} with a pronounced shoulder extending down to 280nm (fig.2.1).

Fig.2.1

U.V. Spectrum Of HBIW ($2.05x10^{-5}$M) In Acetonitrile

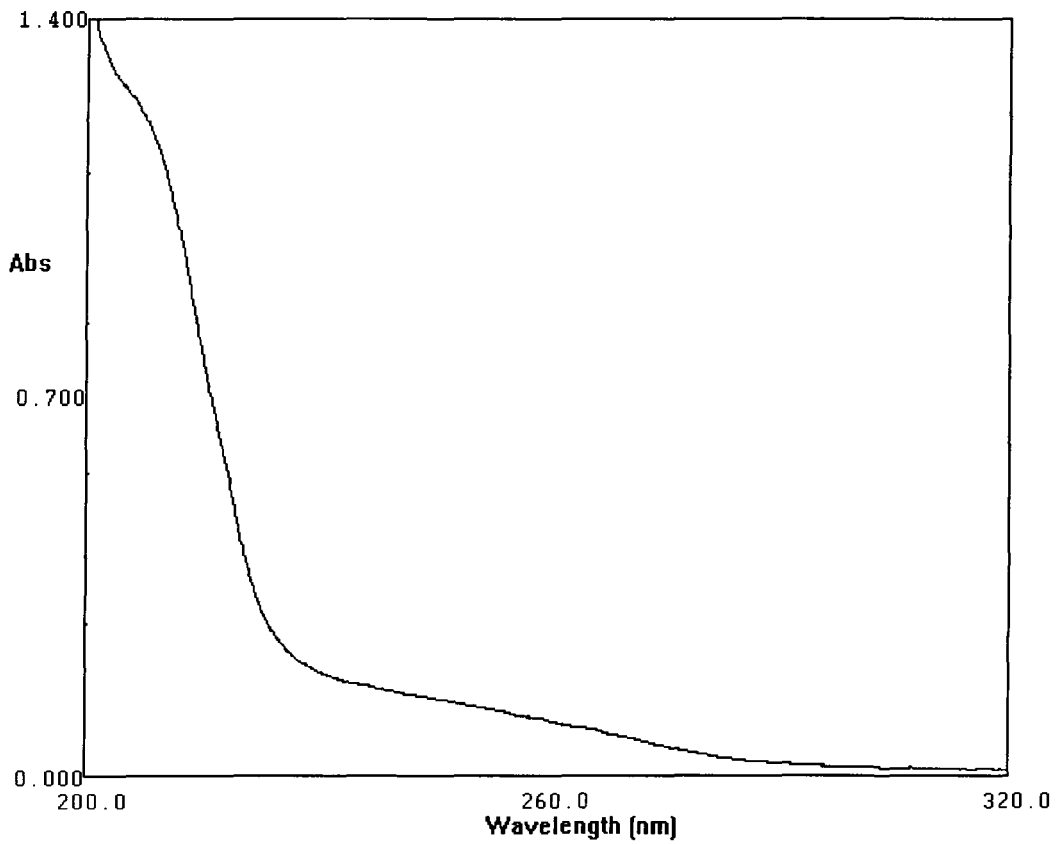

The change with time in U.V. spectrum of a dilute reaction mixture of benzylamine and glyoxal containing an acid catalyst at 40min. intervals is shown in fig. 2.2. Fig. 2.3 is that of the final reaction mixture after 8hrs., which had been subsequently diluted with acetonitrile.

Fig. 2.2

U.V. Spectra Of A Mixture of Benzylamine ($2x10^{-3}M$) And Glyoxal ($1x10^{-3}M$) Containing Trace Of Acid Taken at 40min . Intervals In Acetonitrile

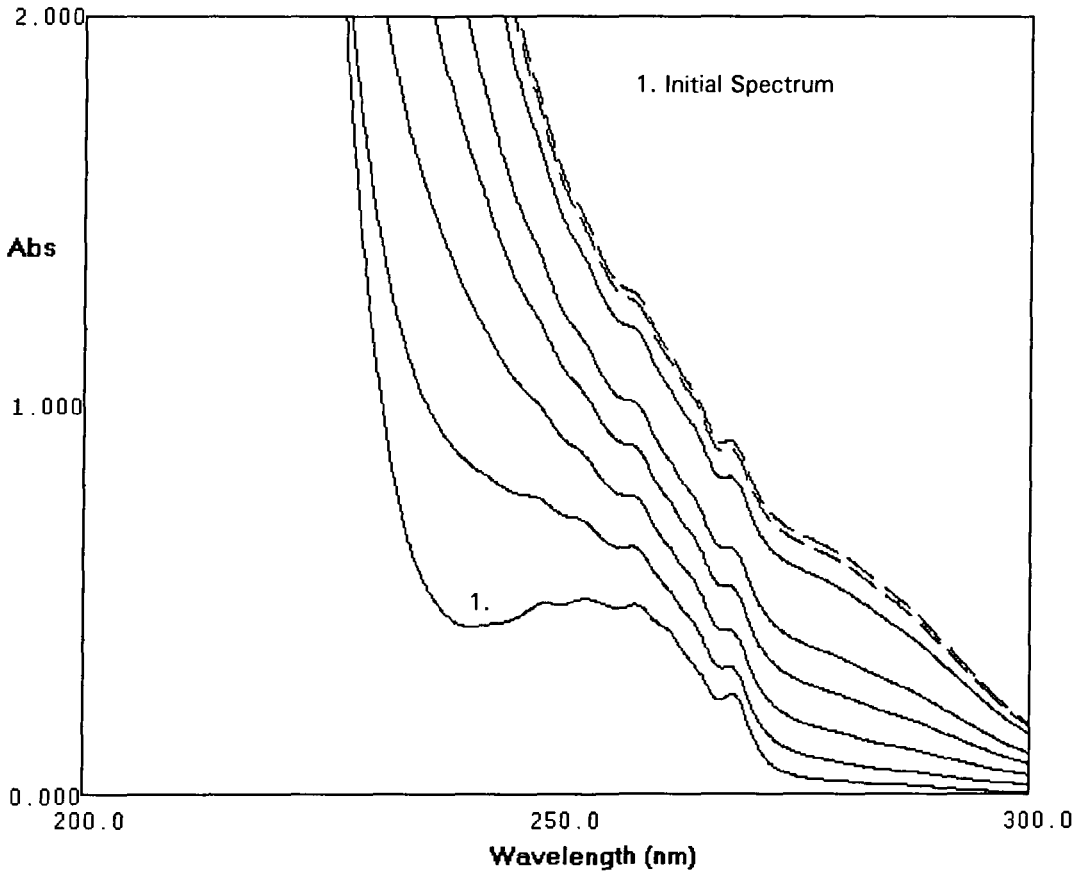

The final spectrum of the reaction mixture shows a series of small peaks between 250-260nm which are characteristic of benzylamine (fig.2.4) and protonated benzylamine (fig. 2.5). Glyoxal shows no appreciable absorbance in this region.

Fig. 2.3

UV. Spectrum Of Reaction Mixture (8hrs.) After Dilution With Acetonitrile

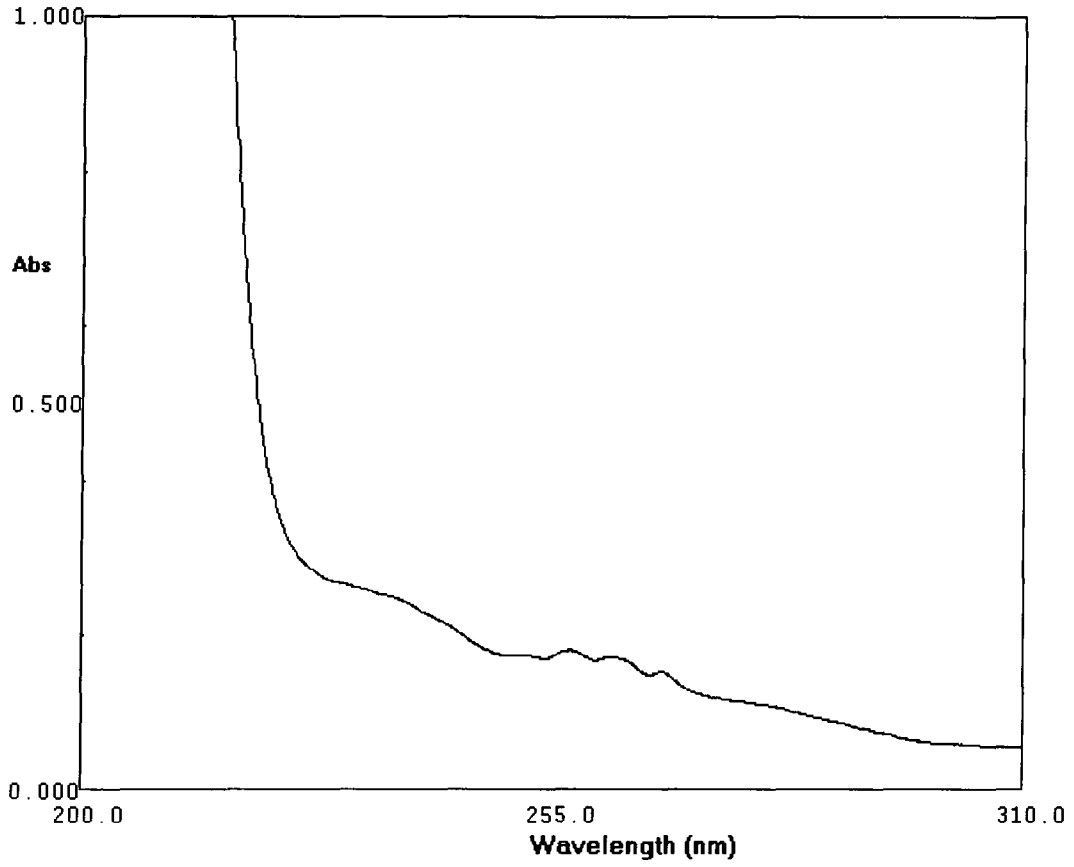

Fig. 2.4

U.V. Spectrum Of Benzylamine ($2x10^{-3}M$) In Acetonitrile

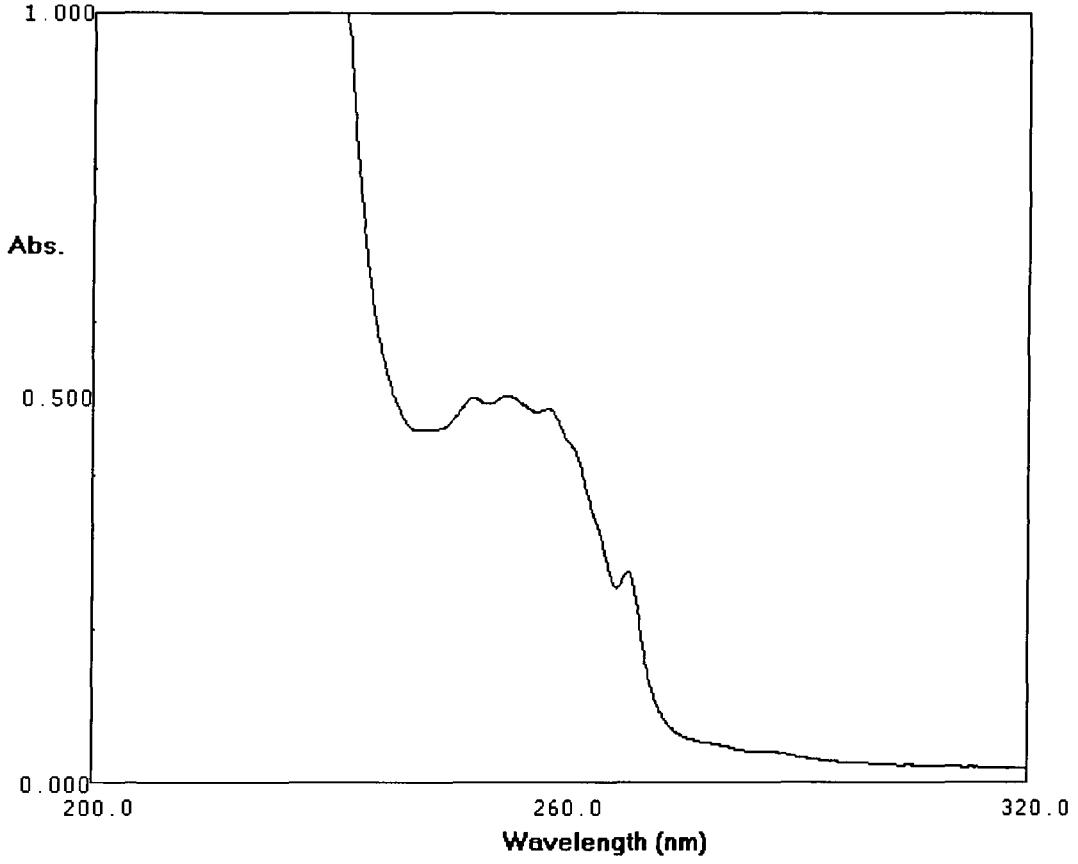

Fig. 2.3 does not resemble the U.V. spectrum of HBIW but it is not possible to rule out the presence of some HBIW in the mixture. It is possible that other products of the reaction that may be produced absorb more strongly and therefore mask the absorbance due to HBIW. It should be noted that in the preparative experiments relatively high concentrations of reactant were used (about 0.5M in benzylamine). For U.V. work very much lower concentrations had to be used.

Fig. 2.5

U.V. Spectrum of Protonated Benzylamine In Acetonitrile

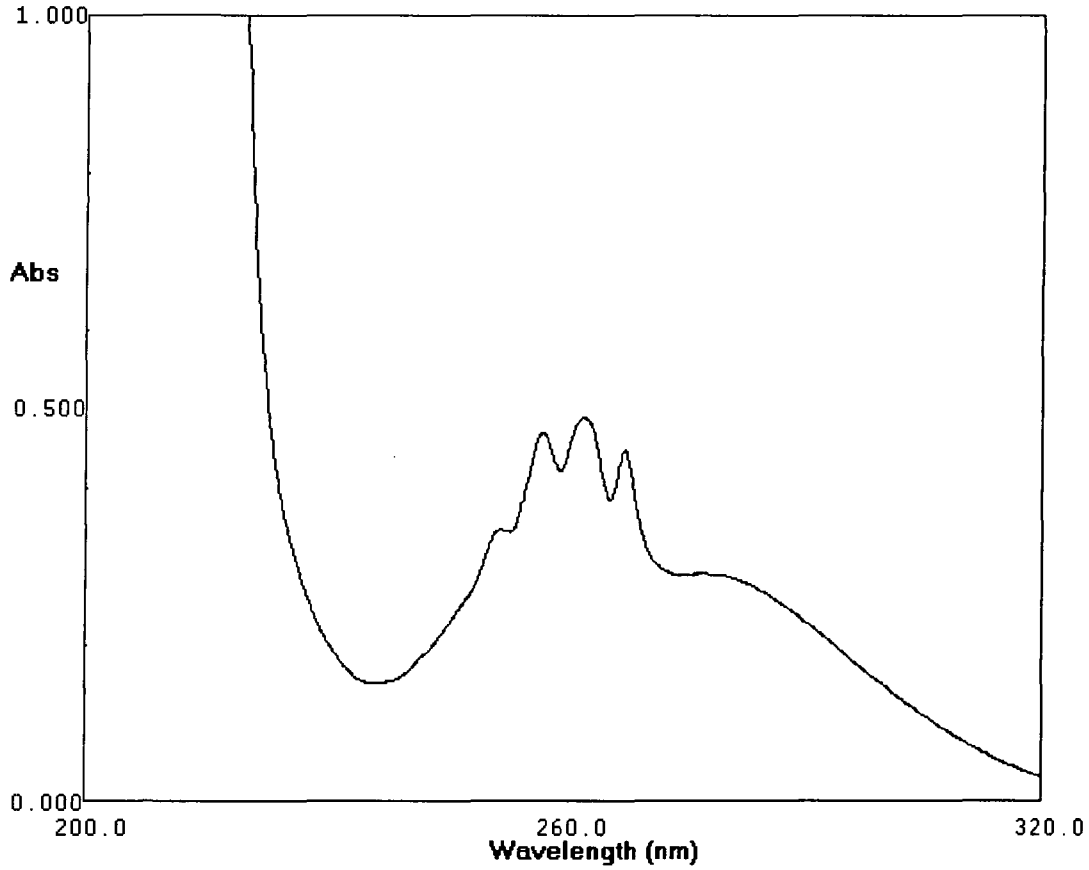

2.4.1 Reactions Of N,N'-Dibenzyl-1,2-ethane-diimine

2.1 is a very reactive intermediate thought to be involved in the formation of HBIW. On standing at 25°C di-imine 2.1 rapidly turns to a brown gum. The U.V. spectrum of 2.1 is that shown in fig.2.6. Since 2.1 cannot be obtained in a completely pure state, there is a possibility of a little benzylamine impurity.

Fig. 2.6

U.V. Spectrum Of Diimine 2.1 In Acetonitrile

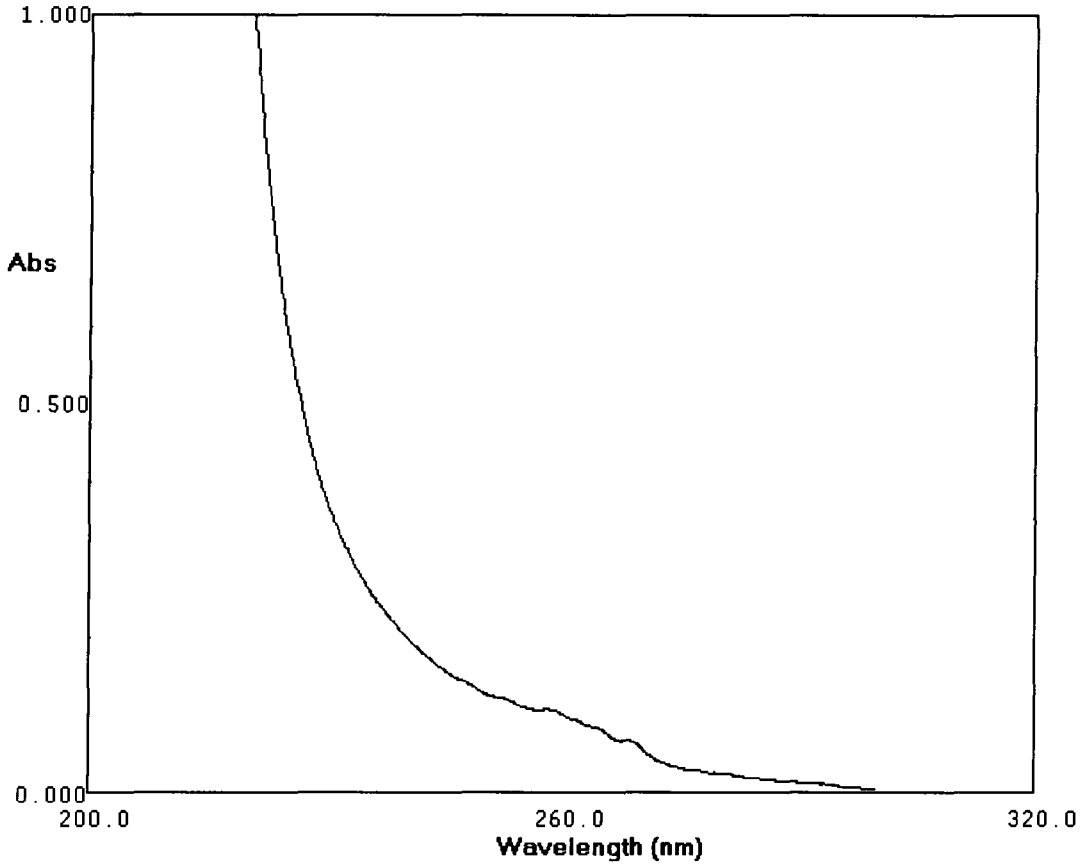

The U.V. spectrum of the diimine shows a similar spectrum to that of HBIW with a λ_{max} at 220nm. One would have expected 2.1 to have an absorption maximum towards higher wavelengths due to conjugation of the double bonds as seen with other diimines.[5-7] A solution of diimine in acetonitrile was scanned at 2hr. intervals and was found to give an increase in absorbance as shown in fig.2.7. In the absence of acid the diimine could be undergoing an alternative reaction to that of cyclisation to give HBIW. Again it is not certain to rule out the possibility that we may also be producing some HBIW.

Fig. 2.7

Change Of U.V. Spectrum Of 2.1 At 2hr. Intervals in Acetonitrile

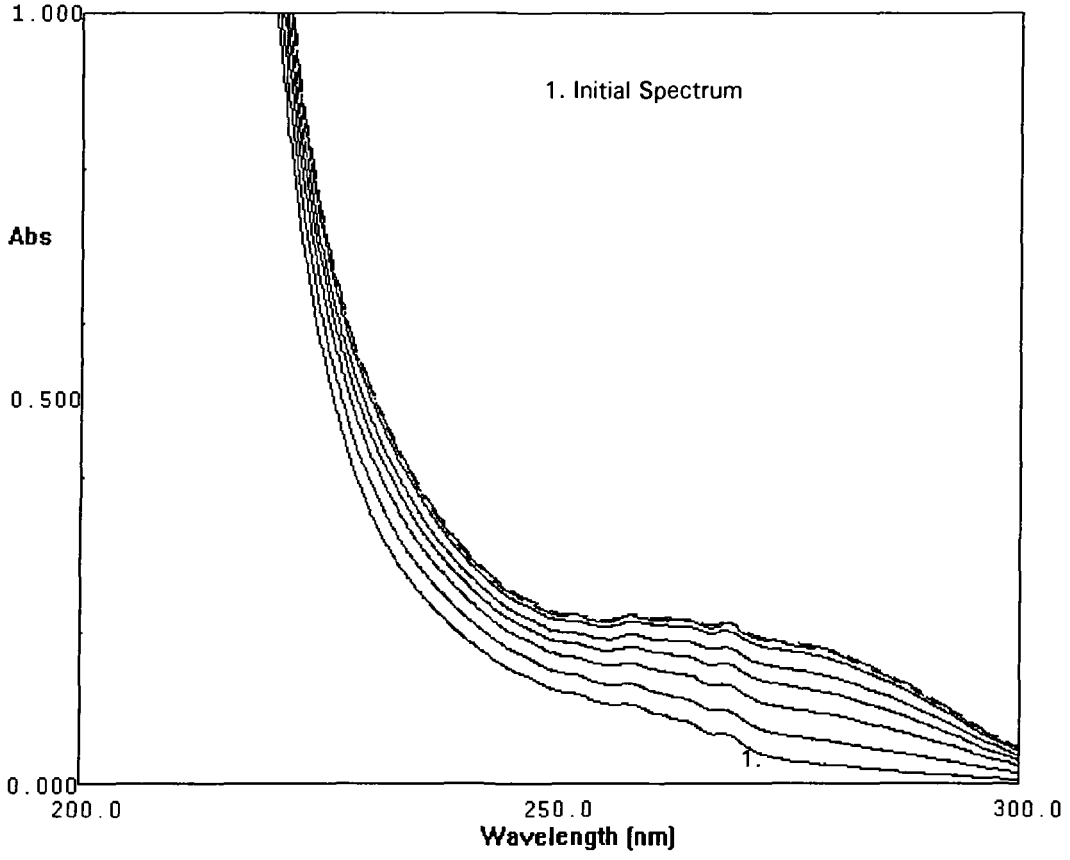

However the U.V. spectrum of the diimine in the presence of perchloric acid taken at 40mins. intervals gave more interesting results (fig.2.8). An initial decrease of absorbance occurred on addition of acid followed by a very much slower increase with time. Close examination of the spectrum of the diimine in acidic media shows strong similarity with the behaviour of HBIW in acidic media. Spectra of HBIW are shown in figs.2.9-2.11.

Fig. 2.8

U.V. Spectrum Of 2.1 In Presence Of Perchloric Acid

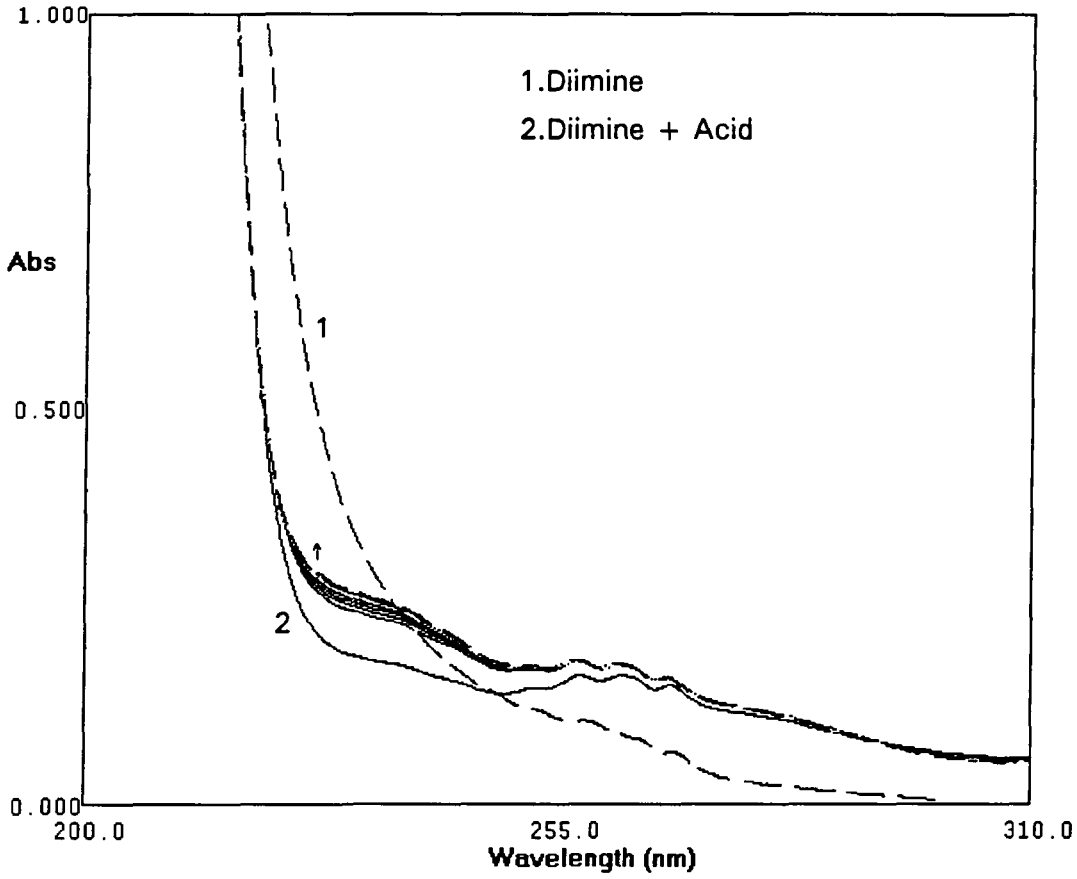

Fig. 2.9

HBIW In 0.05M Perchloric Acid/Acetonitrile (3min. intervals)

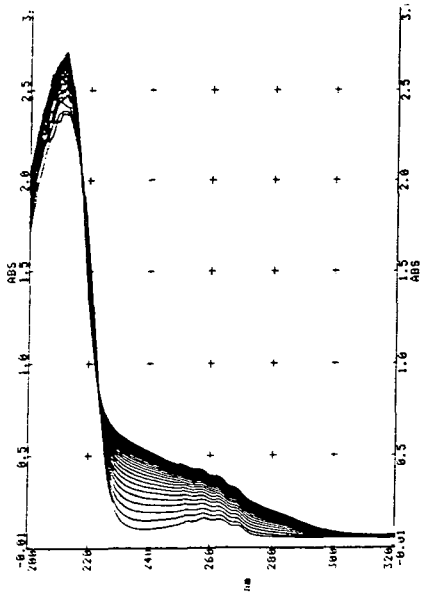

Fig. 2.10

HBIW In 0.05M Perchloric Acid/Acetonitrile Containing 0.25% Water (3min. intervals)

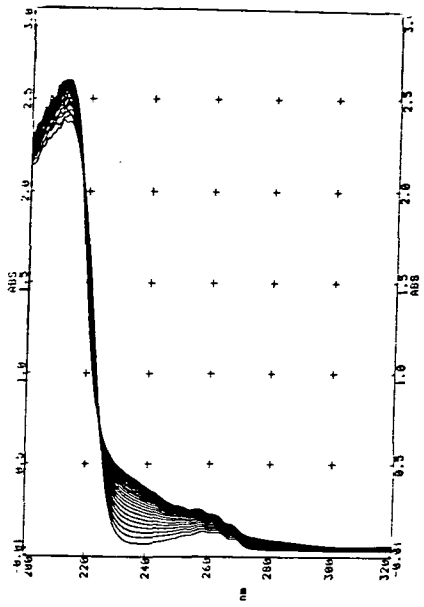

Fig. 2.11

HBIW In 0.05M Perchloric Acid/Acetonitrile Containing 0.50% Water (3min. intervals)

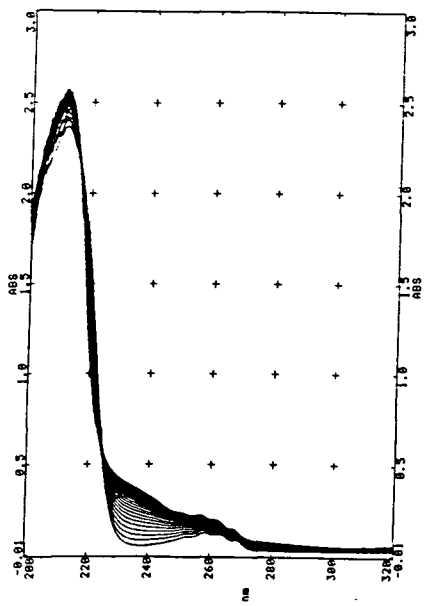

The final spectrum of the benzylamine -glyoxal reaction mixture (after dilution) and that of the diimine/acid mixture are shown to be virtually identical (fig.2.12). From these observations and the similarities in the spectra of HBIW and of the diimine in acidic media, it seems likely that in each case HBIW is formed and then decomposes.

Fig. 2.12

Final U.V. Spectra Of Diimine/Acid And Benzylamine/Glyoxal Reaction Mixtures

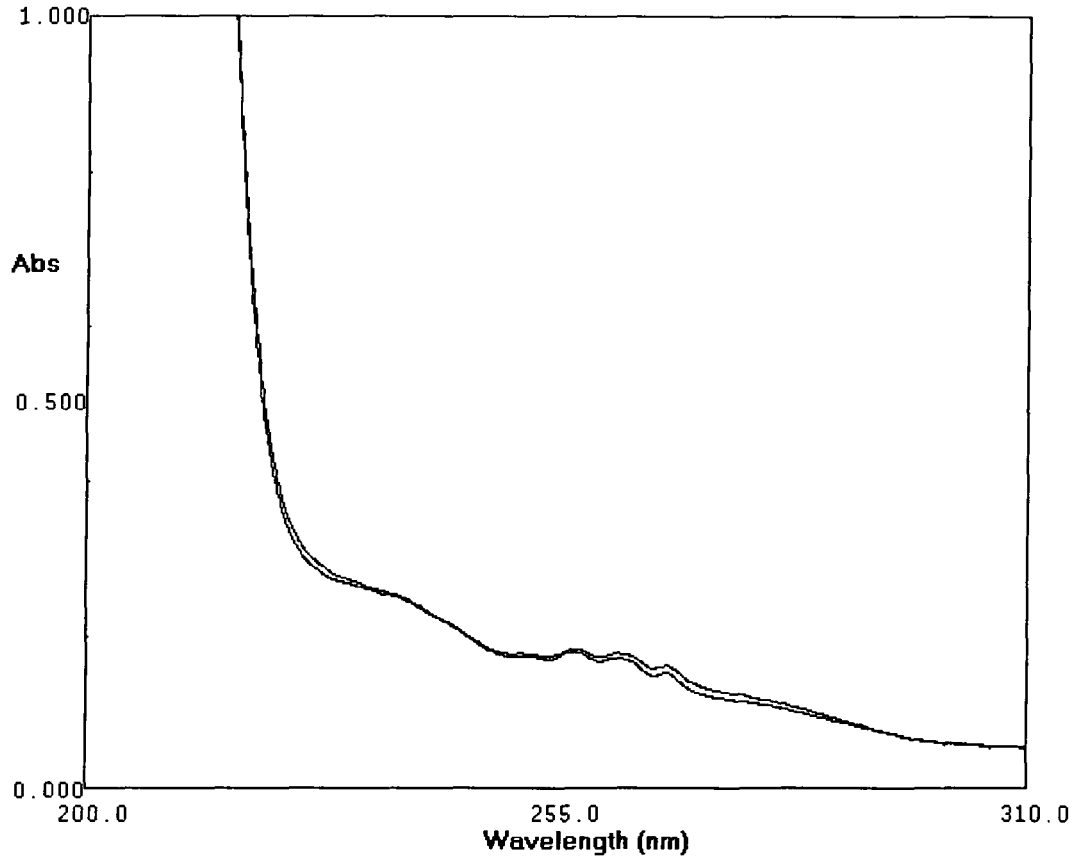

What appears to be happening in the case of the diimine/acid mixture is that HBIW is probably being produced from the trimerisation of the diimine which is thought to be very fast as no observable intermediate is seen. As there will be excess acid present any HBIW formed will be protonated immediately.

The protonated species is unstable and undergoes decomposition , the U.V. spectra of the decomposition of HBIW in acidic media are shown in fig.2.9-2.11.and are very similar to those obtained from the benzylamine-glyoxal reaction mixture and that of the diimine/acid reaction mixture. The initial difference in spectral shape of the bezylamine -glyoxal reaction mixture as opposed to the diimine/acid mixture is due to the fact that in the former case we are probably witnessing formation of the diimine prior to trimerisation and subsequent decomposition.

2.5 Stability Of HBIW In Acidic/Aqueous Media

HBIW is stable indefinitely in acetonitrile and also in acetonitrile containing water. However in the presence of acid decomposition occurs. An initial fast decrease in U.V. absorbance is observed attributed to protonation followed by a slower increase also at 240nm. The final spectra as seen of the reaction mixtures (fig.2.9-2.11) are quite distinct from those of HBIW. There is NMR evidence, described in chapter 4, consistent with the attribution of the initial rapid reaction to reversible protonation.

Perchloric acid was used as opposed to nitric ,sulphuric or hydrochloric acids as it is known to be completely dissociated in acetonitrile.[8]

2.6 Extent Of Protonation Of HBIW

The extent of protonation of HBIW was initially measured at 240nm. However, due to the high extinction coefficient of HBIW at this wavelength measurements were limited to a maximum concentration of HBIW of $2x10^{-4}M$.

The change in absorbance of HBIW at 240nm on addition of perchloric acid is shown in fig.2.18 (values are given in table 2.1). The absorbance values decrease gradually with no distinct inflections, which would be expected if protonation was occurring. An additional complication at this wavelength was the increase in absorbance which occurred with time due to the decomposition of HBIW, also at this wavelength. Therefore all measurements had to be extrapolated to zero time.

Table 2.1

Absorbance Values For HBIW ($2x10^{-4}M$)

At 240nm In Perchloric Acid

Absorbance	10^4 [$HCLO_4$] mol dm^{-3}
1.223	0
1.020	1
0.812	2
0.661	3
0.591	4
0.555	5
0.532	6
0.430	7
0.302	8
0.174	9

Table 2.2

Absorbance Values For HBIW ($1x10^{-3}M$)

At 280nm In Perchloric Acid

Absorbance	10^3 [$HCLO_4$] mol dm^{-3}
1.043	0
0.291	1
0.029	2
0.029	3
0.032	4
0.035	5
0.039	6
0.044	7
0.050	8
0.053	9

Fig.2.18

Absorbance Plot

For HBIW ($2x10^{-4}M$) At 240nm In Acetonitrile

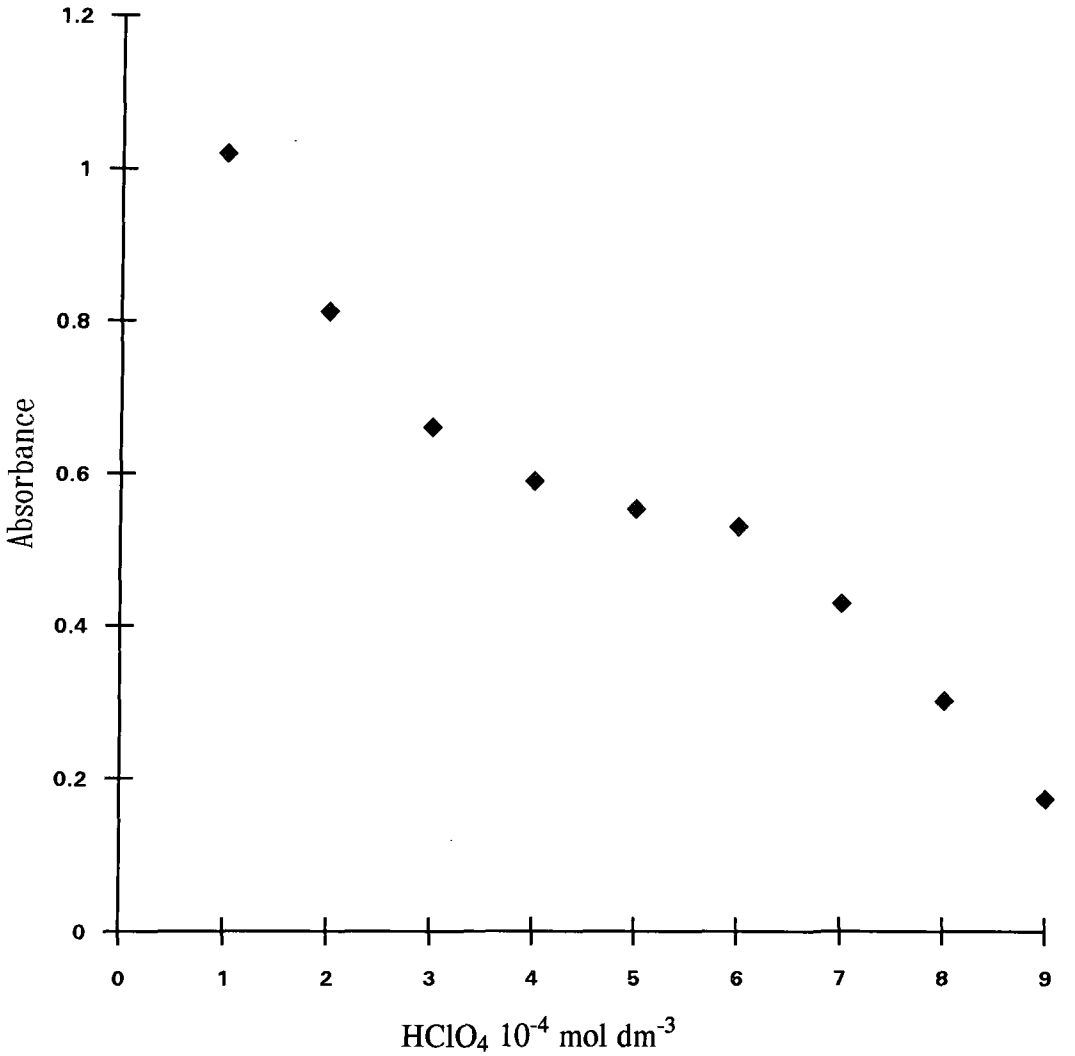

Fig. 2.19

Absorbance Plot

For HBIW ($1x10^{-3}M$) At 280nm In Acetonitrile

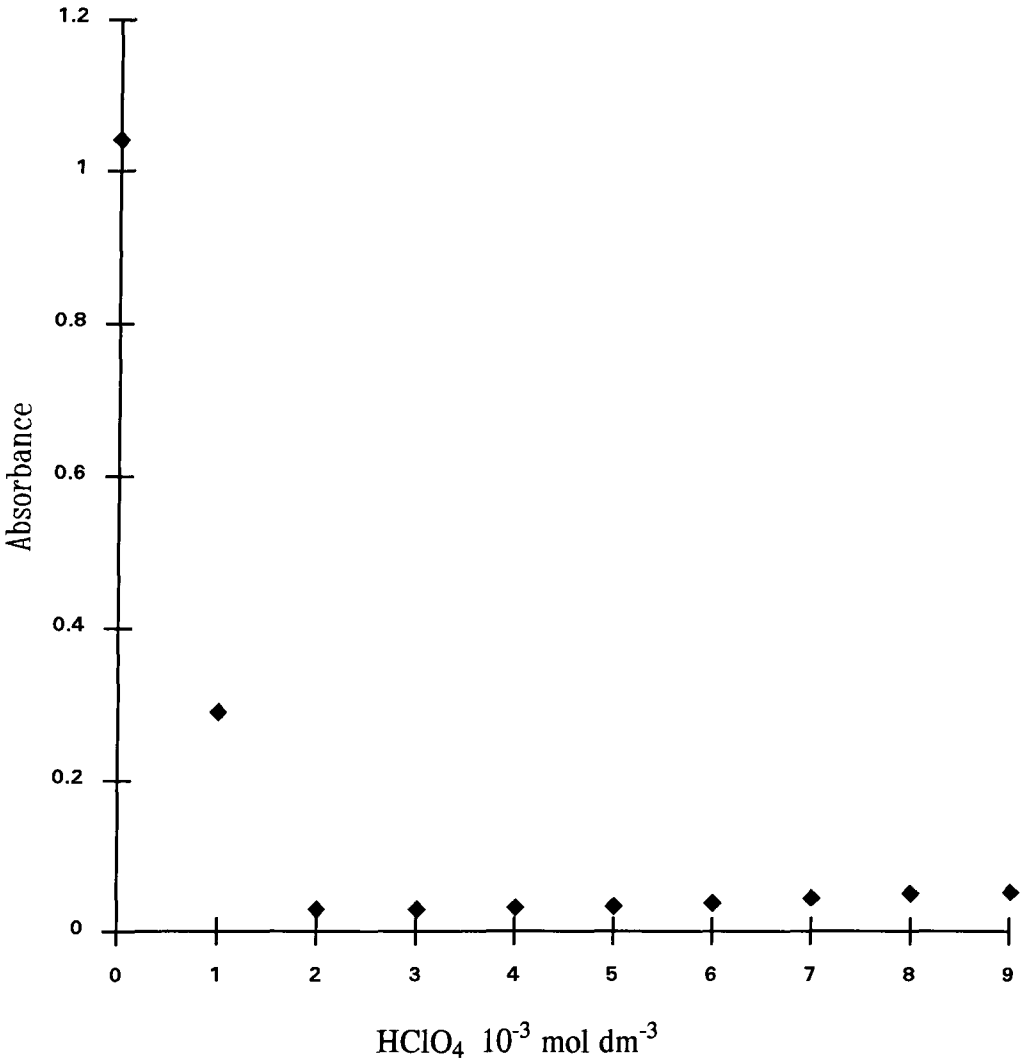

Measurements at 280nm gave more promising results as much higher concentrations of acid and HBIW could be used (table 2.2). On addition of 1 and 2 equivalents of acid two distinct decreases of absorbance were observed. Further additions of acid resulted in no noticeable change (fig.2.19). These results indicated two possibilities:-

i) HBIW was being diprotonated.

ii) These were the stages of gradual monoprotonation which seems to be complete by 2 equivalents of acid

A further experiment was carried out to help verify these observations. When $1x10^{-4}$M aliquots of acid are added to a $1x10^{-3}$M solution of HBIW in acetonitrile at 280nm the graph shown in fig.2.20 was obtained (values given in table 2.3).

Table 2.3

Absorbance Values For HBIW ($1x10^{-3}M$) At 280nm In Perchloric Acid

$10^3[HBIW]_{(stoich)}$ mol dm^{-3}	$10^4[HCLO_4]_{(stoich)}$ mol dm^{-3}	Absorbance 280nm	Absorbance 280nm*	[HBIW]/ $[HBIWH^+]$**	$[H+]_{free}$*** $/10^{-4}$	k_a $/10^4$
1.00	0.00	1.062	1.062			
0.99	0.99	0.964	0.974	10.7	0.14	1.6
0.98	1.96	0.872	0.890	4.98	0.32	1.6
0.97	2.91	0.782	0.806	3.02	0.50	1.5
0.96	3.85	0.699	0.728	2.08	0.73	1.5
0.95	4.76	0.617	0.650	1.50	0.96	1.4
0.94	5.66	0.538	0.570	1.09	1.16	1.3
0.93	6.54	0.460	0.492	0.80	1.37	1.1
0.93	7.41	0.382	0.412	0.58	1.52	0.9
0.92	8.26	0.308	0.335	0.41	1.74	0.7
0.91	9.09	0.225	0.248	0.26	1.87	0.5
0.90	9.91	0.168	0.186	0.174	2.24	0.4
0.89	10.70	0.105	0.118	0.089	2.53	0.2
0.88	11.50	0.060	0.068	0.034	3.00	0.1
0.88	12.30	0.028	0.032	-	-	-
0.87	13.00	0.030	0.034	-	-	-
0.86	13.80	0.030	0.035	-	-	-

* normalised for $1x10^{-3}M$ HBIW, to allow for dilution.

** $$\frac{HBIW}{HBIWH^+} = \frac{Abs.* - 0.034}{1.062 - Abs.*}$$

*** $$[H^+]_{free} = [HCLO_4]_{stoich} - [HBIWH^+]$$

Fig.2.20

Absorbance Plot

For HBIW ($1x10^{-3}M$)

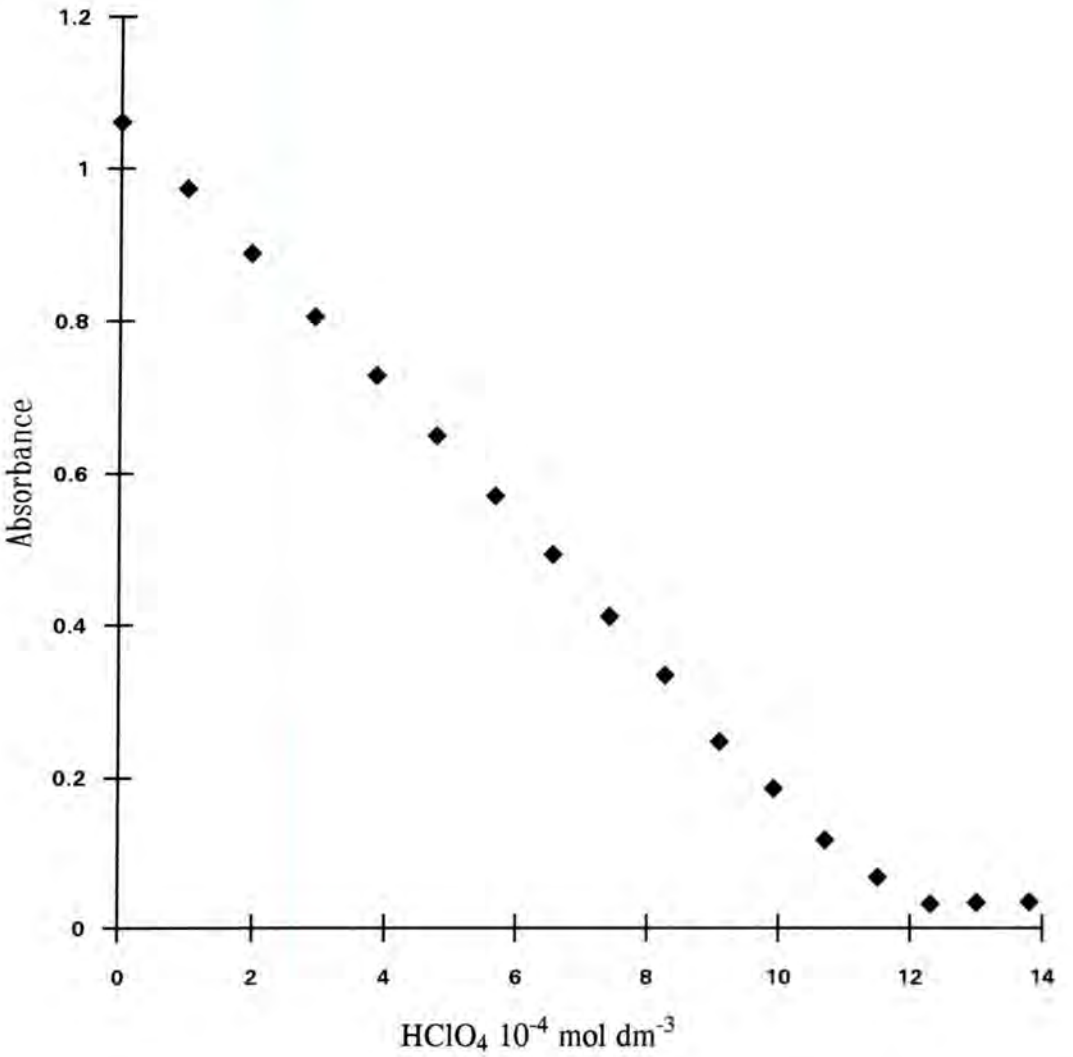

If monoprotonation is occurring then K the equilibrium constant should be a constant value irrespective of acid concentration. From the absorbance values it is possible to calculate the amounts of free HBIW and monoprotonated HBIW (referred to as $HBIWH^+$) at any point (scheme 2.1).

Scheme 2.1

$$HBIW + H^+ \Leftrightarrow HBIWH^+$$

$$K_a = \frac{[HBIW][H^+]}{[HBIWH^+]}$$

Absorbance of HBIW = 1.062

Absorbance of $HBIWH^+$ = 0.034

Assuming monoprotonation ratio of HBIW:$HBIWH^+$ is given by:-

$$\frac{HBIW}{HBIWH^+} = \frac{Abs.* - 0.034}{1.062 - Abs.*} \quad (1)$$

$$[HBIW]_{stoich} = [HBIW] + [HBIWH^+] = x \quad (2)$$

$$\frac{[HBIW]}{[HBIWH^+]} = y \quad (3)$$

From (2) and (3)

$$HBIWH^+ = \frac{x}{y+1}$$

$$[H^+]_{free} = [HCLO_4]_{stoich} - [HBIWH^+]$$

Table 2.3 gives the calculated values of the absorbance, free $[H^+]$, and K_a taking into account the dilution effect of the acid. The values of K_a are constant at low acid concentration but tend to decrease at higher acid concentrations. One problem with these results is that the acid concentrations used are necessarily very low so that any acidic or basic impurities in the solvent may affect the residual acidity of the solvent.

The results in table 2.3 show that the decrease in absorbance at 280nm is complete after the addition of 1.3 equivalents of acid, and that further increases in acid concentration cause no further spectral change. Clearly monoprotonation is occurring, however because of the spread of the values obtained for K_a it is only safe to set a lower limit on the pK_a value for HBIW of $pK_a \geq 4$.

It is of interest to compare this value with those obtained for hexamine (2.4). Measurements made in water have given values of 6.30 at 25°C[9], 5.18 at 45°C[10], 4.86 at 25°C[11] and most recently 4.89 at 25°C.[12]

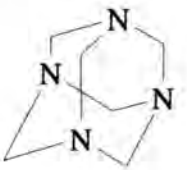

2.4

It seems likely that HBIW may be a weaker base than hexamine due to the presence of electron withdrawing phenyl groups. However there is evidence (Kolthoff *et al*[8]) that pK_a values are considerably higher in acetonitrile than in water. Values are typically 5pK units higher in the organic solvent. This derives partly from the much poorer solvation of protons in acetonitrile due to it being a much weaker base than water. Thus it seems probable the pK_a values of HBIW would be greater than the minimum value of 4 obtained here.

It is also worth pointing out that the results presented here do not rule out the possibility of diprotonation. Thus if the diprotonated form does not absorb at 280nm, then diprotonation would not be detectable by U.V. spectrophotometry.

2.7 Kinetics Of Decomposition

Following the very rapid decrease in absorbance (230-280nm) on addition of acid, an instantaneous process was observed resulting in an increase in absorbance. Kinetics were measured at 240nm with acid concentration in large excess of the HBIW concentration.

In general for the slower process reactions followed excellent first order kinetics with the rate constant of reaction being independent of HBIW concentration. However, in a number of cases (notably those at low acid concentration i.e. high water content) there was evidence for a biphasic reaction in which the initial reaction was followed by a very much slower second reaction; both of these reactions resulting in an increase in absorbance at 240nm.

Where the slower secondary reaction occurred the rate coefficients were determined for the initial reaction using infinity values obtained by linear extrapolation to zero time of absorbance time plots.

A point of interest was that in the presence of added water the values of the absorbance at 240nm at infinity were considerably reduced relative to those obtained where no water was added. This could possibly indicate a different decomposition pathway when water is present.

The results in tables 2.1-2.3 show that the value of k_{obs} increases with increasing acid concentration (fig.2.21). However the effects of added water are different at different acidities. Thus in solutions where $[HClO_4] < 0.04M$ values of k_{obs} increase with increasing water content of the solvent (fig. 2.22-2.24), while in more acidic solutions k_{obs} decreases with increasing water content (fig.2.25-2.27).

Table 2.4

Rate Constants For The Decomposition Of HBIW (9.7×10^{-5}M) In Acetonitrile/Water Containing Perchloric Acid

	$10^4 k_{obs}$ s^{-1}			
$10^3[HCLO_4]$ mol dm^{-3}	0.0% H_2O	0.50% H_2O	0.75% H_2O	1.00% H_2O
1	0.25	1.21	2.19	3.28
2	0.39	1.88	2.17	3.40
3	0.52	2.20	3.50	4.50
4	0.68	2.10	2.85	4.46
5	0.75	2.82	3.40	4.10
6	0.84	2.50	4.30	5.40
7	1.03	3.30	4.30	5.20
8	2.50	2.62	4.21	5.42
9	1.21	3.10	4.51	6.10

Table 2.5

Rate Constants For The Decomposition Of HBIW ($9.7x10^{-5}M$) In Acetonitrile/Water Mixtures Containing Perchloric Acid

	10^3 k_{obs} s^{-1}			
$10^2[HClO_4]$ mol dm^{-3}	0.0% H_2O	0.25% H_2O	0.50% H_2O	1.0% H_2O
1	0.11	0.16	0.22	0.51
2	0.25	0.28	0.36	0.58
4	0.53	0.60	0.69	-
5	0.73	0.45	0.53	-
6	0.81	0.46	0.39	-
7	0.91	0.48	0.44	0.19
8	1.15	0.74	0.46	0.05
9	1.28	0.87	0.45	-

Table 2.6

Rate Constants For The Decomposition Of HBIW ($9.7x10^{-5}M$) In Acetonitrile/Water Mixtures Containing Perchloric Acid

	10^2 k_{obs} s^{-1}			
$10^1[HClO_4]$ mol dm^{-3}	0.0% H_2O	0.25% H_2O	0.50% H_2O	1.0% H_2O
1	0.21	-	-	-
2	0.47	0.34	0.24	-
4	1.12	-	-	-
5	1.34	0.88	0.62	0.15
7	2.26	-	-	-

Fig. 2.21

Rate Constants For Decomposition Of HBIW ($9.7x10^{-5}M$)
In Acetonitrile Containing Perchloric Acid.

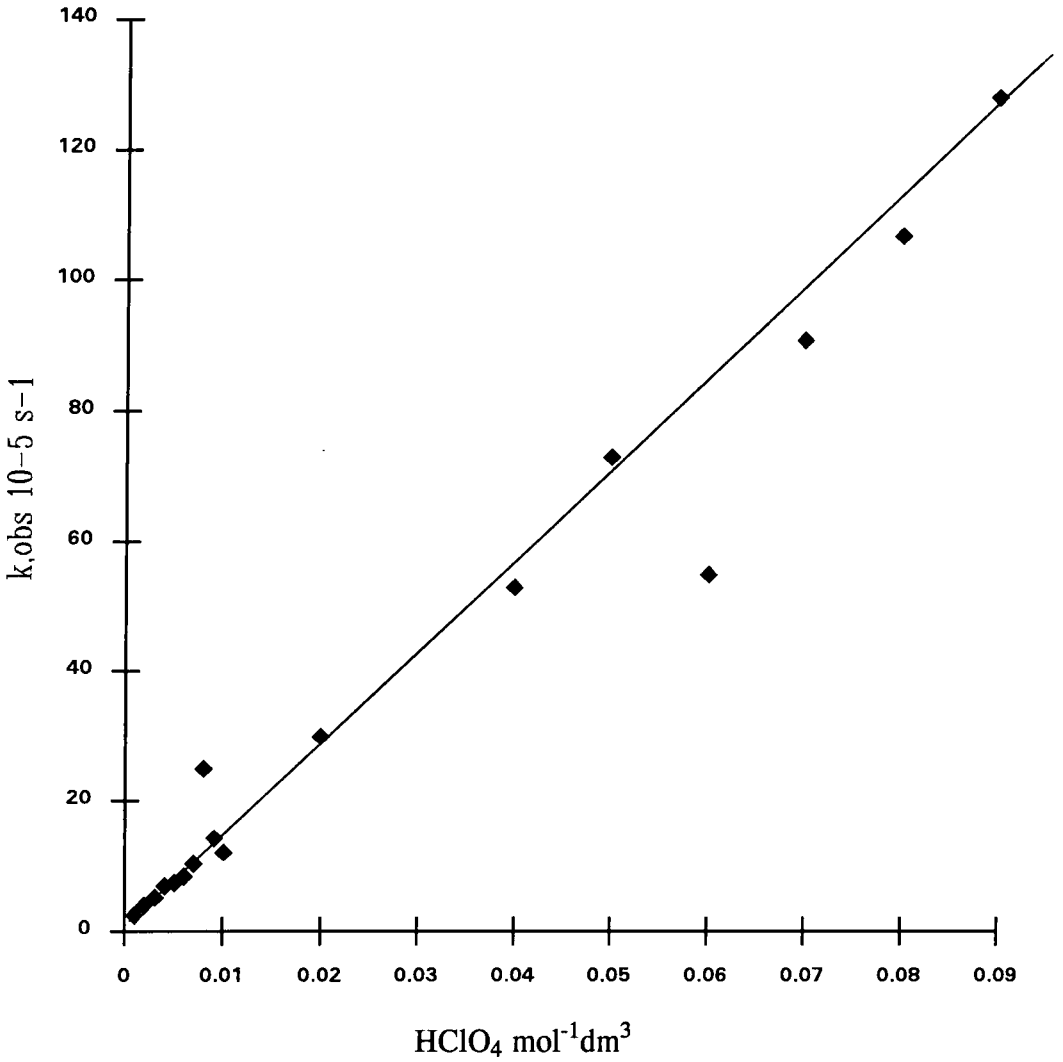

Fig. 2.22

Rate Constants For Decomposition Of HBIW ($9.7x10^{-5}M$)
In Acetonitrile Containing Perchloric Acid ($2x10^{-3}M$)

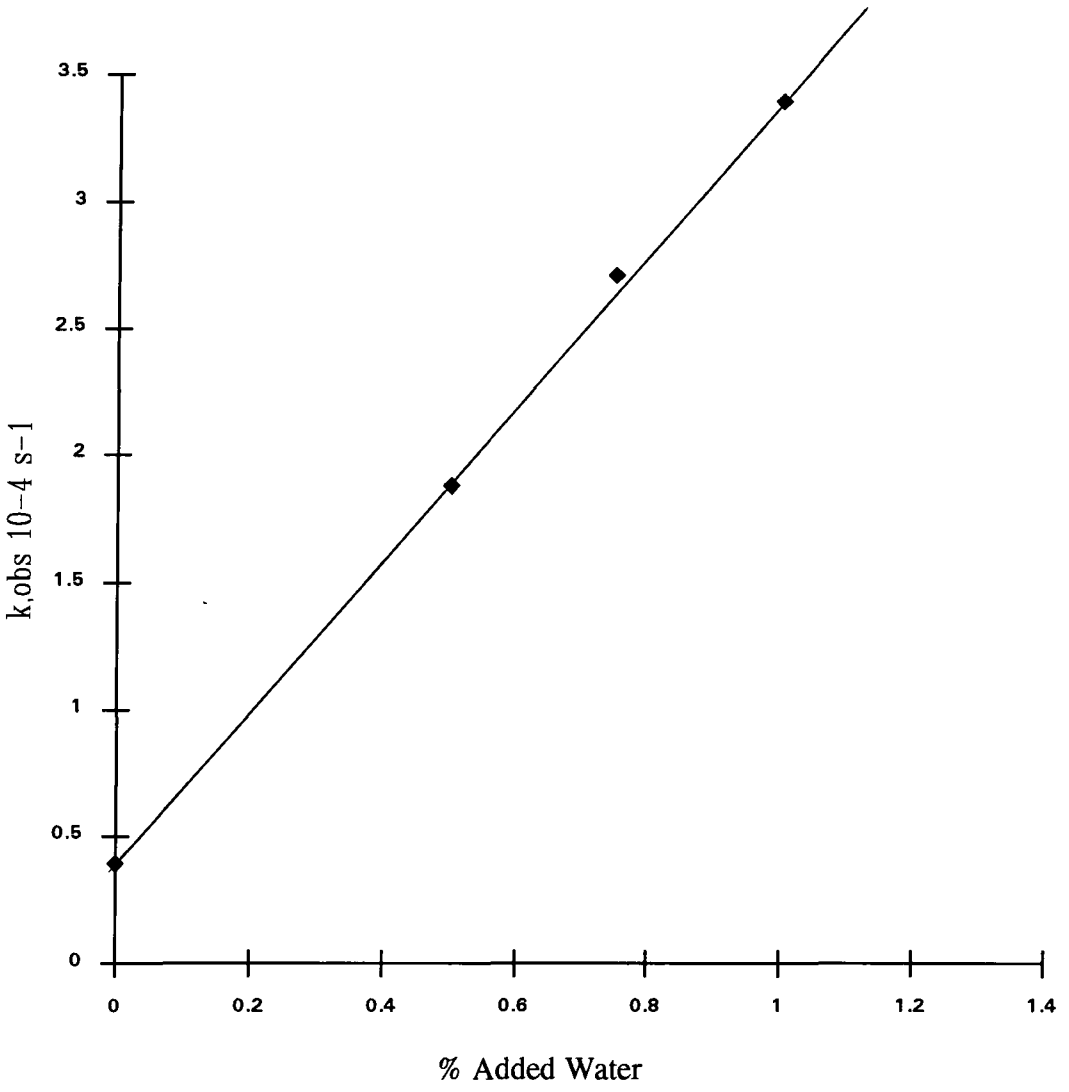

Fig. 2.23

Rate Constants For Decomposition Of HBIW ($9.7x10^{-5}M$)
In Acetonitrile Containing Perchloric Acid ($5x10^{-3}M$)

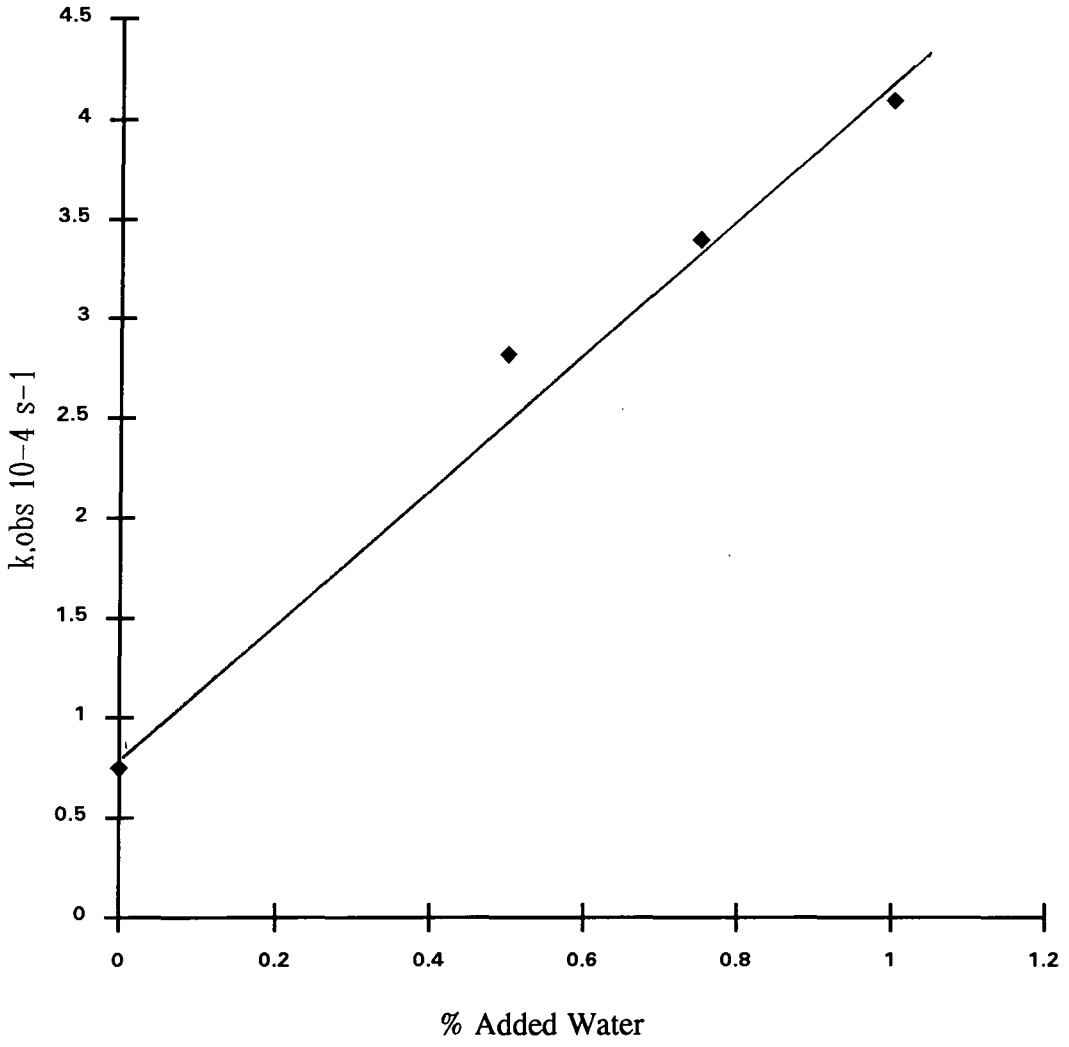

Fig. 2.24

Rate Constants For Decomposition Of HBIW ($9.7x10^{-5}M$)
In Acetonitrile Containing Perchloric Acid ($7x10^{-3}M$)

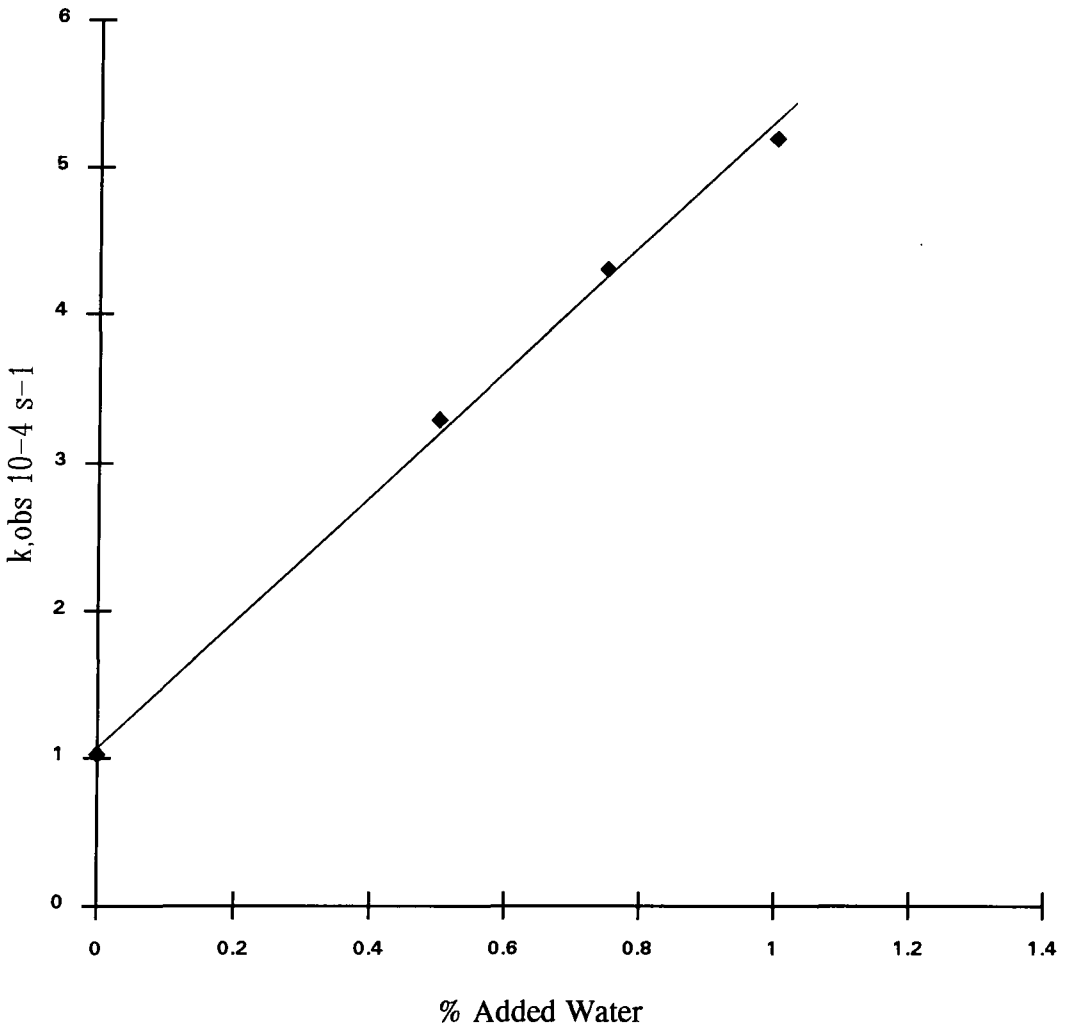

Fig. 2.25

Rate Constants For Decomposition Of HBIW ($9.7x10^{-5}M$)
In Acetonitrile Containing Perchloric Acid ($2x10^{-1}M$)

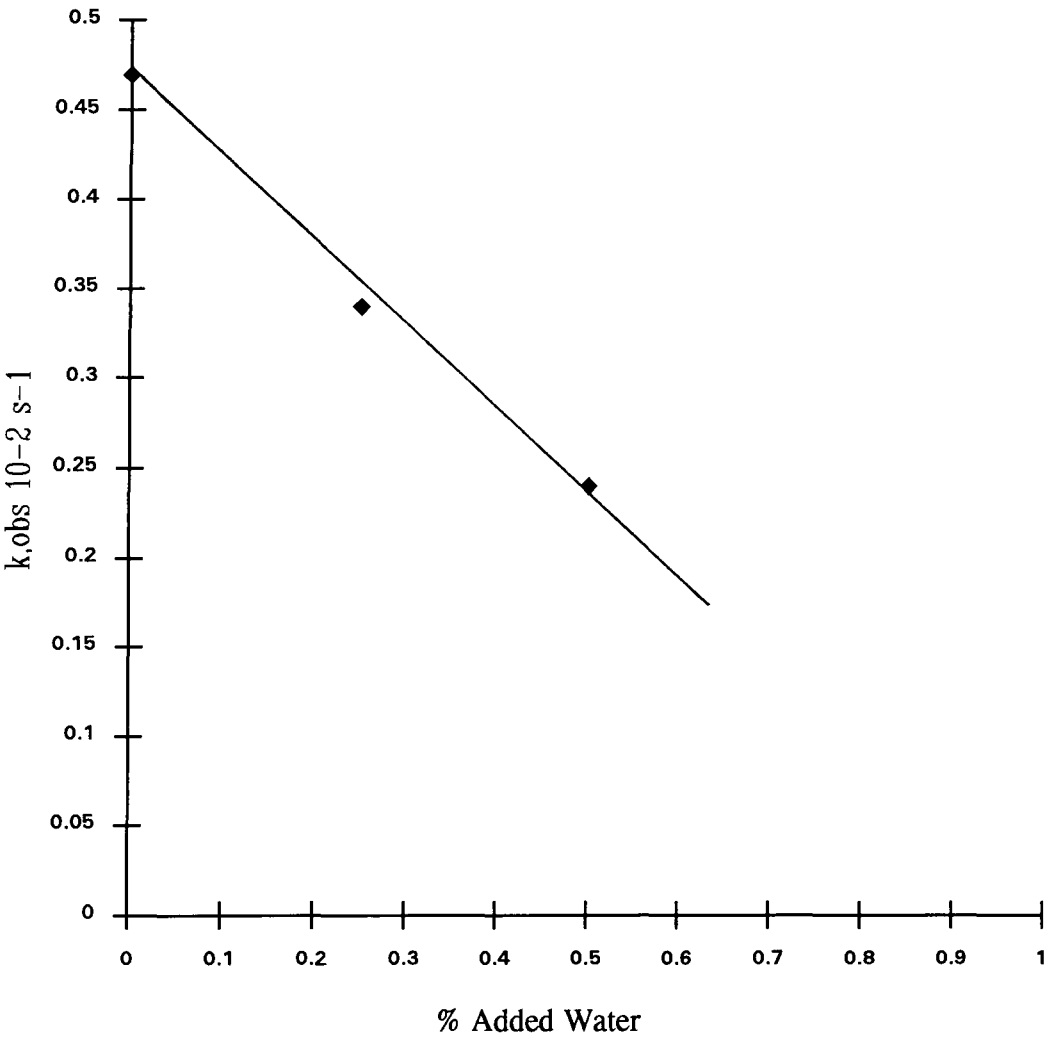

Fig. 2.26

Rate Constants For Decomposition Of HBIW ($9.7x10^{-5}M$)
In Acetonitrile Containing Perchloric Acid ($9x10^{-2}M$)

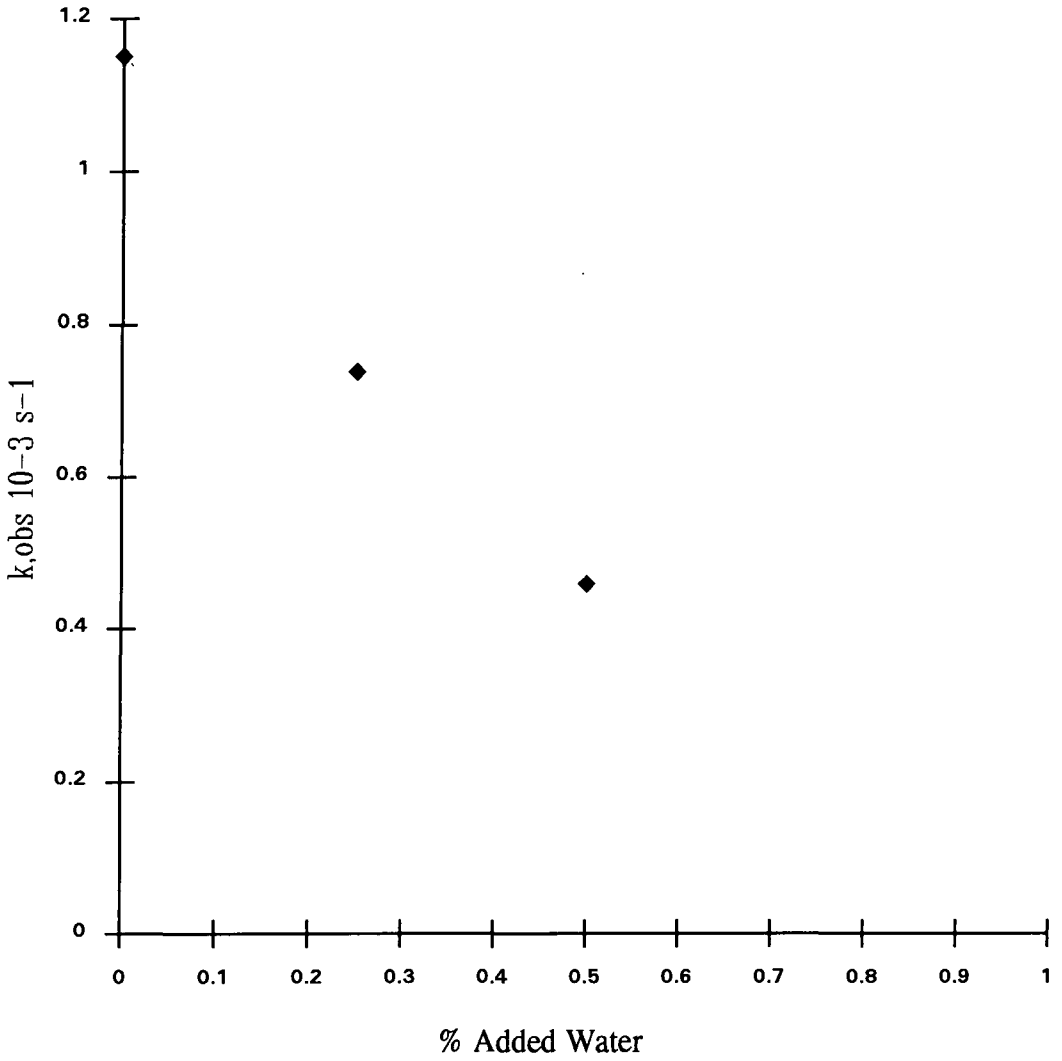

Fig. 2.27

Rate Constants For Decomposition Of HBIW ($9.7x10^{-5}M$)
In Acetonitrile Containing Perchloric Acid ($5x10^{-1}M$)

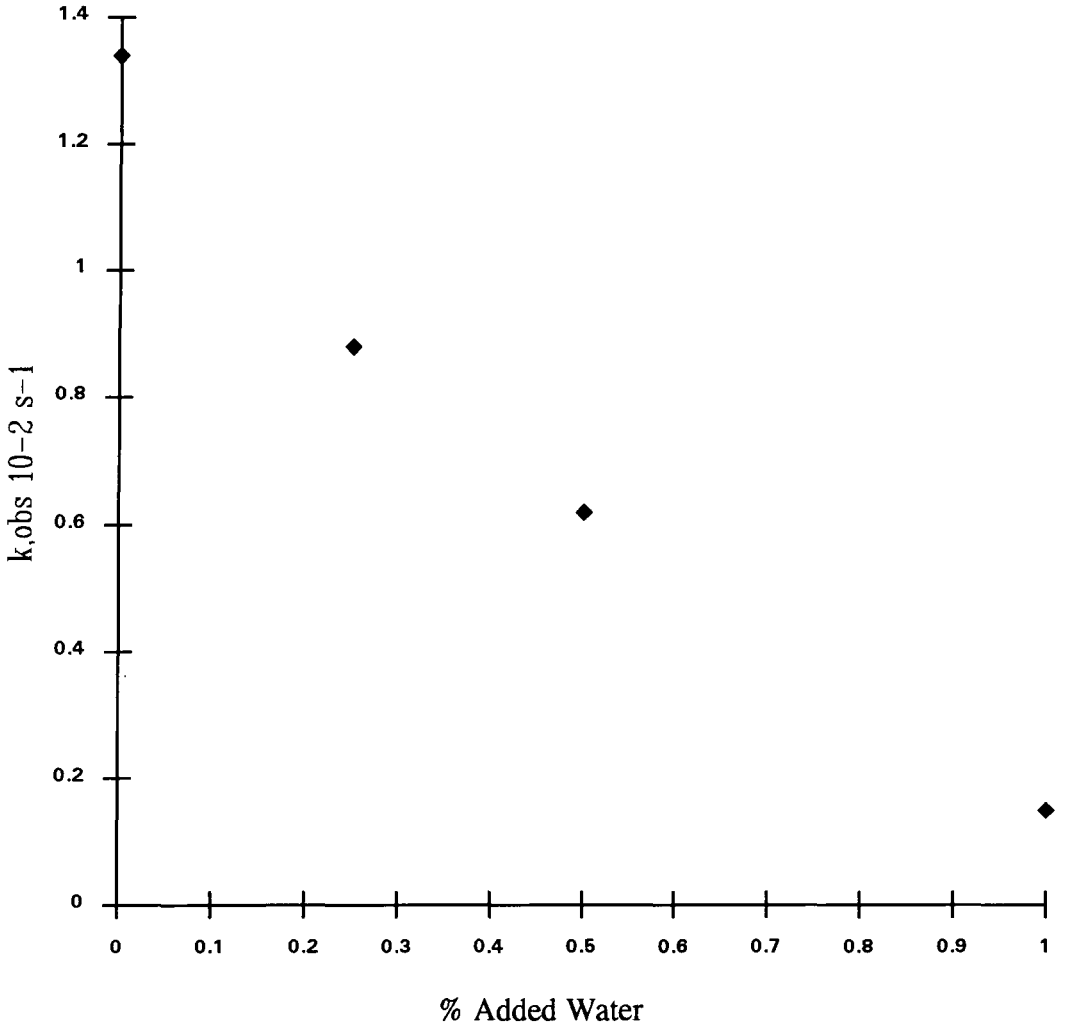

These changes are compatible with a scheme involving two competing reaction pathways (scheme 2.2).

Scheme 2.2

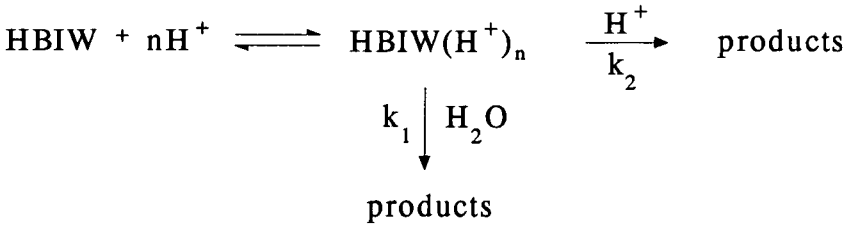

The initial equilibrium is written in terms of n protons. The U.V. measurements indicate that n must have a value of ≥1. The NMR spectra obtained in the presence of acid give clear evidence for successive monoprotonation and diprotonation. The NMR measurements in acetonitrile show that in the presence of two equivalents of perchloric acid HBIW is present largely in the diprotonated form.

Here it seems most likely that n=2, although the possibility that only monoprotonation occurs cannot be ruled out. the kinetic analysis does not depend on whether mono-or di-protonation occurs as long as the substrate is almost completely present in its protonated form. In that case k_{obs} is given by eqn. 2.2, showing

$$k_{obs} = k_1[H_2O] + k_2[H^+] \qquad \textbf{eqn. 2.2}$$

One pathway involves water catalysed decomposition of the protonated form, and a second pathway involves attack by acid on the protonated form. Analysis of the data in table 2.9 obtained in the absence of added water give a good fit with equation 2.2 with a value k_1 at 1% water of 2.5×10^{-4} s^{-1} and a value for k_2 of 0.012 dm^3 mol^{-1} s^{-1}. The value of k_1 obtained may be used to calculate a value for a second order rate constant of 4.5×10^{-4} dm^3 mol^{-1} s^{-1} (obtained by dividing k_1 by the molarity of water).

The variation of k_{obs} with added water can be explained in terms of equation 2.2.

Thus at low acid concentrations the first term in equation 2.2 is dominant so that k_{obs} increases with increasing water content in the solvent. At higher acid concentrations the second term of equation 2.2 is the more important one and the decrease in k_{obs} with added water may be explained by the decrease in the value of k_2 with increasing water. Before discussing the reason for this it is useful to consider possible mechanisms for the acid catalysed decomposition.

One possibility is rate determining attack by the acid on the protonated species. A second possibility for the acid catalysed pathway is equilibrium protonation, giving a low concentration intermediate, followed by rate determining decomposition (eqn.2.3).

$$\underset{2}{H^+ + HBIW(H^+)_n} \overset{K}{\rightleftharpoons} \underset{3}{HBIW(H^+)_{n+1}} \xrightarrow{k} \text{products}$$

eqn. 2.3

In the latter case k_2 is related to K and k by eqn.2.4

$$k_2 = \frac{kK}{1+K[H^+]} \qquad \textbf{eqn.2.4}$$

which is derived as follows :-

$$\text{Velocity} = k[3]$$

$$K = \frac{[3]}{[2][H^+]}$$

$$[2] + [3] + [\text{products}] = \text{constant}$$

$$[2] + K[2][H^+] + [\text{product}] = \text{constant}$$

$$[2](1 + K[H^+]) + [\text{product}] = \text{constant}$$

$$\frac{d[2](1 + K[H^+]}{dt} + \frac{d[\text{product}]}{dt} = 0$$

$$\frac{d[2](1 + K[H^+])}{dt} + kK[2][H^+] = 0$$

$$\frac{-d[2]}{dt} = \frac{kK[H^+]}{1 + K[H^+]}$$

$$k_{obs} = \frac{kK[H^+]}{1 + K[H^+]}$$

The data in table 2.7 show that k_2 does not decrease with increasing acid concentration. Hence if this is the mechanism then $K[H^+] << 1$. In fact k_2 tends to increase at high acidities and this may be due to the fact that here the acidities should be represented by an acidity function rather than the acid concentration.

Hence k_2 might reflect direct attack by the acid on protonated HBIW or equilibrium protonation followed by unimolecular decomposition. There is evidence[13] that with increasing water content in acetonitrile protons are stabilised by solvation. That is to say protons are better solvated by water than by acetonitrile. Hence the decrease in k_2, by either mechanism, with increasing water content in the solvent may be rationalised.

Table2.7

Rate Constants For The Decomposition Of HBIW ($9.7x10^{-5}M$) In Acetonitrile Containing Aqueous Perchloric acid

$[HCLO_4]$ mol dm^{-3}	$\%H_2O$ In Acid	Total[c] $\%H_2O$	10^5 k_{obs} s^{-1}	10^5 $k_2[H^+]$ [a]	10^2 k_2 $dm^3mol^{-1}s^{-1}$[b]
0.001	0.004	0.054	2.50	1.15	1.15
0.002	0.008	0.058	3.90	2.40	1.20
0.003	0.012	0.062	5.20	3.60	1.20
0.004	0.016	0.066	6.80	5.10	1.30
0.005	0.020	0.070	7.50	5.70	1.20
0.006	0.024	0.074	8.40	6.50	1.10
0.007	0.028	0.078	10.3	8.30	1.20
0.008	0.032	0.082	25.0	22.9	2.80
0.009	0.036	0.086	14.4	12.2	1.30
0.010	0.040	0.090	12.0	9.80	1.00
0.020	0.080	0.130	30.0	27.0	1.30
0.040	0.160	0.210	53.0	48.0	1.20
0.050	0.200	0.250	73.0	67.0	1.30
0.060	0.240	0.290	55.0	48.0	0.80
0.070	0.280	0.330	91.0	83.0	1.20
0.080	0.320	0.370	107.0	98.0	1.20
0.090	0.360	0.410	128.0	118.0	1.30
0.100	0.400	0.450	210.0	192.0	1.90
0.200	0.800	0.850	470.0	450.0	2.20
0.400	1.600	1.650	1050.0	1009.0	2.50
0.500	2.000	2.050	1340.0	1289.0	2.60
0.700	2.800	2.850	2260.0	2189.0	3.10

a) $k_2[H^+] = 10^5\ k_{obs}-k_1x\%H_2O$ from eqn. 2.2

b) $k_2 = (k_{obs}-k_1x\%H_2O)/[HCLO_4]$

c) Assuming acetonitrile contains 0.05% water.

d) $k_1 = 2.5x10^{-4}\ s^{-1}$ for 1% H_2O

The results suggest that the initial C-N bond breaking in HBIW is rate determining, and that the subsequent steps follow rapidly. Eventually HBIW breaks down completely and ammonium perchlorate crystals were isolated from the reaction mixture. It is of interest to speculate on the decomposition pathway. The water catalysed route may involve attack on an iminium ion intermediate[14] present in a low concentration in equilibrium with protonated forms. Possible structures for iminium ion intermediates for mono- and di-protonated species are shown in fig.2.28 and 2.29.

Fig.2.28

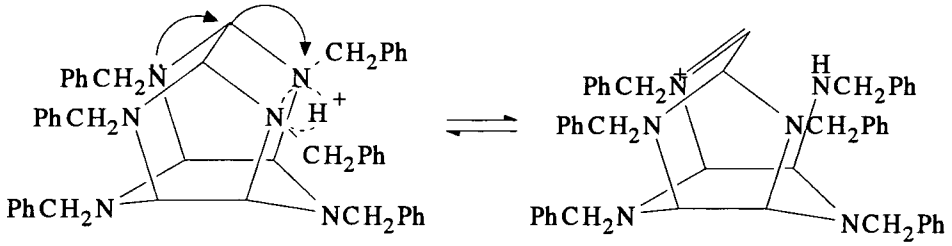

2.3

Fig.2.29

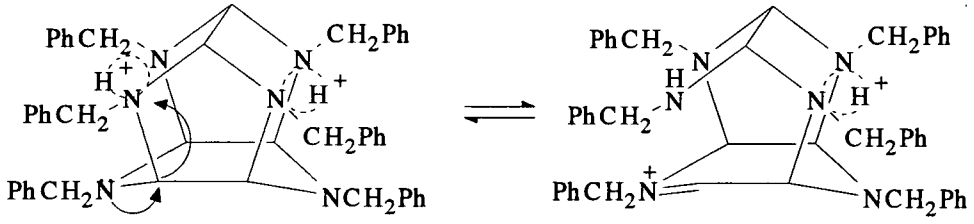

2.4

2.8 References

1. A. T. Nielsen, R. A. Nissan and D. J. Vanderah, *J. Org. Chem.*, 1990, 55, 1459.
2. (a) A. T. Nielsen, R. L. Atkins, D. W. Moore, R. Scott, D. Mallory and J. M. La Berge, *J. Org. Chem.*, 1973, 38, 3288. (b) A. T. Nielsen, R. L. Atkins, J. DiPol, D. W. Moore, *J. Org. Chem.*, 1974, 39, 1349.
3. E. M. Smolin and L. Rapoport, " The Chemistry Of Heterocyclic Compounds"; A. Weissberger Ed. Interscience, New York, Vol. 13, Chapter 9.
4. A. R. Katritzky, R.C. Patel and F. G. Ridell, *Angew, Chem., Int. Ed. Engl.* 1981, 20, 521.
5. I. M. Kolthoff, S. Bruckenstein and M. K. Chantooni Jr., *J. Am. Chem. Soc.*, 1961, 83, 3927.
6. M. R. Crampton , J. K. Scranage and P. Golding, *J. Chem. Research,* 1990, 6, 182.
7. M. R. Crampton J. K. Scranage and A. P. Cooney *J. Chem. Soc. Perkin Trans (ii),* 1989, 77.
8. J. F. Coetzee *Prog. Phys. Org. Chem.*, 1967, 4, 45.
9. R. Pummerer and J. Hofmann, *Ber. Dtsch. Chem. Res.*, 1923, 56, 1255.
10. H. Tada, *J. Am. Chem. Soc.*, 1960, 82, 255, 266.
11. L. Meurling, *Chem. Scr.*, 1975, 7, 23.

Chapter 3

Synthesis Of Hexabenzylhexaazaisowurtzitane (HBIW) And Derivatives

3.1 Introduction

It was found that condensation of glyoxal and benzylamine leads to a new polyazapolycyclic compound known as 2,4,6,8,10,12-hexabenzyl-2,4,6,8,10,12-hexaazatetracyclo [5.5.0.$0^{5,9}$. $0.^{3,11}$] dodecane or more trivially as HBIW (3.1a). Similarly reaction of seven substituted benzylamines gave corresponding structures (eqn.3.1).

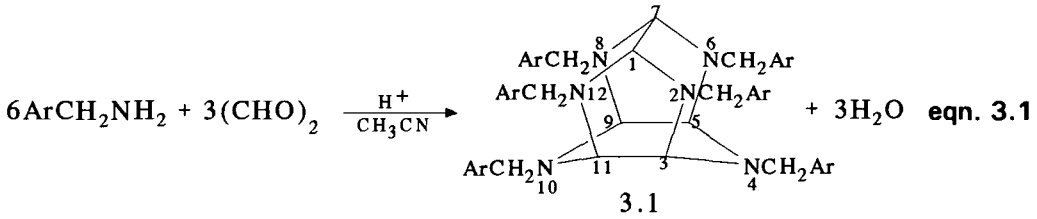

3.1

3.1a,	$Ar = C_6H_5$	3.1f,	$Ar = 2\text{-}BrC_6H_5$
3.1b,	$Ar = 2\text{-}ClC_6H_5$	3.1g,	$Ar = 2\text{-}FC_6H_5$
3.1c,	$Ar = 4\text{-}ClC_6H_5$	3.1h,	$Ar = 2\text{-}MeOC_6H_5$
3.1d,	$Ar = 2\text{-}CH_3C_6H_5$	3.1i,	$Ar = 4\text{-}ClC_6H_{5(D_{12})}$
3.1e,	$Ar = 4\text{-}CH_3C_6H_5$	3.1j,	$Ar = C_6H_{5(D_{12})}$

The compound is described as an isowurtzitane derivative due to its close relationship to wurtzitane (tetracyclo [5.3.1.$1^{2,6}$.0.^{4,9}] dodecane (3.2).[1,2] These isomeric cages have the same adjacent grouping of atoms consisting of six methylene bridges, six methines at bridgeheads and three CHCH groups bonded through the methylenes. The wurtzitane structure contains five six-membered rings while the related isowurtzitane structure has two five-membered rings, two seven-membered rings and one six-membered ring. The hydrocarbon wurtzitane is known but the parent hydrocarbon isowurtzitane is not (3.3).

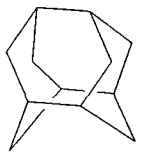

3.2

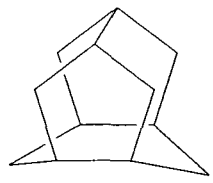

3.3

The caged compound (3.1) is unusual in that all the endocyclic nitrogens are at bridges and none at bridgeheads as in hexamethylenetetramine (3.4)

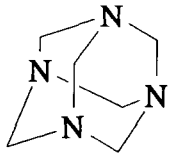

3.4

Wurtzitanes have been known since 1974[3,4] and derivatives incorporating a ring hetero atom have been synthesised by Ganter and co-workers (3.5)[5] and Hamon and co-workers (3.6).[6]

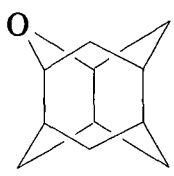

3.5

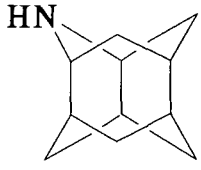

3.6

More recently wurtzitanes incorporating more than one ring hetero atom (3.7) within the ring have been synthesised by Nielsen and co-workers.[7]

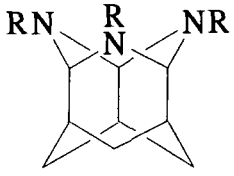

3.7

a, R = CH_3

b, R = C_2H_5

c, R = $C_6H_5CH_2$

d, R = 4-$CH_3OC_6H_4CH_2$

Primary amines and anilines react with glyoxal to give either dicarbinolamines or diimines.[8-12] Certain aryl amines notably aniline and 2-chloroaniline give either 1,2-diimines, dicarbinolamines or tri and tetraaminoethane derivatives depending on the stoichiometry of reactants and solvent composition.[9]

The condensation of benzylamine with glyoxal had not been reported before the commencement of this work although Nielsen and co-workers[13] showed in 1990 that formation of 3.1 was possible. In the same year Boyer and co-workers[14] synthesised a tetraoxaisowurtzitane (4,10,-Dinitro-4,10-diaza-2,6,8,12-tetraoxatetracyclo [5.5.0.$0^{5,9}$.$0^{3,11}$]-dodecane (3.9). The synthesis involved two steps, starting with the condensation of formamide with glyoxal at pH 8-9 (sodium bicarbonate buffer) to yield *trans*, *trans*-1,4-diformyl-2,3,5,6-tetrahydroxypiperazine (3.8). Conversion of 3.8 to 3.9 occurs by addition of a mixture of 3.8 and glyoxal to sulphuric acid at 0^0C, followed by addition of nitric acid to produce 3.9 in 92% yield (scheme 3.1). The mechanism of formation of 3.9 is unknown.

Scheme 3.1

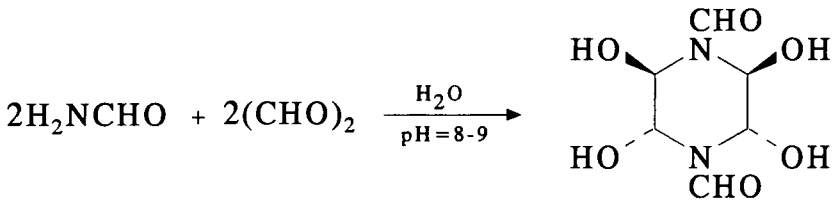

3.8

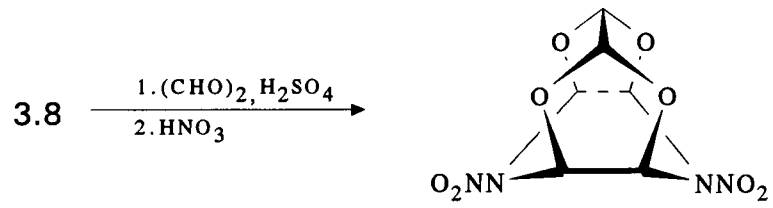

3.9

It is known that α-methyl and α,α-dimethyl benzylamines react with glyoxal to produce stable diimines and not isowurtzitane derivatives.[11,12]

Ethylenediamine and N,N'-disubstituted ethylenediamines react with glyoxal to give cis and trans-1,4,5,8-tetraazadecalins and 2,2'-biimidazolidines.[15-17] However, in one instance condensation of ethylenediamine with glyoxal led to the isolation of a tetraazadioxa caged compound also an isowurtzitane derivative (3.10).[18,19]

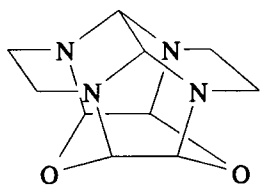

3.10

3.2 Synthesis Of HBIW (3.1a)

HBIW (3.1a) can be prepared in a facile manner by condensation of benzylamine in a 2:1 molar ratio in acetonitrile containing a catalytic amount of acid. The reaction is usually complete within a few hours. The HBIW (3.1a) precipitates out of the reaction mixture and can be obtained by filtration and washing. Initially HBIW (3.1a) was prepared by a procedure which will be denoted as 1. Procedure 1 gave poor yields of 3.1a so a second procedure denoted as 2 was employed to optimise the yield of 3.1a. Best yields were obtained when benzylamine was added over a 40 min. period. Ten phenyl-substituted derivatives were prepared by procedure 2. Full details are given in the experimental section at the end of this chapter.

The effects of acid catalyst and temperature on the yield of 3.1a was studied. Results are given in tables 3.1-3.3. The highest yield of 3.1a was 67% (pure) at 25^{0}C

Table 3.1
Effects Of Acid Catalysts On The Yield
Of HBIW At <16^{0}C

	% YIELD OF HBIW (PURE)							
Acids	Acid/μl	100	150	200	250	300	350	400
HNO_3[a]		29	35	39	45	50	54	60
H_2SO_4[b]		26	30	35	40	44	48	52
HCl[c]		28	32	36	43	47	51	56
HCOOH[d]		23	26	28	30	30	30	30
CH_3COOH[e]		23	27	29	31	30	31	31
$HCLO_4$[f]		25	29	34	38	41	46	51

Table 3.2
Effects Of Acid Catalysts On The Yield Of
HBIW At Room Temperature (25^{0}C)

	% YIELD OF HBIW (PURE)				
Acids	Acid/μl	100	200	300	400
HNO_3[a]		36	43	55	67
H_2SO_4[b]		27	32	37	46
HCl[c]		32	39	40	59
$HCLO_4$[d]		27	33	40	48

Table 3.3
Effects Of Acid Catalysts On The Yield Of HBIW At 35^{0}C.

Acids	%YIELD OF HBIW (PURE)				
	Acid/μl	100	200	300	400
HNO_3[a]		34	41	52	65
H_2SO_4[b]		28	31	36	41
HCl[c]		30	36	44	56
$HCLO_4$[d]		29	30	38	45

Similarly 2 and 4-chlorobenzylamines when reacting with glyoxal gave initially low yields of 3.1b and 3.1c respectively. Tables 3.4 and 3.5.give yields of 3.1b and 3.1c when reaction conditions were optimised.

Table 3.4
Effects Of Acid Catalysts On The Yield Of 4-Chloro HBIW At 25^{0}C

Acids	%YIELD OF 4-CHLORO DERIVATIVE (PURE)				
	Acid/μl	100	200	300	400
HNO_3[a]		4	10	14	20
HCl[c]		3	7	11	16
HCOOH[d]		-	3	6	11

Table 3.5
Effects Of Acid Catalysts On The Yield Of 2-Chloro HBIW At 25^{0}C

Acids	%YIELD OF 2-CHLORO DERIVATIVE (PURE)				
	Acid/μl	100	200	300	400
HNO_3[a]		3	8	12	15
HCl[c]		3	5	9	11
HCOOH[d]		-	2	5	8

Table 3.6
Effects Of Acid Catalysts On The Yield Of HBIW At 25^0C

Amount of HNO_3 added μl	%Yield of Pure HBIW
450	60
500	55
550	51
600	46
700	39
800	33
900	29
1000	26

a) 70%; *b*) 98%; *c*) 37.5% w/w; *d*) 96%; *e*) 98%; *f*) 70%
All acids were of analytical grade.

It was also found that using an excess of benzylamine did not result in an increase in yield nor did increasing the amount of acid catalyst above the its optimum amount (400μl). On the contrary increasing the amount of acid catalyst above its optimum resulted in a decrease in yield (table 3.6). Table 3.7 gives yields of isowurtzitane derivatives 3.1a-j using procedure 2.

Table 3.7
Characterisation Data For Compounds 3.1a-j

Deriv. 3.1	Phenyl Sub.	M.P°C	Yield %	Mr.	Molecular formula	Calculated C	Calculated H	Calculated N	Found C	Found H	Found N
a	H	152-153	67	708.91	$C_{48}H_{48}N_6$	81.32	6.83	11.86	81.37	6.77	11.80
b	2-Cl	180-182	15	915.63	$C_{48}H_{42}N_6Cl_6$[a]	62.90	4.58	9.17	62.88	4.49	9.14
c	4-CL	188-191	20	915.63	$C_{48}H_{42}N_6Cl_6$[b]	62.90	4.58	9.17	62.85	4.50	9.10
d	2-Me	201-203	45	793.11	$C_{54}H_{60}N_6$	81.70	7.56	10.59	81.61	7.48	10.41
e	4-Me	172-174	62	793.11	$C_{54}H_{60}N_6$	81.70	7.56	10.59	81.64	7.52	10.51
f	2-Br	209-210	22	1182.36	$C_{48}H_{42}N_6Br_6$[c]	48.71	3.55	7.10	48.68	3.50	7.05
g	2-F	124-126	33	816.90	$C_{48}H_{42}N_6F_6$[d]	70.50	5.14	10.28	70.44	5.10	10.20
h	2-MeO	134-136	28	889.11	$C_{54}H_{60}N_6O_6$	72.88	6.74	9.44	72.81	6.70	9.39
i	4-$Cl(d_{12})$	190-192	10	927.63	$C_{48}H_{30}D_{12}Cl_6N_6$	62.09	-	9.05	62.01	-	9.00
j	$H(d_{12})$	145-147	43	720.91	$C_{48}H_{36}D_{12}N_6$	79.89	-	11.65	79.81	-	11.58

a) Calc. for Cl=23.26%, found 22.57. (b) Calc. for Cl=23.26%, found 22.97. (c) Calc. for Br=40.59%, found 39.21. (d) Calc. for F=13.95%, found 13.34. (e) Calc. for Cl=22.96%, found 22.05.

It was also found that 3.1 could also be generated from 1,4-dioxane-2,3-diol (3.11) (eqn. 3.2) which is the hemiacetal derivative of glyoxal. This is a useful precursor as it does not require the 40% solution of glyoxal.[20] However, the yields of 3.1 were found to be very much lower (12-26%).

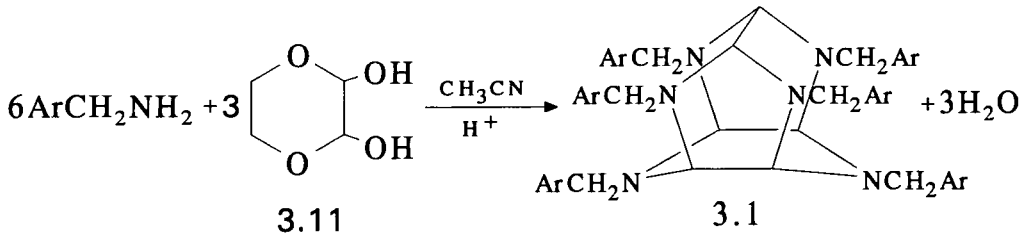

3.11 3.1

eqn. 3.2

3.2.1 N.M.R. Spectra

The ^1H NMR spectra of the purified products were measured in deuteriochloroform, in which they were very soluble. Other possible solvents were deuteriated dichloromethane, acetone, benzene or dimethyl sulphoxide. However, the highest solubility was in deuteriochloroform which also facilitated ^{13}C NMR spectra.

Data was collected in table 3.8 and representative spectra are in figures 3.1-3.7. The assignments of bands was aided by comparison with spectra of HBIW derivatives 3.1i and 3.1j (fig. 3.8 and 3.9) obtained using deuteriated benzylamines ($PhCD_2ND_2$) (fig. 3.10).

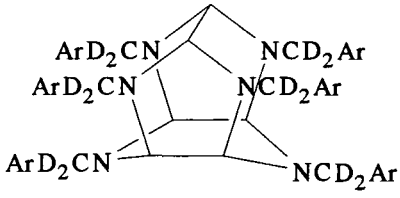

fig. 3.10

3.1j, Ar = C_6H_4Cl
3.1j, Ar = C_6H_4

These spectra show singlets due to methine protons at δ3.55 (2H) and 4.06 (4H) for 3.1i and for 3.1j at δ3.57 (2H) and 4.16 (4H). These characteristic signals also occur, of course, in the derivatives prepared from non-deuteriated benzylamines. These spectra also show bands due to methylene protons of the benzyl groups. The four benzyl groups in the five-membered rings give an AB quartet (J = 13Hz) representing eight protons. The coupling is typical of that expected for geminal hydrogens. The two benzyl groups in the six-membered ring give a singlet representing four protons. The coupling is seen more clearly in spectra at higher fields as shown in fig.3.11 and 3.12.

Nielsen[13] attributed the signals at δ4.16 to methylene hydrogens and that at δ 4.03 to methine hydrogens in 3.1a. The work repeated here using deuteriated benzylamine shows that this is incorrect and the assignments should be reversed.

The spectra of the phenyl ring hydrogens in 3.1 absorb at *ca* δ7.17, at similar positions to those of the parent benzylamine. The methylene hydrogens are found to appear slightly up field in the parent benzylamine than those in 3.1a. Spectra of the parent benzylamine for 3.1a is shown in fig. 3.13.

Table 3.8

NMR Data For Compounds 3.1a-j

Compound 3.1	Phenyl Subst.	Solvent	Phenyl Protons[a]	Benzyl CH_2[c]	Methine CH[c]	Phenyl Subst.
a	H	$CDCl_3$	7.17-7.25	4.03(4H) 4.08(8H)[b]	3.57(2H) 4.16(4H)	-
b	2-Cl	$CDCl_3$	6.71-7.48	4.24(4H) 4.16(8H)[b]	3.57(2H) 4.29(4H)	-
c	4-Cl	$CDCl_3$	6.97-7.27	3.89(4H) 3.99(8H)[b]	3.55(2H) 4.06(4H)	-
d	2-Me	$CDCl_3$	6.38-7.23	4.10(4H) 3.99(8H)[b]	3.49(2H) 4.24(4H)	Me 2.35(12H) 2.27(6H)
e	4-Me	$CDCl_3$	7.03-7.24	3.97(4H) 4.01(8H)[b]	3.51(2H) 4.10(4H)	Me 2.33(12H) 2.32(6H)
f	2-Br	$CDCl_3$	6.68-7.54	4.26(4H) 4.19(8H)[b]	3.56(2H) 4.33(4H)	
g	2-F	$CDCl_3$	6.92-7.32	4.09(4H) 4.07(8H)[b]	3.66(2H) 4.19(4H)	
h	2-MeO	$CDCl_3$	6.70-7.47	4.12(4H) 4.02(8H)[b]	3.59(2H) 4.21(4H)	MeO 3.73(12H) 3.76(6H)
i	4-Cl(d12)	$CDCl_3$	7.27-7.01	- -	3.55(2H) 4.06(4H)	
j	H(d12)	$CDCl_3$	7.19-7.25	- -	3.57(2H) 4.16(4H)	

a) Range of chemical shifts

b) Centre of AB quartet (J=13Hz).

c) Assignments confirmed by specific deuteration experiments.

Fig. 3.1

^{1}H NMR Spectrum Of 3.1a

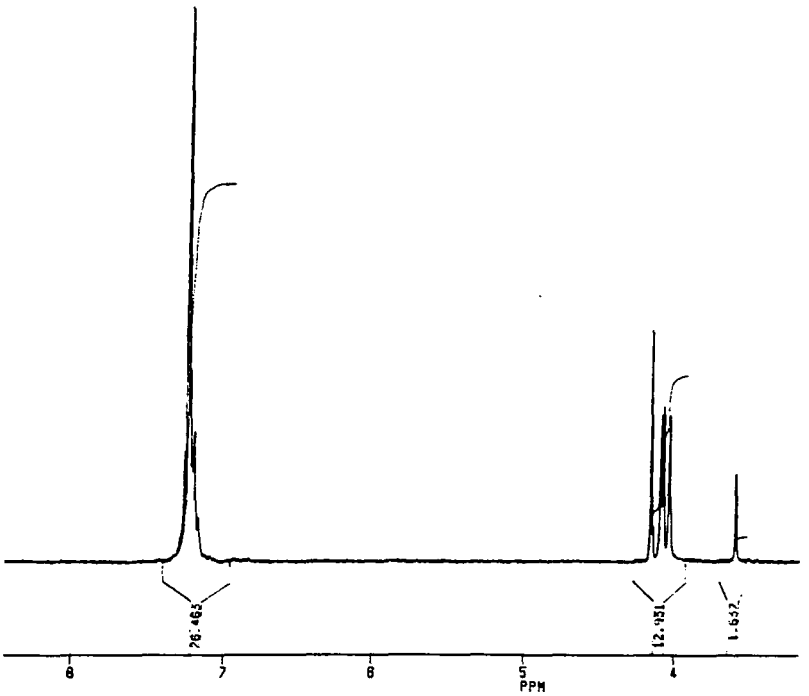

Fig. 3.2

^{1}H NMR Spectrum Of 3.1c

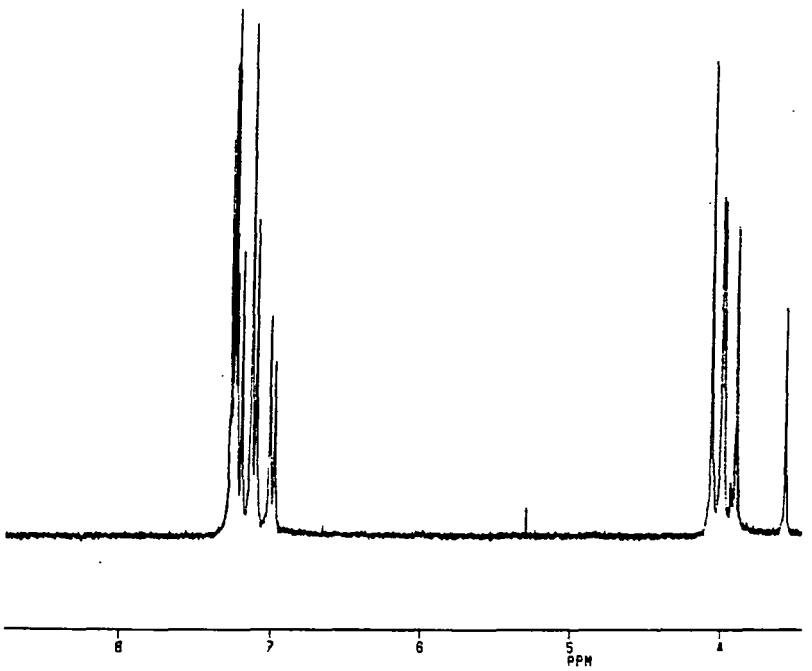

Fig.3.3

^{1}H NMR Spectrum Of 3.1d

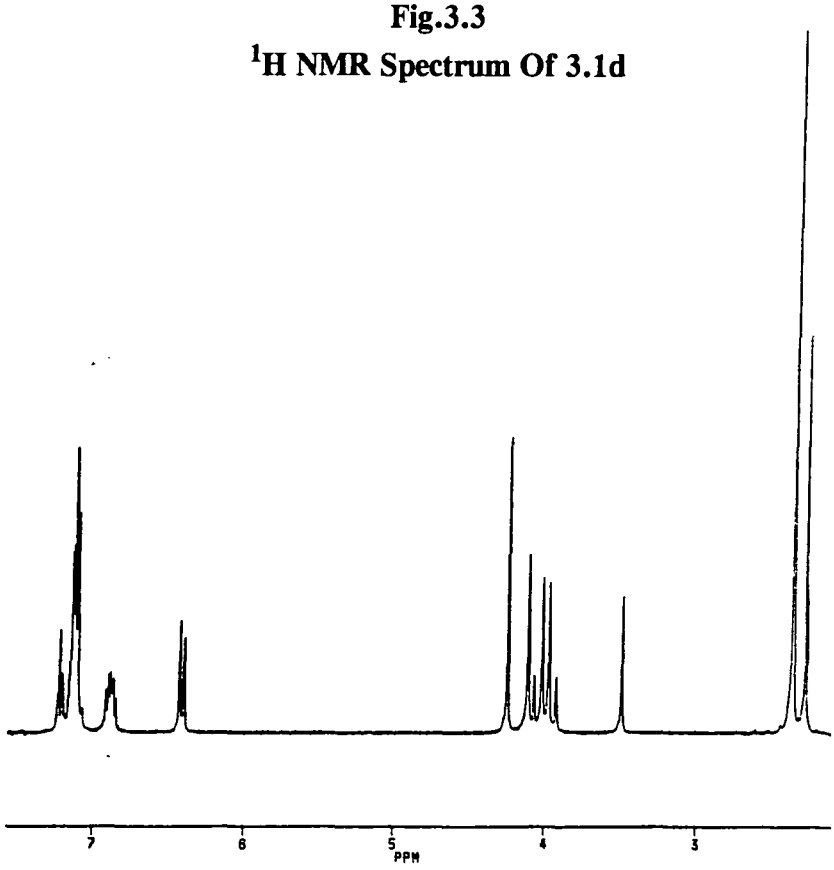

Fig. 3.4

^{1}H NMR Spectrum Of 3.1f

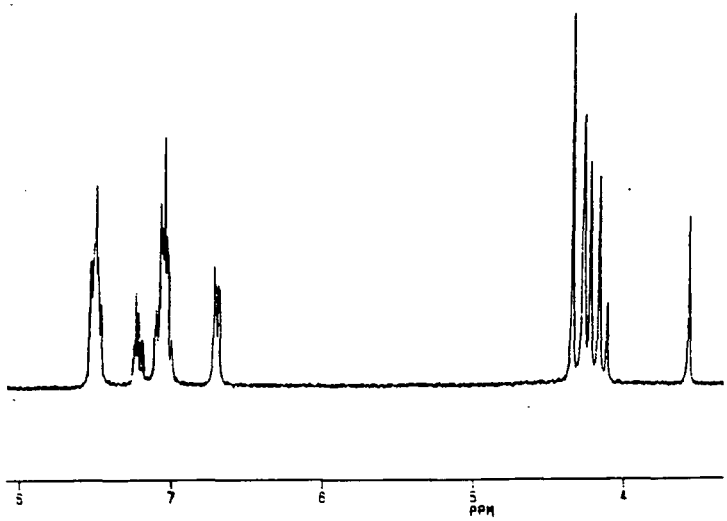

Fig. 3.5

^{1}H NMR Spectrum Of 3.1g

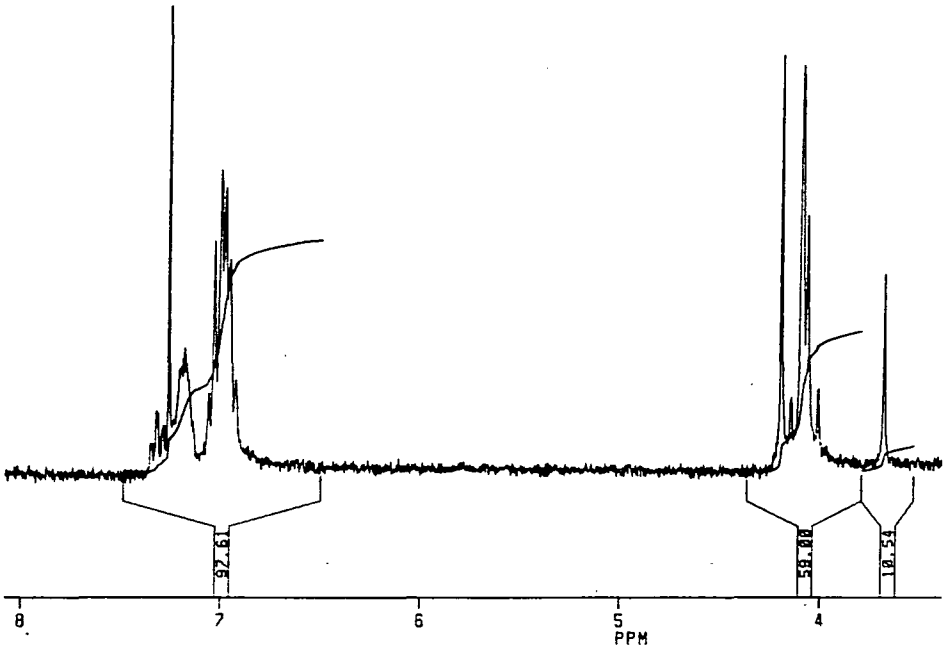

Fig. 3.6

^{1}H NMR Spectrum Of 3.1h

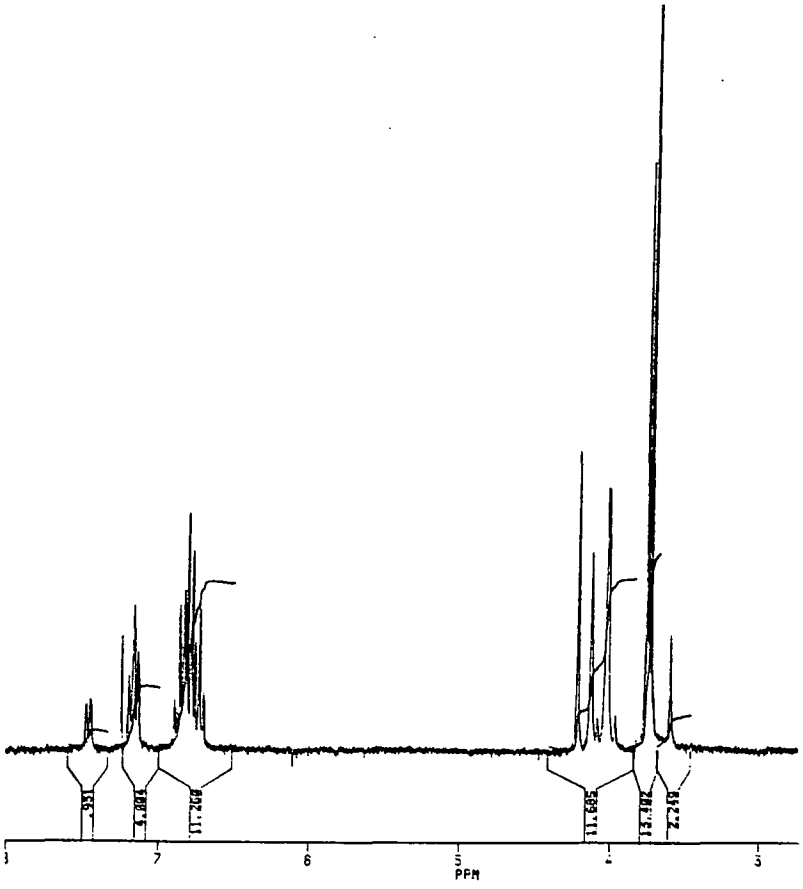

Fig. 3.7

^{1}H NMR Spectrum Of 3.1i

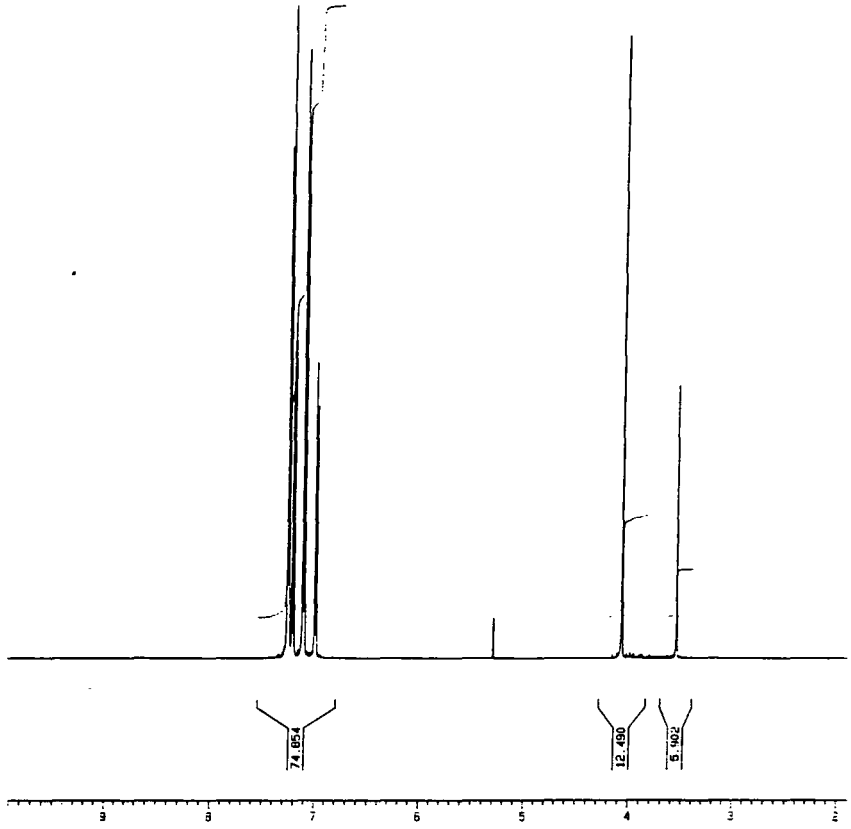

Fig. 3.8

^{1}H NMR Spectrum Of 3.1j

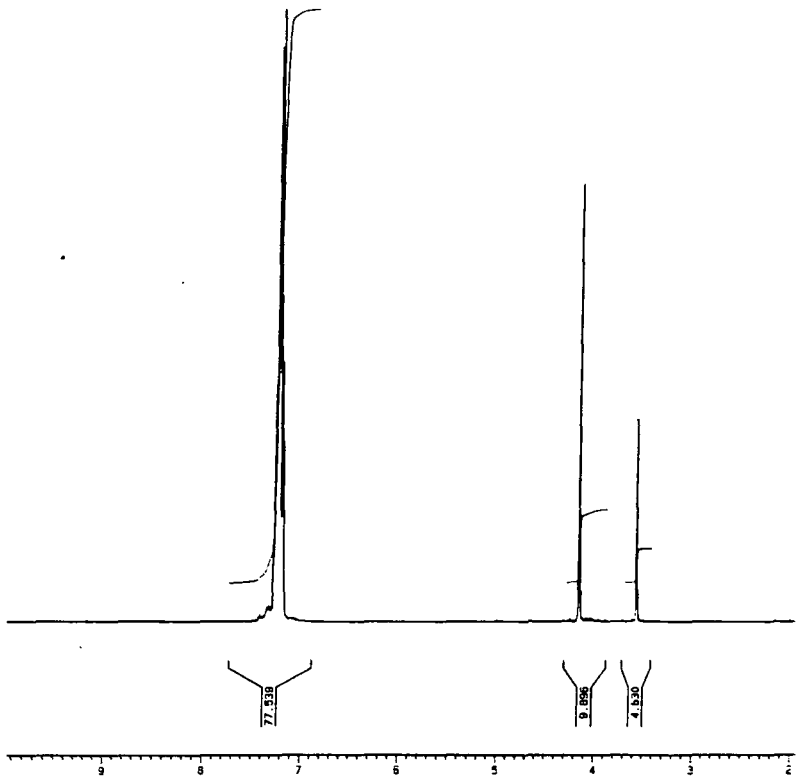

Fig. 3.9

^{1}H NMR Spectrum Of 3.1e

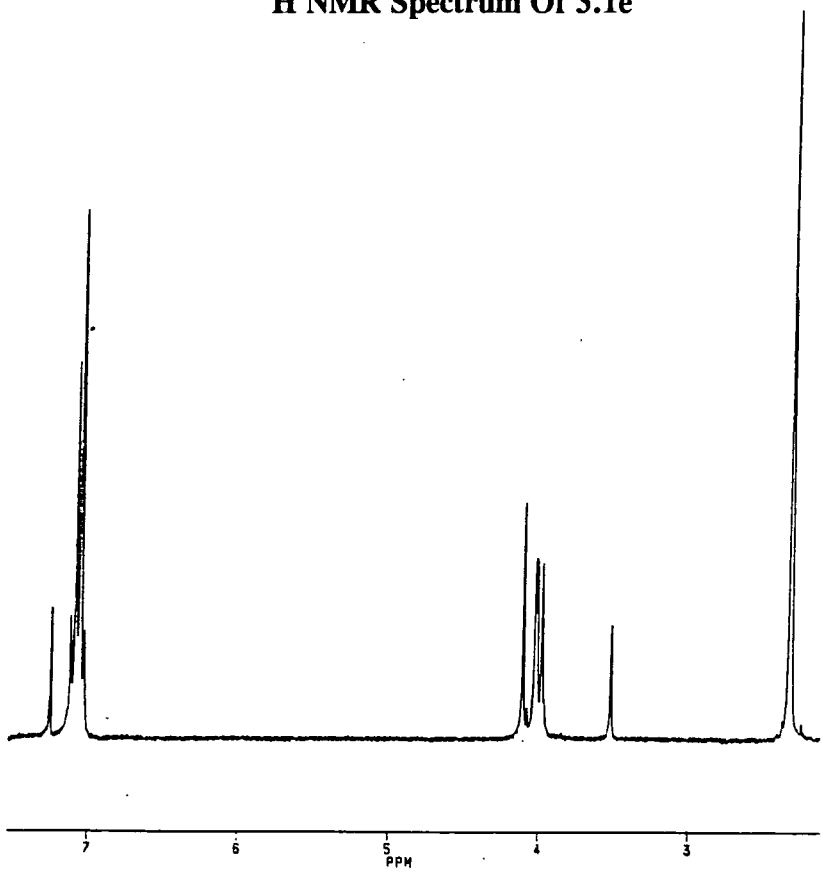

Fig. 3.10

^{1}H NMR Spectrum Of 3.1a (500MHz)

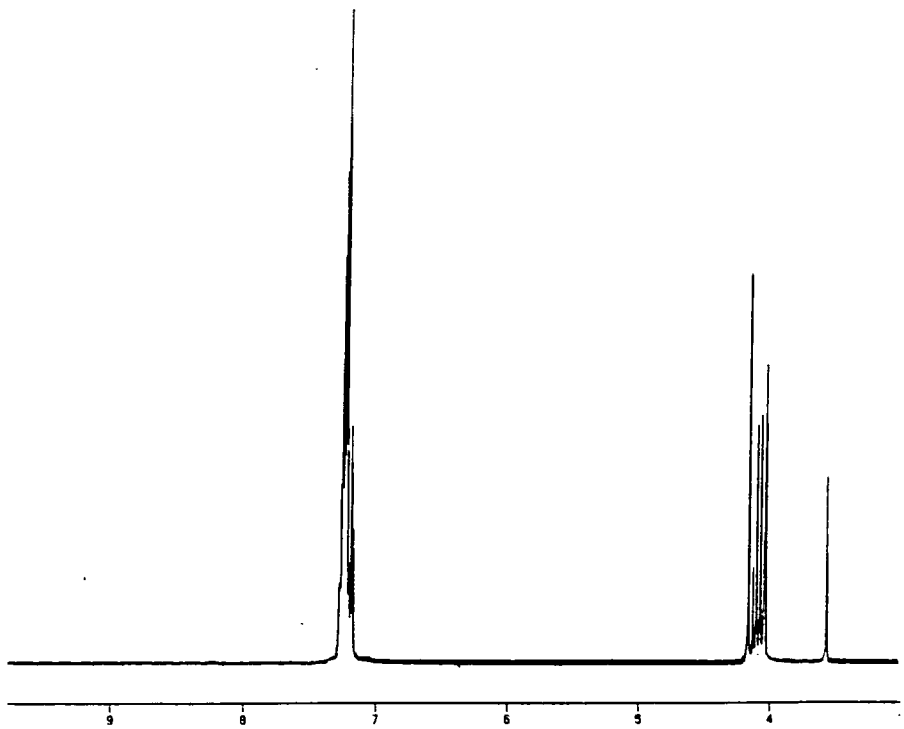

Fig. 3.11

^{1}H NMR Spectrum Of 3.1h (500MHz)

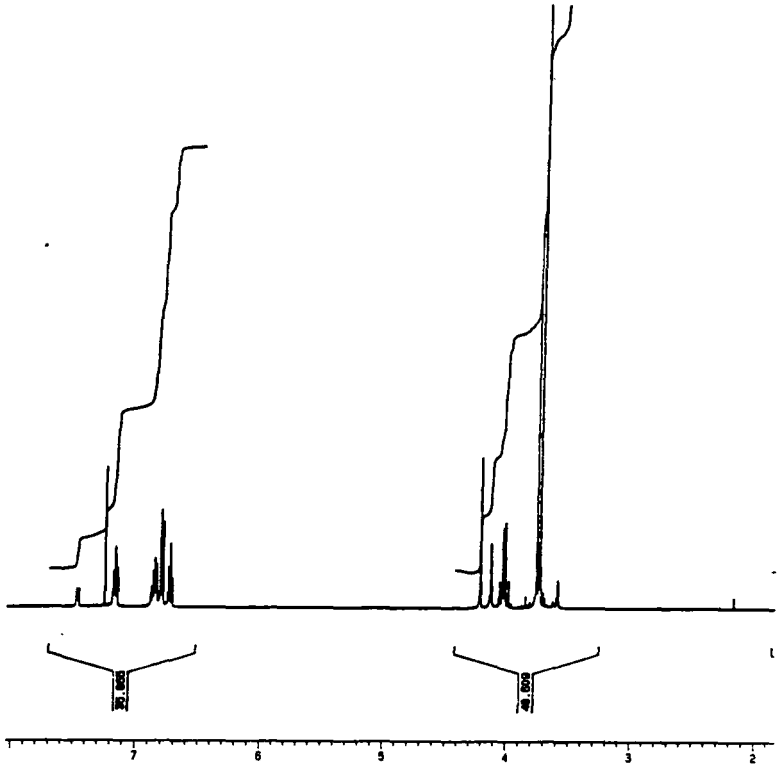

Fig. 3.12

^{1}H NMR Spectrum Of Benzylamine

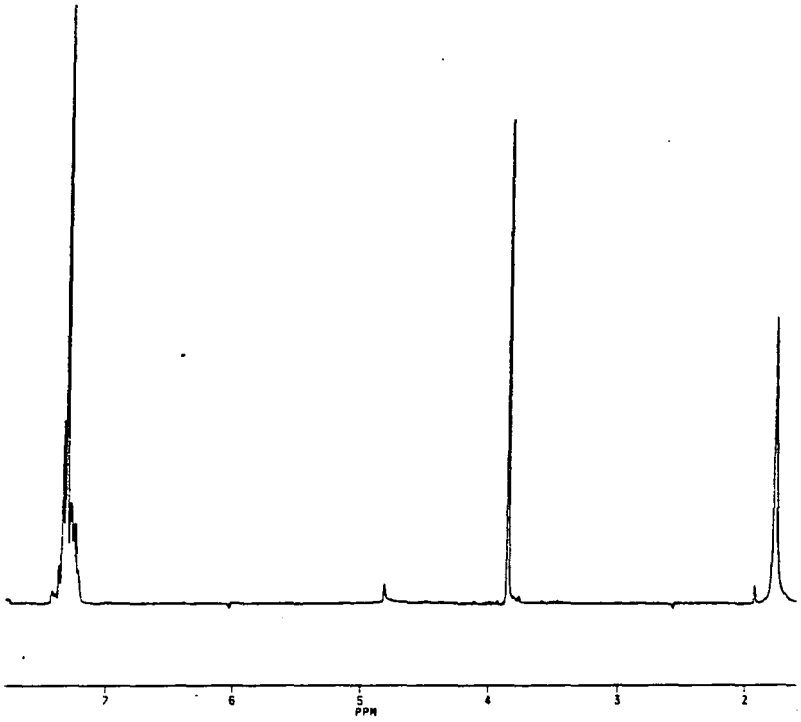

Data for proton-decoupled ^{13}C NMR spectra are given in table 3.9. Methine carbon atoms characteristically[21] absorb at *ca* δ75 while side chain carbon atoms of benzyl groups absorb around δ40 to δ60. In the compounds 3.1a-j the methine carbons appeared at *ca* δ80 with an intensity ratio of *ca* 2:1 (fig. 3.13-3.15). In the absence of proton decoupling each of these bands appeared as a doublet (fig.3.16).

The methylene carbons gave two bands at *ca* δ45-60 with an intensity ratio of 4:8. In the absence of proton-decoupling these bands appeared as triplets (fig. 3.16). The aromatic carbons gave a series of bands in the range δ130-140. Further confirmation of assignments was confirmed using 3.1i, 3.1j and also by comparison with spectra of the parent benzylamines (fig.3.17). Both deuteriated compounds showed benzyl signals of very low intensity at *ca* δ45-60 (fig. 3.18 and 3.19). The very low intensity signals of the C-D benzyl carbons has been attributed to saturation of the ^{13}C signal.[22] The relaxation of the ^{13}C nuclei after a pulse is aided by the attached hydrogen atoms. However, when deuterium is substituted for hydrogen the ^{13}C nuclei do not relax fully before the next pulse which effectively decreases the no. of ^{13}C in the ground state. This results in less nuclei being excited on application of the following pulse resulting in a very much weaker signal.

Fig. 3.13

^{13}C-Decoupled Spectrum Of 3.1a

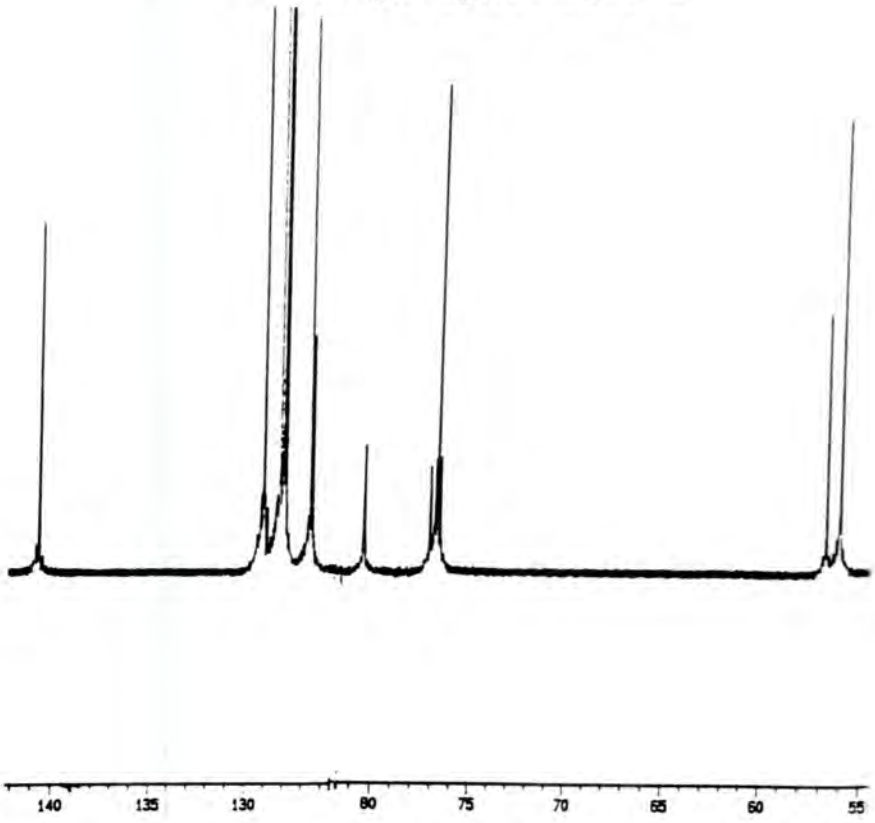

Fig. 3.14

^{13}C-Decoupled Spectrum Of 3.1d

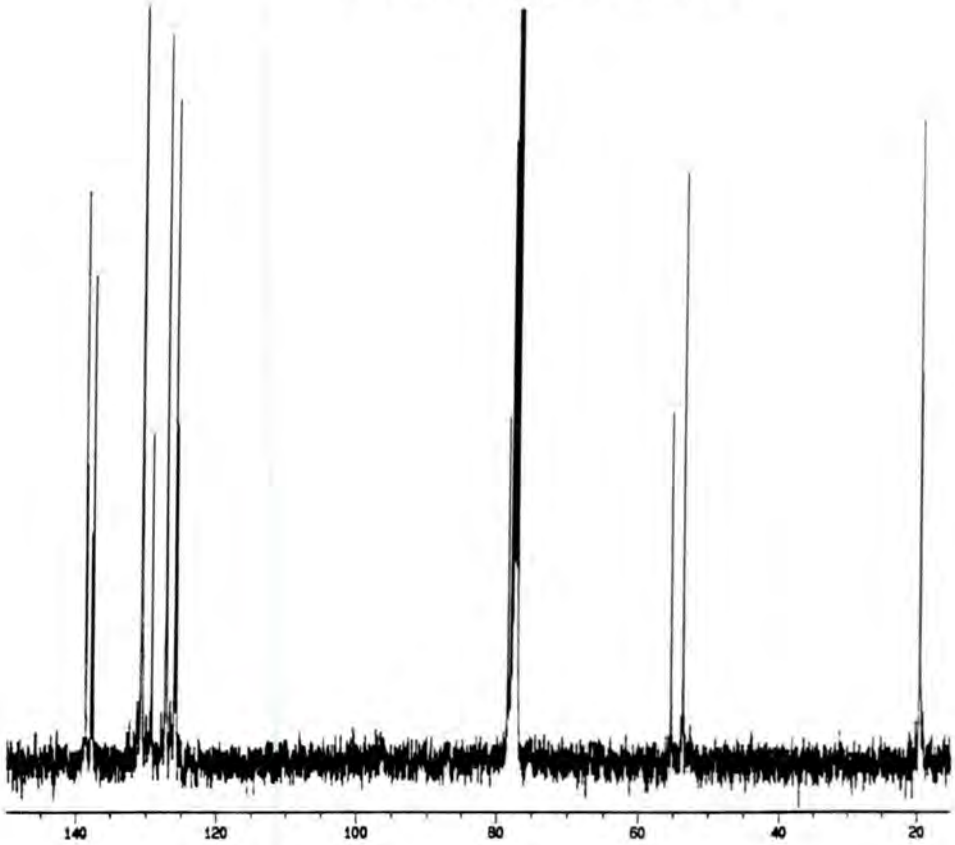

Fig.3.15

^{13}C Decoupled Spectrum Of 3.1f

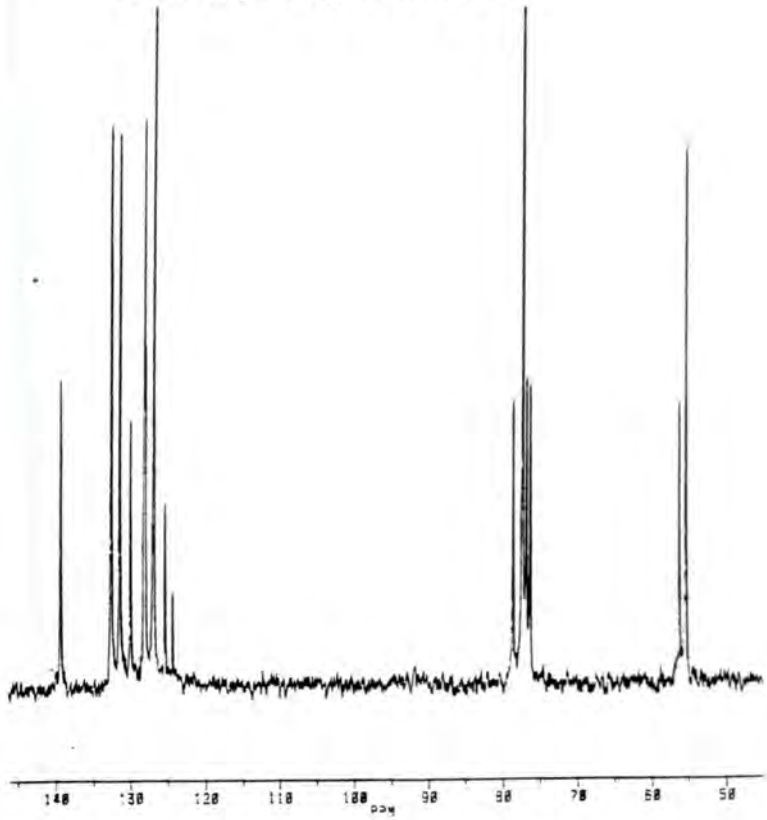

Fig. 3.16

^{13}C Coupled Spectrum Of 3.1a

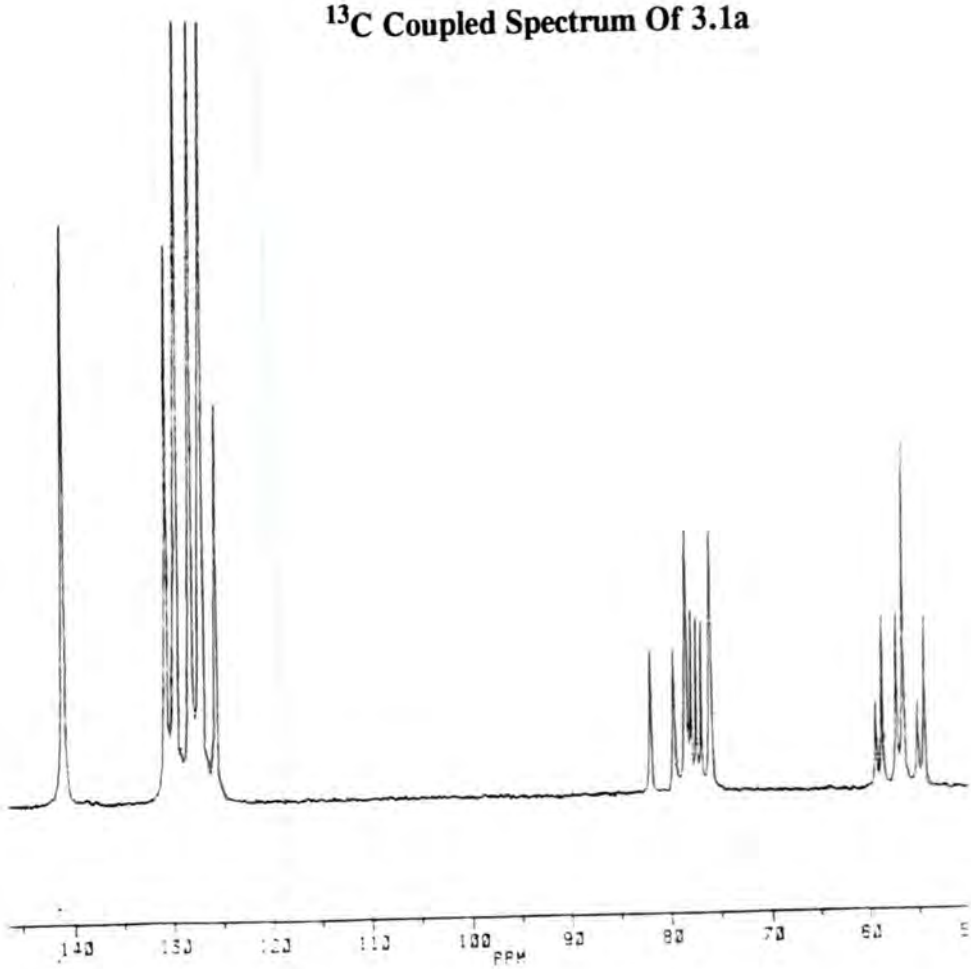

Fig. 3.17

^{13}C-Decoupled Spectrum Of Benzylamine

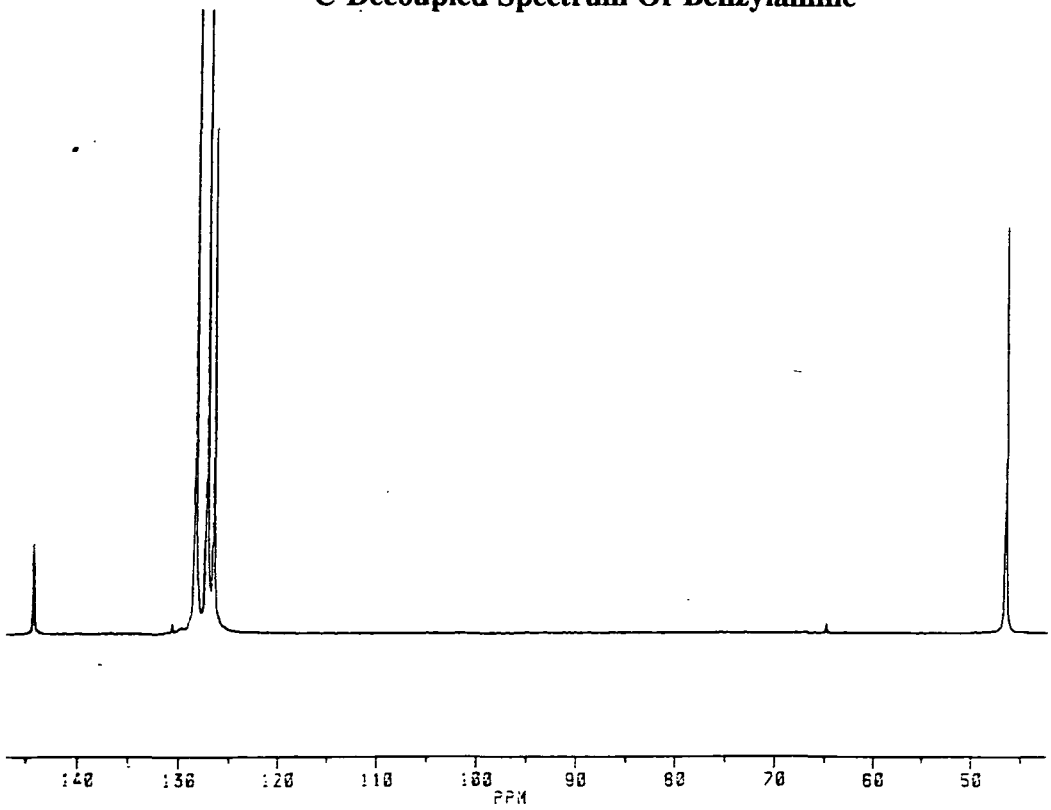

Fig.3.18

^{13}C-Decoupled Spectrum Of 3.1i

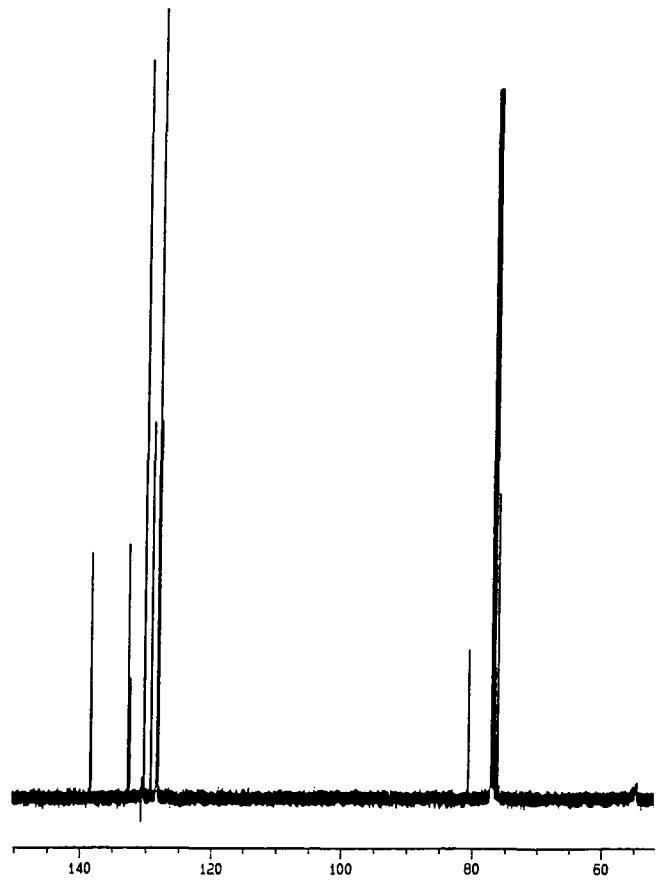

Fig. 3.19

^{13}C-Decoupled Spectrum Of 3.1j

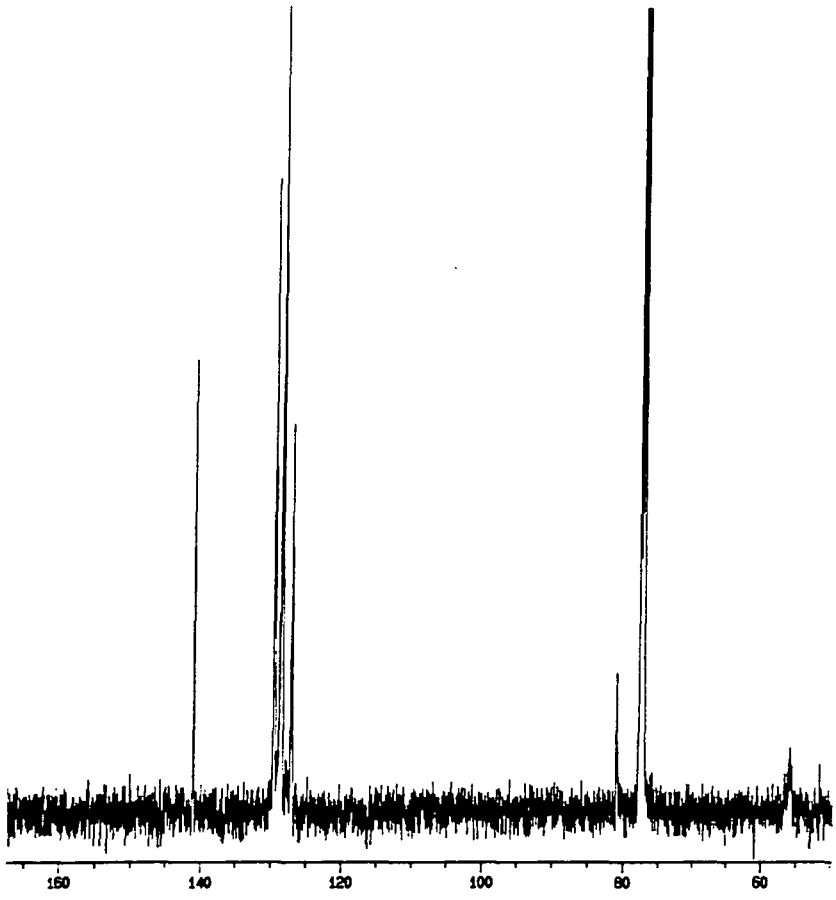

Table 3.9
^{13}C NMR Data for Compounds 3.1a-j

Compound 3.1	Solvent	Phenyl Carbons	CH_2 Carbons[a]	CH Carbons[a]	Phenyl Substit.
a	$CDCl_3$	140.39,128.86,127.98,127.7, 126.33	56.51(2C) 55.84(4C)	80.15(2C) 76.99(4C)	-
b	$CDCl_3$	137.94,134.96,131.43,129.95 129.58,129.45,128.05,126.44	54.34(2C) 53.15(4C)	79.69(2C) 76.77(4C)	-
c	$CDCl_3$	138.62,132.83,132.55,130.35 129.37,128.5, 128.48,128.40	56.18(2C) 55.54(4C)	80.95(2C) 76.47(4C)	-
d	$CDCl_3$	137.61,137.50,136.79,136.55 129.69,126.23,125.01,124.77	54.35(2C) 52.46(4C)	77.01(2C) 75.95(4C)	Me 18.76(4C) 18.68(2C)
e	$CDCl_3$	137.84,136.01,129.24,129.02 128.73,128.43,128.33,128.23	56.56(2C) 55.81(4C)	80.38(2C) 76.77(4C)	Me 21.11(4C) 21.00(2C)
f	$CDCl_3$	139.42,132.81,131.57,130.07 128.25,127.03,125.47,124.41	56.29(2C) 55.41(4C)	78.77(2C) 77.53(4C)	-
g	$CDCl_3$	131.26,130.23,128.37,128.26 128.11,127.99,127.55,127.32 123.63,115.38,115.19,115.04 114.85	49.57(2C) 49.21(4C)	80.83(2C) 76.84(4C)	-
h	$CDCl_3$	157.97,157.63,130.75,129.79 129.60,129.10,127.30,126.8, 119.99,119.83,109.95,109.79	54.94(2C) 50.36(4C)	80.36(2C) 77.12(4C)	Me 26.85(4C) 26.74(2C)
i	$CDCl_3$	138.52,138.39,132.80,130.74 130.41,129.37,128.45,128.28	-	80.76(2C) 76.36(4C)	-
j	$CDCl_3$	140.97,129.59,129.37,128.77 128.56,128.44,127.05,126.94	-	80.84(2C) 77.07)4C)	-

a) Assignments confirmed from coupled/decoupled spectra and from comparison with spectra of 3.1i and 3.1j.

3.2.2 Mass Spectroscopy

The Chemical Ionisation mass spectrum of 3.1a gives a molecular ion peak at m/z 708 corresponding to HBIW and one of the protonated N,N'-dibenzyl-1,2-ethanediimine cation formed as a breakdown product at m/z of 237 (M+1=237) (fig. 3.20).

M+1 and M+2 peak intensities predicted theoretically using the formulae given in eqn. 3.3. agreed closely with those obtained. These formulae predict the peak intensities expected due to isotopic abundances of ^{13}C, ^{15}N and ^{2}H.

$$\%(M+1)=100([M+1]/[M])$$

$$\approx 1.08 \text{ x No. of C atoms} + 0.36 \text{ x No. of N atoms} + 0.016 \text{ x No. of H atoms}$$

$$\%(M+2)=100([M+2]/[M] \qquad \textbf{eqn. 3.3}$$

$$(1.08 \text{ x No. of C atoms})^2/200 + 0.36 \text{ x No. of N atoms} + 0.016 \text{ x No. of H atoms}$$

where M is the molecular ion peak.

For HBIW (3.1a) using values of (M), (M+1) and (M+2) of 92.22, 49.54 and 13.68 (obtained from spectrum) respectively gave %(M+1) and %(M+2) of 53.72% (calc. 54.76), and 13.68% (calc. 14.83). The mass spectrum for 3.1a and 3.1c are shown in figs. 3.20 and 3.21. It must be noted that in many cases no molecular ion peak was observed although M+1 and M+2 peaks due to the diimine moiety were observed in many cases.

Fig. 3.20
C.I. Mass Spectrum Of 3.1a

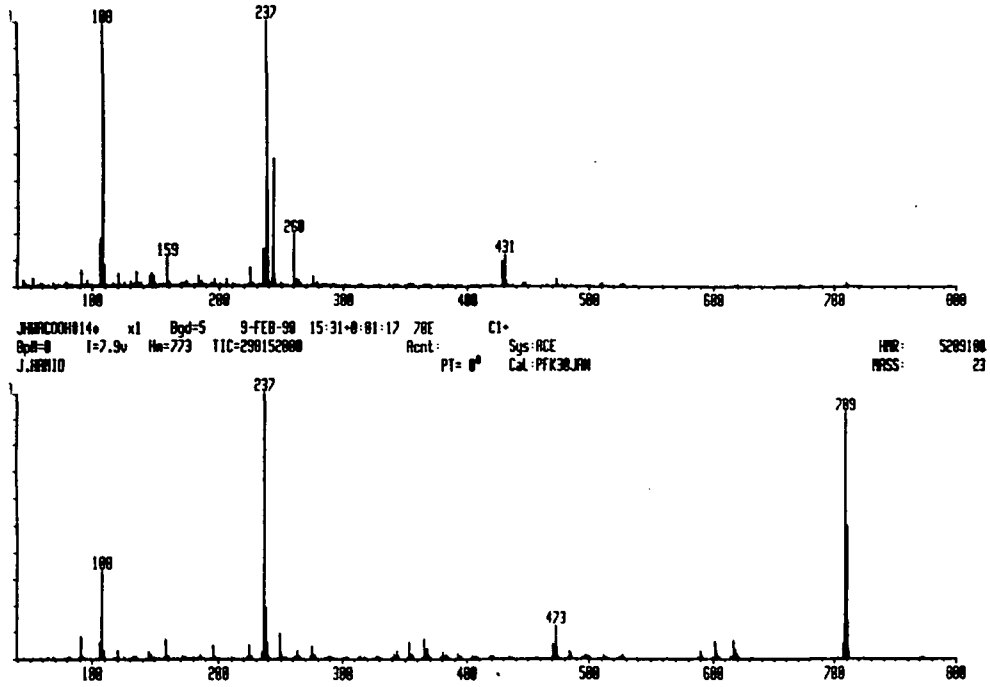

Fig. 3.21
C.I. Mass Spectrum Of 3.1c

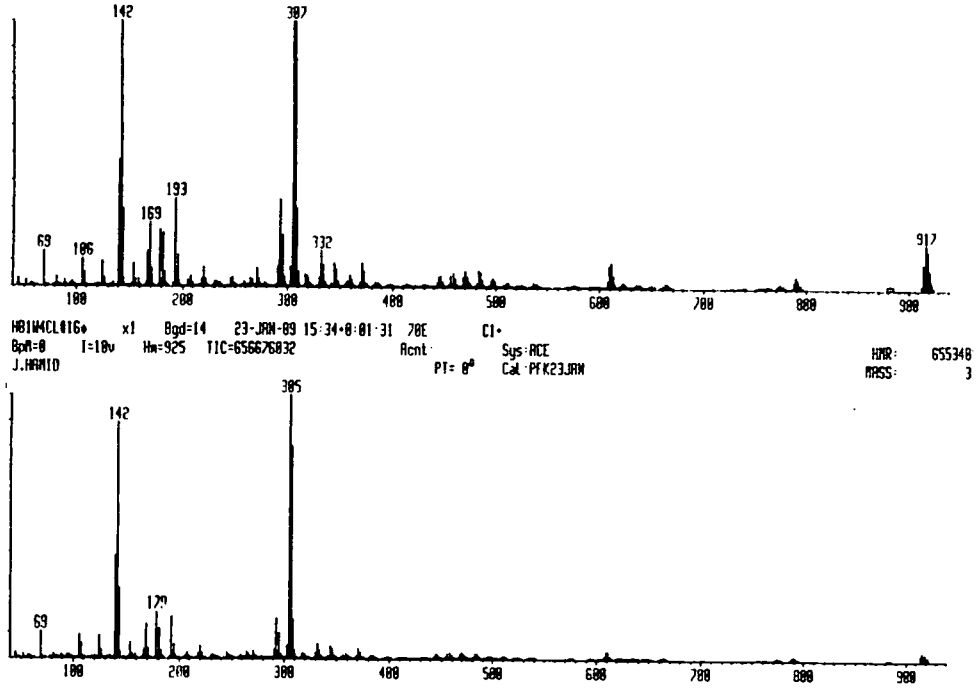

3.3 X-ray Crystal Structure

The crystal structure of 4-chlorobenzyl-hexaazaisowurtzitane (3.1c) was established by x-ray crystallography and is shown in fig. 3.22. Dr. George Ferguson at Guelph, Canada is thanked for this structure determination. The structure in the solid is quite regular with a symmetry element. The six membered C_4N_2 ring at the base of the molecule forms a well defined boat structure with the two benzyl groups pointing downwards. The methylene hydrogens are exocyclic to the six-membered ring.

In the five-membered C_3N_2 rings the atoms N2, C3, C4 and N5 are almost planar and with C1 give a classic envelope conformation. The arrangement of atoms about N2 and about N6 is nearly planar whereas N5 has a pyramidal environment showing that the lone-pair is stereochemically active. In the solid state two of the benzyl groups at the top of the molecule are pointing upwards, with the methylene hydrogens exocyclic, and two are pointing downwards, with the methylene hydrogens endocyclic.

The crystal structure of the 3.1d was also established by x-ray crystallography and is shown in fig. 3.23 (many thanks to Prof. Howard André Bastinov and colleagues at Bristol University). As can be seen the solid state stucture is slightly different to that of 3.1c. In this cage structure all the benzyl methylene hydrogens in the two five-membered rings are all exocyclic including those in the six-membered ring.

Fig.3.22

X-Ray Crystal Structure Of 4-Chlorobenzyl-hexaazaisowurtzitane

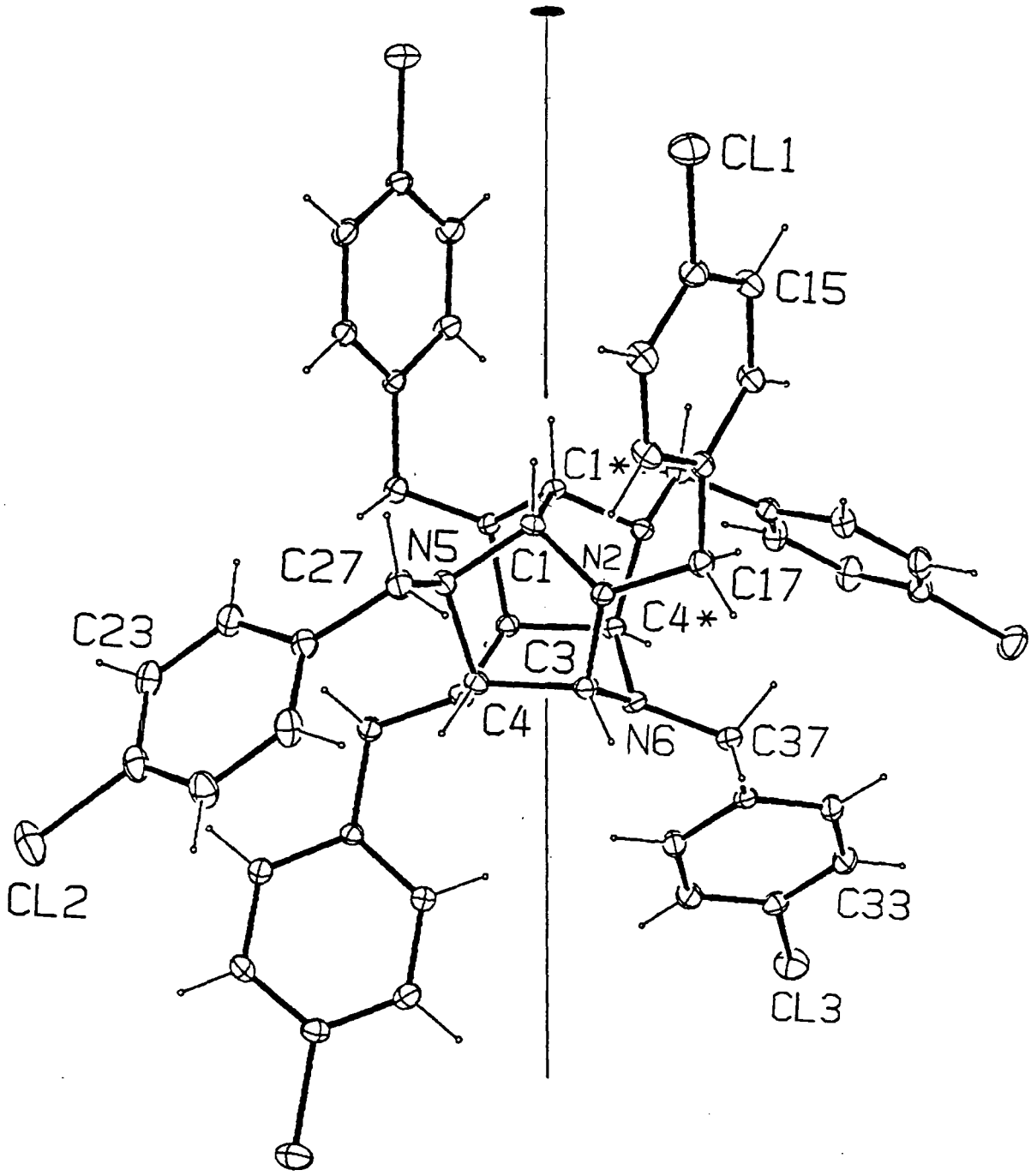

Fig. 3.23

X-Ray Crystal Structure Of 2-Methylbenzyl-hexaazaisowurtzitane

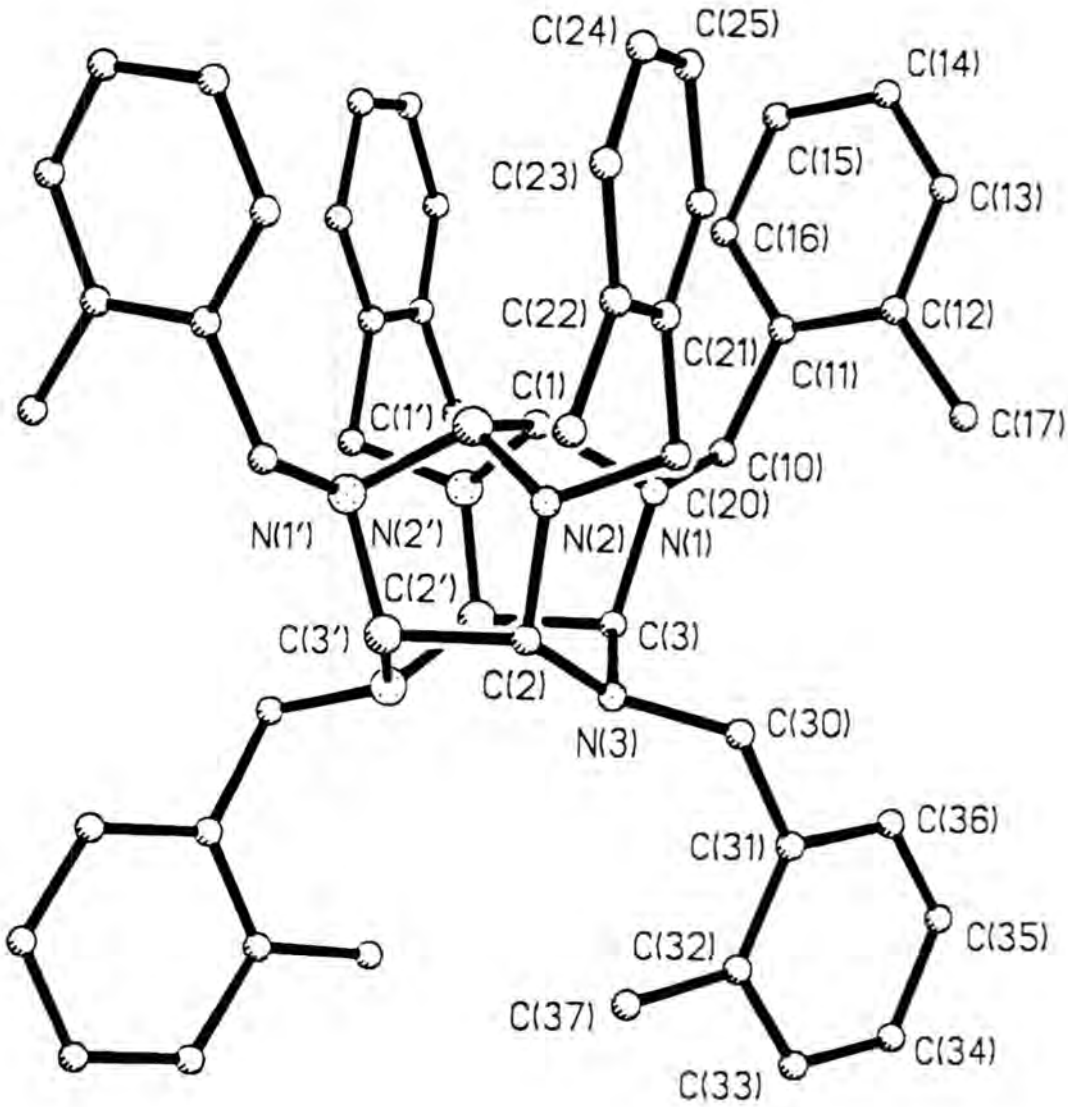

The ^1H NMR spectra of 3.1c (and all the derivatives) show that in solution the four methylene groups of the benzyl systems at N2 and N5 give a single AB quartet, with geminal coupling of 13Hz. This indicates that in solution the benzyl groups at N2 and N5 must, on time averaging, be equivalent. This might be achieved by rapid inter conversion of the environments about N2 and N5 A further possibility is that in solution the arrangements at N2 and N5 become equivalent. However, the fact that in each of these four CH_2 groups coupling is observed between the two hydrogens indicates that there is restricted rotation about the N-C bonds.

3.4 Preparation Of Intermediates In The Synthesis Of HBIW

N,N'-Dibenzyl-1,2-ethanediimine (3.12) is thought to be an intermediate in the formation of HBIW (3.1a). It can be prepared in a rather similar manner to HBIW but substituting aqueous ethanol (50% v/v) for acetonitrile as solvent and keeping the temperature at 0°C. Here the aqueous glyoxal is added over a five minute period to the benzylamine solution. In the HBIW preparation the benzylamine is the added component.

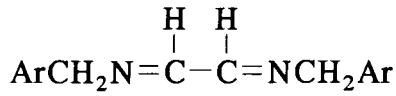

3.12

Ar=C_6H_5

Ar = C_6H_4Cl

Another intermediate involved in the formation of HBIW is thought to be the dicarbinolamine, 3.13 (1,2-bis(benzylamino)-1,2-ethanediol) and this may be prepared by reaction of benzylamine with glyoxal in aqueous THF (50% v/v) at 0°C. Dehydration of the dicarbinolamine can be achieved by pumping under vacuum (0.1mm Hg) for about an hour to give 3.12 (eqn.3.4). The dehydration may be catalysed by acid remaining from the preparation.

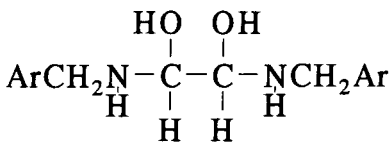

3.13

Ar=C_6H_5

Ar = C_6H_4Cl

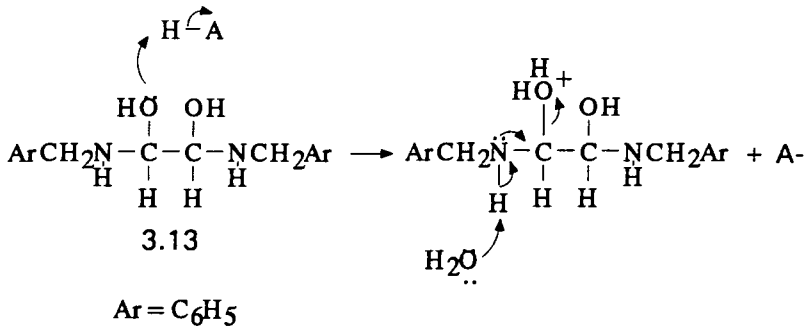

3.13

$Ar = C_6H_5$

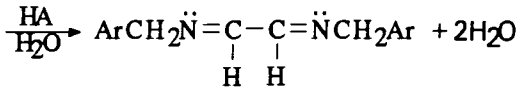

3.12

eqn. 3.4

The diol and the diimine can be readily distinguished from their characteristic ^1H NMR spectra. The diimine ($CDCl_3$) shows a signal at δ8.07 typical of N=CH-CH=N groups.[26] The spectrum in fig. 3.24 shows that the diimine is fairly pure apart from a little water (δ1.78 (b)) and some oligomers of 3.12 (δ3.2-4.5). The benzyl methylene protons give a singlet at δ4.77 and the aromatic ring protons a multiplet at δ7.10-7.37.

Fig. 3.24
^1H NMR Spectrum Of 3.13

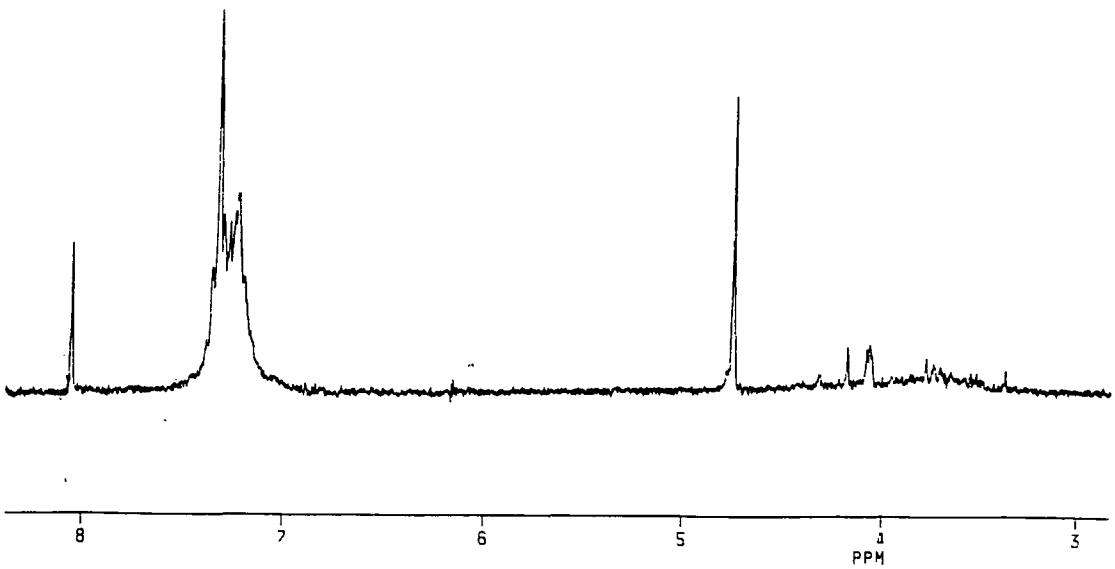

If the diimine is dissolved in acetonitrile and the solution left for several minutes HBIW precipitates out. The yield of HBIW is about 70-75%.

The diol ($CDCl_3$) gives a sharp signal due to methylene protons at δ4.68, and a broader band at δ4.66 which collapses on addition of D_2O, and is thus attributed to exchangeable NH and/or OH protons. The aromatic protons appear as a multiplet at δ 7.12-7.35 while the CHCH signal appears as a multiplet along with other signals at δ 3.2-4.0.

3.5 Formation Of HBIW

Nielsen and co-workers[13] gave a possible mechanism for the production of 3.1a (scheme 3.2). Formation of HBIW is thought to involve trimerisation of diimine 3.12. They have shown that the diol (3.13) seems to react much more slowly than the diimine to give 3.1a indicating that dehydration of the diol is slower than trimerisation of 3.12 to form 3.1a. Of the total 3.1a formed in 17 hours, 92% is formed within the first half an hour from diimine, but only 75% from the diol during the same time period.

Scheme 3.2

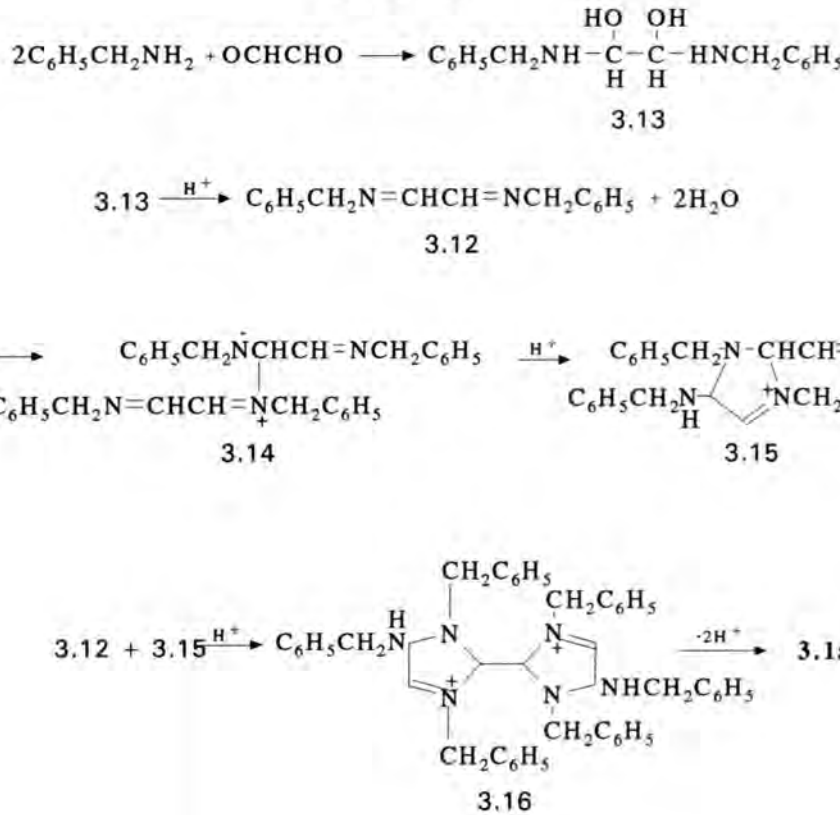

Dibenzyl diimines are unusual in their very reactive behaviour to produce 3.1a because most other diimines obtained from other amines and glyoxal are stable materials that do not polymerise nor do they self react to produce isowurtzitanes.

The diimine trimerisation is thought to involve addition of an imine (diimine in this case) 1,2-dipole to a second imine molecule (scheme 3.2). Initially the dicarbinolamine 3.13 is formed which in the presence of an acid catalyst readily dehydrates to yield the dibenzyl diimine 3.12. Dimerisation of 3.12 gives the acyclic dimer 3.14. This can readily protonate and cyclise to give the monocyclic dimer 3.15 which is cationic. Further reaction of 3.15 with another molecule of diimine 3.12 and protonation leads to the formation of a bicyclic trimer 3.16, a dication. Intramolecular cyclisation of 3.16 and loss of two protons then leads to 3.1a.

There are many reports in the literature which show that monoimines derived from aldehydes and ammonia also undergo similar, extremely rapid trimerisation to produce 2,4,6-trisubstituted-1,3,5-hexahydrotriazines. These reactions also involve self addition of imine 1,2-dipoles.[23,24] Anilines and benzylamine are also found to react with aldeyhdes to form N,N,N-trisubstituted-1,3,5-hexahydrotriazines. However, for most amines the reaction is limited to those with formaldehyde.[25-28] Other amines react with aldehydes to produce stable imines RCH=NR which do not cyclise to give hexahydrotriazines. Methylamine and allylamine have also been observed to produce 1,2,3,4,5,6-hexasubstituted-1,3,5-hexahydrotriazines and only when reacting with acetaldehyde.[26-30]

Cordes and Jencks[31] have shown in the reaction of anilines with aromatic aldehydes to form Schiff bases, the rate limiting step at basic pH is dehydration of the carbinolamine intermediate ArNHCHOHAr. Pratt and Kamlet[31] have shown that the rate of Schiff base formation is slower for anilines bearing electronegative substituents.

Similarly it was found that formation of HBIW derivatives from benzylamines containing electron withdrawing ring substituents (2-Cl, 4-Cl, 2-F, 2-Br and 2-MeO) was slower and gave lower yields than formation of HBIW (3.1a) itself or the 4-methyl and 2-methyl derivatives.

If reaction occurs according to scheme 3.2 there are several steps which may be affected by the electronic effect of the substituents in the benzyl ring. The steps involved in the formation of diimine are shown in scheme 3.3.

Scheme 3.3

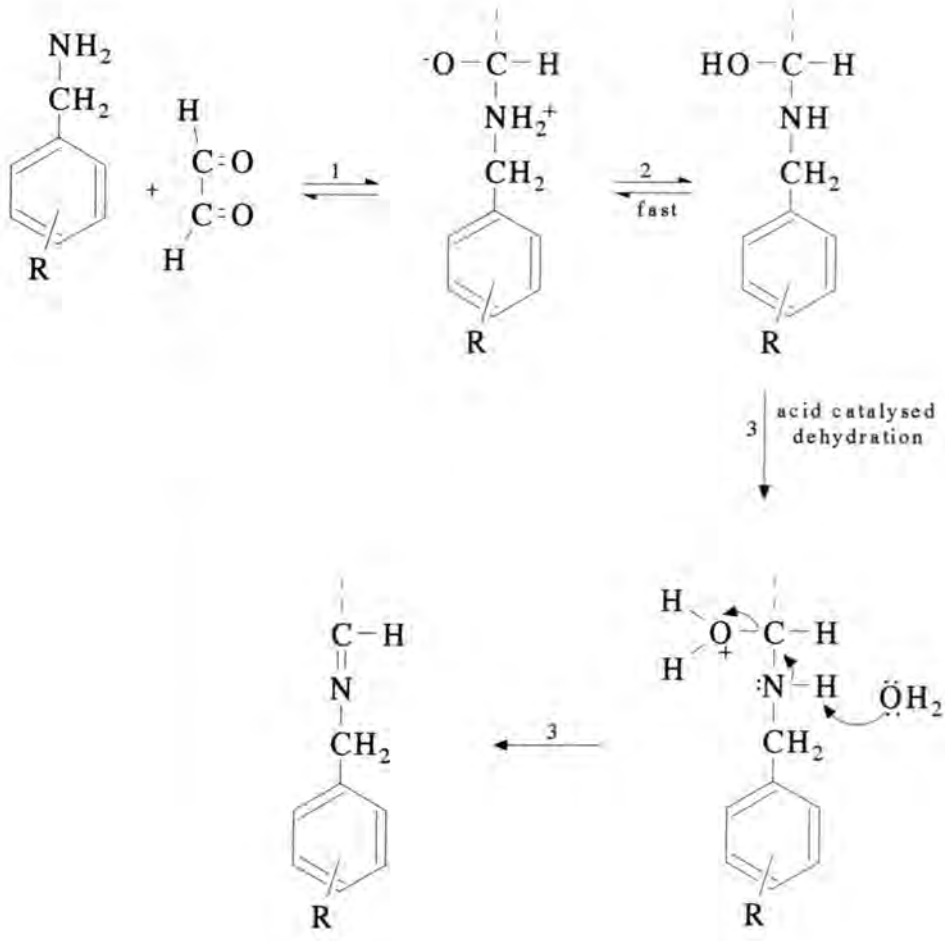

Step 1. Slowed by electron withdrawing R group. Reduction in nucleophilicity of benzylamine.

Step 2. Rapid intramolecular proton transfer.

Step 3. Slowed by electron withdrawing R group. More difficult for electrons to move from nitrogen.

Further the dimerisation of the diimine (scheme 3.2) will also involve nucleophilic attack by nitrogen which may also be inhibited by the presence of electron withdrawing groups in the benzyl ring.

Derivatives 3.1i and 3.1j containing deuteriated methylene groups were successfully prepared using benzylamines deuteriated in the methylene and amino positions ($ArCD_2ND_2$). It was also thought to be worthwhile to carry out a preparative experiment using N,N'-dideuteriobenzylamine, ($C_6H_5CH_2ND_2$). Since glyoxal is available only as an aqueous solution, which would introduce exchangeable protons into the system. The experiment here used 1,4-dioxan-2,3-diol (3.11) which is the hemiacetal derivative of glyoxal available as a solid. Reactions of $C_6H_5CH_2ND_2$ with 3.11 in CD_3CN/D_2O containing DNO_3 gave 3.1a in a yield of 12% after 24 hours reaction. No incorporation of deuterium into the product was found, as evidenced by the ^1H NMR. The corresponding reaction using non-deuteriated reagents gave a yield of 26% after 24 hours. Similarly Nielsen and co-workers obtained a lower yield from the reaction of N,N'-dideuteriobenzylamine and interpreted this as suggesting that the rate determining step, is proton (deuteron) transfer from the carbinolamine (scheme 3.3 step 3). This interpretation is open to question since no rate measurements were made, and it is possible that the overall yield is lower using the deuteriated material but rate constants are unaffected.

As no deuterium was isolated in 3.1a from experiments using deuteriated medium and reactants then mechanisms involving exchange of benzyl α-methylene protons may be discounted. Monoimines and also those derived from benzylamine or α-substituted benzylamines have been shown to undergo 1,3-dipolar additions with dipolarophiles such as styrene or methyl maleate to give substituted pyrrolidines.[33,34] These cyclisations require removal of α-benzyl methylene protons which is clearly not the case here. It has been shown[13] that benzylidenebenzylamine $C_6H_5CH_2N{=}CHC_6H_5$ does not exchange any of its protons in deuteriated systems. Thus 1,3-dipolar mechanisms of this type can be discounted.

The formation of hexaazaisowurtzitane ring system appears to be fairly specific to reactions of benzylamine and ring-substituted benzylamines. Analogues have not been reported from other aliphatic or aromatic amines. The benzyl group plays an active role possibly by stabilising and activating the ionic intermediates formed during the course of the reaction. Although diimines and dicarbinolamines may be formed from aniline derivatives and some aliphatic amines, cyclisation to give caged structures has not been observed. The t-butyl group should be effective in stabilising cationic intermediates but may be too sterically hindered to allow further reaction. Also α-substituted benzylamines yield diimines but these fail to dimerise or trimerise probably due to steric effects which are known to inhibit imine 1,2-dipole additions.[1,10,23,24]

3.6 Stability Of HBIW

The new hexaazaisowurtzitane ring system is much more stable towards acids then the related triazaisowurtzitane ring system,[7] which undergo very facile ring opening in the presence of acid catalysts even weak ones.[7] The triazaisowurtzitanes in both deuteriochloroform and acetonitrile are shown to be in equilibrium with their monocyclic triimines (scheme 3.4).

Scheme 3.4

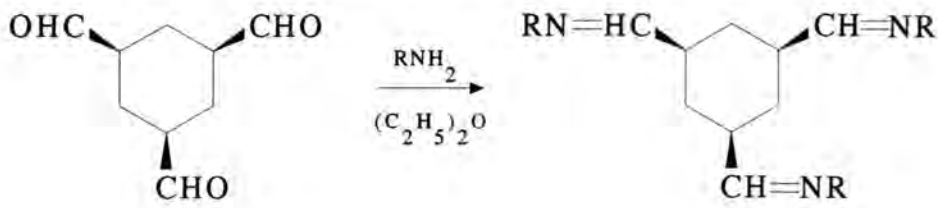

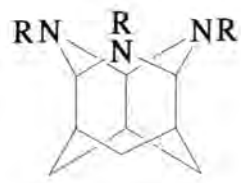

a, R = CH_3

b, R = C_2H_5

c, R = $C_6H_5CH_2$

d, R = 4-$CH_3OC_6H_4CH_2$

On the other hand hexabenzylhexaazaisowurtzitanes synthesised here show no evidence of decomposition in neutral aprotic solvents by ^1H NMR. However, 3.1a has been shown to break down in acetonitrile in the presence of acids (see chapter 2).

3.7 Salt Formation

As HBIW is a tertiary amine one would expect it to form salts. In this study it has been possible to isolate stable hydrobromide, hydrochloride and hydroperchlorate salts from aprotic solvents such as chloroform, benzene and methylene dichloride. In all cases the salts formed are hydrated dibasic salts which is in accord with ^{1}H NMR studies showing that in excess acid HBIW exists primarily as the diprotonated species. 3.1a can be regenerated from salts by treatment with aqueous sodium hydroxide. Elemental analysis support the structure. However, in solution the salts have been shown to decompose within several hours to give unidentified products. Due to insolubility of these salts it was difficult to obtain ^{1}H NMR spectra except for the hydroperchlorate salts (fig. 3.25) (see next chapter for full details).

Fig. 3.25

^{1}H NMR Spectrum Of Hexabenzylhexaazaisowurtzitane Dihydroperchlorate Monohydrate

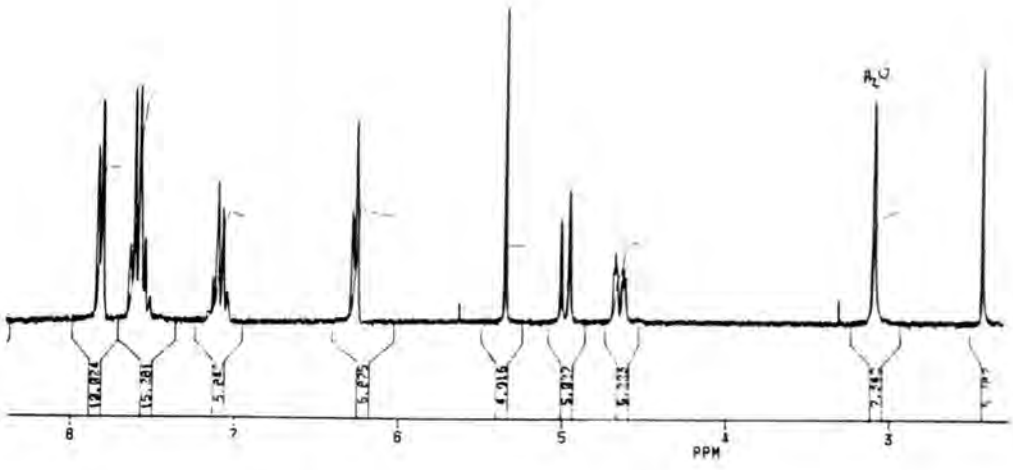

3.8 Analysis Of HBIW Reaction Mixture

It was thought of interest to see if any other cage compounds could be formed as by-products in the reaction leading to the formation of HBIW. In order to assess this possibility the reaction was carried out as outlined in procedure 2.

After allowing the reaction to proceed for 24 hours the precipitated HBIW was filtered off and the orange mother liquor was concentrated under reduced pressure. This resulted in a dark orange tar which was analysed by HPLC using 60/40 acetonitrile/water as the mobile phase. Comparison of the chromatogram with those of standard solutions of benzylamine and diimine allowed positive identification of these compounds. There were also several other unidentified components present.

An attempt was made to separate the components of the dark orange tar using column chromatography with 9:1 cyclohexane:diethylether as eluent on a silica column. Initial TLC experiments indicated that at least five components were present. The most soluble component(s) gave a yellow solution which was concentrated under reduced pressure at 45°C to give an orange-red solution which changed to a gummy solid (M.P. 50-60°C). The ^{1}H NMR spectrum is shown in fig 3.26. When suspended in acetonitrile the gummy solid gave an off-white precipitate whose ^{1}H NMR in deuterioacetone is shown in fig.3.27.

Fig. 3.26 shows a complex mixture but shows peaks which are in similar positions for those expected for HBIW (3.1a) (δ7.17-7.24 (m) Ar, δ4.16 (s) and 3.57 (s) methine CH, δ4.03 (s) and 4.08 (only singlet seen instead of quartet due to overlap). The ^{1}H NMR of the gummy solid in deuteriated acetone is found to be virtually identical. It seems likely that there is some diimine in the reaction mixture which must have subsequently formed HBIW when suspended in acetonitrile

Fig. 3.26

^{1}H NMR Spectrum Of Gummy Solid (yellow eluant)

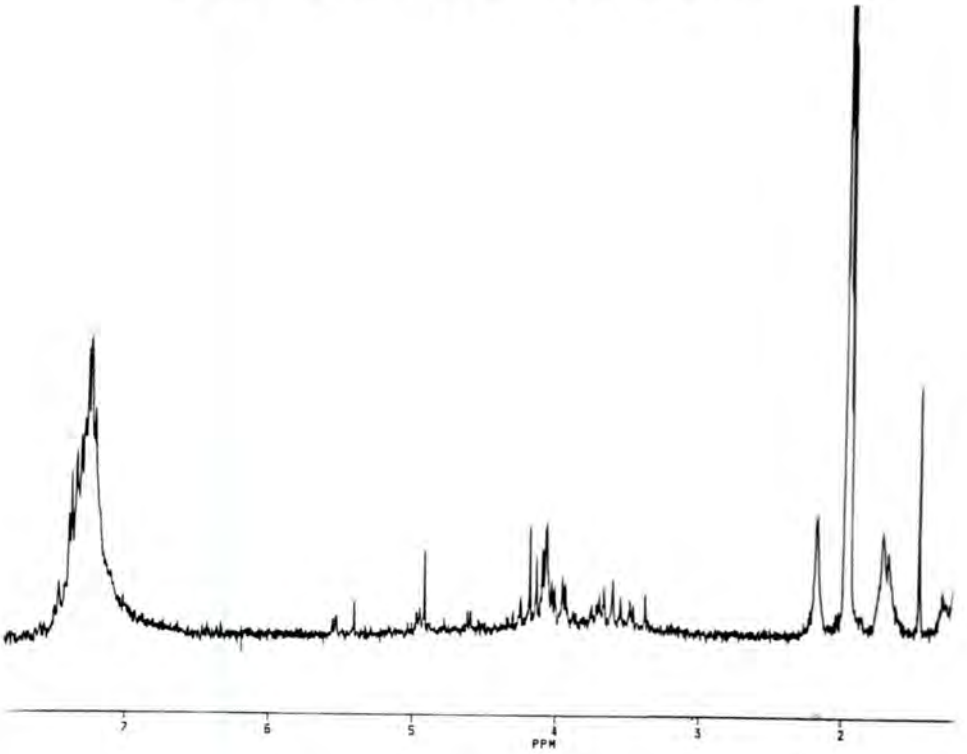

Fig. 3.27

^{1}H NMR Spectrum Of White Precipitate

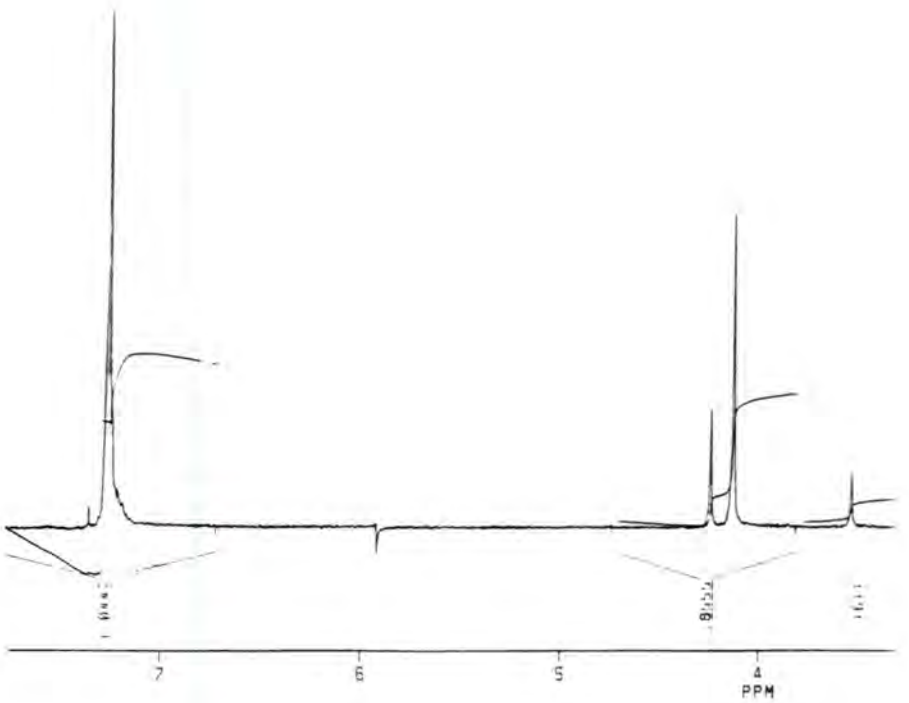

Since the yield of 3.1c obtained from reaction of 4-chlorobenzylamine is considerably less than the yield of 3.1a obtained from benzylamine it seemed possible that more/other products might be produced. It was of interest to try and identify these other products. Hence further investigations were carried out on the reaction mixture produced from 4-chlorobenzylamine and glyoxal.

Initially standard solutions of the 4-chlorbenzyl-diimine, 4-chloro-HBIW (3.1c), 4-chlorobenzylamine and the 4-chloro-dicarbinolamine were run and the following chromatograms obtained with their respective U.V. spectra (fig.3.28-3.31). The peaks due to the respective compounds have been labelled for simplicity.

The mother liquor from the reaction of 4-chlorobenzylamine and glyoxal using procedure 2 was obtained as a red/orange tar after concentration under reduced vacuum. A separation was attempted using initially a solvent system of 60:40 v/v cyclohexane:diethyl ether on a silica column. The initial fractions separated were referred to as Mix 1 and Mix 2 (see scheme 3.5).

Scheme 3.5

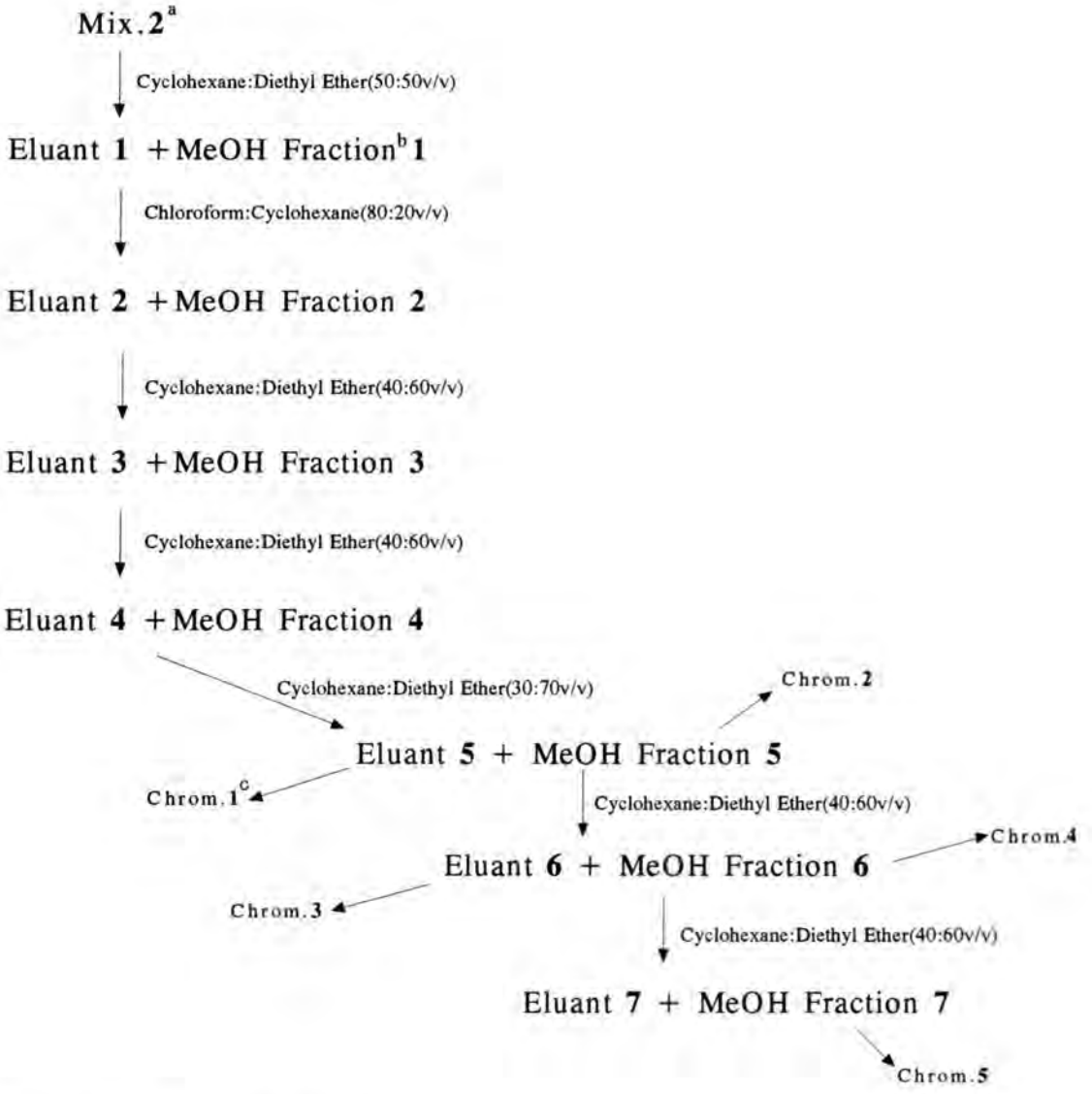

a) **Mix 1**. Remnant on column.
Mix 2. Eluant from column.

b) MeOH fractions refer to residue left on column after elution, which is then washed out with methanol.

c) Refers to HPLC chromatograms.

Fig. 3.28

HPLC Chromatogram Of Diimine (3.12)

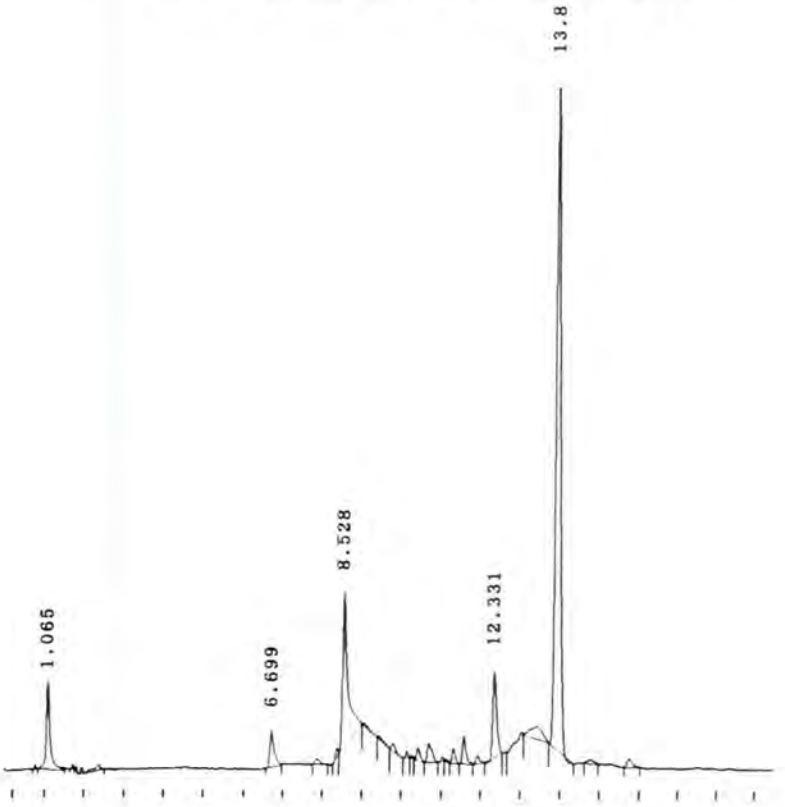

U.V. Spectra Of Components

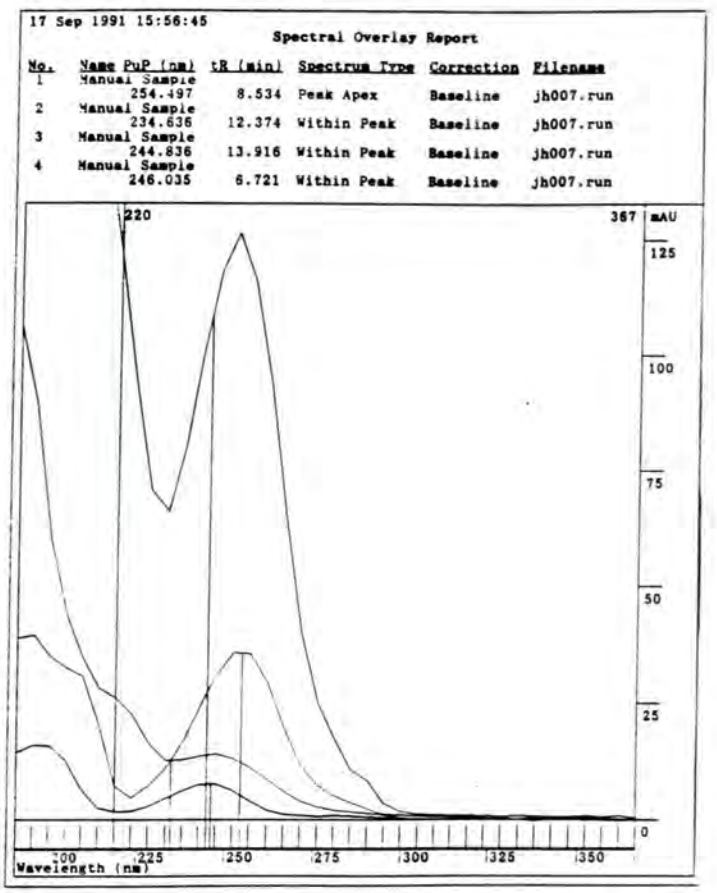

Fig. 3.29

HPLC Chromatogram Of 3.1c (CH_2Cl_2)

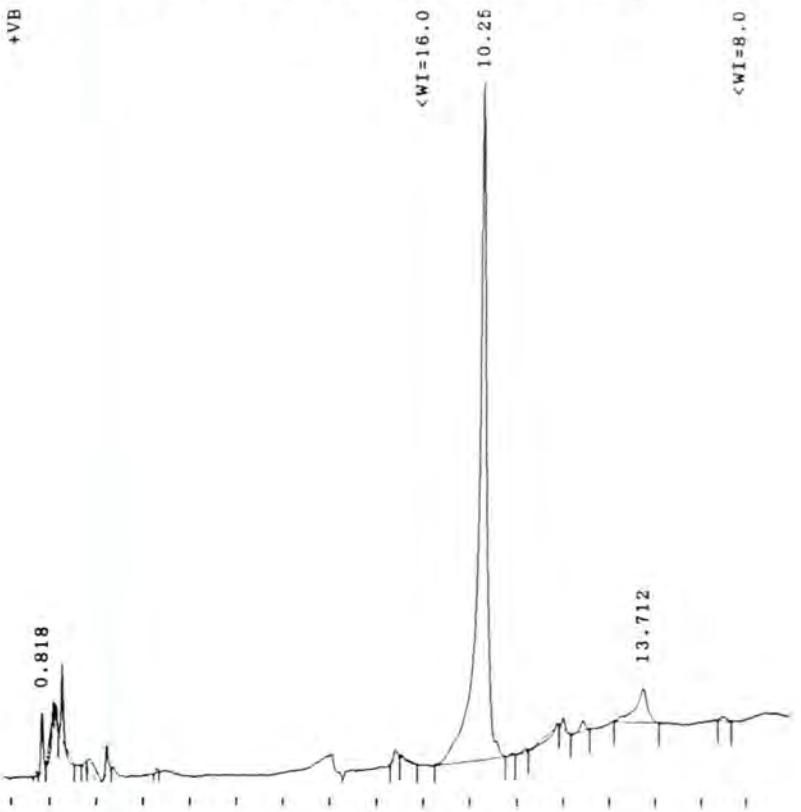

U.V. Spectrum Of 3.1c

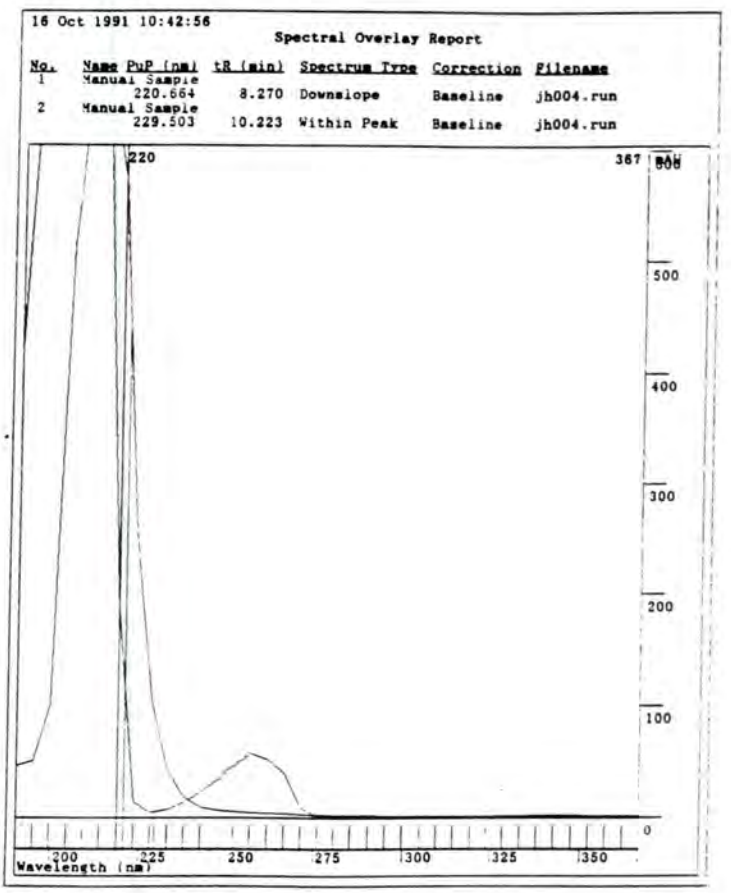

Fig. 3.30
HPLC Chromatogram Of Diol (3.13)

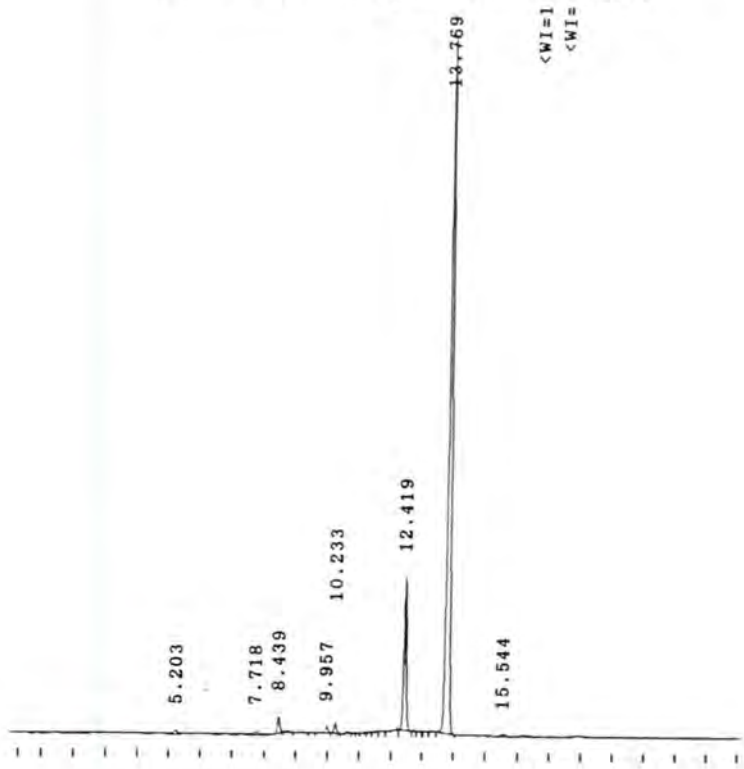

U.V. Spectra Of Components

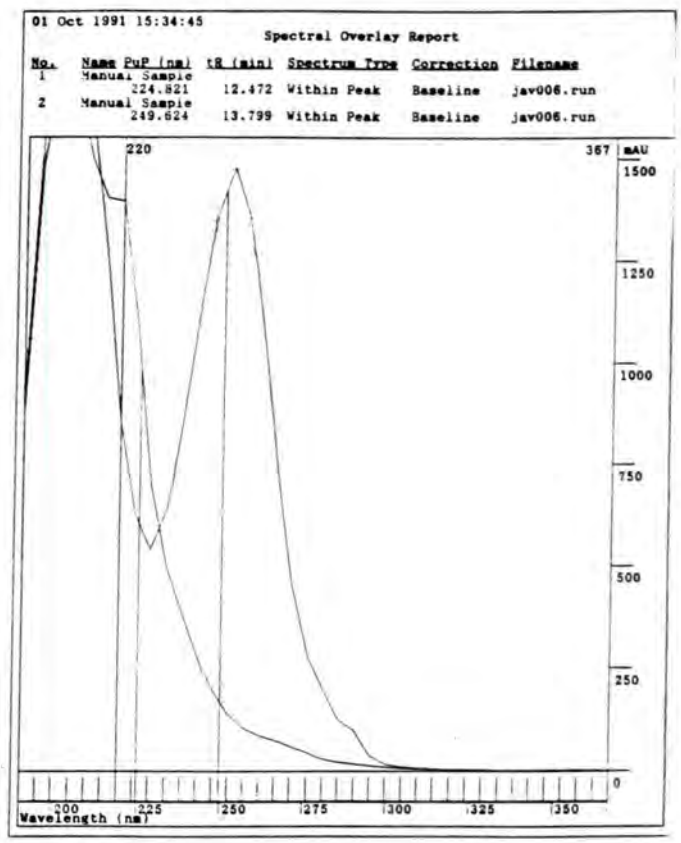

Fig. 3.31

HPLC Chromatogram Of 4-Chlorobenzylamine

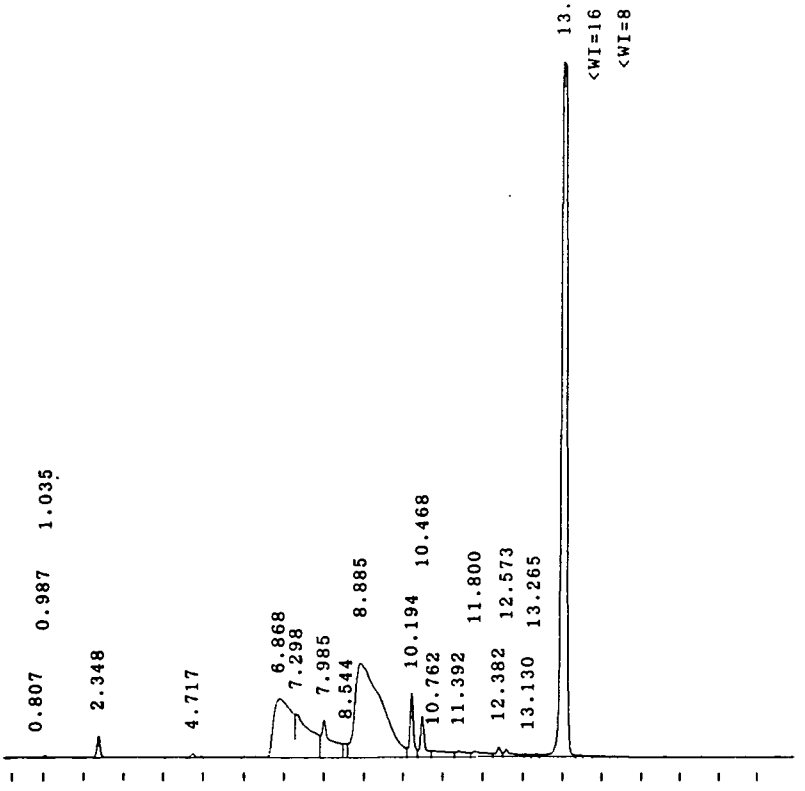

U.V. Spectra Of Components

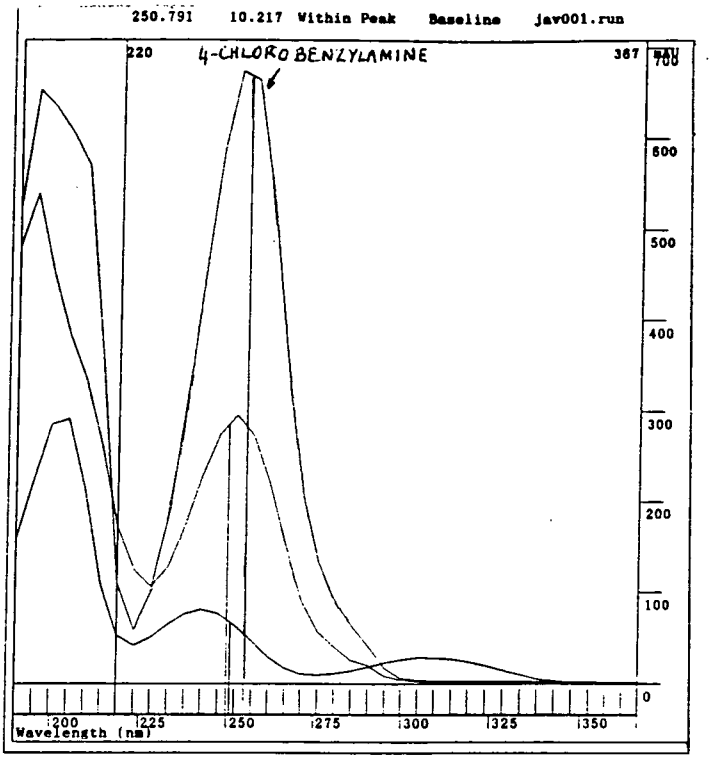

Mix.2 was separated several times to give various fractions as shown in scheme 3.5. Even after five separations MeOH fraction 5 is still shown to be a complex mixture (chrom.2(fig.3.32)).

Fig. 3.32

HPLC Chromatogram 2

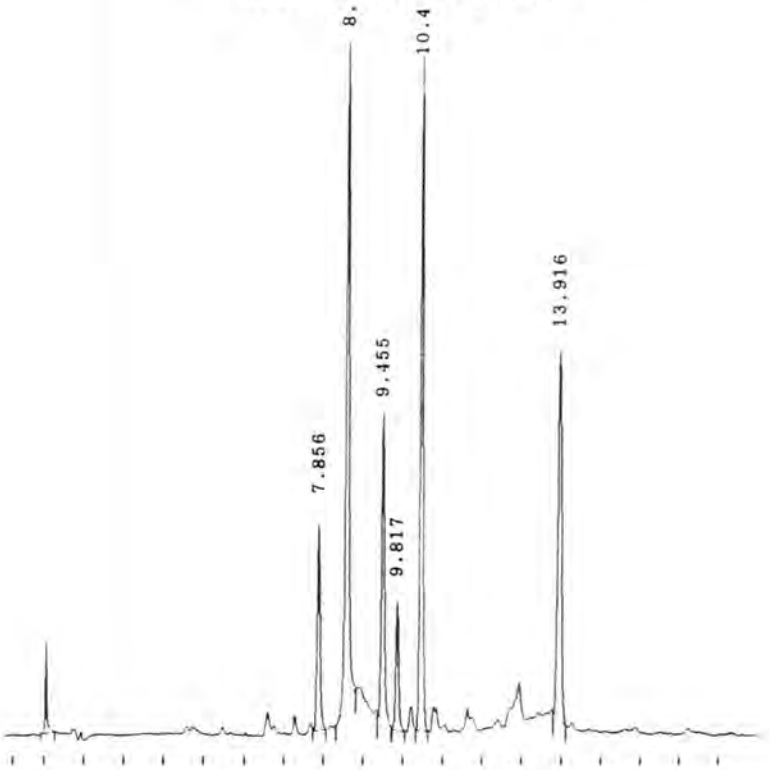

U.V. Spectra Of Components

No.	Name PuP (nm)	tR (min)	Spectrum Type	Correction	Filename
1	Manual Sample 255.342	7.784	Within Peak	Baseline	jh005.run
2	Manual Sample 255.071	8.571	Within Peak	Baseline	jh005.run
3	Manual Sample 285.151	9.498	Downslope	Baseline	jh005.run
4	Manual Sample 268.776	9.836	Within Peak	Baseline	jh005.run
5	Manual Sample 233.691	10.420	Peak Apex	Baseline	jh005.run
6	Manual Sample 250.389	13.953	Within Peak	Baseline	jh005.run

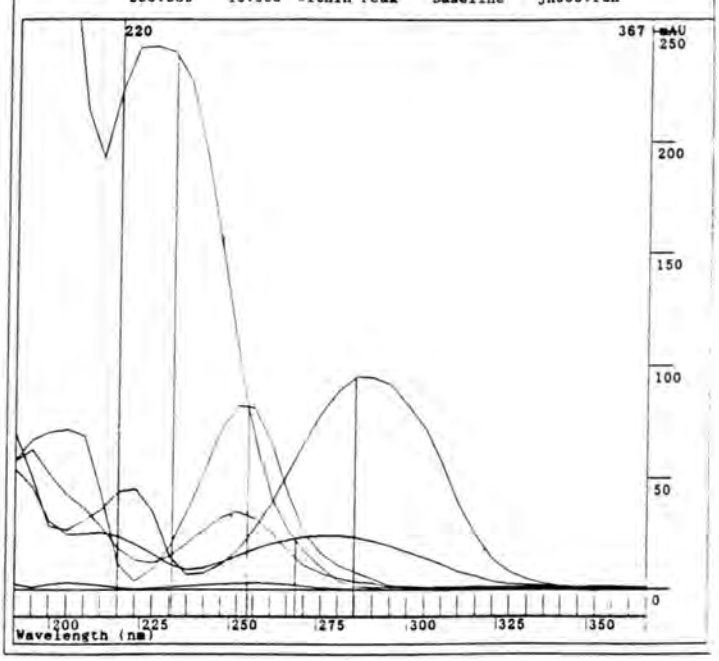

From the known standard solutions run previously it was possible to identify those peaks having retention times of 8.5, 10.42 and 13.91 as the 4-chloro-diimine, 4-chloro-HBIW (3.1c) and 4-chlorobenzylamine respectively. The U.V. spectra of these compounds gave further confirmation. There were also several peaks in the chromatogram which remained unidentified. The eluant 5 on the other hand showed mainly the presence of 4-chloro-diimine (chrom.1(fig.3.33)).

Further separation of MeOH fraction 5 gave eluant 6 (chrom.3(fig.3.34)) revealing a major peak due to 4-chloro-diimine with a much smaller one due to 4-chloro-benzylamine. The MeOH fraction 6 was also shown to contain some 4-chloro-benzylamine and possibly some diimine (chrom.4(fig. 3.35)). The final separation gave a MeOH fraction 7 containing again some 4-chloro diimine and possibly some 4-chloro-HABIT.(chrom.5(fig. 3.36)).

Again from these investigations the results show that these reaction mixtures are fairly complex containing several compounds of which the 4-chloro-diimine, 4-chloro-HBIW and 4-chloro-benzylamine have been positively identified.

Fig. 3.33

HPLC Chromatogram 1

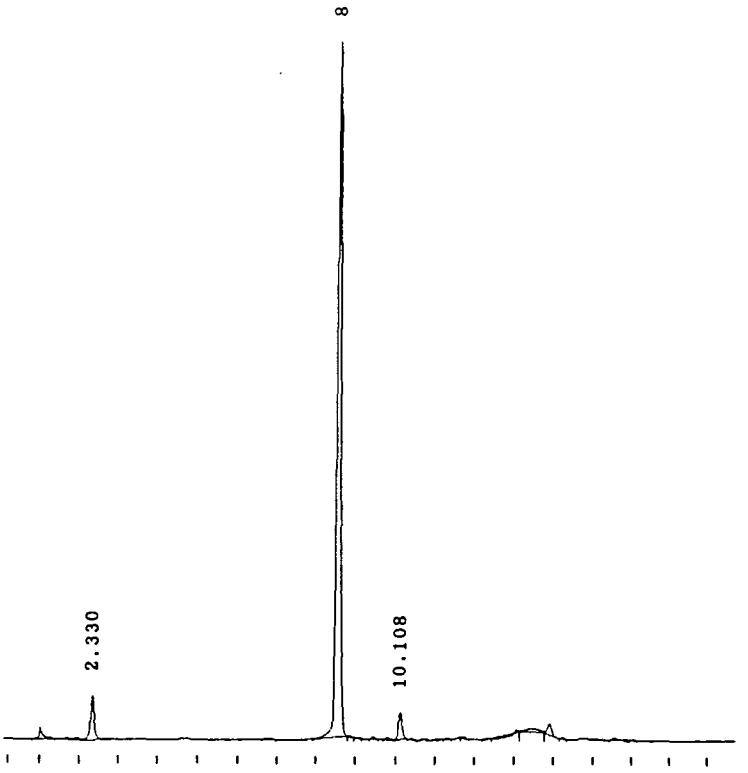

U.V. Spectra Of Components

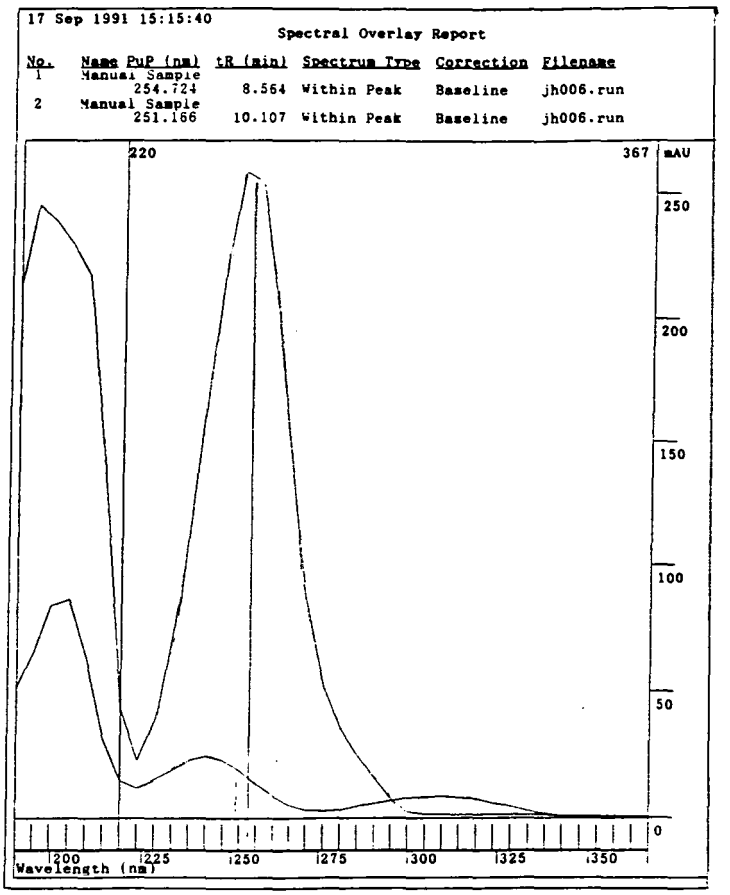

Fig. 3.34

HPLC Chromatogram 3

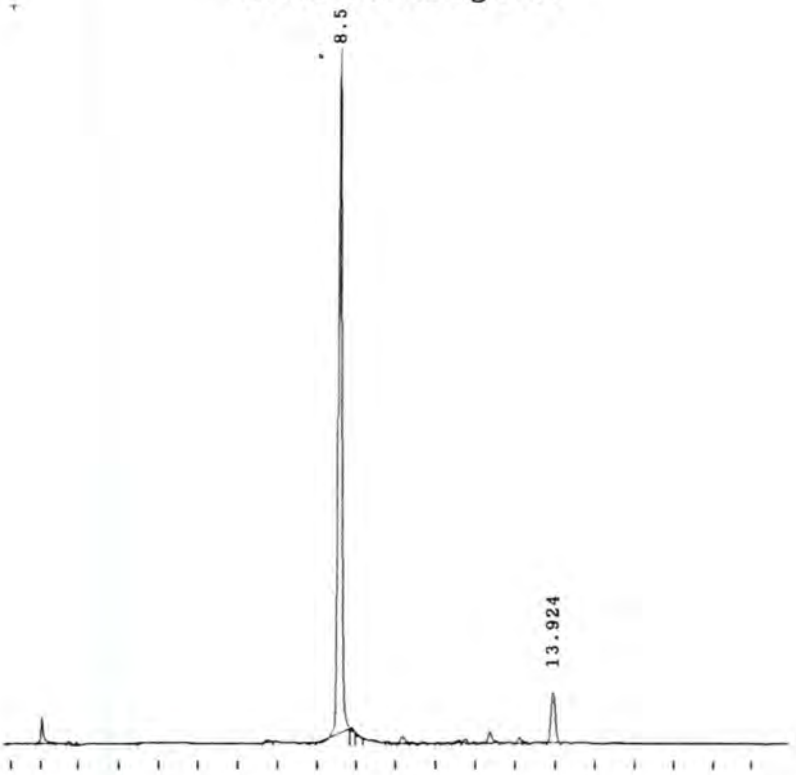

U.V. Spectra Of Components

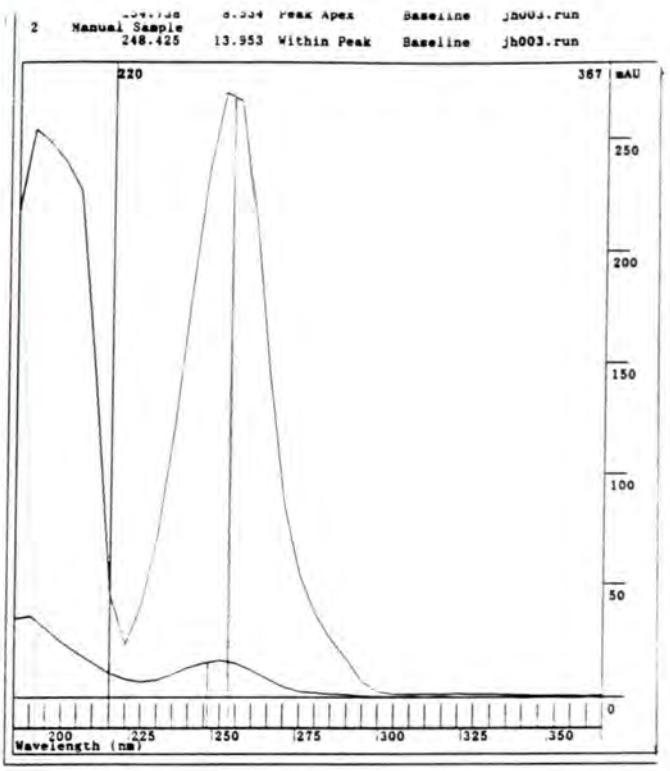

Fig. 3.35
HPLC Chromatogram 4

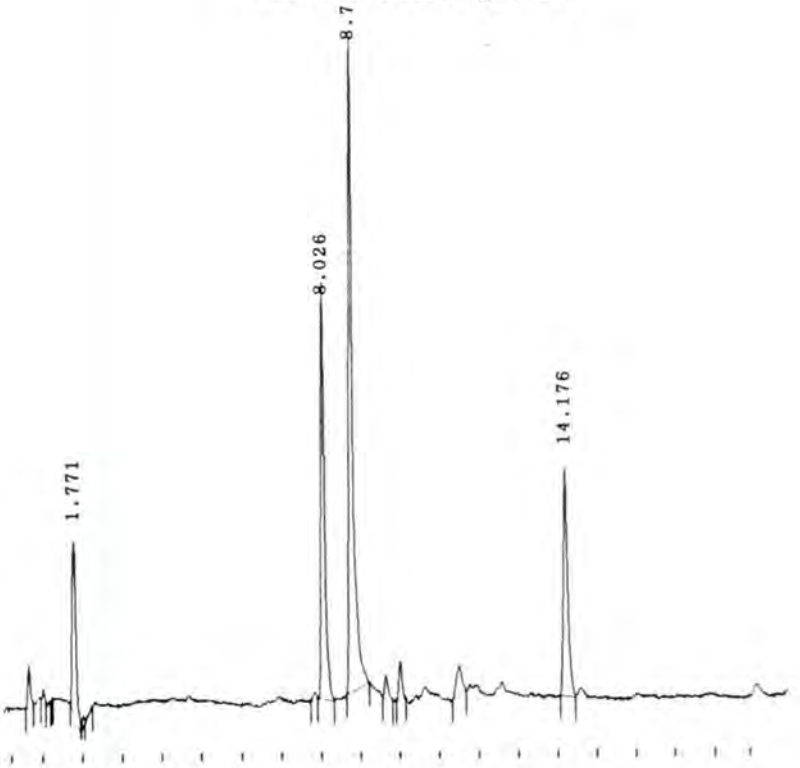

U.V. Spectra Of Components

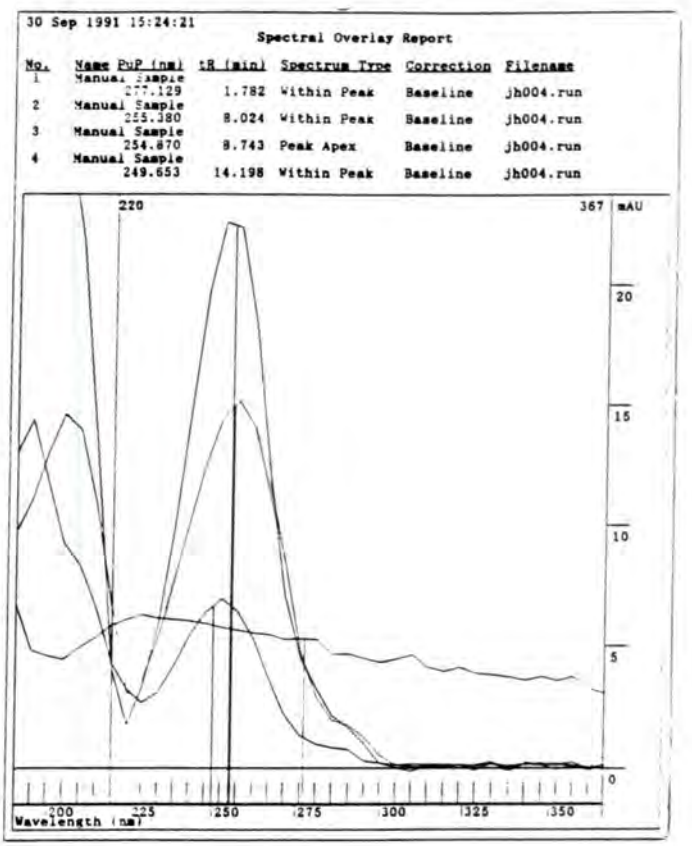

Fig. 3.36
HPLC Chromatogram 5

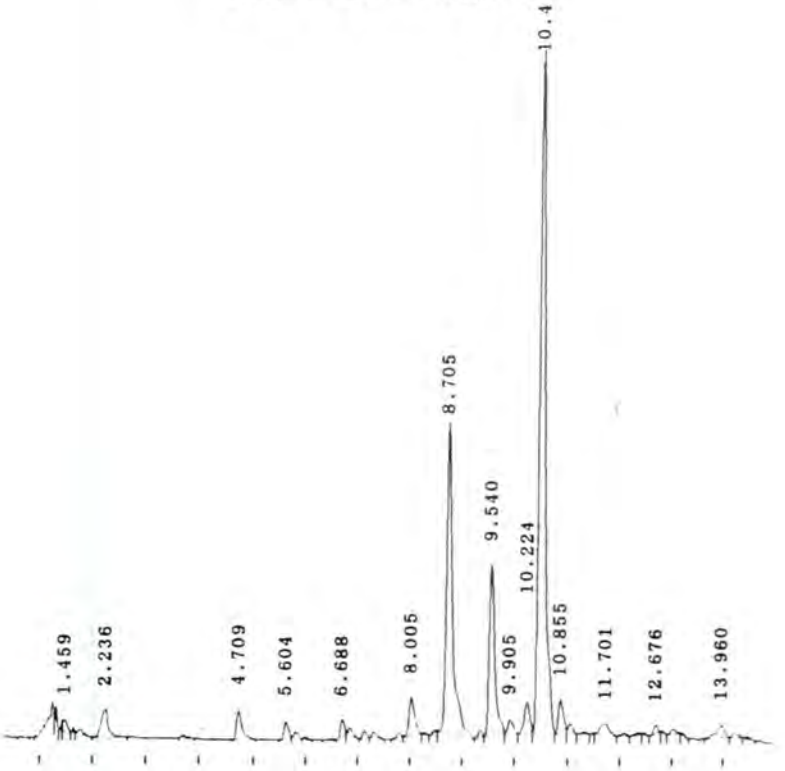

U.V. Spectra Of Components

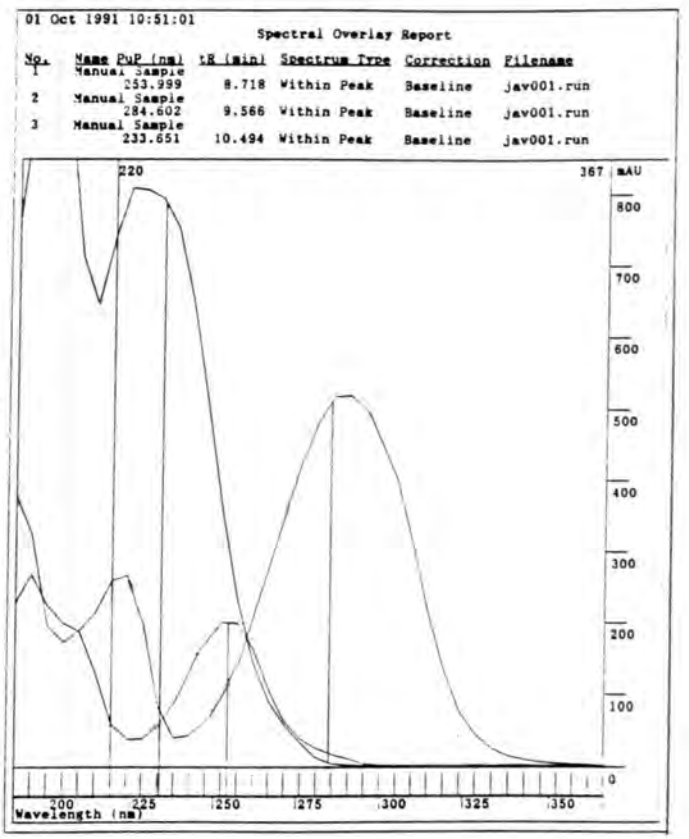

3.9 Synthesis Of Tetraacetyl-tetraazaisowurtzitane (TAIW)

It was found that reductive debenzylation of HBIW (3.1a) and simultaneous acetylation gave a tetra-acetylated isowurtzitane derivative known as TAIW[34] (3.17 (eqn.3.5).

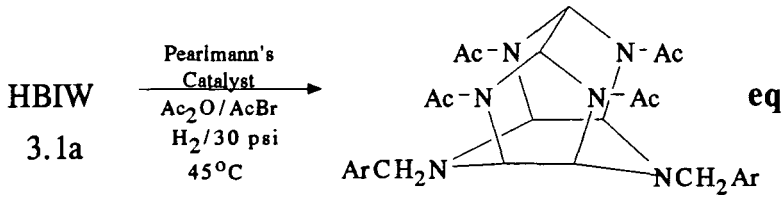

eqn. 3.5

3.17

Ar = C_6H_5
Ac = CH_3CO

^{1}H NMR of 3.17 shows debenzylation and acetylation has only occurred at the nitrogens in the two five-membered rings. A deuteriated derivative was also prepared using HBIW-d_{12} (3.1j).

TAIW (3.17) is found to be very stable in acidic media showing no decomposition. The ^{1}H NMR of 3.17 was unaffected in the presence of three equivalents of acid. The U.V. spectrum after 24 hours in acetonitrile containing a twenty fold excess of acid also showed no change.

3.9.1 Mass Spectrum

The C.I. mass spectrum is that expected for TAIW. There are peaks at at 517 (M+1) and 518 (M+2) (fig. 3.37).

Fig. 3.37

C.I. Mass Spectrum Of TAIW

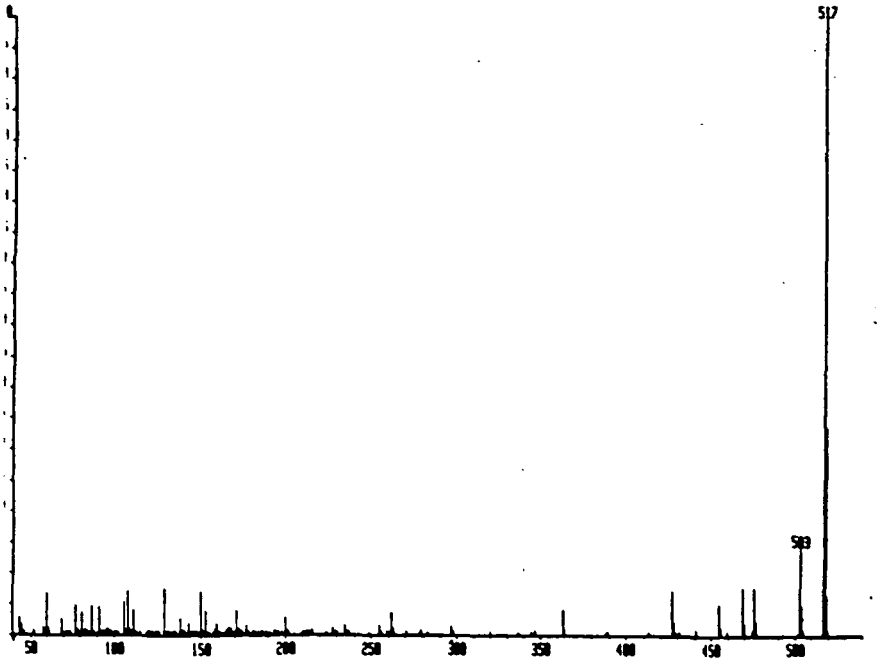

3.9.2 ^{1}H NMR

The ^{1}H NMR spectrum (500MHz) of 3.17 in $CDCl_3$ is fairly complex indicating the presence of two, possibly three isomers due to restricted rotation about the N-Ac bonds (fig. 3.38) (table 3.9). Assignments were also aided by comparison of ^{1}H NMR spectra using TAIW-d_4 (3.18) (fig. 3.39).

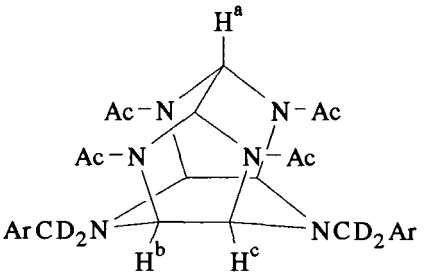

3.18

Ar = C_6H_5

The spectrum is compatible with three isomers 1, 2, and 3 in each case of which two carbon functions point down. In isomer 1 the carbonyl groups at nitrogens N1 and N3 point down while those at N2 and N4 point up. This leads to equivalence of the methine hydrogens H^a which give a singlet, but to non-equivalence of H^b and H^c which exhibit coupling (J=6.7Hz). Similarly non-equivalence of the benzyl methylene protons results in spin-coupled bands (J=14Hz).

In isomer 2, with the carbonyl functions at N1 and N2 pointing up and the carbonyl groups at N3 and N4 pointing down, the methine hydrogens H^a are again equivalent and give a singlet. The H^b and H^c protons are non-equivalent and give spin-coupled bands. Now the two methylene hydrogens at N5 are equivalent, and give a singlet, but are distinct from the two hydrogens of the methylene group at N6.

There is also evidence for the presence of the isomer 3 where the carbonyl functions at N2 and N3 point up while those at N1 and N4 point down. Here the two H^a hydrogens are non-equivalent and give doublets while H^b and H^c are equivalent.

Fig. 3.38

^{1}H NMR Spectrum Of TAIW (500MHz)

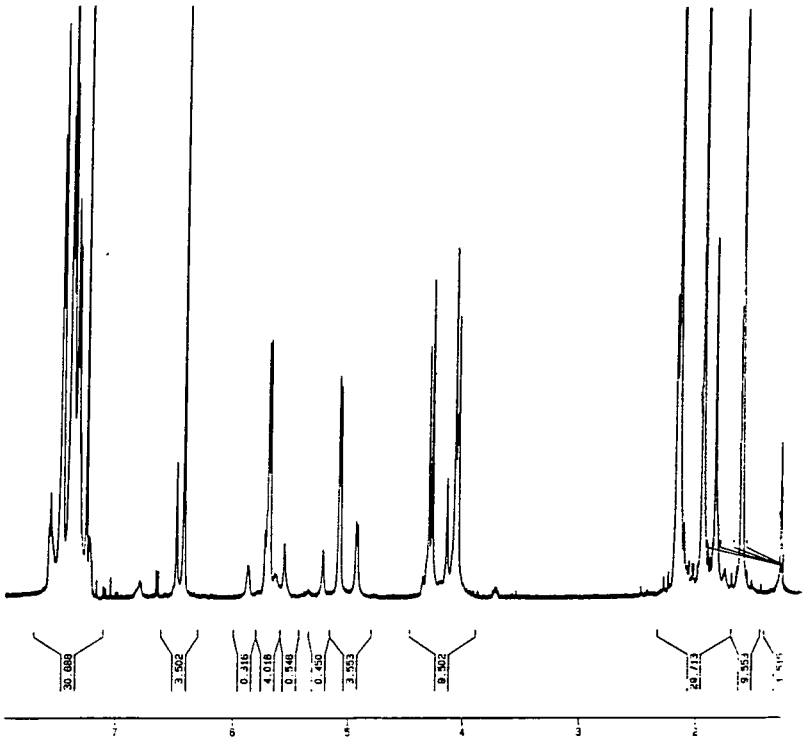

Fig.3.39

^{1}H NMR Spectrum Of TAIW-d_4

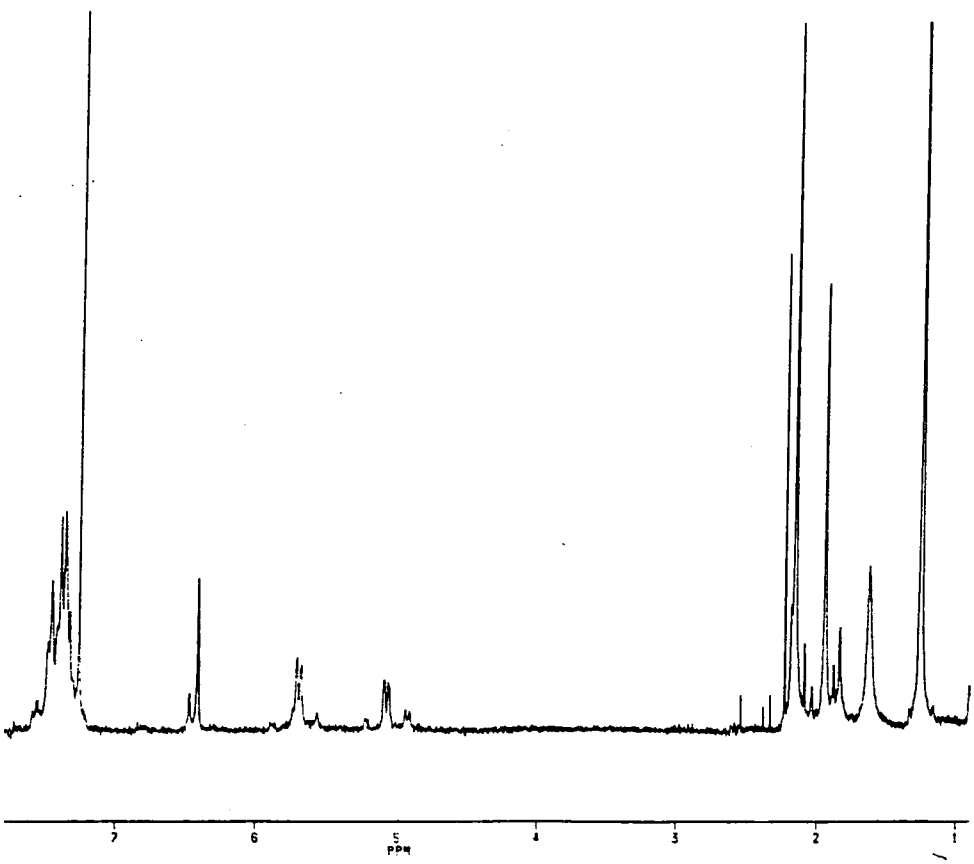

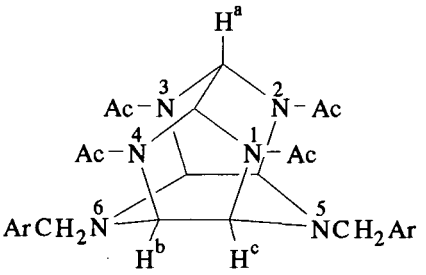

Ar = C_6H_5

Table 3.9
^{1}H NMR Data Of TAIW/$CDCl_3$

	H^a/ppm	H^b/ppm	H^c/ppm	$H(CH_2)$ Benzyl/ppm	CH_3/ppm
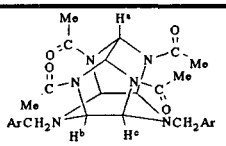 1	6.42(s)	5.69(d) J=6.7Hz	5.08(d) J=6.7Hz	4.28(d) 4.04(d) J=14Hz	2.16(s) 1.95(s)
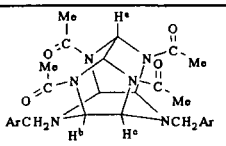 2	6.50(s)	4.93(d) J=6.7Hz	5.72(d) J=6.7Hz	4.14(s) 4.06)(s)	2.18(s) 1.89(s)
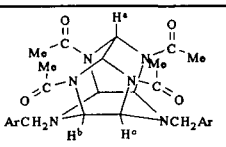 3	6.6(d)	5.23(s)	5.57(s)	a	a

a) Bands obscured by those due to other isomers

The ^{13}C NMR (fig. 3.40) shows only bands for the major isomer (1) (table 3.10)

Table 3.10
^{13}C NMR Data For TAIW/$CDCl_3$

	CH_3/ppm	CH_2 Benzyl/ppm	CH Methine/ppm	C Aromatic/ppm	CO Carbonyl/ppm
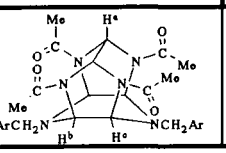	22.13, 20.70	56.32	70.44, 69.56	128-136	168.25

Fig. 3.40

^{13}C Decoupled NMR Of TAIW

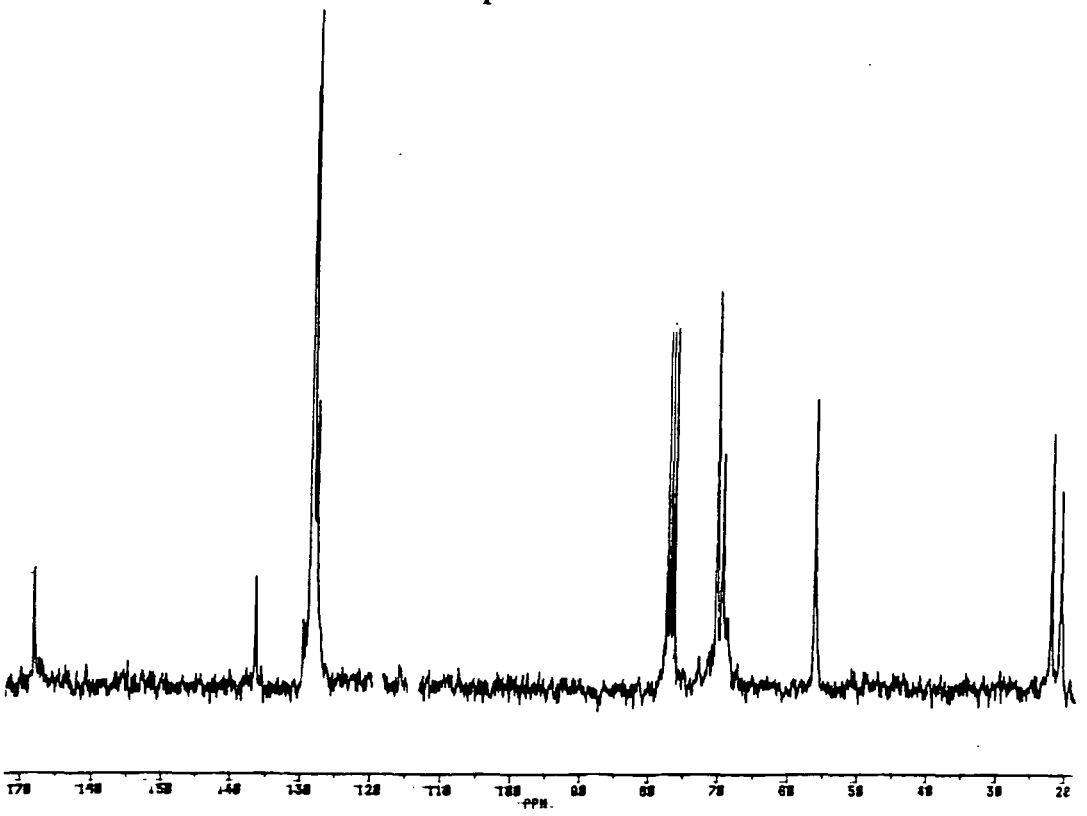

3.10 Attempted Preparation Of The 4-Nitrobenzyl Derivative Of HBIW

Reaction of 4-nitrobenzylamine with glyoxal under reaction conditions used previously for preparation of other derivatives of 3.1 gave only a red tar after several days. Washing the precipitate with methanol (1-2 hours) and filtration afforded a red/brown powder which could not be recrystallised (M.P. 160-165°C). However, elemental analysis gave results close to those expected for an HBIW (3.1) structure. Calculated for 4-Nitrobenzyl derivative of HBIW (3.1) ($C_{48}H_{42}N_{12}O_{12}$) gave C=58.89, H=4.29, N=17.17 and O=20.79%. Obtained C=57.30, H=4.15, N=16.03 and O=22.52%.

The mass spectrum was inconclusive as no evidence of a cage structure could be detected. But it is known that these cage structures are unstable and most readily fragment under the conditions employed for obtaining the spectrum into smaller fragments such as the diimine. The mass spectrum did however show a strong M+1 peak at 311 which may be due to a diimine structure produced as a decomposition product.

The ^1H NMR spectrum of the compound even in very large concentrations (very soluble) in DMSO-d_6 gave a very poor spectrum (fig.3.41). The spectrum, however, did indicate two types of nitro group (δ7.1-7.50) as would be expected for HBIW derivatives (4 nitro groups in the two five-membered rings and two nitro groups in the

six-membered ring) The aliphatic region does show several peaks which may possibly due to those of a HBIW derivative (δ3.5-4.2). A ^{15}Nitrogen NMR confirmed the presence of two types of nitro groups in the compound (fig.3.42). From this evidence it is possible to conclude that we may have formed some 4-nitrobenzyl derivative of HBIW (3.1).

Fig. 3.41
^{1}H NMR Of Red Solid/DMSO-d_6

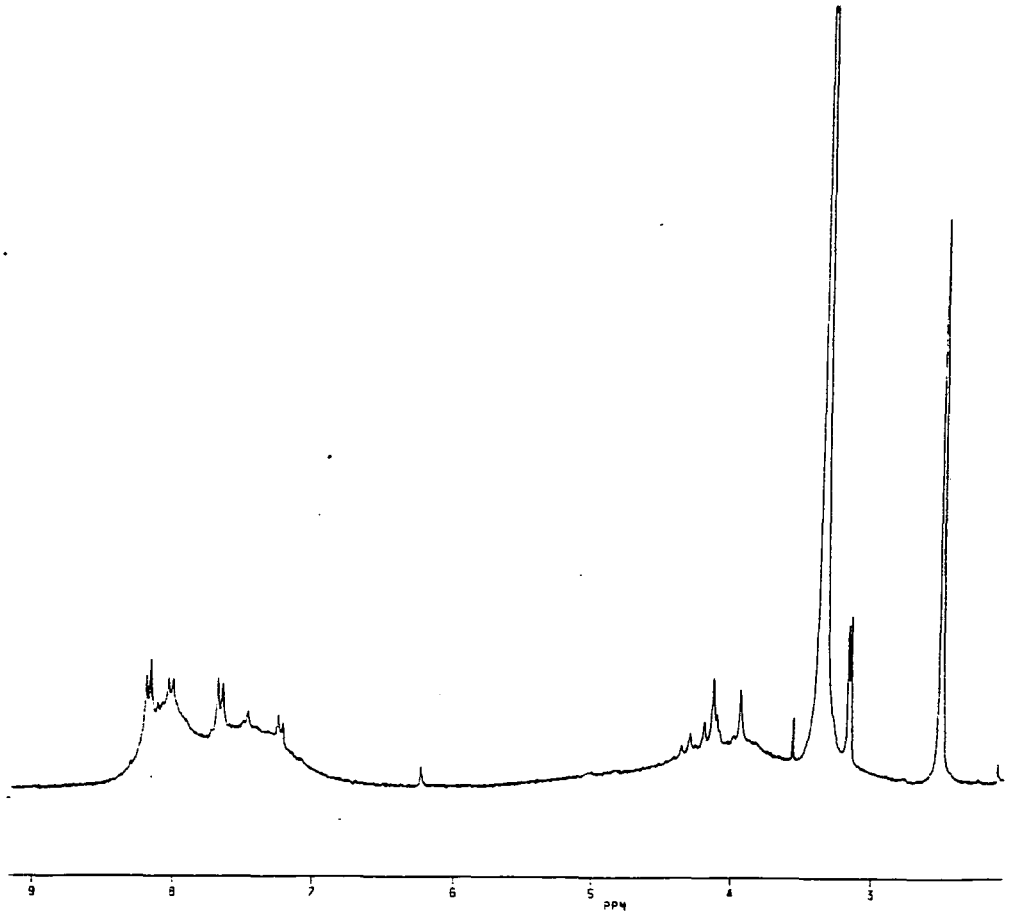

Fig. 3.42
^{15}N NMR Spectrum Of Red Solid/CH_3NO_2

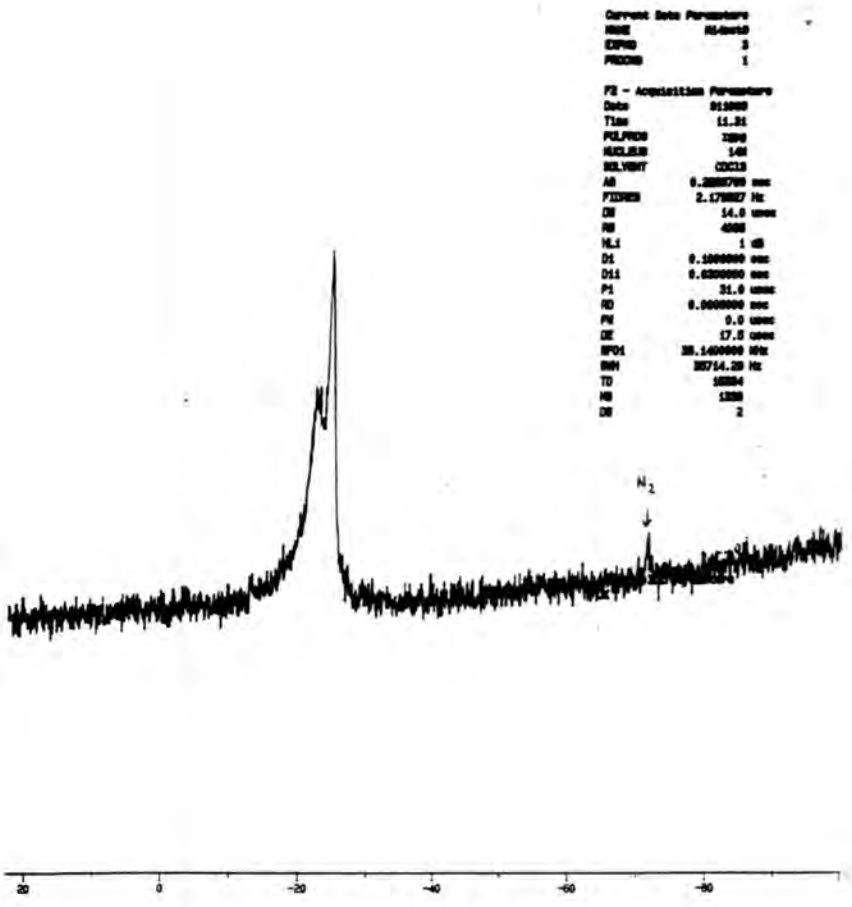

3.11 Experimental

3.11.1 Synthesis Of HBIW Using Procedure 1

40% Glyoxal (121g, 0.83mol) was dissolved in acetonitrile (900cm^3) containing formic acid (0.5cm^3 (98%)). Benzylamine (179g, 1.67mol) was added, with stirring over 30 minutes while keeping the temperature of the reaction mixture below 16°C by cooling it in ice. A further two (0.5cm^3) aliquots of formic acid (98%) were added during the addition of benzylamine. Once all the benzylamine had been added the cooling bath was removed and the mixture was stirred overnight.

The acetonitrile was decanted off from the crude sticky product and 500cm^3 of methanol was added. The mixture was stirred vigorously for *ca* 1 hour then allowed to settle, the methanol decanted off and the process repeated with a second portion of methanol. Finally after decanting the methanol, acetonitrile (250cm^3) was added and a further stirring gave a fine white precipitate which was filtered off, washed with acetonitrile (100cm^3) and dried in a current of air (1-2 hours) and under vacuum overnight to give crude HBIW (3.1a) as a fine white powder, 61g (31%) M.P. 148.5-150.5°C. Recrystallisation from boiling acetonitrile (800cm^3/20g) gave pure HBIW (3.1a) as colourless needles M.P. 153°C.

Procedure 2 was a scaled down version of procedure 1 in which benzylamine (14g, 0.13mol) was added to 40% glyoxal (9.48g, 0.065mol) containing nitric acid catalyst (0.4cm^3, (70%)) in 250cm^3 of acetonitrile over 40 minutes at 25°C. No further aliquots of acid were added after the initial addition.

All derivatives were obtained by following procedure 2 except 3.1g (2-fluoro) and 3.1h (2-methoxy). In the case of 3.1g the reaction was carried out according to procedure 2 but after all the benzylamine had been added the mixture was left for several days, after which all the acetonitrile solvent was taken off on a rotary evaporator at 45°C. Addition of methanol (10cm^3) to the resulting tarry red/brown solid induced precipitation of crude 3.1g. A further 150cm^3 of methanol was added to complete precipitation and the solution filtered. The crude 3.1g was finally washed with cold methanol (30cm^3) to give a white solid. Recrystallisation from hot methanol gave pure 3.1g as colourless needles M.P. 124-126°C.

In the case of 3.1h the acetonitrile was taken off on a rotary evaporator after 24 hours and then the tarry red liquid left for 4-5 days. Cyclohexane:chloroform (80:20 v/v) was added (2cm^3) to facilitate precipitation and the mixture left for 10-15 minutes. Once precipitation occurred cold methanol was added (150cm^3) and the resulting crude 3.1h isolated by filtration and washed with 30cm^3 of methanol to yield a white solid. Recrystallisation from cyclohexane gave pure 3.1h M.P. 134-136°C.

3.11.2 Synthesis Of TAIW (Reductive Debenzylation)

In a Parr shaker-type hydrogenator equipped with a 2L glass pressure bottle and heating jacket, recrystallised HBIW (3.1a) (47g) was reduced using Pearlmann's catalyst under 1-2 atmospheres H_2 in the following manner:-

The bottle was filled with argon and charged with the catalyst (8-9g). Freshly distilled acetic anhydride[a] (*ca* 750cm^3) was then added, followed by the HBIW and finally acetyl bromide co-catalyst (*ca* 1g). The bottle was then briefly evacuated and flushed four times with hydrogen and finally pressurised to 28-29 psi. Shaking was then started and the pressure and temperature were monitored.[b] Typically, an exotherm of 7 to 8°C occurred within 30-40 minutes of the start of the reaction (pressure dropped 12-15 psi at this time); after 2 hours, heating was commenced and the temperature was raised progressively to 45^{0}C over 1.5 hours. At this time, or once the pressure had fallen below *ca* 5 psi, the system was recharged with hydrogen to 21-22 psi and shaking was continued until the uptake of hydrogen had fallen off to less than 1.5 psi in 0.5 hours (approximately 3.5 hours after commencement of heating. Heating and shaking were then discontinued and the reactor was allowed to stand (under 12-14 psi of hydrogen) overnight.

The bottle was vented, filled with argon, then cautiously unstoppered with washing of catalyst from the neck of the bottle using a little acetic anhydride. The mixture was then filtered (filter paper) such that the residue (product and spent catalyst) did not dry out; the slurry was transferred to a large round-bottomed flask, chloroform (750cm^3) was added, and the suspension was refluxed with gentle heating (caution-bumping) for 2-3 hours. Meanwhile, the solvent was removed from the filtrate (Rotavap./oil pump, temperature below 55°C) to give, after *ca* 3 hours, a sticky pale-brown solid which was triturated with acetonitrile to give TAIW (6g). Finally, the chloroform solution was filtered and the filtrate evaporated to dryness (final conditions as before) to give TAIW as a fine white powder (17g). The IR spectrum shows ν_{max} (C=O) 1687, 1650 and 1642cm^{-1} (fig.3.44) and the U.V. spectrum gives λ_{max} 230nm, ε= 23,000 mol^{-1}dm^{3}cm^{-1}. The spent catalyst from the above filtration was stored under water. The total yield of TAIW thus obtained was 23g (67%) (M.P.°C 298-300°C (darkening of sample occurs prior to melting)).

Fig.3.44
I.R. Spectrum Of TAIW

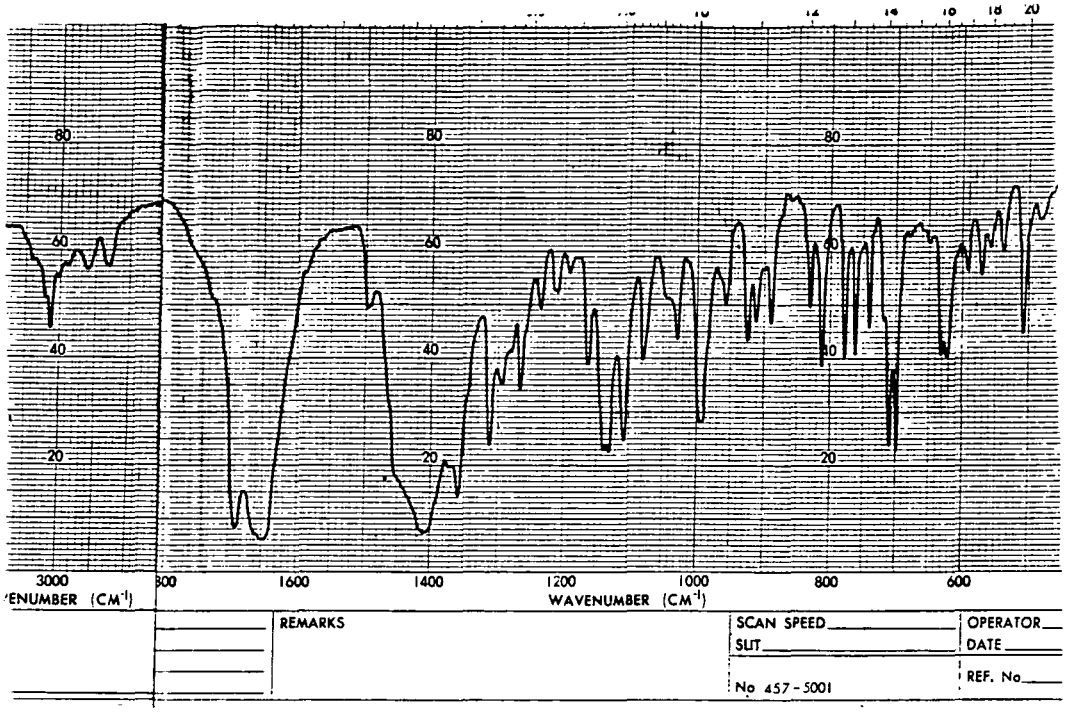

3.11.3 Synthesis Of TAIW-d_4

TAIW was prepared on 1/47th scale of that for TAIW using HBIW-d_{12} (3.1j). The overall yield of TAIW-d_4 was 19%. The ^1H NMR showed absence of benzyl CH_2 protons δ4.04-4.28 (M.P. 303-305°C).

3.11.4 Preparation Of Salts Of HBIW

3.11.4a Preparation Of Hexabenzylhexaazaisowurtzitane Dihydrochloride Monohydrate

HBIW (3.1a) (2g, 0.003mol) was dissolved in methylene dichloride (5cm^3). Hydrochloric acid (12M, 3cm^3) was added dropwise and the mixture stirred vigorously for a few minutes until precipitation of the salt was complete. The salt was immediately filtered and washed with cold methanol to give 1.78g of the dihydrochloride salt (79% yield). The salt was then dried for 6 hours at 0.1mm Hg to give a white powder M.P. 123-125°C. Elemental analysis calculated for HBIW2HCl.H_2O ($C_{48}H_{52}N_6Cl_2O$) gave C=72.21, H=6.25, N=10.50 and Cl=8.75. Found C=72.01, H=6.19, N=10.42 and Cl=8.60.

3.11.4b Preparation Of Hexabenzylhexaazaisowurtzitane Dihydrobromide Monohydrate

Prepared as above except using hydrobromic acid (47%, 3cm^3). Gave 1.7g dihydrobromide salt (68% yield) after 15 minutes stirring. The salt was dried as above to give a white powder M.P. 122-124°C. Some decomposition occurred during drying. Elemental analysis, calculated for HBIW2HBr.H_20 ($C_{48}H_{52}N_6Br_2O$) gave C=64.86, H=5.85, N=9.45 and Br=18.01. Found C=64.63, H=5.69, N=9.42 and Br=17.90.

3.11.4c Preparation Of Hexabenzylhexaazaisowurtzitane Dihydroperchlorate Monohydrate

Prepared as for dihydrochloride except using perchloric acid (10M, 3cm^3). Gave 2.1g of the dihydroperchlorate salt after 5 minutes (80% yield), which after drying gave white solid (some decomposition occurs during drying) M.P. 127-128°C. Elemental analysis calculated for HBIW2$HClO_4$.H_20 ($C_{48}H_{52}N_6Cl_2O_9$) gave C=62.20, H=5.61, N=9.07 and Cl=7.55. Found C=62.03, H=5.55, N=9.02 and Br=7.02.

3.11.4d Preparation Of Salts Using 4-Chlorobenzylisowurtzitane (3.1c)

Similarly hydrated salts of 3.1c were prepared using the same procedures.

4-Cl-HBIW2HClO$_4$.H$_2$O (white solid) M.P. 126-128°C Yield 73%.

4-Cl-HBIW2HBr.H$_2$O (whit solid) M.P. 130-133°C Yield 60%.

4-Cl-HBIW2HCl.H$_2$O (white solid) M.P. 110-112°C Yield 71%.

3.11.5 Preparation Of Deuteriated HBIW-d$_{12}$ (3.1j) And 4-Cl-HBIW-d$_{12}$ (3.1i)

40% Aqueous glyoxal (1.52g, 0.010mol) was added to benzylamine-α,α-d$_2$-N,N-d$_2$ (2.3g, 0.021mol) in acetonitrile (100cm^3) containing nitric acid catalyst (0.007cm^3, 70%) over 40 minutes with continuous stirring. After an hour precipitation of crude HBIW-d$_{12}$ occurred and the mixture was left to stir overnight. The crude HBIW-d$_{12}$ was then filtered, washed twice with methanol (two 100cm^3 aliquots) before being recrystallised from boiling acetonitrile (100cm^3) to give 1.1g of HBIW-d$_{12}$ as fine colourless needles M.P. 145-147°C. ^{1}H NMR shows absence of benzyl methylene protons (δ4.03 and 4.08). Methine ring protons and aromatics appear at δ3.57 (2H) and 4.16 (4H) and δ7.19-7.25 (30H) respectively (fig.3.8).

Preparation of 4-chloro-HBIW-d$_{12}$ was conducted in a similar manner except 4-chlorobenzylamine-α,α-d$_2$-N,N-d$_2$ (1.40g 0.009mol) was used instead of benzylamine-α,α-d$_2$-N,N-d$_2$. The amount of glyoxal was adjusted accordingly to give the correct stoichiometry. The yield of 4-chloro-HBIW-d$_{12}$ was only 0.32g (10%) M.P. 190-192°C. The chloro derivative was recrystallised from methylene dichloride. ^{1} H NMR spectrum shows the absence of benzyl methylene protons (δ3.89 and 3.99). Methine ring protons and aromatics apppear at δ3.55 (2H) and 4.06 (4H) and δ7.01-7.27 (24H) respectively (fig.3.7).

3.11.6 Preparation Of N,N'-Dibenzyl-1,2-ethanediimine (3.12)

40% Aqueous glyoxal (4.00g, 0.027mol) was added dropwise, with stirring to a mixture of benzylamine (5.90g, 0.055mol) in aqueous ethanol (40cm^3 50% v/v) containing nitric acid catalyst (0.005cm^3 (70%)) over 10 minutes while keeping the temperature below 0°C (dry-ice or ice-salt cooling). The precipitated crude diimine was stirred for a further 5 minutes before being filtered. The solid white product was washed with ice cold aqueous ethanol (10cm^3) before being dried under vacuum at 0.1mm of Hg for about 1-2hrs. 5.82g crystalline diimine (91%) was obtained containing water of hydration (M.P. 50-60°C) as indicated by the proton NMR. ^{1}H NMR ($CDCl_3$) gave characteristic CHCH vinyl signal at δ8.07 (s) (2H), 4.77 (s) (4H) CH_2 benzyl methylenes and aromatic ring protons at δ7.10-7.37 (m) (10H). Also observed were possible signals due to oligomers of 3.12.

The 4-chloro-diimine was prepared in a similar manner using same molar quantities to give after drying 6.17g (74%) (M.P. 50-70°C). The ^1H NMR ($CDCl_3$) gave CHCH signal at δ8.05 (s) (2H), benzyl methylenes δ4.73 (s) (4H) and aromatic ring protons at δ7.15-7.34 (m) (8H).

3.11.7 Preparation Of 1,2-Bis(benzylamino)-1,2-ethanediol (3.13)

40% aqueous glyoxal (4.00g, 0.027mol) was added dropwise, with stirring to a mixture of benzylamine (5.90g, 0.055mol) in aqueous tetrahydrofuran (40cm^3 50% v/v) containing nitric acid catalyst (0.005cm^3 (70%)) over 10 minutes while keeping the temperature below 0°C (dry-ice or ice-salt cooling). The precipitated crude diol was stirred for a further 5 minutes before being isolated by suction filtration. The gummy white solid product was washed with ice cold water (10cm^3) before being dried by suction for several minutes to give 9.4g of 3.13. The diol contains much water of hydration (M.P. 50-60°C). ^1H NMR spectrum ($CDCl_3$) gave CHCH signal at δ3.2-4.4 (m), (along with signals of THF and possible oligomers of 3.12), 4.63 (s) (4H) CH_2 benzyl methylenes, OH/NH (s) δ4.66 (disappears on addition of D_2O) and aromatic ring protons at δ7.21-7.28 (m) (10H).

The 4-chloro-diol was prepared in a similar manner to give a similarly gummy product (8.2g) (M.P. 50-70°C). ^1H NMR spectrum ($CDCl_3$) gave CHCH signal at δ 3.2-4.4 (m), (along with signals of THF and possible oligomers of 3.21), 4.59 (s) (4H) CH_2 benzyl methylenes, OH/NH (s) δ4.66 (disappears on addition of D_2O) and aromatic ring protons at δ7.22-7.32 (m) (8H).

3.12 References

1. C. A. Cupas; L. Hodakowski, *J. Am. Chem. Soc.*, 1974, 96, 4668.
2. H. Tobler, R. O. Klaus and C. Ganter, *Helv. Chim. Acta,* 1975, 58, 1455
3. L. F. Fieser, *J. Chem. Educ.*, 1965, 42, 408.
4. D. P. G. Hamon and C. F. Taylor *Tetrahedron Lett.* 1975, 155.
5. R. O. Klaus; C. Ganter, *Helv. Chim. Acta,* 1980, 63, 2559.
6. D. P. G. Hammon, G. F. Taylor and R. N. Young, *Aust. J. Chem.*,1977, 03, 589.
7. A. T. Nielsen , S. L. Christian and W. D. Moore, *J. Org. Chem.*, 1987, 52, 1656.
8. J. M. Kliegman and R. K. Barnes, *Tetrahedron,* 1970, 26, 255.
9. J. M. Kliegman and R. K. Barnes, *J. Org. Chem.*, 1970,35, 3140.
10. H. tom Dieck and J. Dietrich, *Chem. Ber.*, 1984, 117, 694.
11. M. D. Hurwitz U. S. Patent 2582,128 Jan 8, 1952; *Chem Abstr.* 1952, 46, 8146f
12. H. tom Dieck and W. I. Renk, *Chem. Ber.*, 1971, 104, 92
13. A. T. Nielsen, R. A. Nissan and D. J. Venderah, *J. Org. Chem.*, 1990, 55, 1459.
14. V. T. Ramakrishnan, M. Vedachalam J. H. Boyer, *Heterocycles* 1990, 31, 479.
15. B. Fuchs; A. Ellencweig, *Recl. Trav. Chim.*, 1979, 98, 326.
16. R. L. Willer, D. W. Moore, and C. K. Lowe-Ma, *J. Org. Chem.*, 1985, 50, 2368.
17. R. L. Willer and D. W. Moore, *J. Org. Chem.*, 1985, 50, 2365.
18. J. M. Edwards, U. Weiss, R. D. Gilardi and I. L. Karle, *Chem. Commun.*, 1968, 1649.
19. R. D. Gilardi, *Acta Crystallogr.*, 1972, B28, 742.
20. M. C. Venuti, *Synthesis,* 1982, 61.
21. R. J. Abraham, J. Fischer and P. Loftus, "Introduction to NMR Spectroscopy", Wiley and Sons Ltd. 1988.
22. E. Breitmaier, G. Haas, M. Voelter, "Atlas of ^{13}C NMR Data", Vol I, Heyden and Sons Ltd. 1979.

23. A. T. Nielsen, R. L. Atkins, A. T. Moore, R. Scott, D. Mallory and J. M. La Berge, *J. Org. Chem.*, 1973, 38, 3288.

24. A. T. Nielsen, D. W. Moore, R. L. Atkins, J. Di Pol, *J. Org. Chem.*, 1974, 39, 1349.

25. A. G. Giumanini, G. Verardo, L. Randaccio, N. Bresciani-Pahor and P. Traldi, *J.Prakt. Chem.* 1985, 327, 739.

26. B. Mauze, J. Pornet, M. L. Martin and L. Miginiac, *C. R. Acad. Sci. Paris Ser. C* 1970, 270, 562.

27. J. Graymore, *J. Chem. Soc.* 1932, 1353.

28. A. G. Giumanini, G. Verardo, E. Zangrando, L. Lassiani, *J.Prakt. Chem.* 1987, 329, 1349.

29. G. B. Carter, M. C. McIvor and R. G. J. Miller, *J. Chem. Soc. C* 1968, 2591.

30. Y. S. Dolskaya, G. Y. Kondrateva, N. I. Golovina, A. S. Shashkov and V. I. Kadentsev, *Izv. Akad. Nauk SSSR, Ser. Khim.* 1975, 1812.

31. E. H. Cordes and W. P. Jencks, *J. Am. Chem. Soc.*, 1962, 84, 832.

32. E. F. Pratt and M. J. Kamlet, *J. Org. Chem.* 1961, 26, 4029.

33. R. Grigg and J. Kemp, *Tetrahedron Lett.* 1980, 21, 2461.

34. A. T. Kazaryan, S. O. Misaryan and G. T. Martirosyan, *Arm. Khim. Zh.* 1978, 31, 913; *Chem. Abstr.* 1970, 90, 186707x.

35. Ministry Of Defence, private communication.

Chapter 4

^{1}H N.M.R. Studies Of Protonation Of HBIW And Its Derivatives And, Of The Formation Of HBIW

4.1 Introduction

It has been shown in chapter 3 that NMR spectroscopy can be usefully used to examine the structures of HBIW and its derivatives. In this chapter ^{1}H and ^{13}C NMR measurements are used to investigate the protonation of HBIW and its derivatives. There is the possibility of identifying protonated intermediates in acidic solution prior to decomposition.

An attempt was also made to examine by NMR spectroscopy the formation of HBIW from 1,4-dioxan-2,3-diol (3.11) or from 40% aqueous glyoxal. Measurements were made in both deuterioacetonitrile and deuteriochloroform with the aim of identifying any intermediates during the formation of 4.1.

4.2 Protonation Of HBIW (4.1)

Due to the insolubility of HBIW and its derivatives in acetonitrile measurements were most conveniently made using deuteriochloroform as solvent. Acid was added in the form of 70% aqueous perchloric acid dissolved in deuterioacetonitrile. The concentration of HBIW was 0.01M and all measurements were made on a 250MHz instrument at 25°C unless otherwise stated.

Although HBIW itself is not sufficiently soluble in acetonitrile for NMR measurements, it was found that on the addition of acid (1 equivalent or 2 equivalents) the mono- or di-protonated derivatives dissolved so that spectra could be obtained.

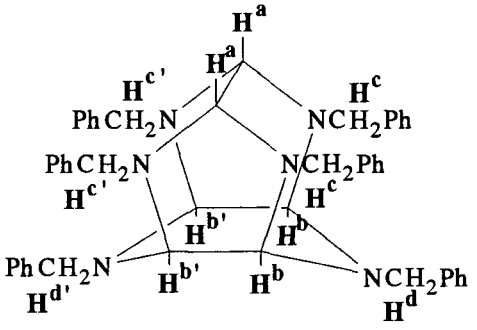

4.1

In deuteriochloroform HBIW gives the spectrum shown in fig.4.1. Comparison with the spectrum of HBIW in which all twelve methylene protons have been deuteriated allows the assignment of bands at δ3.57 (H^a) and 4.16 (H^b and $H^{b'}$) to the ring cage methine protons. These appear in the intensity ratio 2:4. The four methylene protons , H^d and $H^{d'}$, give a singlet at δ4.04, while the eight methylene protons H^c and $H^{c'}$ give an AB quartet centred at δ4.08. The coupling (J=13Hz) is due to geminal interactions between hydrogens on the same carbon atom. The aromatic protons give a multiplet at δ7.17-7.25 representing thirty hydrogens.

Fig. 4.1

^{1}H NMR Spectrum Of 4.1 In $CDCl_3$

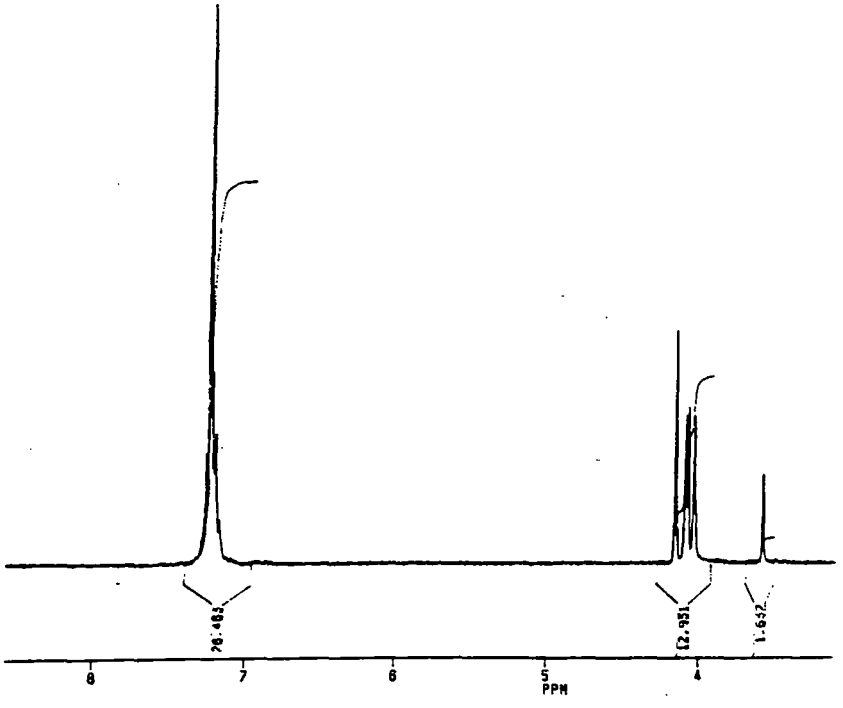

On addition of 1 equivalent of acid an interesting change occurred giving the spectrum shown in fig.4.2. It is known from kinetic studies that HBIW will decompose in the presence of excess acid, however there was no evidence from the NMR spectrum for decomposition over several days when only one equivalent of acid was present. The spectrum is compatible with monoprotonation to give the structure 4.2 in which the proton bridges two nitrogen atoms.

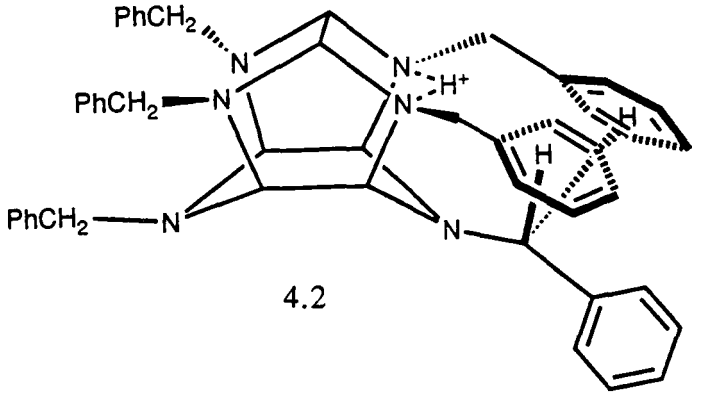

4.2

Data are given in table 4.1. The methine protons H^a show a large downfield shift from δ3.55 to δ5.20 consistent with protonation on the adjacent nitrogens. The methine protons H^b show a smaller shift from δ4.16 to δ4.41. It would be expected that H^b and $H^{b'}$ should have different chemical shifts since protonation occurs only on one side of the cage. It seems probable that these shifts coincide. However, it has been shown by low temperature ^1H NMR in $CDCl_3$ at -60°C that the singlet actually does appear as an AB quartet (J=7Hz) at δ4.39 and δ4.33 respectively. It is shown later on that the spectrum of the monoprotonated species in acetonitrile shows an AB quartet for the H^b and $H^{b'}$ protons. As the two sides of the cage are non-equivalent the H^c and $H^{c'}$ methylene protons are non-equivalent and now appear as two AB quartets (J=13Hz) with shifts of δ3.81 and 4.75 and δ4.12 and 4.41. The band at δ 3.81 appears as a doublet, J=13Hz and the lines are considerably broader than those due to the other methylene protons. This broadening may be attributed to spin-coupling with the added NH proton. This amino proton shows a broad band at δ8.71. the broadness of the bands at δ8.71 and 3.81 is likely to be due to slow exchange of the amino proton with free protons, so that spin-coupling is partially eliminated.

The methylene protons H^d and $H^{d'}$ give bands at δ2.35 and 3.61, compared with a value of δ4.04 in the parent. The non-equivalence of H^d and $H^{d'}$ is expected since protonation occurs on one side of the molecule. The large upfield shift from δ4.04 to δ2.35 may be attributed to a conformational effect which results in the methylene protons being located below the aromatic ring(s) of the benzyl groups at the N2 and N6 (H^c) positions.

Fig. 4.2

^{1}H NMR Spectrum Of HBIW In The Presence Of 1 Equivalent Of Acid In $CDCl_3$

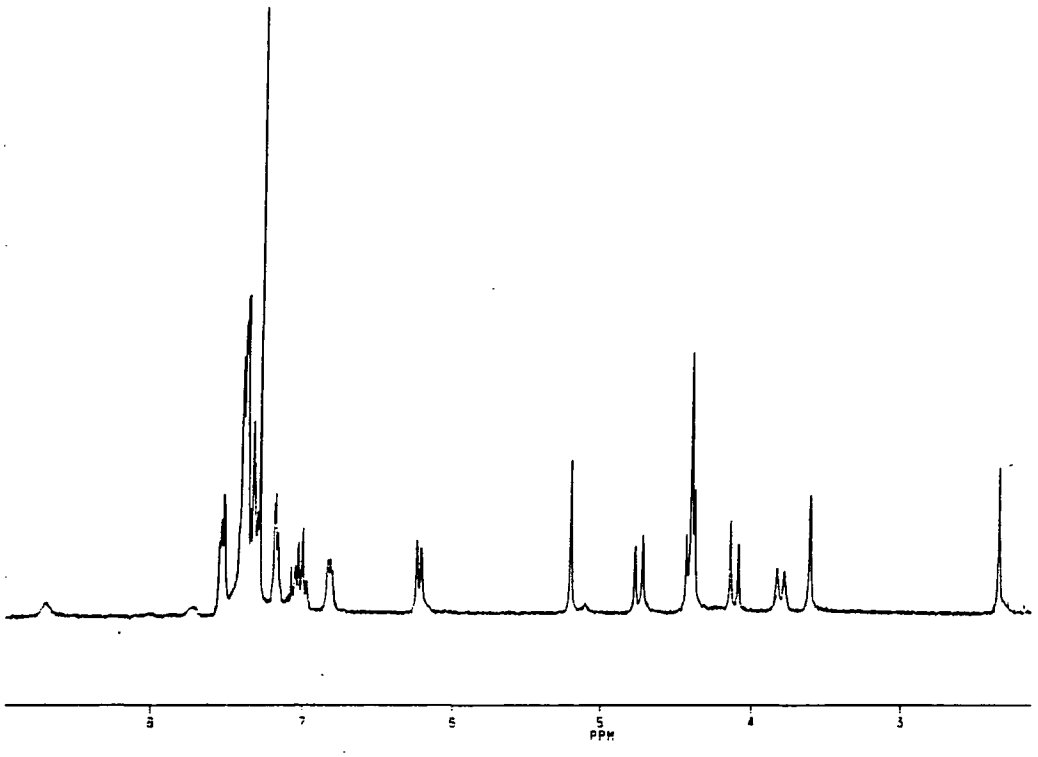

It is known that the ring current in aromatic derivatives may cause shielding of hydrogens directly above and below the ring. A previously noted example[1] is in the spectrum of scopolamine (4.3) where the hydrogens H6 and H7 appear at δ3.37 and 2.70 respectively, considerably upfield from the expected position.

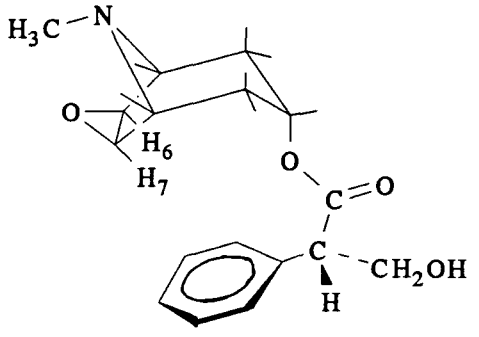

4.3

Table 4.1
^{1}H NMR Protonation Data For HBIW And Its Deuteriated Derivative In $CDCl_3$

Derivative 4.1	H^a /ppm	H^b /ppm	$H^{b'}$ /ppm	H^{c**} /ppm	$H^{c'**}$ /ppm	H^d /ppm	$H^{d'}$ /ppm	Aromatic Protons	NH*** proton
HBIW	3.57	4.16	4.16	4.09	4.09	4.04	4.04	7.17-7.25	-
$HBIWH^+$	5.20	4.41	4.41	3.81 4.75	4.12 4.41	2.35	3.61	6.21-7.59	8.71
$HBIWH_2^{2+}$	6.17	5.06	5.06	4.23	4.73	2.28	2.28	6.20-7.72	8.01
HBIW*	3.56	4.15	4.15	-	-	-	-	7.20-7.26	-
$HBIWH^+$*	5.19	4.40	4.40	-	-	-	-	6.22-7.54	8.71
$HBIWH_2^{2+}$*	6.19	5.08	5.08	-	-	-	-	6.20-7.74	8.01

* Deuteriated derivative

** Coupling J=13Hz is observed between geminal hydrogens.

*** Coupling J=5Hz may be observed between the NH proton and one of the methylene protons on each of the H^c groups. This coupling is lost when proton exchange becomes more rapid.

A further interesting feature is the doublet J=7Hz attributable to two aromatic hydrogens. The fact that a doublet is observed indicates that these are in the 2-position of the benzyl ring. The bands may reasonably be attributed to the hydrogens at the 2-position of the rings at the positions which will be in the closest proximity to the positive charge.

Also seen in the ^1H NMR spectrum are signals due to deuterioacetonitrile (from the acid) and water (δ2.0 and 1.79 respectively). The 500MHz ^1H NMR spectrum of the monoprotonated species is shown in fig. 4.3.

The spectrum is then, consistent with structure 4.2 in which the proton is strongly associated with the two nitrogen atoms in the five-membered rings. It is not possible to say whether the proton is situated symmetrically between the nitrogen atoms (4.4) or rapidly equilibrates between two equivalent structures (4.5).

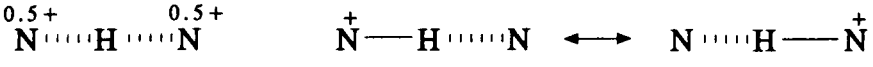

4.4 4.5 4.5

Fig. 4.3
^1H NMR Spectrum Of HBIW In The Presence Of 1 Equivalent Of Acid In $CDCl_3$

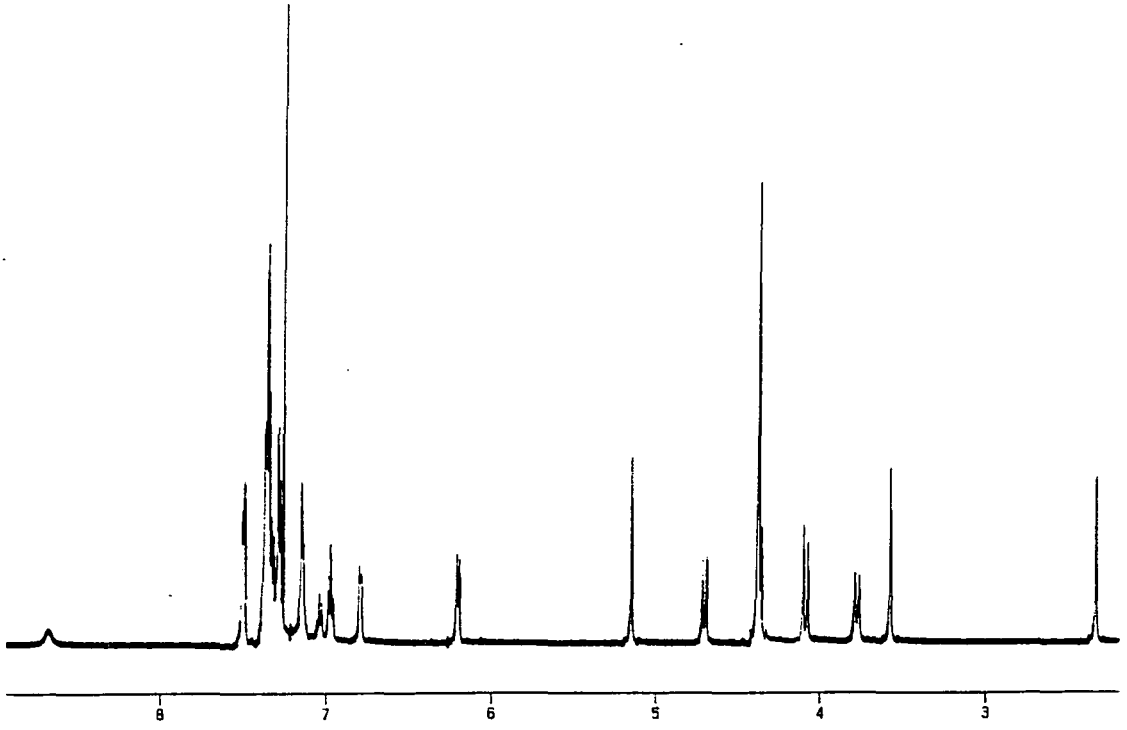

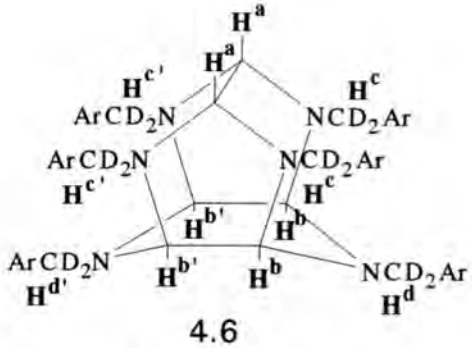

4.6

a) $Ar = C_6H_5$

b) $Ar = C_6H_4Cl$

Fig. 4.4 shows the ^1H NMR spectrum of 4.6a in which the methylene hydrogens have been deuteriated in deuteriochloroform in the presence of 1 equivalent of acid. The aromatic ring protons appear as a multiplet between δ6.21-7.54. The ring cage methine protons appear as a singlet in a 2:4 ratio at δ5.19 and 4.40 respectively. AB quartets due to benzyl methylene protons are absent. No signals due to protons H^d and $H^{d'}$ are observed confirming assignments as previously discussed that these were due to benzyl methylene protons. Peaks due to water and deuterioacetonitrile are also seen at δ2.15 and 1.83 respectively.

The spectrum of 4.6a is shown in fig. 4.5. The aromatic protons are seen to appear between δ7.20-7.26 with the methine ring cage protons H^a and H^b and $H^{b'}$appearing at δ3.56 and 4.15 respectively (see table 4.1).

Fig. 4.4

^{1}H NMR Spectrum Of 4.6a In The Presence Of 1 Equivalent Of Acid In $CDCl_3$

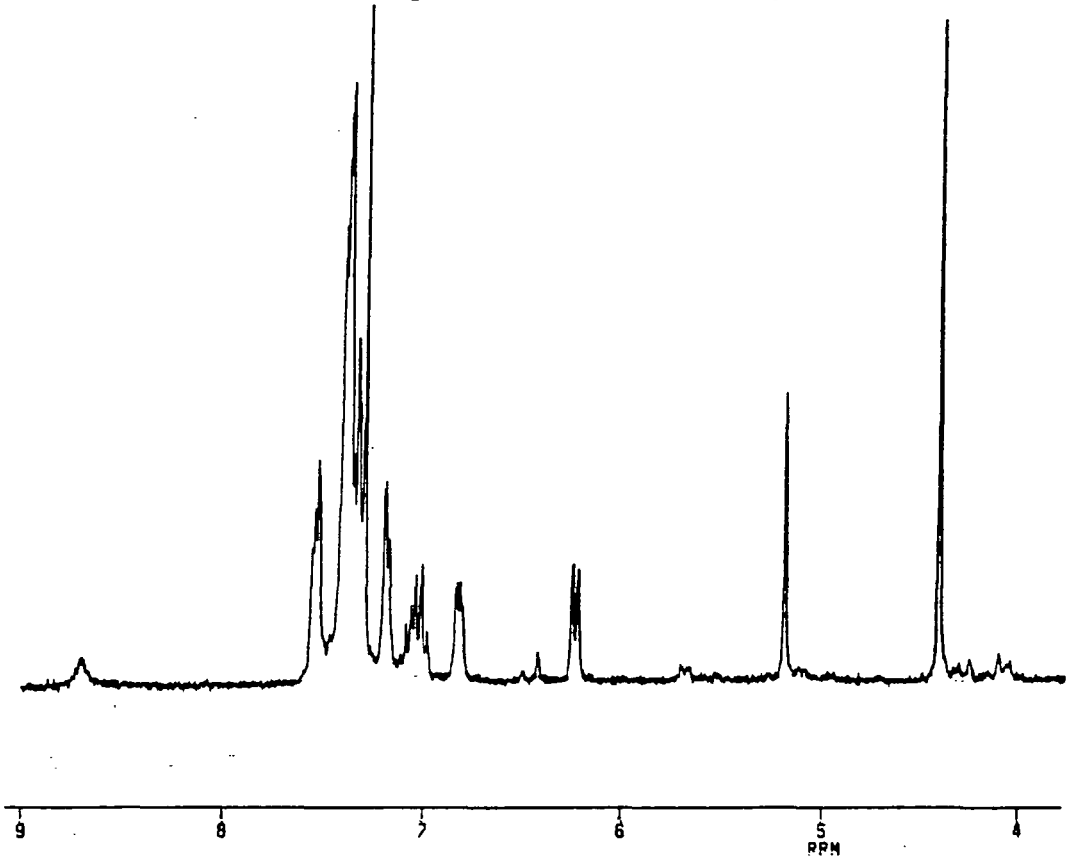

Fig. 4.5

^{1}H NMR Spectrum Of 4.6a In $CDCl_3$

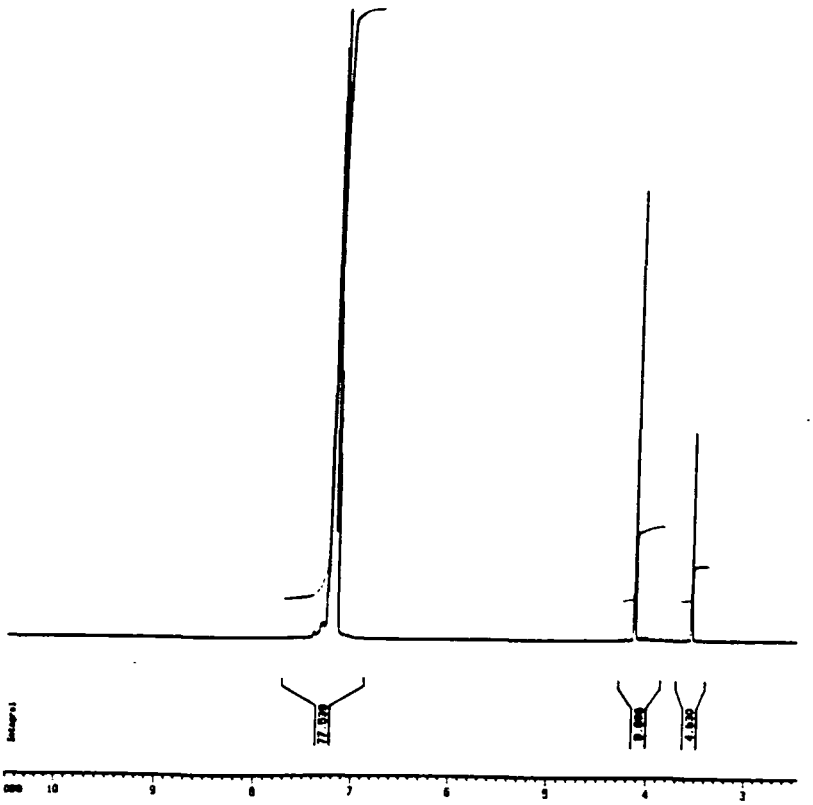

Studies of the protonation of diimines[2-4] have similarly found evidence for monoprotonation involving a proton associated with two nitrogen atoms. Recent studies by Hine and Yeh[5] and Karabatsos and Lande[6] have confirmed that for imines the anti-conformation (E) is generally more stable. There is also evidence from the work of Blackwood[7] and co-workers that aromatic aldimines in which the carbon-nitrogen bond is conjugated with an aromatic ring exist preferentially in the E conformation where E and Z refer to structures 4.7 and 4.8 respectively.

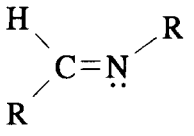

E

4.7

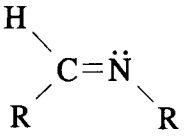

Z

4.8

It is found that the sterically more stable conformations of diimines are 4.9 and 4.10 as only these two conformations allow coplanarity of the aromatic rings with the two carbon-nitrogen double bonds thereby extending the conjugated system.

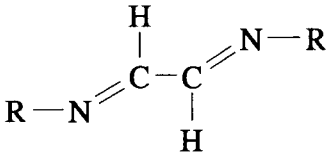

4.9

E-s-trans*-E

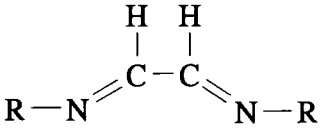

4.10

E-s-cis*-E

* Where *s-cis* and *s-trans* refer to torsional isomers around the central carbon-carbon bond of a 1.3 diene system.

It is thought that in solution 4.9 is preferred. However if this conformation was to be retained on protonation charge delocalisation would be difficult. As shown in (4.11) delocalisation would require proton switching between the two nitrogen atoms.

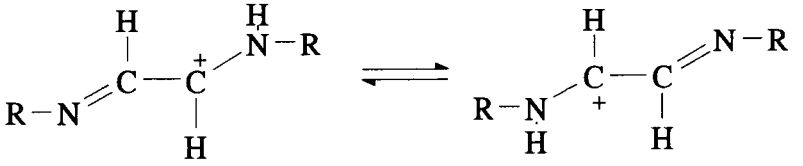

4.11

However, free rotation around the C-C bond of 4.11 will give what is thought to be a planar, resonance stabilised five-membered ring structure containing the diimine linkage and an additional proton (4.12). This is confirmed by titration of the respective diimine with 0.1N perchloric acid in acetic acid[8(*)] which shows them to be essentially monobasic (i.e. titrate for 1 molar nitrogen equivalent and not 2 as would be expected). In one case a crystalline diimine hydroperchlorate salt was isolated.[3] The NMR of 4.12 shows only one type of methine proton as would be expected.

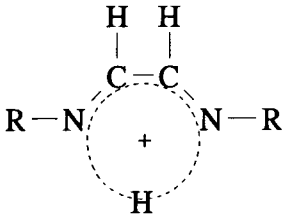

4.12

In the presence of 0.5 equivalents of acid the ^1H NMR spectrum shows bands due to both free HBIW (4.1) and to monoprotonated species (4.2). This indicates that the proton must be held quite strongly by the HBIW molecule so that proton transfer between molecules is slow. This is clearly seen in the spectrum of the 4-Chloro derivative of HBIW (3.1c) (fig.4.6). The spectrum of the 4-Chloro derivative is shown in fig. 4.7 while that of the deuteriated 4-chloro derivative (4.15b) is shown in fig. 4.8. Data are given in table 4.2. Fig. 4.6 shows bands of the ring cage methine protons H^a and H^b and $H^{b'}$ in the 4-Chloro derivative at δ3.55 and 4.06 respectively. The aromatic protons appear between δ6.97-7.27. The benzyl methylene protons H^c and $H^{c'}$ and H^d and $H^{d'}$ appear at δ3.98 and 3.89 respectively. Those due to the monoprotonated species for H^a and $H^{b'}$ and $H^{b'}$ are observed at δ5.15 and 4.36. Protons H^c and $H^{c'}$ appear at δ3.81 and 4.33 and δ4.66 (band at δ4.19 is obscured by parent peak). The methylene protons H^d and $H^{d'}$ appear at δ2.42 and 3.55 the latter appearing as a shoulder on the peak due to the H^a protons in the parent, while the aromatics appear between δ6.21-7.51. The NH proton appears as a broad band at δ 8.68. it was also found that if a slight excess of acid (1.5 equivalents) was used then both the mono- and di- protonated species could be observed (fig. 4.9).

(*) This is the standard titration method using perchloric acid in acetic acid to give the total basicity of amines or Schiff bases, using crystal violet indicator. This involves dissolving the diimine (in this case) in enough acetic acid so that no precipitation of perchlorates takes place. A few drops of 1% crystal violet indicator in acetic acid was added and the solution titrated with 0.1N perchloric acid to a green endpoint. This represents the total basicity.

Table 4.2

^{1}H NMR Data For 4-Chloro HBIW (3.1c) In The Presence Of Acid In $CDCl_3$

Derivative 3.1c	H^a /ppm	H^b /ppm	$H^{b'}$ /ppm	H^{c}** /ppm	$H^{c'}$** /ppm	H^d /ppm	$H^{d'}$ /ppm	Aromatic protons	NH*** proton
4-Cl-HBIW	3.55	4.06	4.06	3.99	3.99	3.89	3.89	6.97-7.27	-
4-Cl-HBIWH$^+$	5.15	4.36	4.36	3.81 4.66	4.19 4.33	2.42	3.55	6.21-7.51	8.68
4-Cl-HBIW*	3.55	4.06	4.06	-	-	-	-	7.01-7.27	-
4-Cl-HBIWH$^+$*	5.16	4.35	4.35	-	-	-	-	6.19-7.51	8.72
(s)4-Cl-HBIWH$_2^{2+}$	6.20	5.30	5.30	4.60	4.93	2.37	2.37	6.20-7.79	8.68

* Deuteriated derivative

** Coupling J=13Hz is observed between geminal hydrogens.

*** Coupling J=5Hz may be observed between the NH proton and one of the methylene protons on each of the H^c groups. This coupling is lost when proton exchange becomes more rapid.

(s) Diprotonated salt of 4-chloro HBIW in deuterioacetone.

Fig. 4.6

^{1}H NMR Spectrum Of 4-Chloro HBIW (3.1c) In The Presence Of 0.5 Equivalents Of Acid In $CDCl_3$

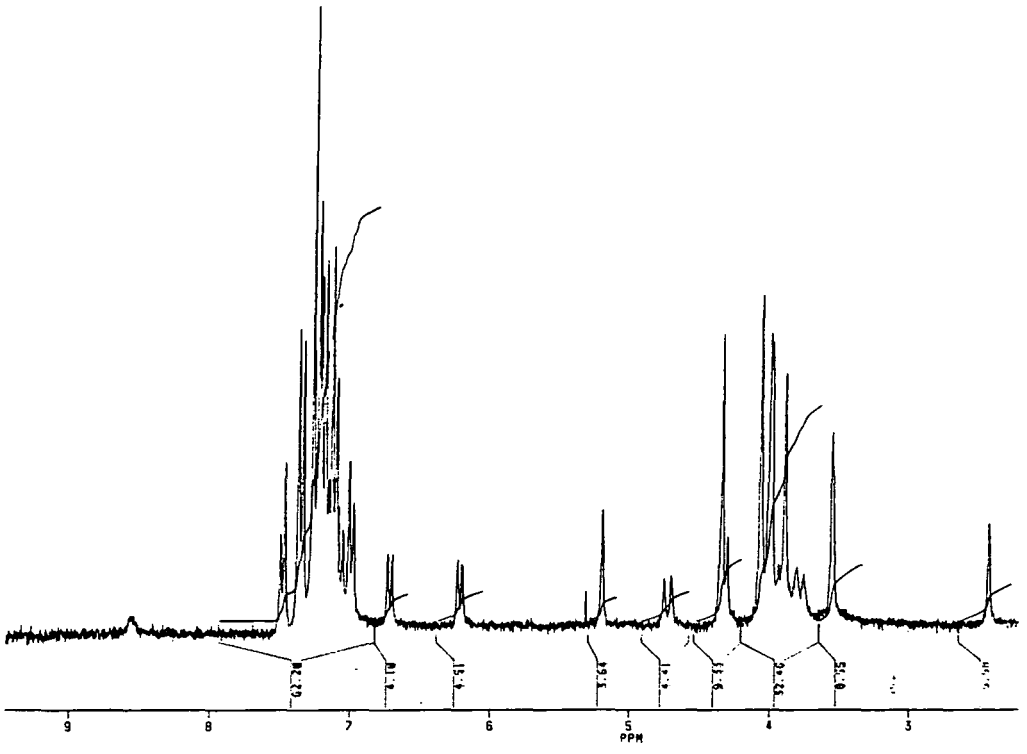

Fig. 4.7

^{1}H NMR Spectrum Of 4-Chloro HBIW In $CDCl_3$

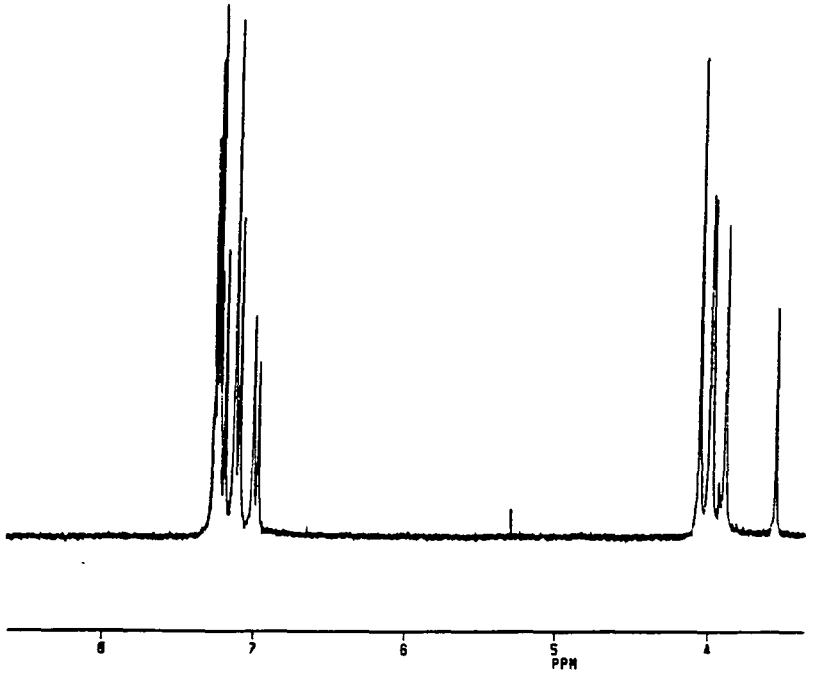

Fig. 4.8

^{1}H NMR Spectrum Of 4-Chloro HBIW (4.6b) In $CDCl_3$

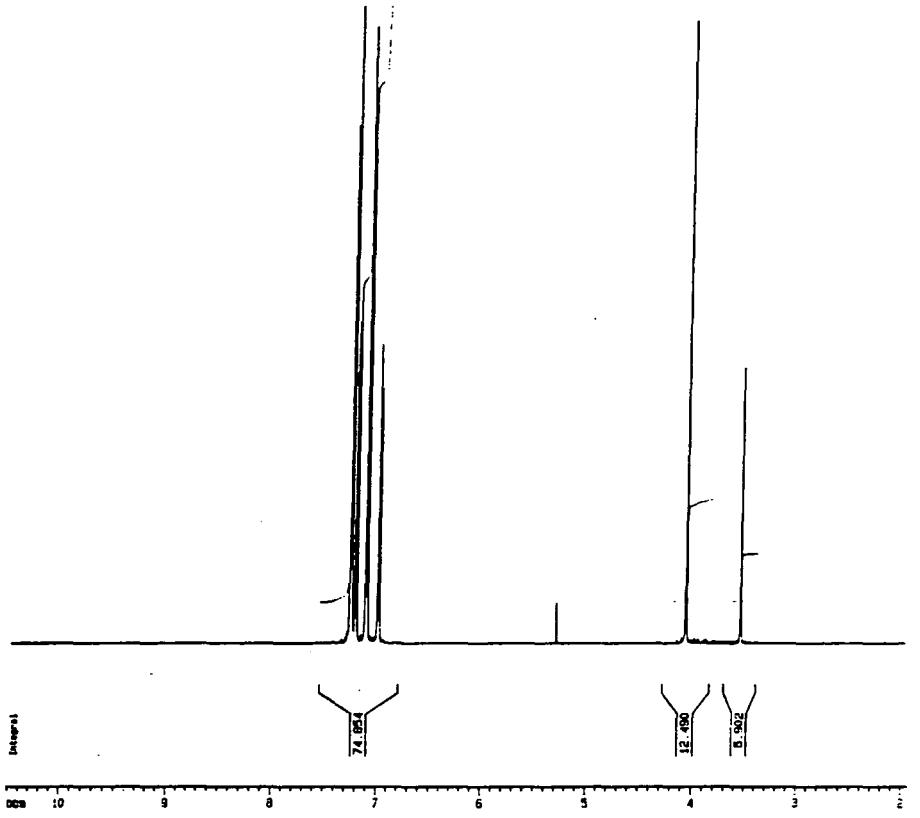

Fig. 4.9

^{1}H NMR Spectrum Of HBIW In The Presence Of 1.5 Equivalents of Acid In $CDCl_3$

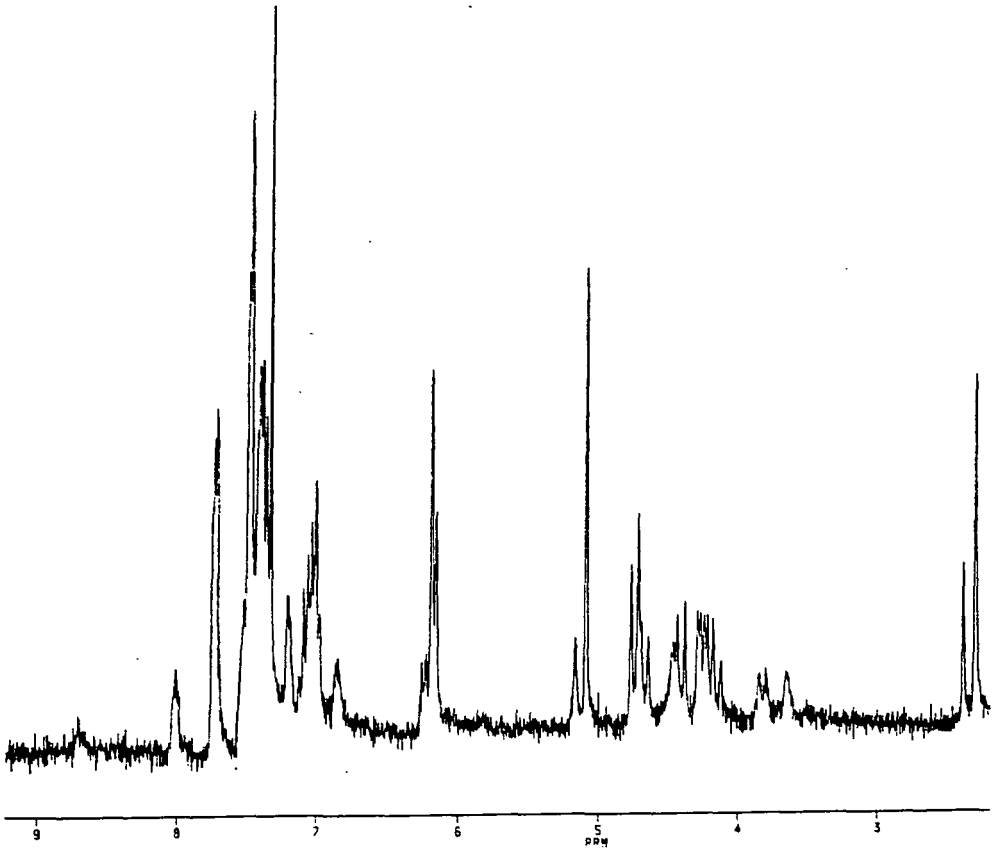

If HBIW is suspended in deuterioacetonitrile and 1 equivalent of acid added all the HBIW dissolves (this is facilitated by placing the solution in a sonic bath for several minutes). This was attributed to the formation of a protonated species, which was shown to be the monoprotonated species (4.2). The ^{1}H NMR spectrum in deutrioacetonitrile (fig. 4.10) showed bands for the monoprotonated species similar to those were also observed in deuteriochloroform. Bands due to benzyl methylene protons H^d and $H^{d'}$ again are found to appear upfield at δ2.55 and 3.69 while the ring cage methine protons H^a are found further downfield at δ4.71. Protons H^b and $H^{b'}$ give an AB quartet (J=7Hz) at δ4.57 and 4.51 (note in deuteriochloroform these appeared as a singlet). One would also expect two AB quartets due to H^c and $H^{c'}$. The H^c protons gave one AB quartet (J=13Hz) at δ3.99 and 4.34. The $H^{c'}$ protons appear as an overlapping quartet (appear as triplet) at δ4.25 and 4.20 respectively, while the aromatics hydrogens appear between δ6.41-7.63. The NH proton signal appearing as a broad band about δ8.49. Fig. 4.11 shows the same spectrum in the presence of a slight excess of acid (1.4 equivalents) except splitting of H^c proton signal due to spin-coupling with the added NH proton is observed indicating proton exchange to be slow. Also seen are signals at δ5.94 (H^a) and 4.92 (H^b and $H^{b'}$) attributed to formation of the diprotonated species.

The spectral assignments were confirmed using deuteriated HBIW (4.6a). The ^{1}H NMR spectrum of deuteriated HBIW (4.6a) in the presence of 1 equivalent of acid in deuterioacetonitrile is shown in fig. 4.12. Only two sets of signals are observed in the aliphatic region due to ring cage methine protons H^a and H^b and $H^{b'}$. H^b and $H^{b'}$ appear as an AB quartet (J=7Hz) at δ4.56 and 4.50 respectively, while the H^a protons appear at δ4.71. The aromatic protons appearing between δ6.42-7.56 with the NH proton signal appearing at δ8.48. The data is summarised in table 4.3.

Table 4.3

^{1}H NMR Data For HBIW (4.1) In The Presence Of Acid In CD_3CN

Derivative 3.1a	H^a /ppm	H^b /ppm	$H^{b'}$ /ppm	H^{c}*** /ppm	$H^{c'}$*** /ppm	H^d /ppm	$H^{d'}$ /ppm	Aromatic protons	NH**** proton
$HBIWH^+$	4.71	4.57**	4.51**	3.99 4.34	4.20 4.25	2.54	3.69	6.41- 7.63	8.49
$HBIWH^+$*	4.71	4.56**	4.50**	-	-	-	-	6.42- 7.56	8.48
$HBIWH_2^{2+}$	5.94	4.92	4.92	4.70	4.21	2.27	2.27	6.19- 7.67	7.91

* Deuteriated derivative

** Coupling J=7Hz is observed between H^b and $H^{b'}$.

** Coupling J=13Hz is observed between geminal hydrogens.

****Coupling J=5Hz may be observed between the NH proton and one of the methylene protons on each of the H^c groups. This coupling is lost when proton exchange becomes more rapid.

Fig. 4.10

^{1}H NMR Spectrum Of HBIW (4.1) In The Presence Of 1 Equivalent Of Acid In CD_3CN

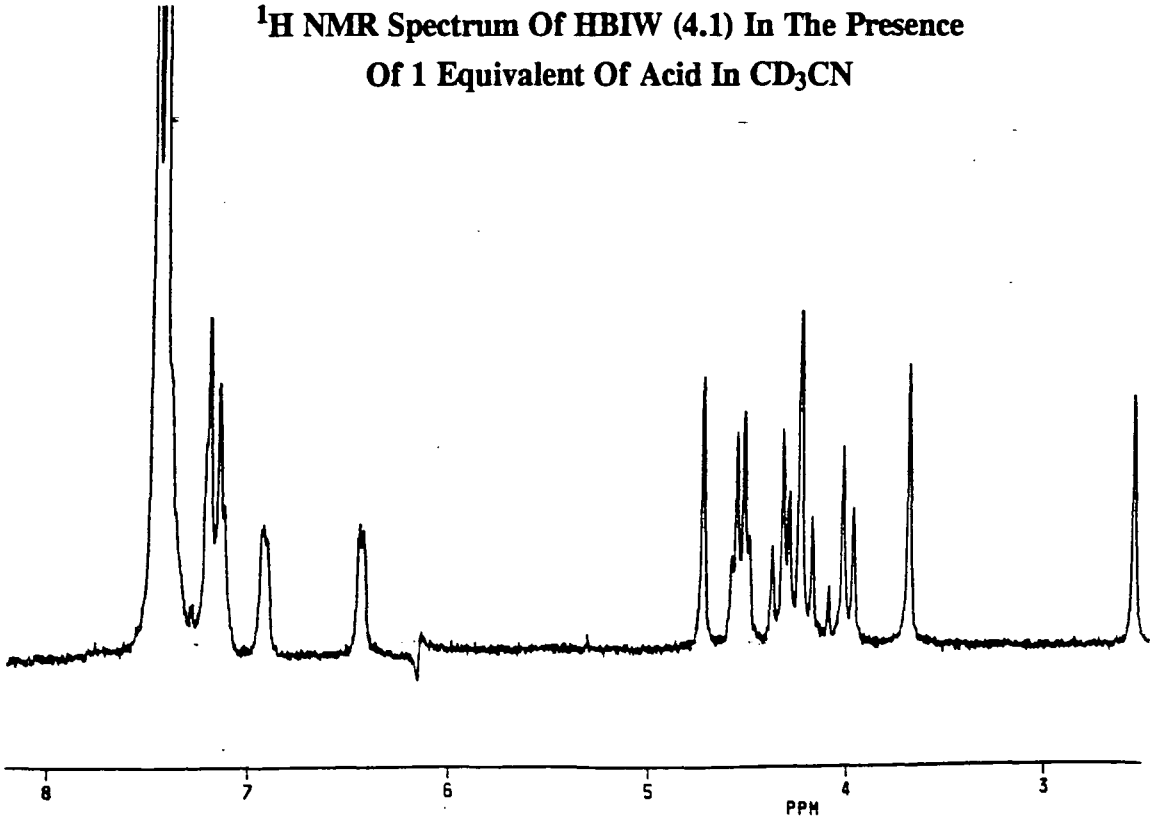

Fig. 4.11

^{1}H NMR Spectrum Of HBIW In The Presence Of 1.4 Equivalents Of Acid In CD_3CN

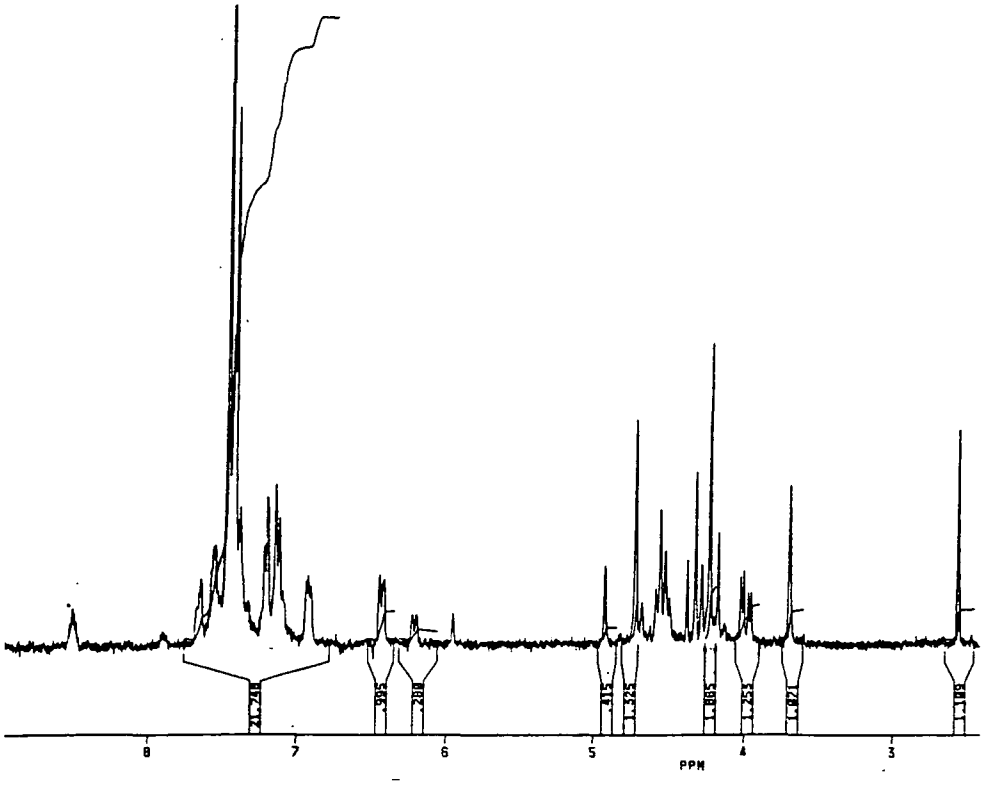

Fig. 4.12

^{1}H NMR Spectrum Of Deuteriated HBIW (4.6a) In The Presence Of 1 Equivalent Of Acid In CD_3CN

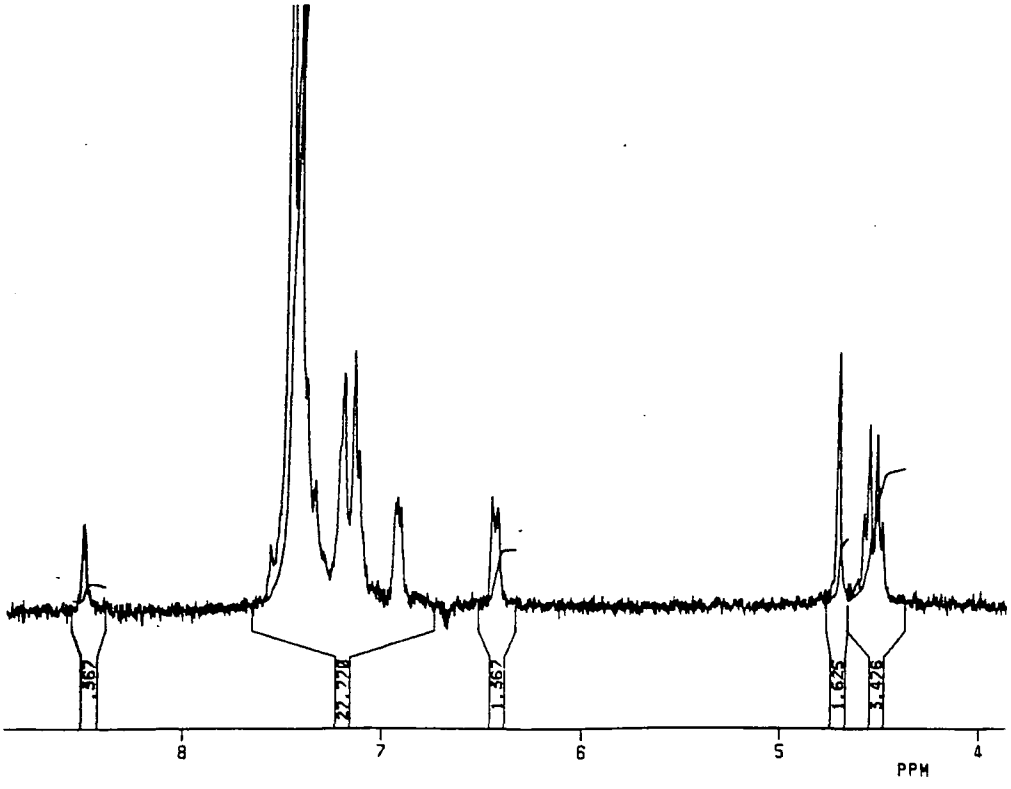

4.3 ^{13}C NMR Of Monoprotonated Species

^{13}C NMR was used as confirmation of the structure of the monoprotonated species. It was shown that the monoprotonated species was stable for several days in deuteriochloroform which facilitated ^{13}C NMR spectra.

The 500MHz ^{13}C proton-decoupled NMR spectrum of the parent is shown in fig. 4.13. The aromatic carbons (structure 4.13) (e) appear between δ126.33-140.39. A signal due to deuterioacetonitrile added with the acid is also observed at δ117. The carbon atoms of the methylene groups C^c and $C^{c'}$ and C^d and $C^{d'}$ appear in a ratio of 8:4 at δ55.84 and 56.51 respectively.

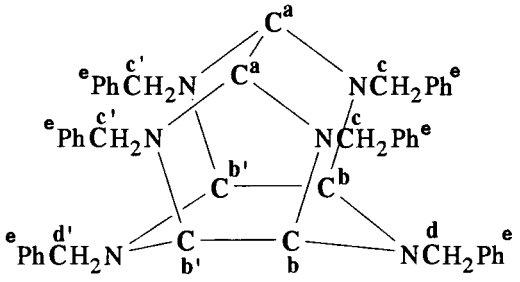

4.13

The methine ring cage carbon atoms C^a and C^b and $C^{b'}$ give bands in a 4:2 ratio at δ76.99 and 80.15.

In the ^{13}C decoupled 500MHz spectrum of the monoprotonated species in deuteriochloroform (fig. 4.14) the methine ring cage carbon atoms C^a and C^b and $C^{b'}$ give three bands of equal intensity at δ84.31, 80.89 and 75.09. The benzyl methylene carbon atoms C^c and $C^{c'}$ give bands at δ58.15 and 55.81 with those at C^d and $C^{d'}$ give bands at δ54.52 and 56.20 respectively. The aromatic carbons (e) appearing between δ127.31-139.43.

Similarly it was also possible to obtain a ^{13}C decoupled NMR spectrum of the monoprotonated species in deuterioacetonitrile as shown in fig. 4.15. In this case the aromatic carbon atoms are found to appear between δ127.31-138.34. The benzyl methylene carbons C^c and $C^{c'}$ give bands at δ57.21 and 54.72 and those due to C^d and $C^{d'}$ appear at δ54.13 and 55.23. The ring cage methines C^a and C^b and $C^{b'}$ again appear as three singlets at δ82.82, 81.53 and 75.36 (see table 4.4).

Table 4.4
^{13}C NMR Data For HBIW In The Presence of Acid

Derivative 3.1a	C^{a}** * /ppm	C^{b}*** /ppm	$C^{b'}$*** /ppm	C^{c}*** /ppm	$C^{c'}$*** /ppm	C^{d}*** /ppm	$C^{d'}$*** /ppm	Aromatic carbons
HBIW*	80.15	76.99	76.99	55.84	55.84	56.51	56.51	126.33-140.39
$HBIWH^{+}$*	84.31	80.89	75.09	58.15	55.81	54.52	56.20	127.31-139.43
$HBIWH^{+}$**	82.82	81.53	75.36	57.21	54.72	54.13	55.23	127.31-138.34

* ^{13}C determined in $CDCl_3$

** ^{13}C determined in $CDCN_3$

*** Assignments confirmed using deuteriated HBIW (4.6a) and/or by coupled/decoupled ^{13}C NMR.

Fig. 4.13
500MHz ^{13}C Decoupled NMR Spectrum Of HBIW (4.1) In $CDCl_3$

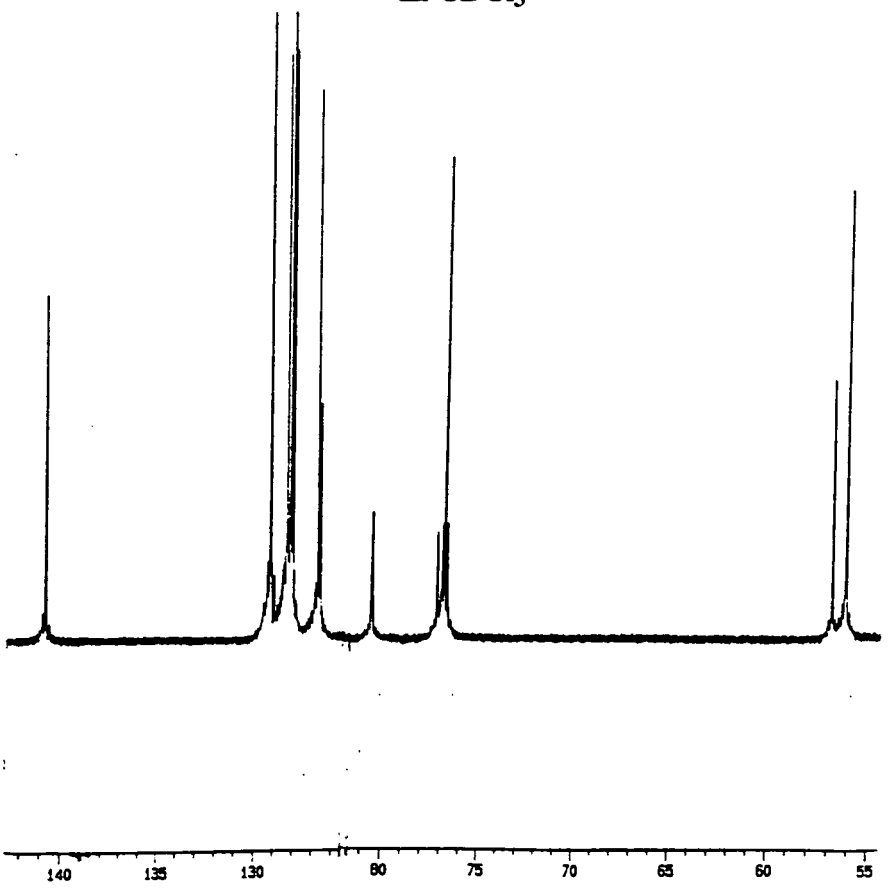

Fig. 4.14

^{13}C Decoupled NMR Spectrum Of HBIW In The Presence Of 1 Equivalent Of Acid In $CDCl_3$

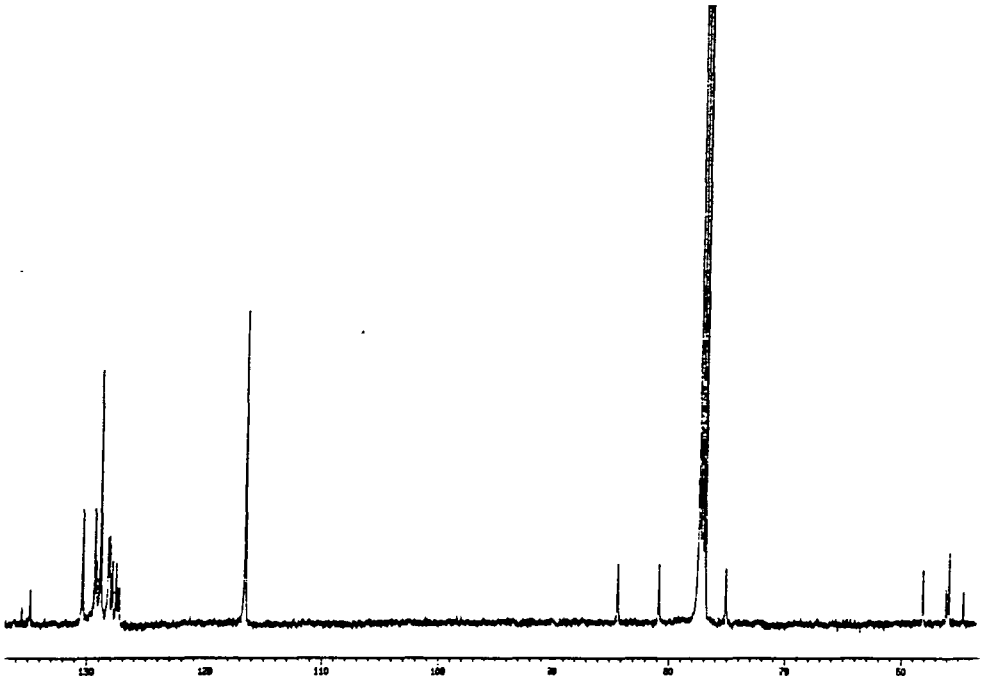

Fig. 4.15

250MHz ^{13}C Decoupled NMR Spectrum Of HBIW In The Presence Of 1 Equivalent Of Acid In CD_3CN

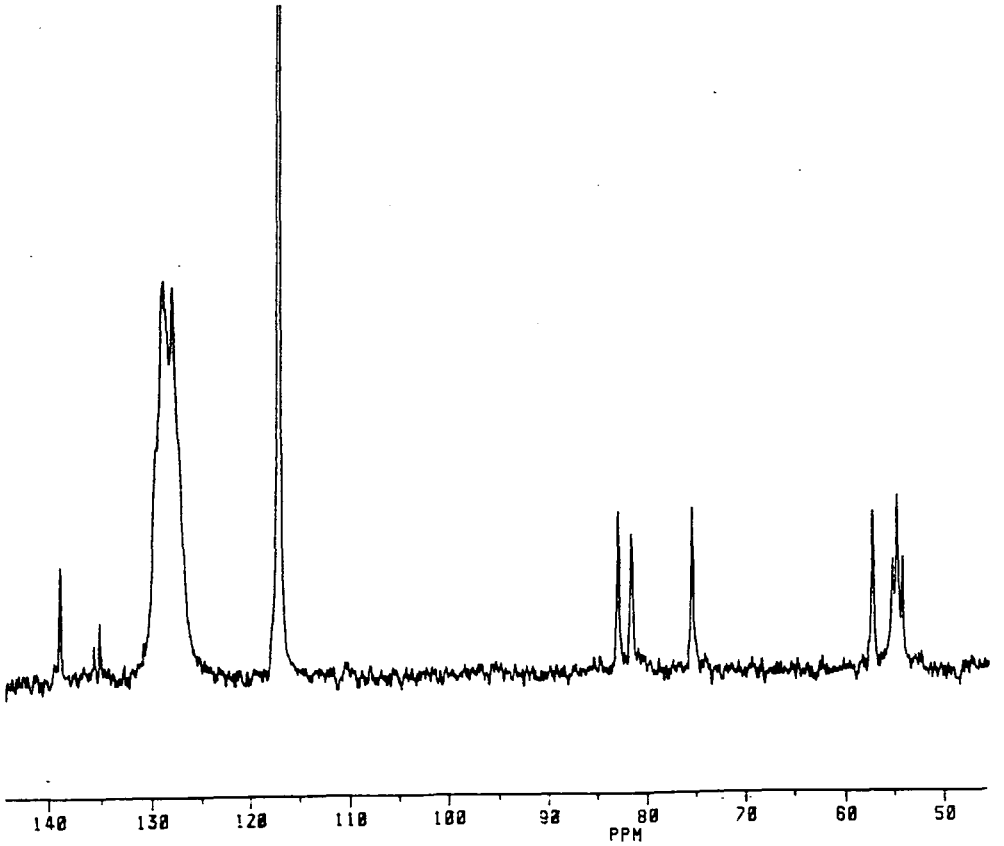

4.4 Diprotonation

In the presence of two equivalents of perchloric acid in deuteriochloroform there is NMR evidence for diprotonation. The spectrum (fig. 4.16) is consistent with structure 4.14 in which the two protons are held by the nitrogen atoms in the five-membered rings.

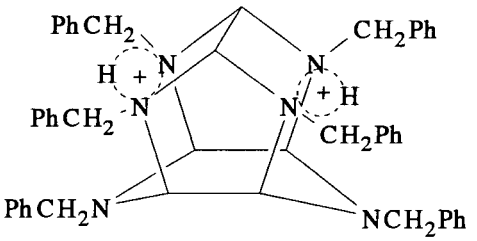

4.14

The spectrum indicates a structure having similar symmetry to the parent. Thus the two AB quartets observed for the H^c and $H^{c'}$ protons in the monoprotonated species are replaced by a single AB quartet with shifts of δ4.23 (4H) and 4.73 (4H). It is noteworthy that the highfield band shows further splitting (J=5Hz) through coupling of the added NH protons with one of each of the two adjacent methylene hydrogens. The H^a hydrogens show a further paramagnetic shift to δ6.17 while the four equivalent H^b and $H^{b'}$ hydrogens are shifted to δ5.06. The four H^d and $H^{d'}$ methylene hydrogens are now equivalent and absorb at δ2.28 which is close to the position of the H^d protons in the monoprotonated species. This may indicate that the diamagnetic shielding resulting from proximity to the aromatic rings is now felt by all four of the methylene hydrogens at H^d and $H^{d'}$. A band representing two protons at δ 8.01 is attributed to the two added amino protons. This is split into a triplet due to coupling of each NH group with two equivalent methylene hydrogens (see table 4.1and 4.3).

Fig.4.16
^{1}H NMR Spectrum Of HBIW (4.1) In The Presence Of 2 Equivalents Of Acid In $CDCl_3$

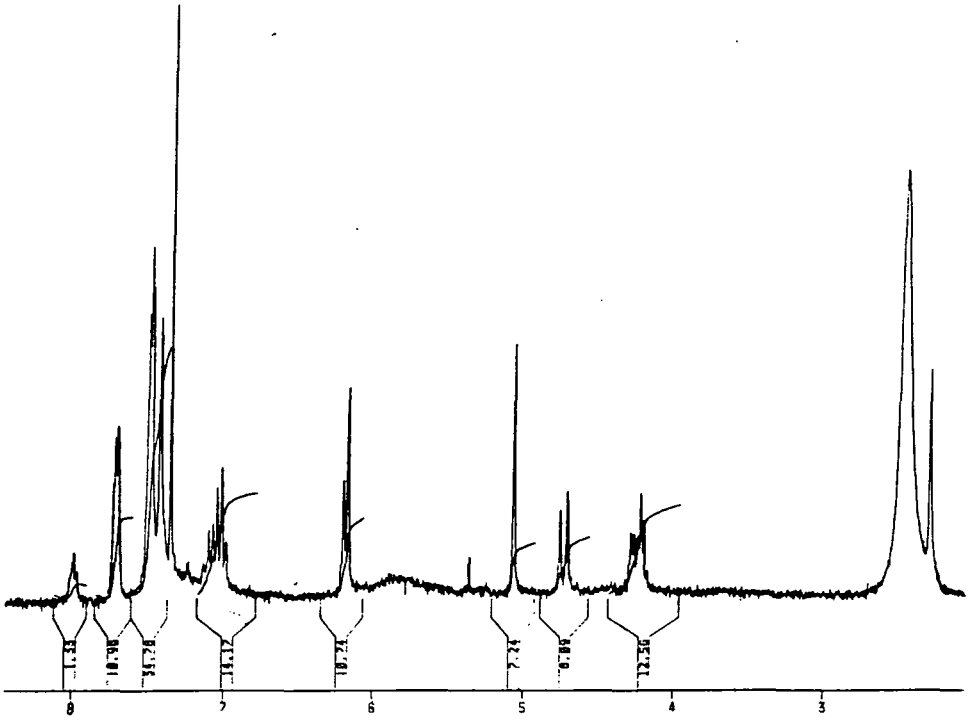

Deuteriated HBIW (4.15a) in deuteriochloroform (fig. 4.17) shows the absence of benzyl methylene protons H^c, $H^{c'}$, H^d and $H^{d'}$ (table 4.1). The methine protons H^b and $H^{b'}$ give a band at δ5.08 (signal appears at δ4.16 in the monoprotonated species) while the H^a protons appear further downfield at δ6.19 (superimposed on one of the aromatic proton peaks) in a 4:2 ratio. The NH signal appears as a sharp singlet at δ 8.01 with the aromatic protons giving amultiplet between δ6.20-7.74.

In deuterioacetonitrile a much clearer picture is seen (fig. 4.18). A similar spectrum is observed showing an AB quartet (J=13Hz) due to geminal coupling of the benzyl methylene protons H^c and $H^{c'}$ at δ4.70 and 4.21 the latter signal being split further to another AB quartet (J=7Hz) due to spin-coupling of the added NH proton with one of the methylene protons on each of the H^c groups. The ring cage methine protons H^a appear downfield at δ5.94 and not superimposed on the aromatic proton signal at δ6.19 as was the case in deuteriochloroform. H^b and $H^{b'}$ appear as a singlet at δ4.92. The aromatic hydrogens appear between δ6.19-7.67 and the benzyl methylene hydrogens H^d and $H^{d'}$ give a single band at δ2.27. The triplet at 7.91 (J=5Hz) is attributed to the NH proton coupling with the H^c hydrogens.

As discussed in the previous chapter several salts of HBIWand its 4-Chloro derivative had been prepared. Elemental analysis suggested hydrated diprotonated salts. This was confirmed by the ^{1}H NMR spectrum in deuterioacetone as shown in fig. 4.19. The spectrum of the diprotonated dihydroperchlorate salt of HBIW (fig. 4.19) is found to be virtually identical to that of the diprotonated species obtained using 2 equivalents of acid in both deuteriochloroform and acetone. Due to the unstable nature of the diprotonated species in solution it was not possible to obtain a ^{13}C NMR spectrum.

Fig. 4.17
^{1}H NMR Spectrum Of Deuteriated HBIW (4.6a) In The Presence Of 2 Equivalents Of Acid In $CDCl_3$

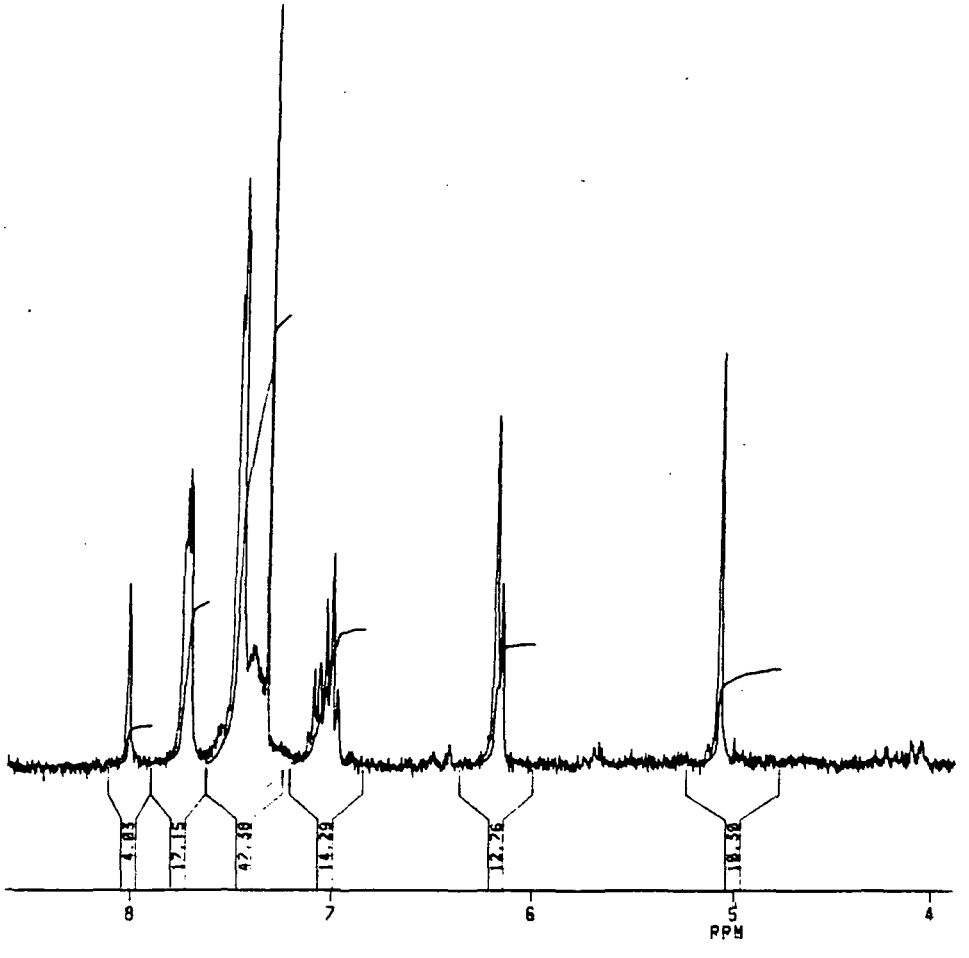

Fig. 4.18

^{1}H NMR Spectrum Of HBIW (4.1) In The Presence of 2 Equivalents Of Acid In CD_3CN

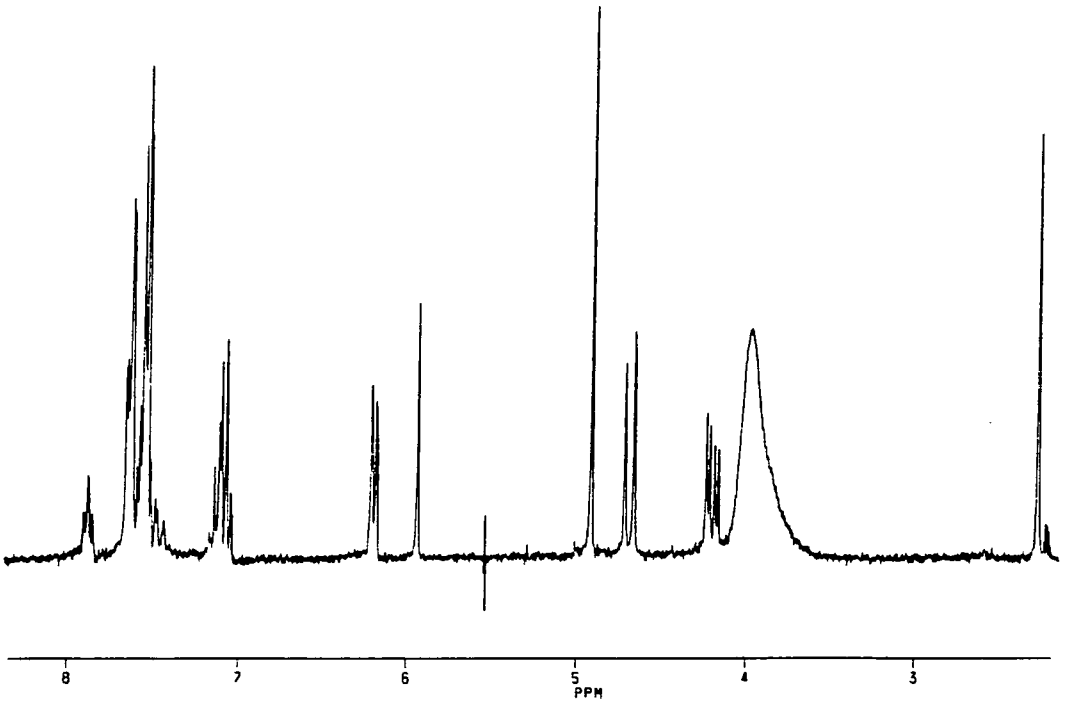

Fig. 4.19

^{1}H NMR Spectrum Of The Diprotonated Dihydroperchlorate Salt Of HBIW In $(CD_3)_2CO$

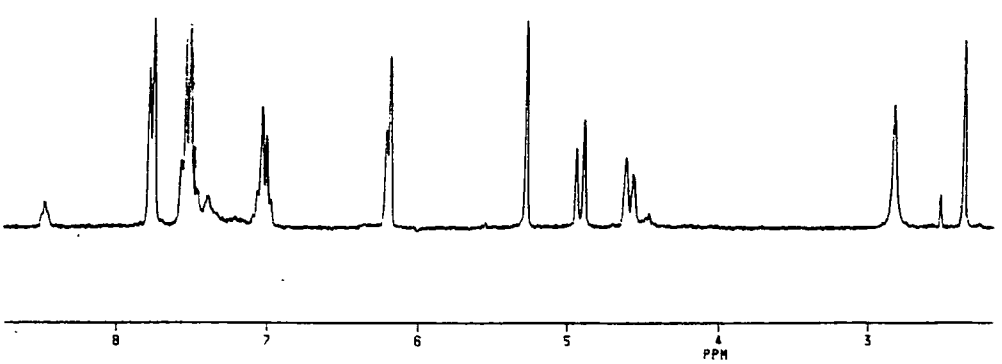

4.5 Protonation Of HBIW In Excess Acid

In the presence of 3 equivalents of acid the ^1H NMR spectrum is shown to consist mainly of the diprotonated species. However, a new band is observed at δ5.31 and an additional splitting of the methylene benzyl signals of H^c and Hc' is seen at δ 4.23 indicating that decomposition of the cage structure is occurring (fig. 4.20).

Fig. 4.21 shows that of deuteriated HBIW derivative in the presence of 3 equivalents of acid. This spectrum is identical to that of the deuteriated diprotonated HBIW in deuteriochloroform (4.6a).

However, addition of sodium deuteroxide gave back the spectrum of the parent compound containing two additional bands at δ3.84 (2H) and 5.35 respectively (fig.4.22). These signals are not seen in the spectrum of the deuteriated HBIW (4.6a) after addition of sodium deuteroxide (fig. 4.23) suggesting that these bands are due to methylene protons which may be some decomposition product. It should be noted that the signal at δ3.84 occurs in a very similar position to that of protonated benzylamine.

In the presence of 4 equivalents of acid in deuteriochloroform rapid decomposition of HBIW occurs, although it is still possible initially to observe the presence of some diprotonated species (fig.4.24). Again addition of sodium deuteroxide gave back the original spectrum of the parent with similar bands probably due to the decomposition product at δ5.35 and 3.84 (fig. 25).

Fig.4.20

^{1}H NMR Spectrum Of HBIW In The Presence Of 3 Equivalents Of Acid In $CDCl_3$

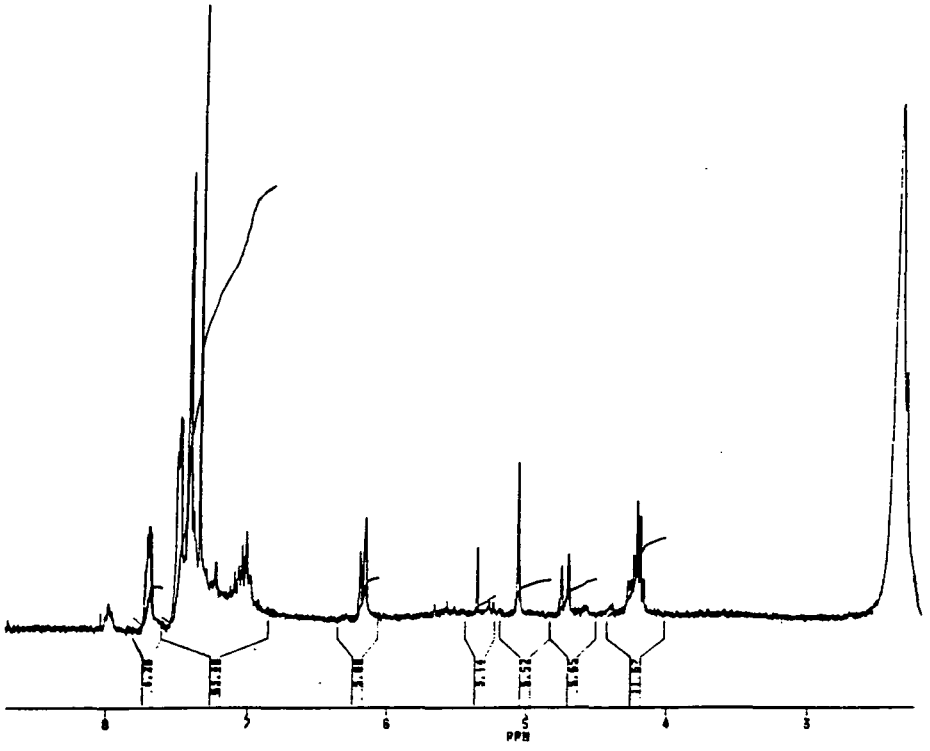

Fig 4.21

^{1}H NMR Spectrum Of deuteriated HBIW (4.6a) In The Presence Of 3 Equivalents Of Acid In $CDCl_3$

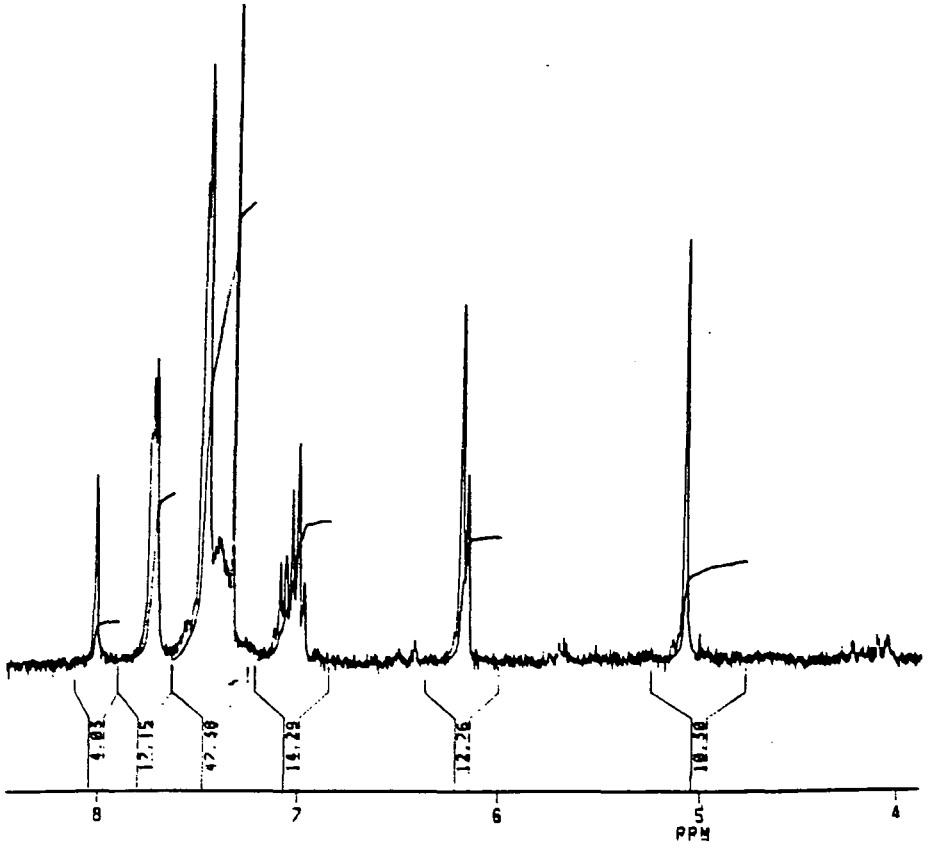

Fig. 4.22

^{1}H NMR Spectrum Of HBIW In 3 Equivalents Of Acid After NeutralisationWith Sodium Deuteroxide

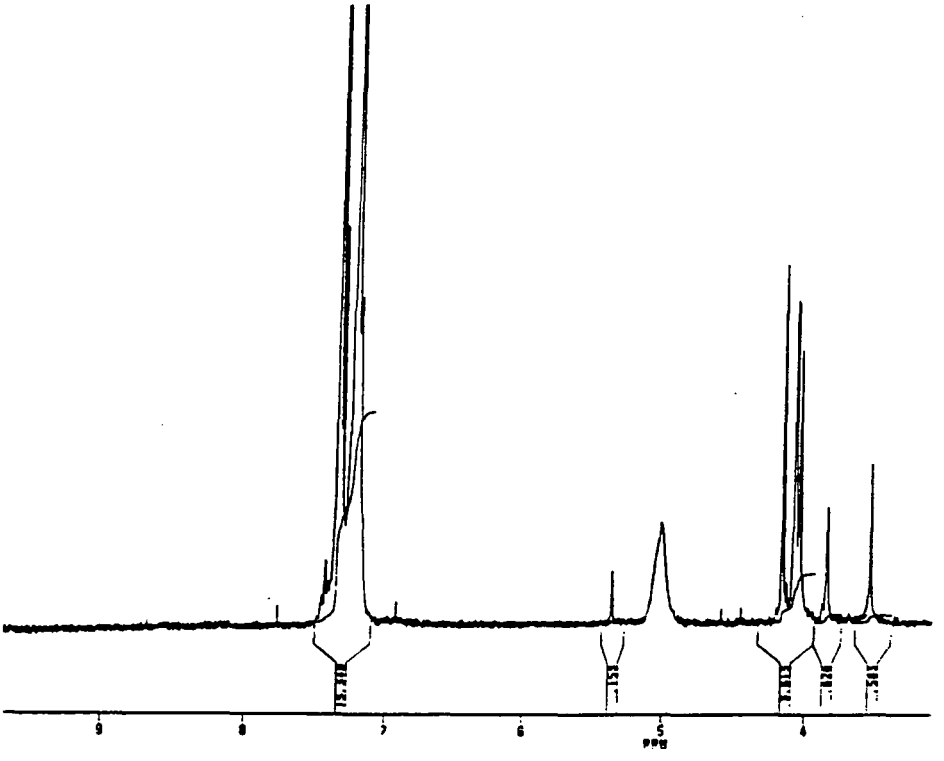

Fig. 4.23

^{1}H NMR Spectrum Of Deuteriated HBIW (4.6a) In The Presence Of 3 Equivalents Of Acid After Neutralisation With Sodium Deuteroxide

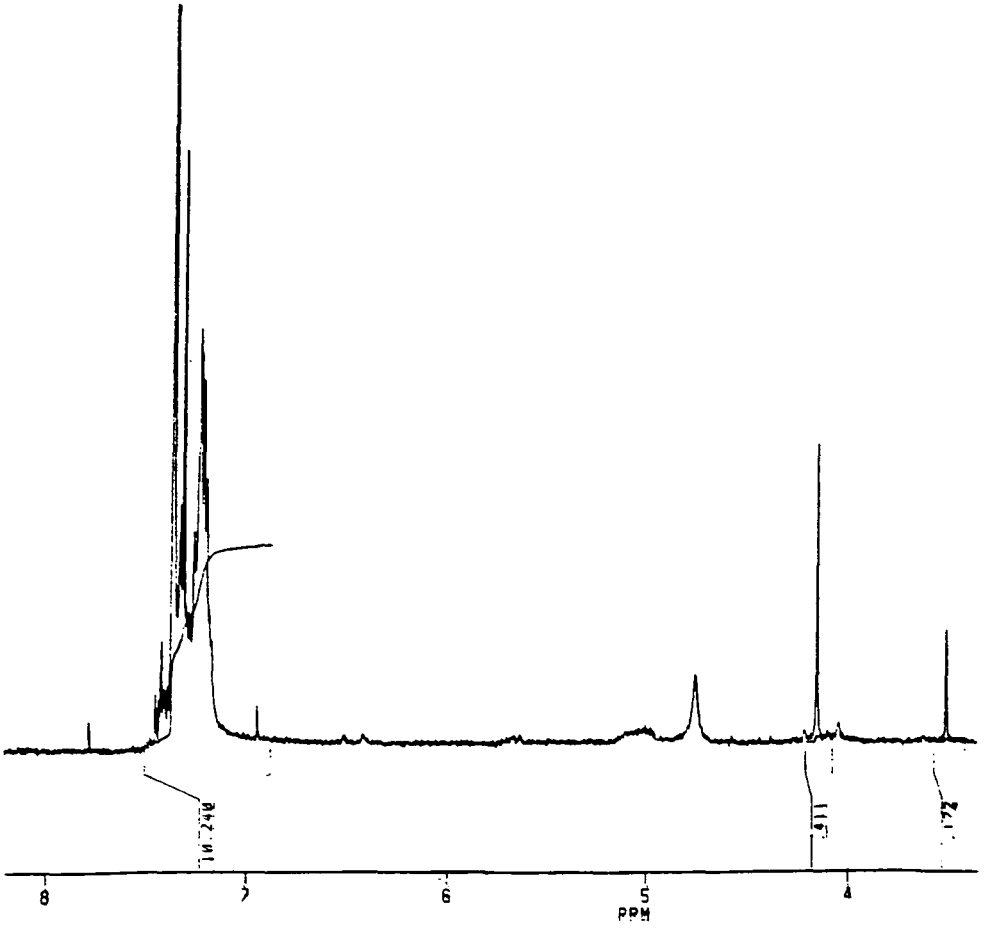

Fig. 4.24

^{1}H NMR Spectrum Of HBIW In The Presence Of 4 Equivalents Of Acid In $CDCl_3$

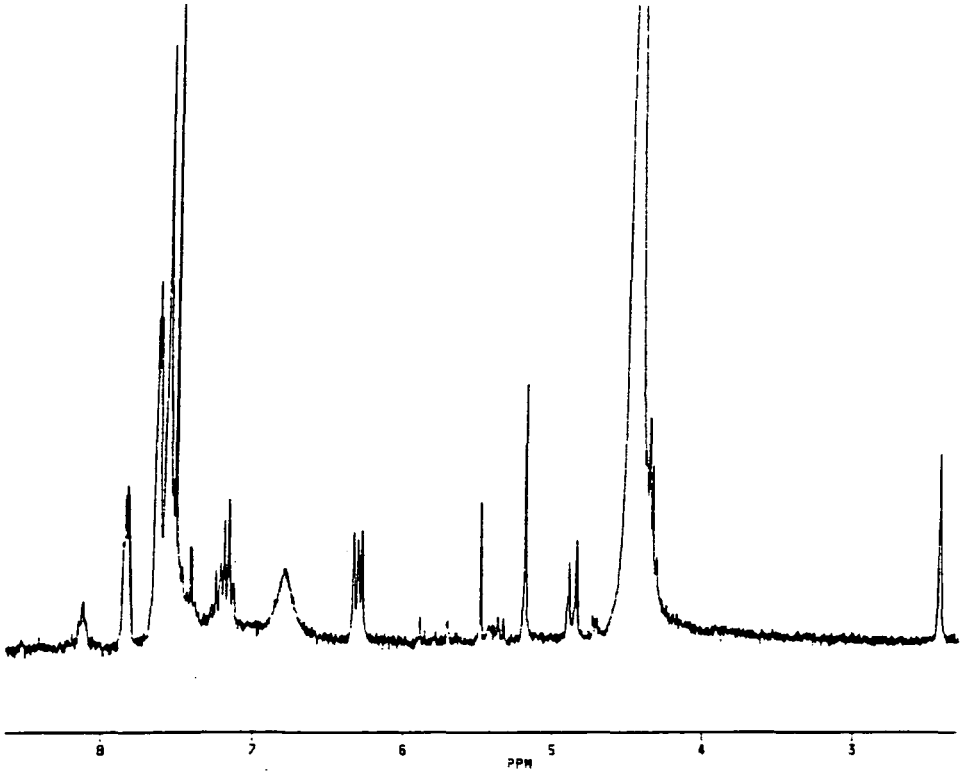

Fig. 4.25

^{1}H NMR Spectrum Of HBIW In 4 Equivalents Of Acid After NeutralisationWith Sodium Deuteroxide

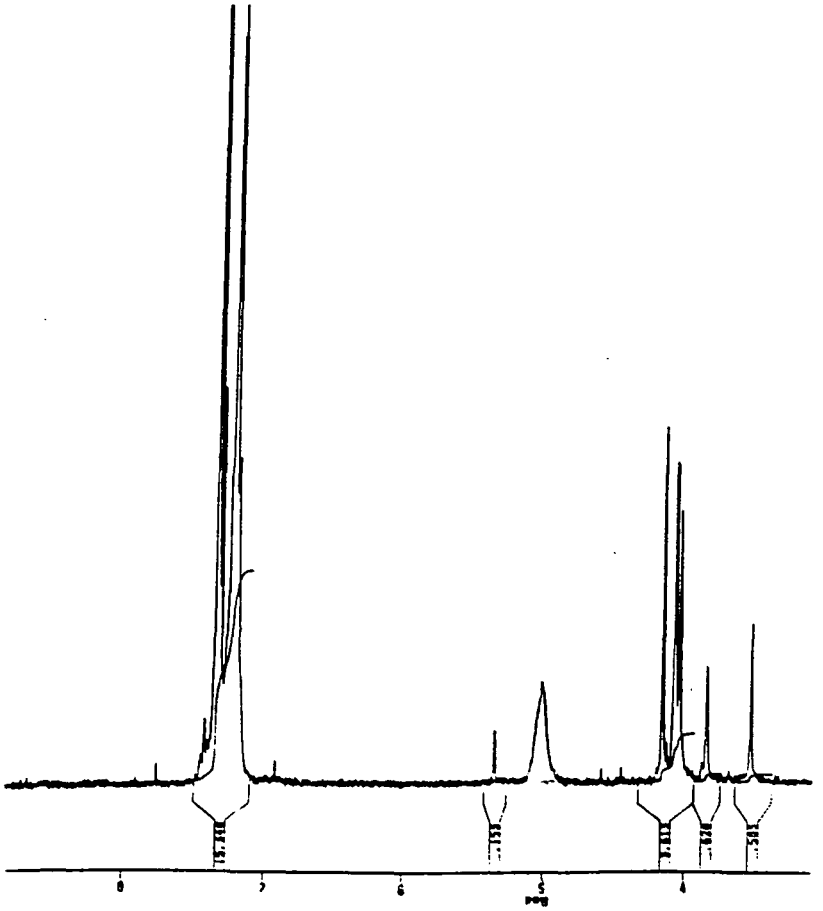

4.6 Stability Of Several Derivatives Of HBIW In Acid

In order to confirm that substituted derivatives of HBIW followed a similar pattern in acidic media it was decided to carry out similar protonation studies on 4-chloro HBIW (3.1c) and 2-methyl HBIW (3.1d).

In 1 equivalent of acid the 4-chloro derivative (table 4.2) gives an almost identical ^{1}H NMR spectrum to that obtained for the monoprotonated species of HBIW (fig. 4.26). The H^a and H^b and $H^{b'}$ protons appear as two singlets (ratio of 2:4) at δ 5.15 and 4.36 respectively. Protons H^c and $H^{c'}$ appear as two AB quartets at δ3.81, and 4.66 and δ4.19 and 4.33. The H^d and $H^{d'}$ protons give bands at δ3.55 and 2.42 with the aromatic protons appearing between δ6.21-7.51.

Due to the insolubility of the 4-chloro HBIW diprotonated species in deuteriochloroform it was not possible to obtain a ^{1}H NMR spectrum. However the spectrum of the diprotonated hydroperchlorate salt dissolved in deuterioacetone is shown in fig. 4.27 and shows bands due to H^a and H^b and $H^{b'}$ at δ6.20 (superimposed on one of the aromatic proton peaks).and 5.30. The benzyl methylene protons H^c and $H^{c'}$ give bands at δ4.93 and 4.60 representing eight protons with the latter band showing spin-coupling between the NH proton and H^c protons, a consequence of which the NH signal appears as a triplet at δ8.68. Protons H^d and $H^{d'}$ give a singlet at δ2.37 with the aromatic protons appearing between δ6.20-7.79 (table 4.2). This spectrum is virtually identical to that of the diprotonated species of HBIW in both deuterioacetonitrile and chloroform.

Fig. 4.26

^{1}H NMR Spectrum Of 4-Chloro HBIW (3.1c) In The Presence Of 1 Equivalent Of Acid In $CDCl_3$

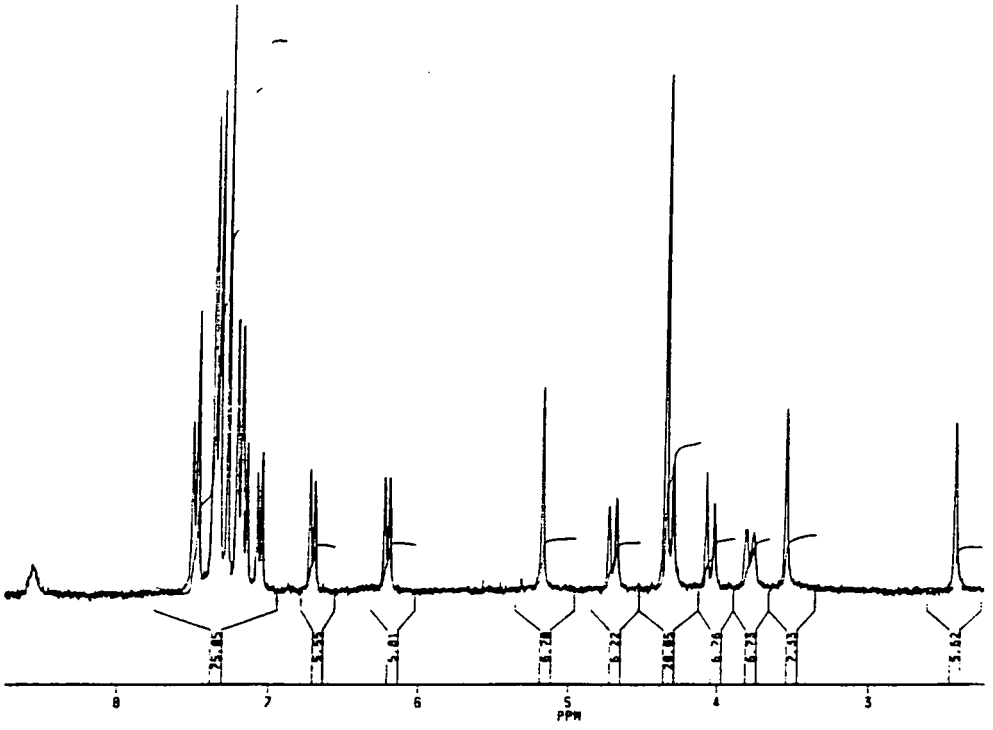

Fig. 4.27

^{1}H NMR Spectrum Of The Dihydroperchlorate Salt Of 4-Chloro HBIW (3.1c) In $(CD_3)CO$

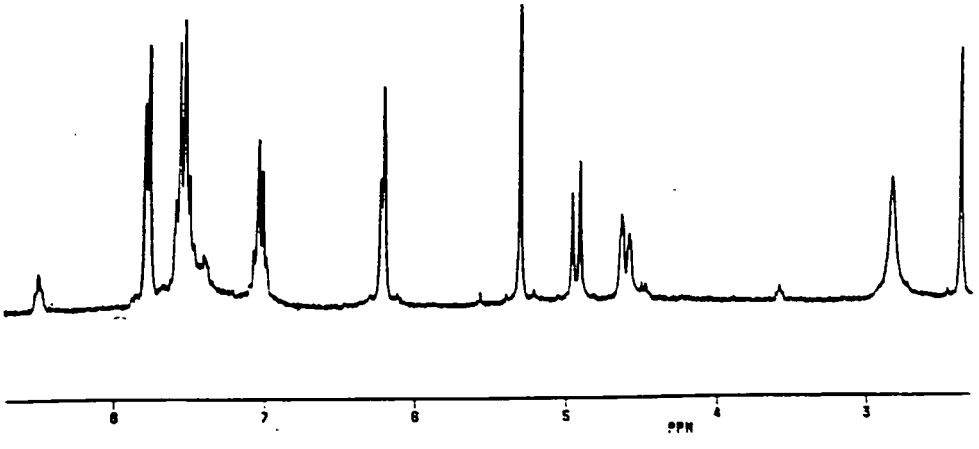

The spectra of the 2-methyl derivative of HBIW (3.1d) in deuteriochloroform is shown in fig. 4.28. In the presence of one equivalent of acid a similar spectrum is obtained as for HBIW. The two AB quartets (J=13Hz) due to the H^c and $H^{c'}$ protons are less pronounced than those in the parent and give bands at δ4.03 and 4.41 and δ 4.11 and 4.34. The methine ring cage protons H^a and H^b and $H^{b'}$ give two peaks in a ratio of 2:4 at δ5.03 and 4.51 respectively. H^d and $H^{d'}$ protons appear further upfield at δ2.52 and 3.56. while the four types of methyl substituents give bands at δ1.61 (H^d), 1.86 ($H^{d'}$), 2.29 (H^c) and 2.21 ($H^{c'}$). The aromatics give a multiplet between δ 6.11-7.26 and the NH proton signal appears as a broad band about 8.52 (fig.4.29) (table 4.5).

In the presence of two equivalents of acid no spectrum similar to that for the diprotonated species of HBIW is obtained. The spectrum is very complex suggesting very rapid decomposition of the diprotonated species (fig. 4.30). This was confirmed when sodium deuteroxide was added to the solution of the diprotonated derivative. This did not give back the simple spectrum of the parent but that of a complex mixture (fig.4.31).

Fig. 4.28
^{1}H NMR Spectrum Of 2-Methyl HBIW (3.1d)
In $CDCl_3$

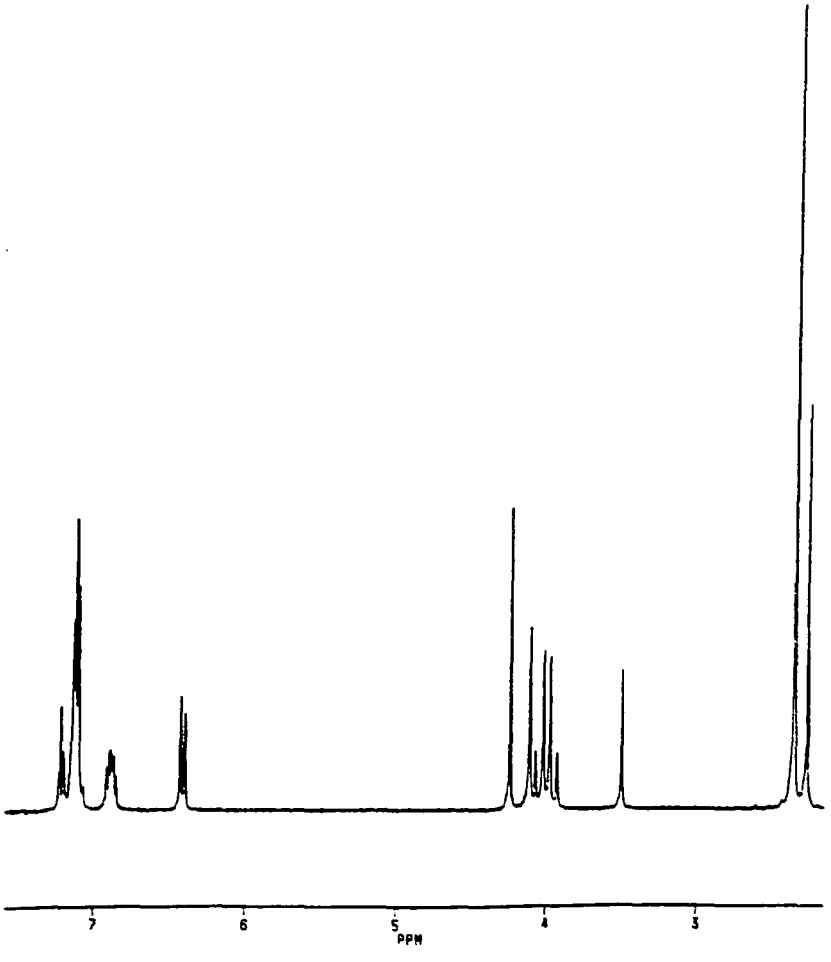

Fig. 4.29

^{1}H NMR Spectrum Of 2-Methyl HBIW (3.1d) In The Presence Of 1 Equivalent Of Acid In $CDCl_3$

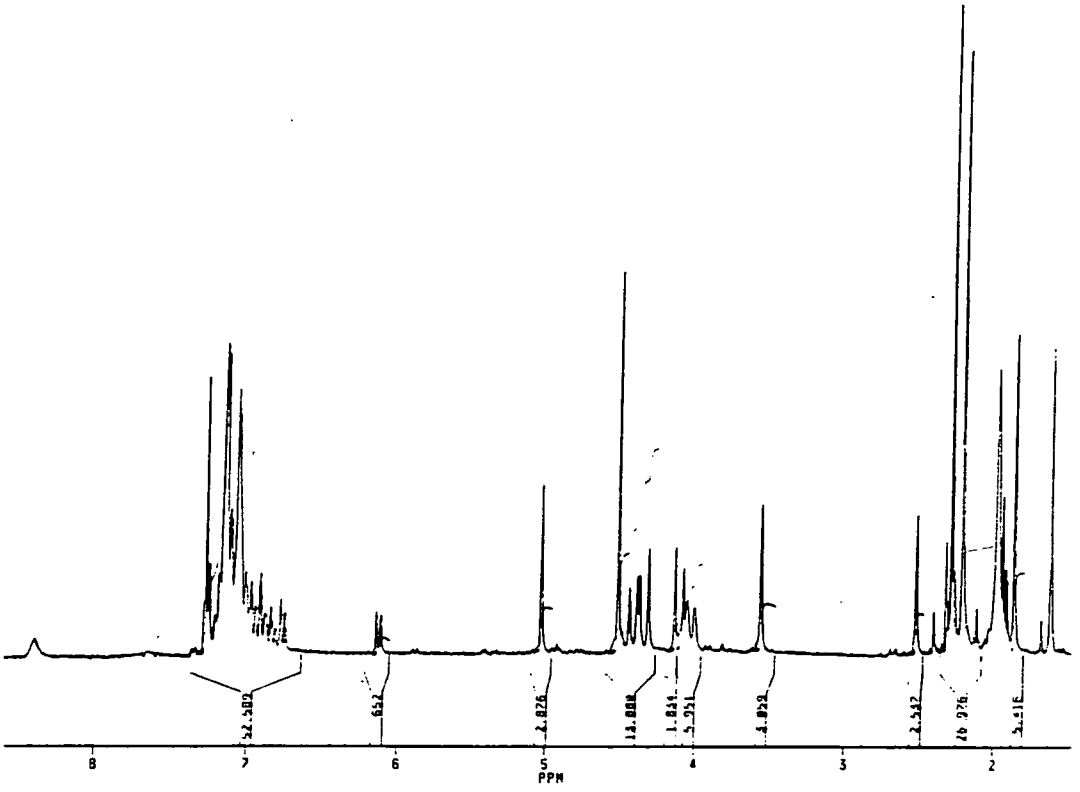

Fig. 4.30

^{1}H NMR Spectrum Of 2-Methyl HBIW (3.1d) In The Presence Of 2 Equivalents Of Acid In $CDCl_3$

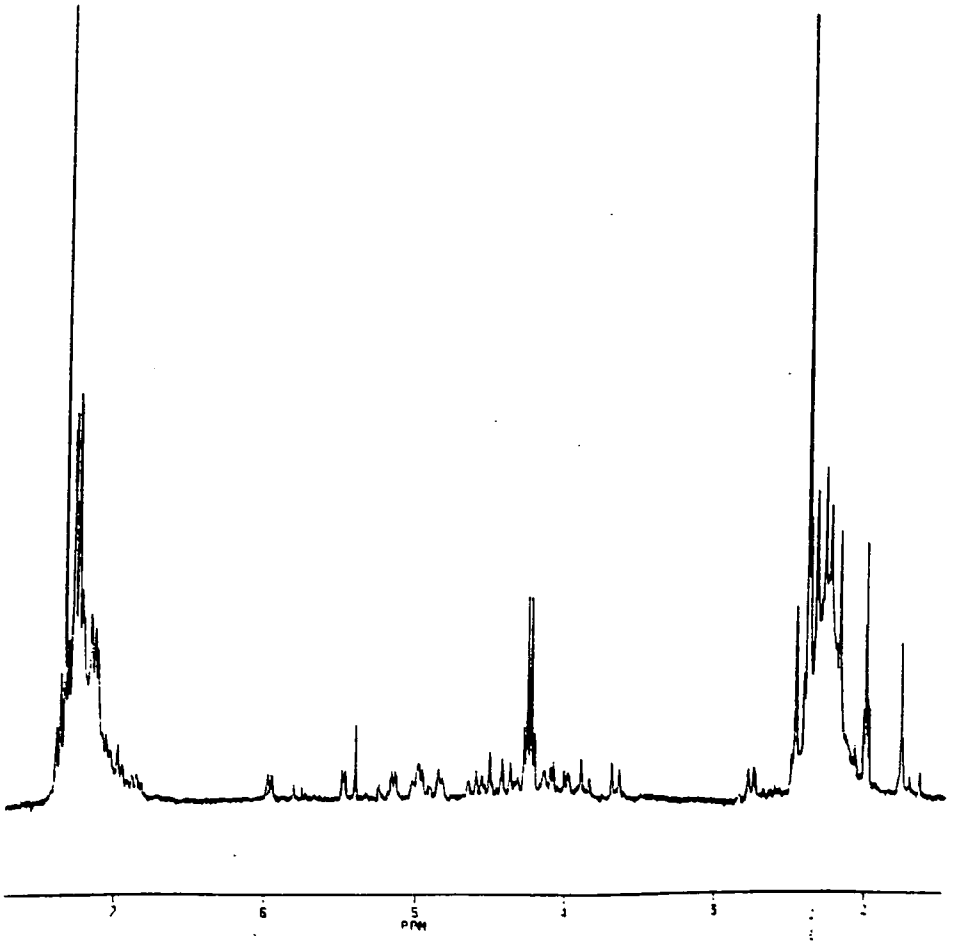

Fig. 4.31

^{1}H NMR Spectrum Of 2-Methyl HBIW (3.1d) In The Presence Of 2 Equivalents Of Acid After Neutralisation With Sodium Deuteroxide

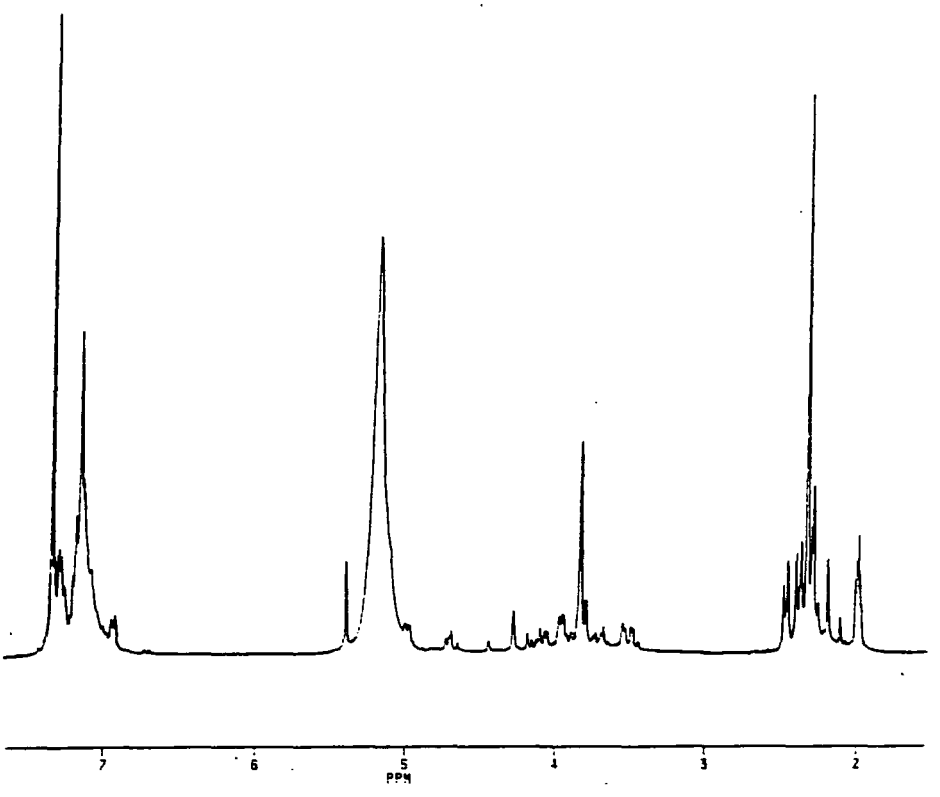

The ^{13}C decoupled NMR spectrum of the monoprotonated species was obtained in deuteriochloroform and is shown in fig. 4.32 (table 4.6). The spectrum is identical to that obtained for HBIW in one equivalent of acid Three types of methine ring cage carbons signals are observed at δ82.13, 81.36 and 75.03 corresponding to those of C^a and C^b and $C^{b'}$. Carbons C^c and $C^{c'}$ appear at δ52.49 and 54.78 while those due to carbons C^d an $C^{d'}$ appear at δ53.43 and 52.71 respectively. The methyl substituents on the aromatic ring appear as overlapping peaks between δ18.72-19.28 with the aromatic rings appearing between δ125.46-136.78. Also seen is a peak due to deuterioacetonitrile from the added acid at δ116.61 (see table 4.6).

Table 4.5
^{1}H NMR Data For 2-Methyl HBIW (3.1d) In Acid

Deriv. 3.1d	H^a /ppm	H^b /ppm	$H^{b'}$ /ppm	H^{c}* /ppm	$H^{c'}$* /ppm	H^d /ppm	$H^{d'}$ /ppm	Aromatic protons	NH proton	Methyl substit.
2-Me HBIW	3.49	4.24	4.24	3.94	4.04	4.11	4.11	6.38-7.23	-	2.36(12H)** 2.27(6H)
2-Me $HBIWH^+$	5.03	4.51	4.51	4.03 4.41	4.11 4.34	2.52	3.56	6.11-7.26	8.52	1.61(H^d), 1.86($H^{d'}$) 2.29(H^c) 2.21($H^{c'}$)

*Coupling J=13Hz is observed between geminal hydrogens

**Methyl substituents on the aromatic rings next to H^c and $H^{c'}$.

Fig. 4.32
^{13}C Decoupled NMR Spectrum Of The Monoprotonated Species Of 2-Methyl HBIW (3.1d) In $CDCl_3$

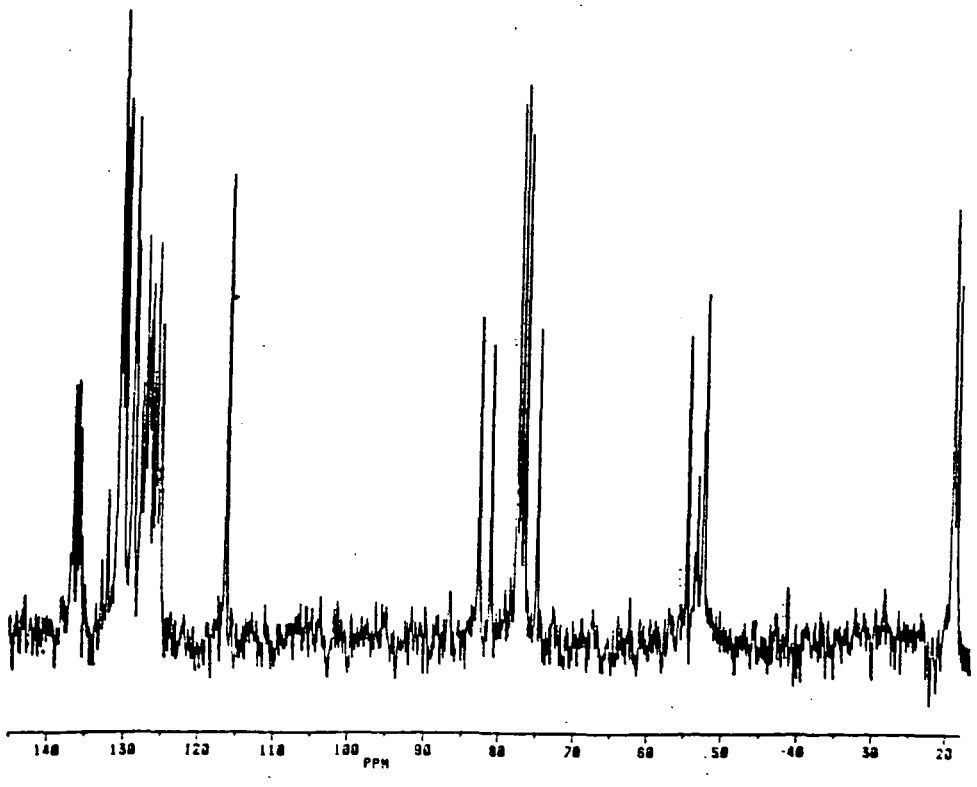

Table 4.6

^{13}C NMR Data For 2-Methyl HBIW (3.1d) In $CDCl_3$

Derivative 3.1d	C^{a}** /ppm	C^{b}** /ppm	$C^{b'}$** /ppm	C^{c}** /ppm	$C^{c'}$** /ppm	C^{d}** /ppm	$C^{d'}$** /ppm	C*** Me	Aromatic carbons
2Me-HBIW*	77.01	75.95	75.95	52.46	52.46	54.35	54.35	18.76[a] 18.68[b]	124.77-137.94
2Me-$HBIWH^{+}$*	82.13	81.36	75.03	52.49	54.78	53.43	52.71	18.72-19.28[c]	125.46-136.78

* ^{13}C determined in $CDCl_3$

** Assignments confirmed using deuteriated HBIW (4.6a) and/or by coupled/decoupled ^{13}C NMR.

*** Methyl substituents on aromatic rings.

a) Methyl carbons at C^{c} and $C^{c'}$.

b) Methyl carbons at C^{d} and $C^{d'}$.

c) Appear as overlapping peaks.

4.7 Formation Of HBIW

It was thought to be of interest to try to follow the progress of the reaction between glyoxal with benzylamine by ^{1}H NMR spectroscopy. The solvents used were deuteriated acetonitrile and chloroform. A major problem for the reaction in acetonitrile was precipitation of HBIW in the NMR tube.

Reactions were also attempted using 1,4-dioxan-2,3-diol (3.11) as a substitute for aqueous glyoxal since the latter reagent gives rise to a large water signal in the NMR spectrum.

The ^{1}H NMR spectrum of 1,4-dioxan-2,3-diol in deuterioacetonitrile is shown in fig. 4.33, consisting of an AB quartet at δ4.41 and 4.35 (J=5Hz) due to axial and equatorial protons of the dioxan ring. A similar AB quartet is observed at δ3.91 and 3.44 (J=5Hz) due to the axial and equatorial protons adjacent to the hydroxyl groups.

Addition of benzylamine and a trace of acid catalyst to 1,4-dioxan-2,3-diol in deuterioacetonitrile gives the spectrum shown in fig. 4.34. The spectrum shows bands due to presence of the diimine at δ8.04 (s, **HC**=N (2H)), 4.73 (s, C**H**$_2$ (4H)) and 7.01-7.24 (m, Ar (10H)). Ethylene glycol is formed as a by-product and gives bands at δ3.50 (s, (C**H**)) and 2.86 (s, (O**H**)). The mixture also indicates the presence of protonated benzylamine at δ3.86 (s, (C**H**$_2$)). The mixture is still very complex but it was seen that several peaks occurring at δ4.26, 4.15 and 4.08 disappeared prior to precipitation of HBIW (*ca* 10 mins. after mixing (fig. 4.35)), these may have been due to another intermediate although this still remains unidentified. No peaks due to starting materials could be observed. Even after precipitation of HBIW it was still possible to detect the presence of the diimine. This indicates not all the diimine formed reacts to give HBIW.

Using deuteriochloroform as solvent rather than acetonitrile it was found that 3.11 and benzylamine in the presence of an acid catalyst gave a similar complex spectrum from which it was possible to identify the diimine (δ8.07, 4.77 and 7.01-7.24), ethylene glycol (δ3.66 and 2.59) and protonated benzylamine (δ3.85) respectively (fig. 4.36). Due to the greater solubility of HBIW in deuteriochloroform it should be possible to detect the presence of HBIW. After 7 hours and after 2 days it can be seen that there is a decrease in the amount of diimine and increase in ethylene glycol indicating probable formation of HBIW (fig. 4.37 and 4.38). From these spectra it is not possible to rule out the formation of HBIW as its bands may be hidden under those due to other compounds also formed during the reaction.

Using aqueous glyoxal in place of 3.11 in deuteriochloroform gave similar complex spectra indicating the presence of diimine and protonated benzylamine (fig.4.39). However after 1 day the mixture showed bands in almost identical positions to those expected for HBIW.

The only conclusions made from these studies indicate that not all the diimine is used in the formation of HBIW, and that it has not been possible to identify any other intermediates apart from the diimine at this stage.

Fig. 4.33
^{1}H NMR Spectrum Of 1,4-Dioxan-2,3-Diol (3.11)
In CD_3CN

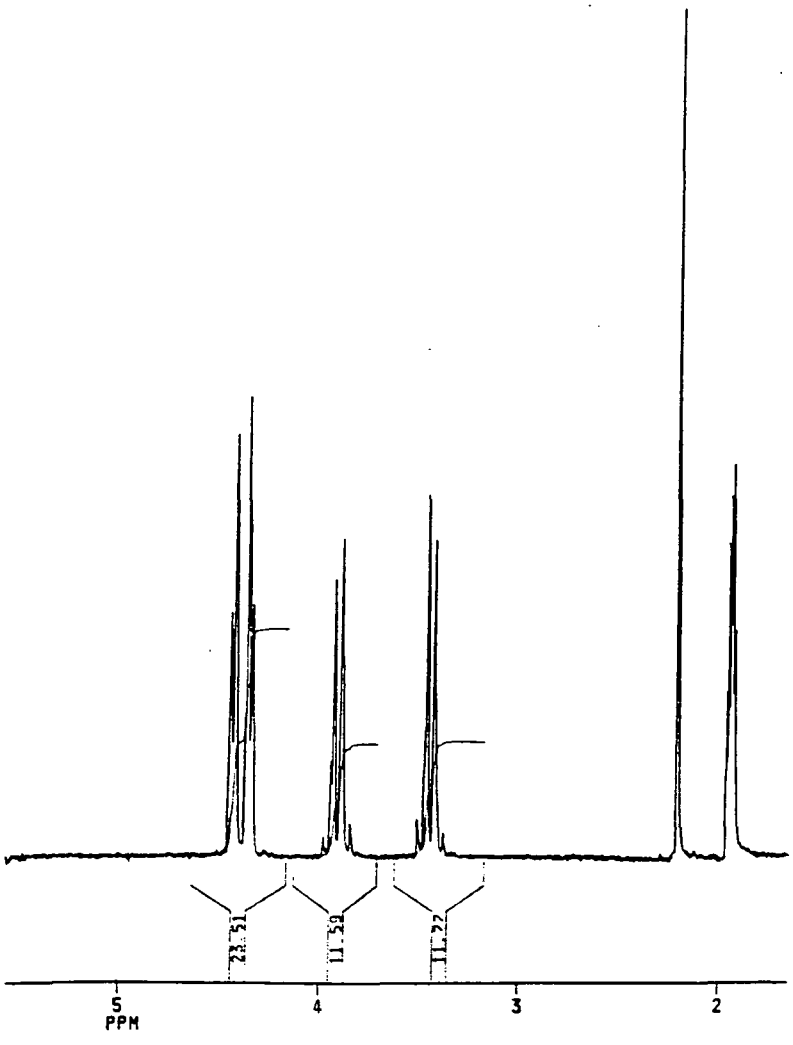

Fig. 4.34

Initial ^1H NMR Spectrum Of 1,4-Dioxan-2,3-Diol And Benzylamine In The Presence Of an Acid Catalyst In CD_3CN

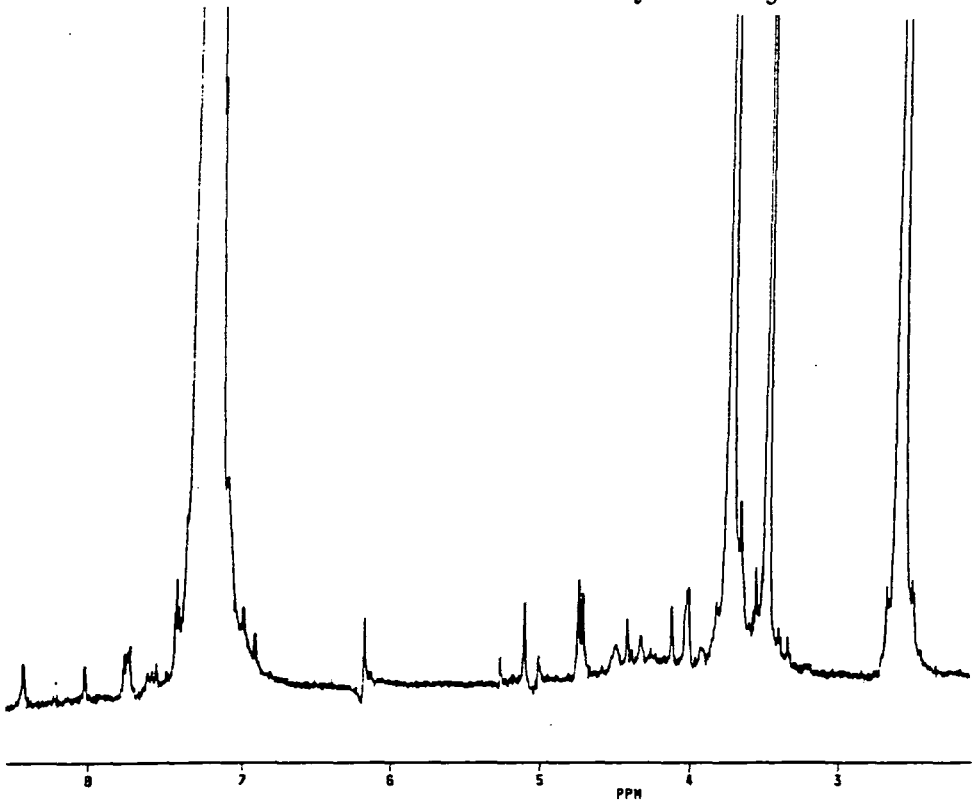

Fig. 4.35

^1H NMR Spectrum Of 1,4-Dioxan-2,3-Diol And Benzylamine In The Presence Of an Acid Catalyst In CD_3CN After 10 mins.

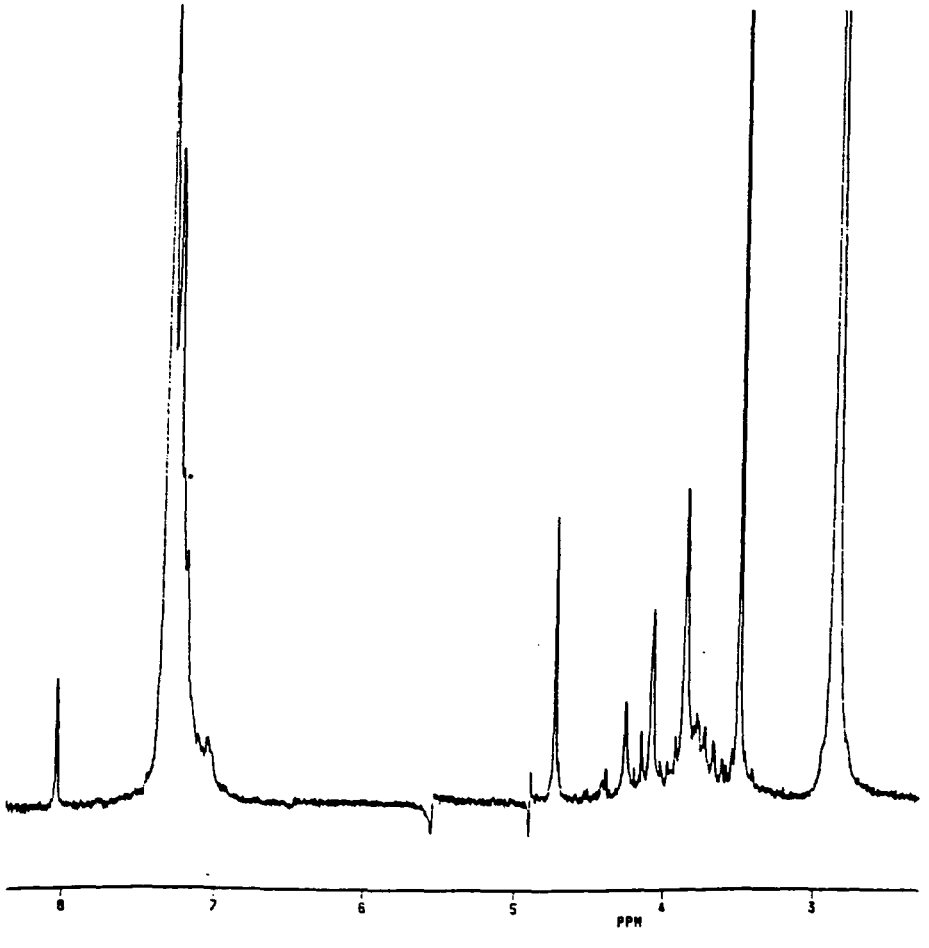

Fig. 4.36

^{1}H NMR Spectrum Of 1,4-Dioxan-2,3-Diol And Benzylamine In The Presence Of an Acid Catalyst In $CDCl_3$ After 7 Hrs.

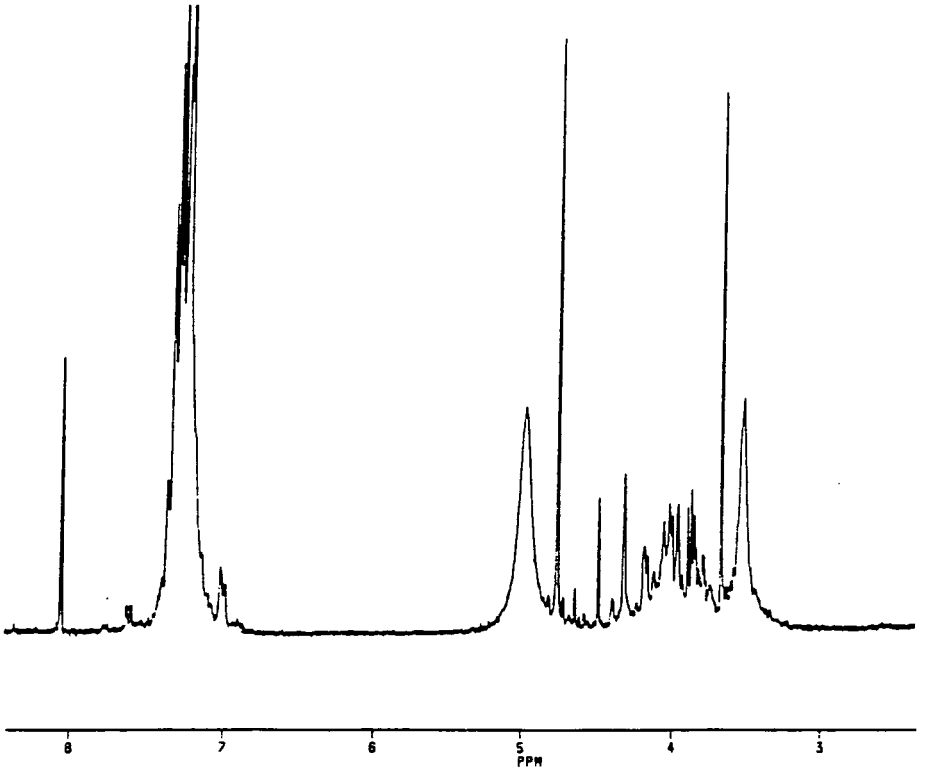

Fig. 4.37

^{1}H NMR Spectrum Of 1,4-Dioxan-2,3-Diol And Benzylamine In The Presence Of an Acid Catalyst In $CDCl_3$ After 2 Days.

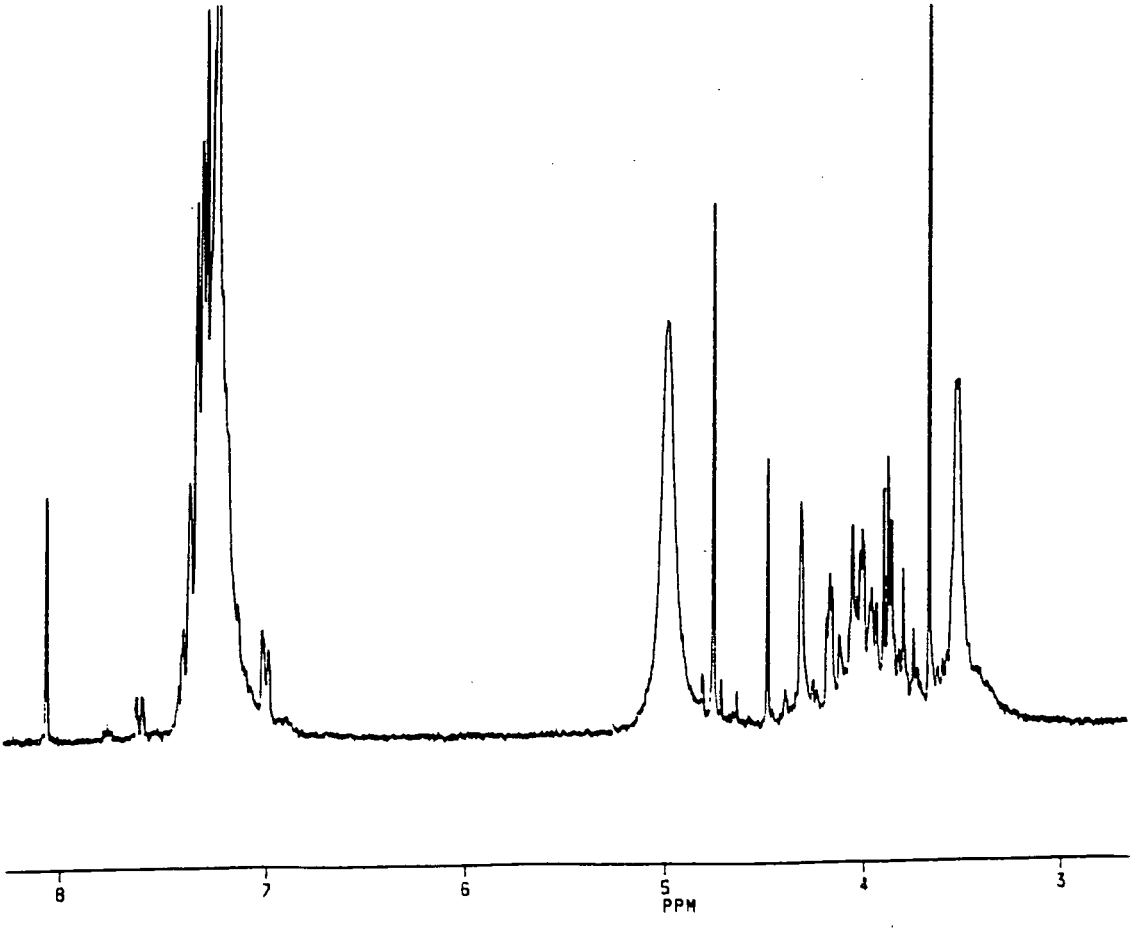

Fig.4.38

Initial ^{1}H NMR Spectrum Of Aqueous Glyoxal And Benzylamine In The Presence Of an Acid Catalyst In $CDCl_3$

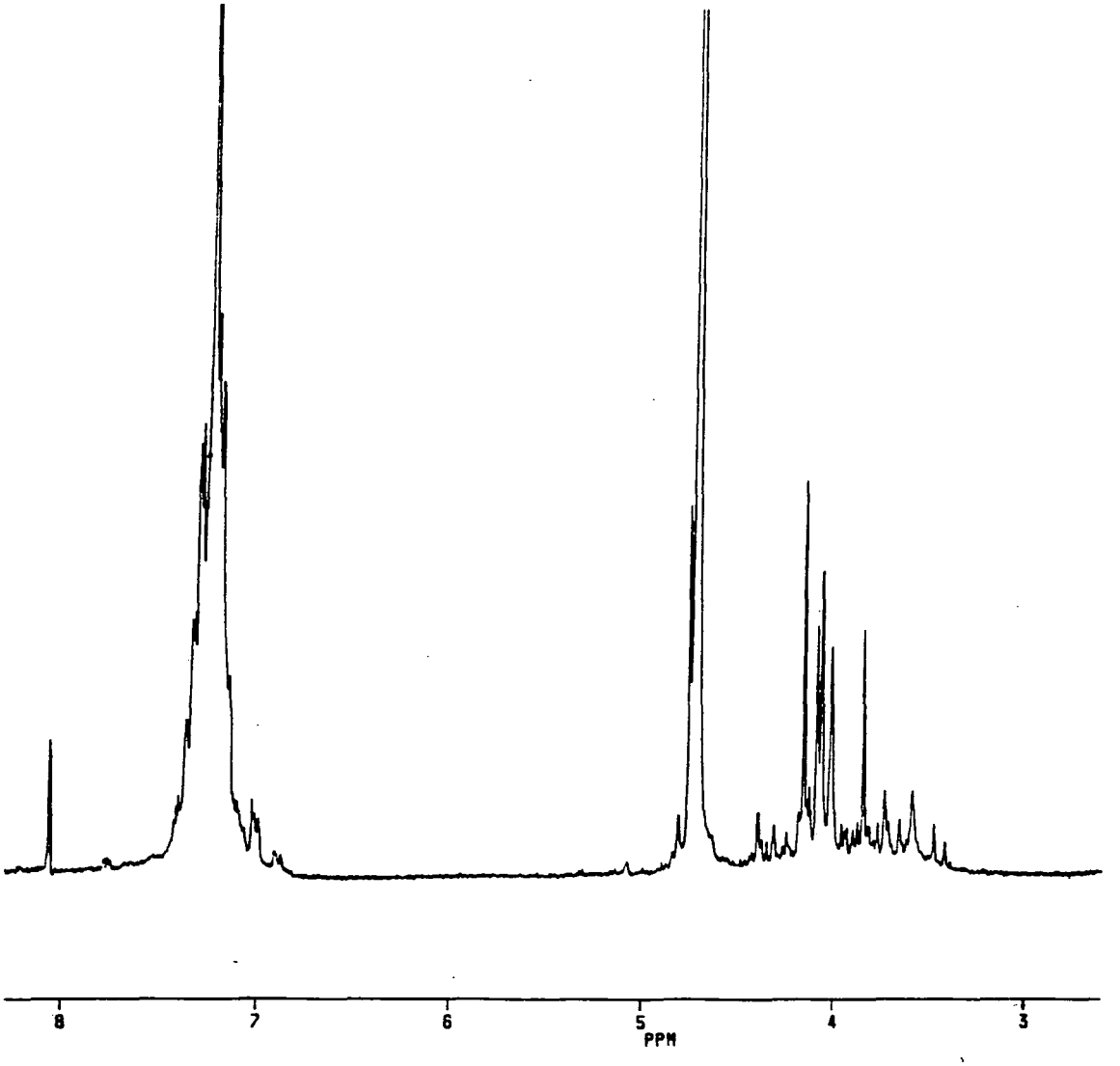

4.8 References

1. C. Sarazin, G. Goethals, J. P. Seguin and J. N. Barbotin, *Magnetic Resonance In Chem.*, 1991, 29, 291-300.
2. J. M. Kliegman and R. K. Barnes, *Tetrahedron Letts.*, 1969, 24, 1953-1956.
3. J. M. Kliegman and R. K. Barnes, *Tetrahedron*, 1970, 26, 2555-2560.
4. J. M. Kliegman and R. K. Barnes, *Tetrahedron*, 1970, 22, 1859-1861.
5. J. Hine and C. Y. Yeh, *J. Am. Chem. Soc.*, 1963, 85, 2669.
6. J. Karabatsos and S. S. Lande, *Tetrahedron*, 1968, 24, 3907.
7. J. E. Blackwood *et al. J. Am. Chem. Soc.*, 1968, 90, 510.
8. E. F. Hillenbrand, Jr. and C. A. Pentz, Organic Analysis Volume III, pp. 145; Interscience, New York, London (1956); S. K. Freeman, *Analyt. Chem.*, 1953, 25 (II), 1750.

Chapter 5

Kinetic Studies Of The Decomposition Of Substituted Bicyclononanes In Acidic Media

5.1 Introduction

There is interest in bicyclononane structures (5.1) because of their relevance to the synthesis of HMX (5.2) which is used as a commercial explosive. Derivatives (5.1) may be produced by the reaction of hexamine (5.3) with electrophiles.

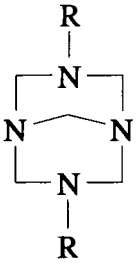

5.1

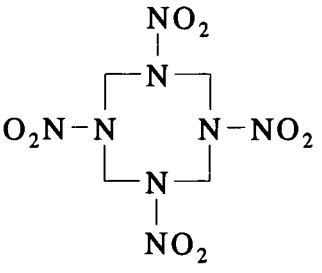

5.2

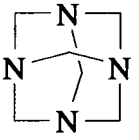

5.3

5.1.1 Nitrosation

Thus it is known that nitrosation of 5.3 in aqueous solution may be achieved by addition of hydrochloric acid and sodium nitrite.[1] The pH of the solution determines the nature of the products. At pH 1-2, trimethylenetrinitrosamine (TMTN) (5.4) is formed, whereas at pH 2 a mixture of TMTN and dinitrosopentamethylenetetramine (DNPT) (3,7-dinitroso-1,3,5,7-tetraazabicyclo [3.3.1] nonane) (5.5) are formed. At higher pH's (3-6) DNPT is the only product (scheme 5.1). If acetic acid is employed instead of hydrochloric acid then the only product over a wide range of conditions is the bicyclononane DNPT (5.5). DNPT was first prepared by Greiss and Harrow.[2]

Scheme 5.1

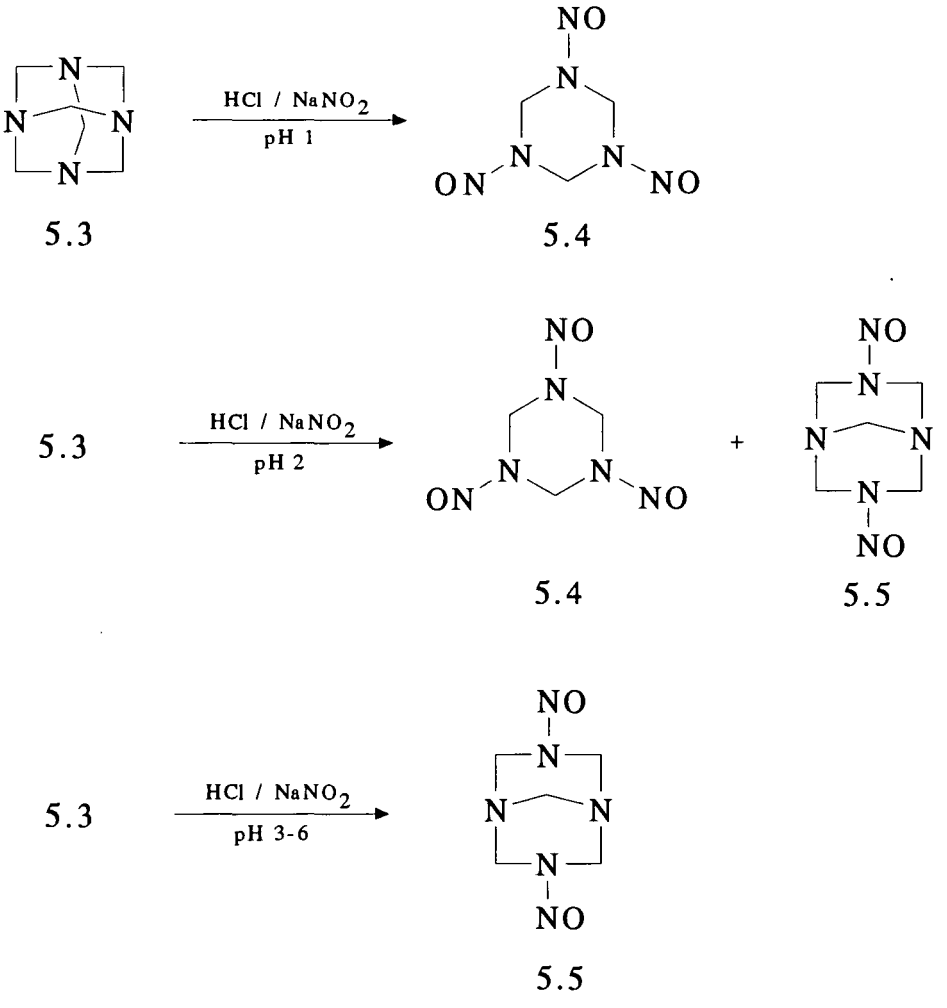

5.1.2 Acetylation

Diacetylpentamethylenetetramine (DAPT) (3,7-diacetyl-1,3,5,7-tetraaza-bicyclo [3.3.1] nonane) (5.6) can be easily prepared from hexamine (5.3) and acetic anhydride in a good yield.[3] However at higher temperatures 1,3,5-triacetyl-1,3,5-triazacyclo hexane commonly known as TRAT (5.7) is formed (scheme 5.2).

Scheme 5.2

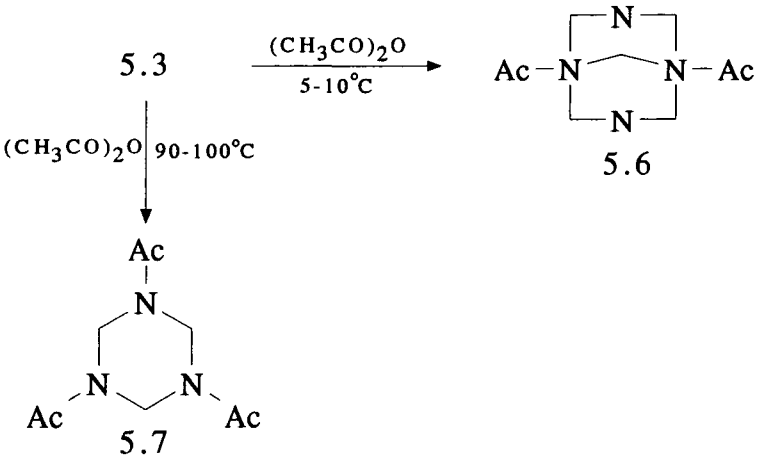

5.1.3 Nitration

Nitration of hexamine[4] gives initially the commercial explosive RDX (5.8) (or HMX (5.2) depending upon nitration conditions). However, if this is removed during the nitration and the mother liquor neutralised with ammonia or an alkali in the cold to about pH 5, precipitation of dinitropentamethylenetetramine (DPT) (3,7-dinitro-1,3,5,7-tetraazabicyclo [3.3.1] nonane) (5.9) occurs.[5-7] Wright and co-workers[5] also synthesised DPT by the reaction of methylene diamine and dimethylol nitramide (5.10) (scheme 5.3).

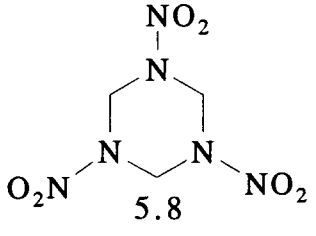

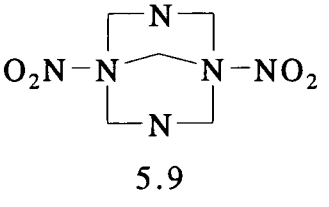

Scheme 5.3

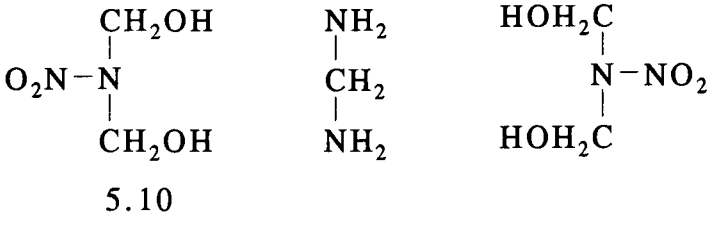

5.1.4 Kinetic Studies

Protonation studies have been reported for the acid catalysed decomposition of hexamine (5.3) and its dinitroso- (5.5), diacetyl- (5.6) and dinitro- (5.9) derivatives in water. Hexamine itself has a pKa value of 4.89 and is resistant to decomposition in weakly acidic solution.[8] In concentrated acid there is evidence for diprotonation pKa_2=-1.7 and decomposition occurs to formaldehyde.

The presence of electron withdrawing groups in the substituted derivatives 5.5, 5.6 and 5.9 results in considerable reductions in the basicity relative to 5.3. Data are given in table 5.1 and show that 5.5, 5.6 and 5.9 have pKa values of *ca* 1.0 so that protonation will be approximately half complete in 0.1M acid.

Kinetic studies[8-10] are consistent with an acid catalysed decomposition pathway involving, equilibrium protonation followed by rate determining breakdown of the monoprotonated derivative as shown in eqn. 5.1 for DAPT. Values of k_{H+}, the rate coefficient for cleavage are given in table 5.1.

$$\text{DAPT} + H^+ \underset{}{\overset{K}{\rightleftharpoons}} \text{DAPTH}^+ \xrightarrow{k_{H^+}} \text{products} \quad \textbf{eqn. 5.1}$$

$$k_{obs} = \frac{k_{H^+}.K[H^+]}{1+K[H^+]} \quad \textbf{eqn. 5.2}$$

Table 5.1
Data In Water At 25°C

Compound	pKa	k_{H+}[b]/s^{-1}	Reference
Hexamine (5.3)	4.89 (-1.7)[a]	$6x10^{-6}$(30°C)	8
DAPT (5.6)	0.74	$9x10^{-4}$	8
DPT (5.9)	0.80	$3.9x10^{-2}$	9
DNPT (5.5)	1.06	$5x10^{-2}$	10

a) pKa_2 for second protonation.
b) Rate constant for decomposition of monoprotonated derivatives.

In addition, it was found[9] that the dinitro (5.9) compound spontaneously decomposed in water in the absence of protonation. The rate coefficient for this process was found to have the value $2x10^{-3}$ s^{-1}.

Of particular interest was the observation[10] that in the decomposition of the dinitroso derivative (5.5), there was evidence for a pathway involving a diprotonated derivative which made a contribution at high acid concentrations.

Measurements have also been reported for the protonation and acid catalysed decomposition of 3,7-bis (arylazo)-1,3,5,7-tetraazabicyclo [3.3.1] nonane (5.11)

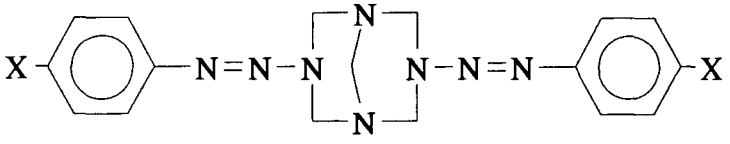

5.11

X =Cl

X =CO_2Et

arene diazonium ions with hexamine (5.3)[11]. Because 5.4 was insoluble measurements here were made in acetonitrile containing small concentrations of water. These results were interesting because they showed that the acid catalysed decomposition occurred in two stages and an intermediate, which may be an iminium ion, was observed. Hence, it was thought to be of interest to examine the reactions of 5.5, 5.6 and 5.9 in acetonitrile.

Measurements were made in acetonitrile solvent containing 0.05% water. Concentrated aqueous perchloric acid was diluted with acetonitrile. This procedure resulted in the addition of some water with the acid so that a solution of 0.01M perchloric acid contains 0.04% water from this source. Other additions of water were made using boiled distilled water.

In the case of DPT (5.9) it has been shown[9] that in acidic solution nitramide (NH_2NO_2) is produced giving a U. V. absorbance at 210nm. It was also shown that the intermediates formed in both acidic and basic media could be interconverted. Although the initial decomposition products were not identified, it seems likely that initial C-N bond cleavage may lead to a primary ring opened product, which may exist at low pH as 5.12, intermediate pH as 5.13 and at high pH as 5.14 although the exact nature of R remains unknown.

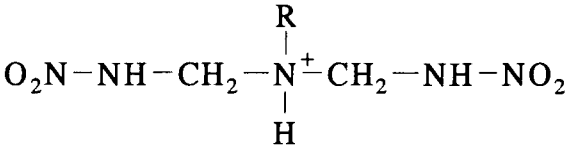

5.12

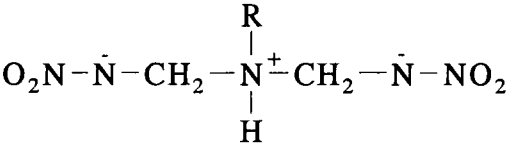

5.13

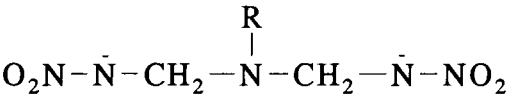

5.14

The initial bond cleavage may involve reaction via an iminium ion species which would undergo subsequent decomposition to give the species shown above. Further reaction may be dependent upon the rate of hydrolysis of the iminium ion with that of further C-N bond cleavage to give ultimately the species of the type 5.12, 5.13 or 5.14 which dependent upon pH decompose to give nitramide.

It has been shown that methylenedinitroamine (MDNA) (5.15) ultimately yields formaldehyde, nitrous oxide (N_2O), and water[12] (eqn. 5.3).

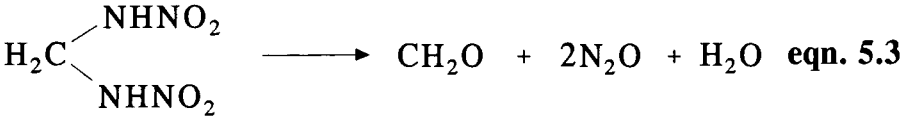

eqn. 5.3

5.15

The primary stage of decomposition was shown[12] to be liberation of nitramide (NH_2NO_2) and conversion of the methylene group of MDNA (5.15) into formaldehyde. The decomposition is thought to proceed via the monoanion 5.16 (scheme 5.4)

Scheme 5.4

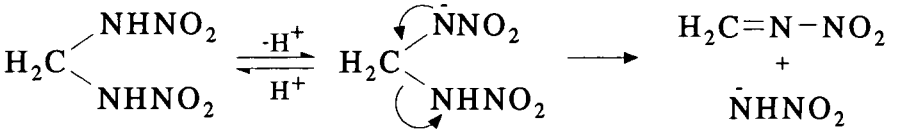

It has been shown[13] that the unionised and dianion species of MDNA have been found to be fairly stable in solution. Since in the doubly ionised MDNA electrons cannot move in either direction to promote bond cleavage as one nitroamine function cannot facilitate ejection of another as the nitroamine anion. However,after monoionisation it is possible due to the relatively greater ability of electrons (scheme 5.5). Therefore,one would suggest that the probable species undergoing decomposition could be 5.13 or some species with a similar structure. A possible mode of breakdown of 5.13 is shown in scheme 5.5.

Scheme 5.5

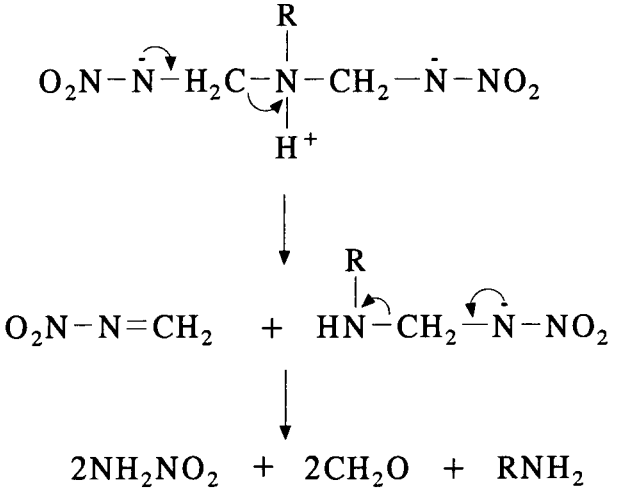

Nitramide is known to be unstable in both acidic and basic media, but the rate of decomposition in acid is very much slower than in base and therefore would be less likely to be detected in basic media.

5.2 Diacetylpentamethylenetetramine (DAPT)

5.2.1 ^{1}H NMR

There is evidence in the diacetyl derivative (5.6) for restricted rotation about the N-C bonds, so that the acetyl groups have fixed conformations.[14] The most stable conformation is expected to be the anti-conformer (5.16).

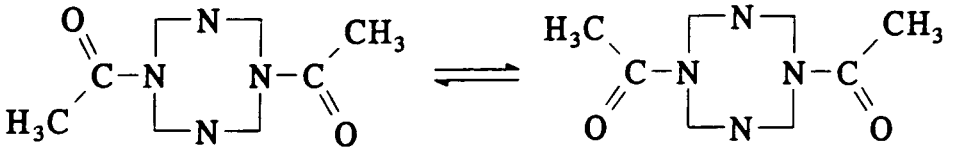

5.16 5.17

The ^{1}H NMR spectrum of DAPT (5.6) in deuteriochloroform (fig. 5.1) show bands at δ2.08 (s, acetyl) and δ4.42 (s, CH_2 bridge protons), with 2 AB quartets (J=13Hz) due to axial and equatorial methylene protons with shifts of δ4.22 and 5.95 and δ5.72 and 4.76.

Fig. 5.1
^{1}H NMR Of DAPT (5.6) In $CDCl_3$

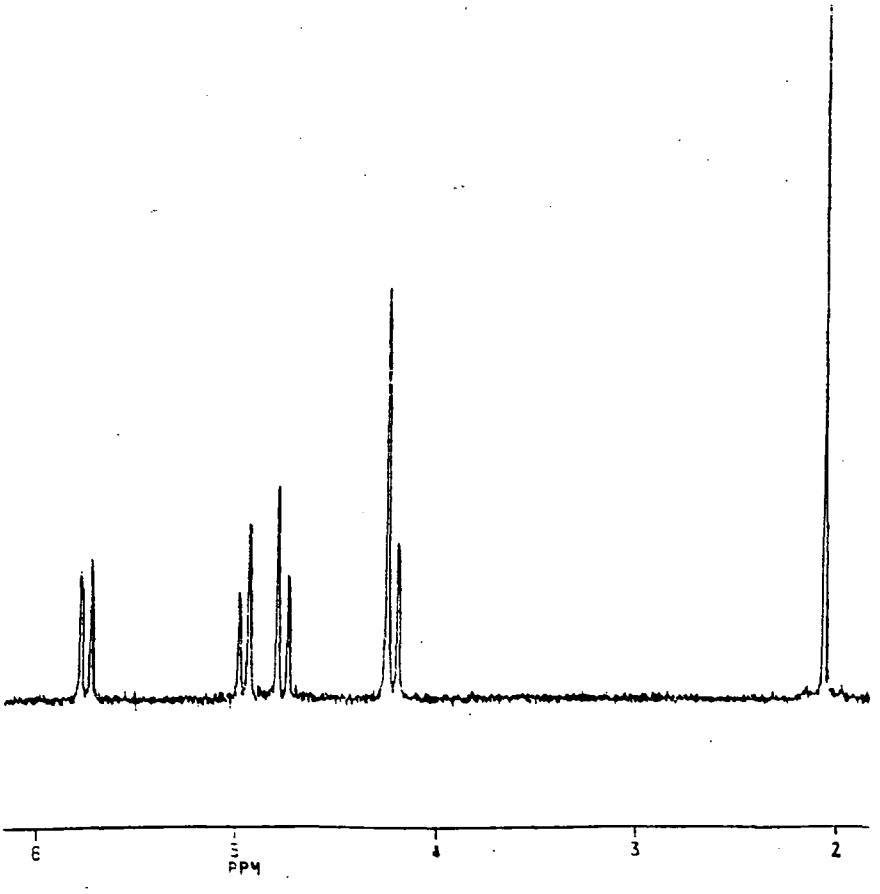

However in acetonitrile two sets of bands are observed consistent with the presence of both conformers 5.16 and 5.17 (fig. 5.2). The minor conformer is present to the extent of *ca* 20%. On addition of acid to 5.16 in acetonitrile all bands shift downfield.

Fig. 5.2
^{1}H NMR Spectrum Of DAPT (5.6) In CD_3CN

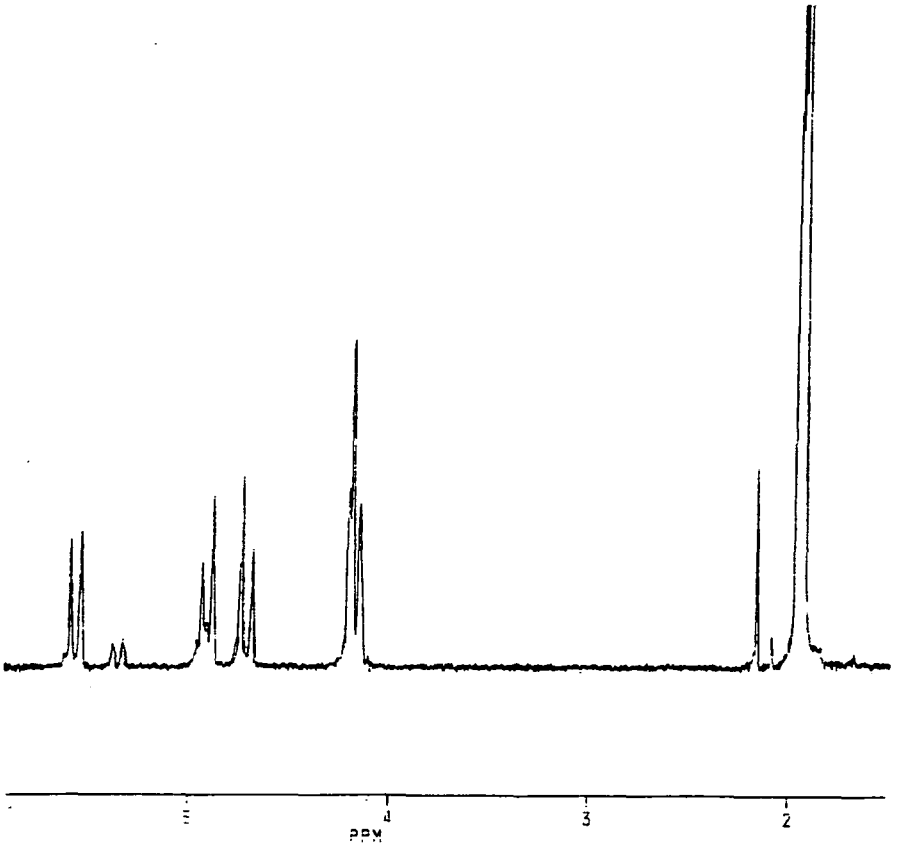

In the presence of 1 equivalent of acid is shown in fig. 5.3 and shifts are given in table 5.2. The change in ^{1}H NMR spectrum is nearly complete in the presence of 1 equivalent of acid so that the results are best interpreted in terms of mono-protonation, with a rapid equilibrium between neutral and protonated species. The largest shift occurs with the CH_2 bridge protons indicating protonation on an attached nitrogen atom. In the presence of 1 equivalent of acid the spectrum remains unchanged over several hours. However, in the presence of excess acid (fig. 5.4-5.6) the spectra indicate rapid decomposition. The spectra show triplets, J *ca* 50Hz in the region δ6-7 which may be attributed to amino protons in protonated NHR groups. Bands are also observed in the region expected for hydrated formaldehyde (δ4.8)[15] and to species containing -NCH_2OH groups (δ4.5).[16]

Fig. 5.3

^{1}H NMR Spectrum Of DAPT (5.6) In The Presence Of 1 Equivalent Of Acid In CD_3CN

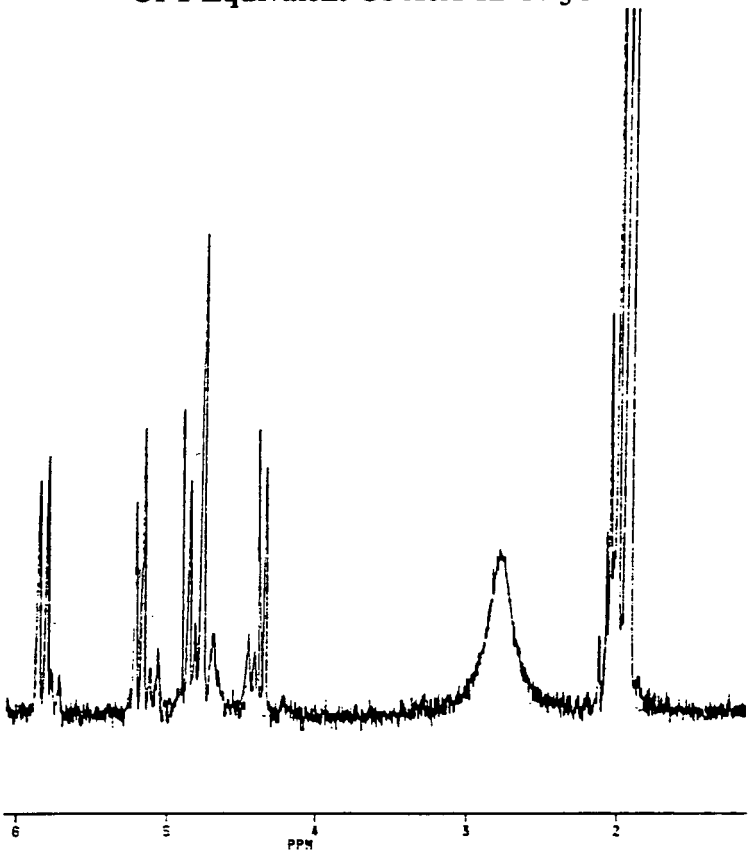

Fig. 5.4

^{1}H NMR Spectrum Of DAPT (5.6) In The Presence Of 2 Equivalents Of Acid In CD_3CN

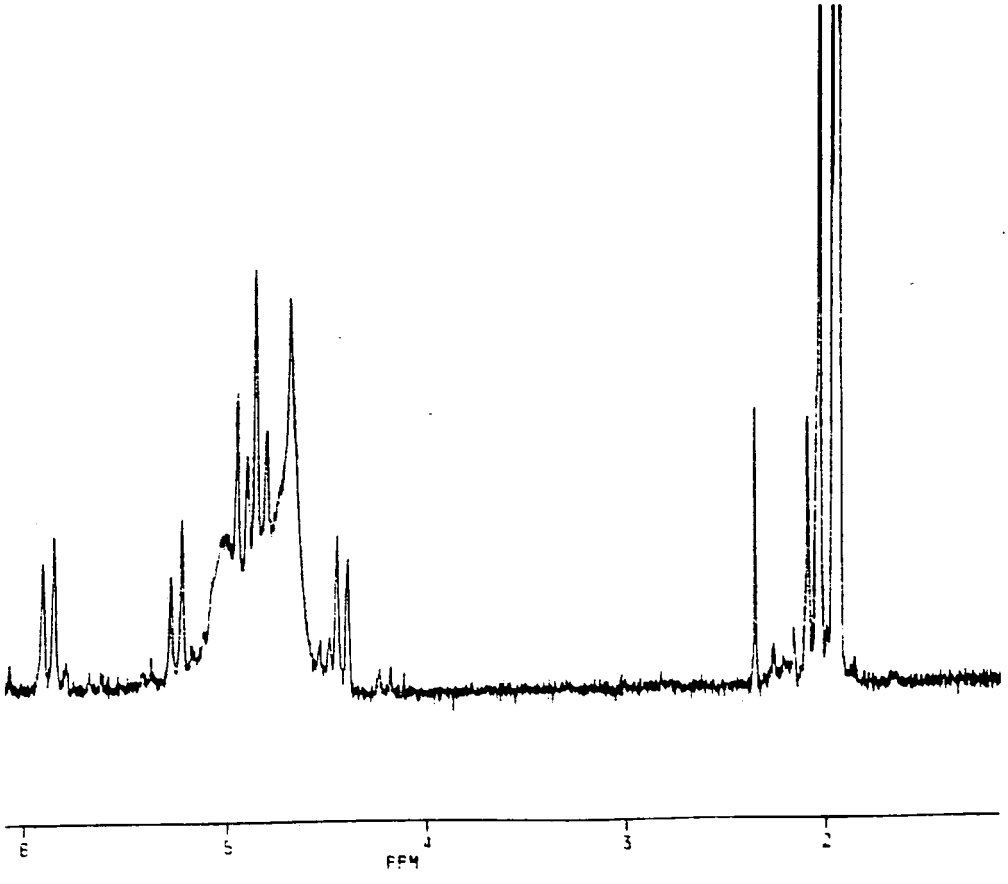

Fig. 5.5

^{1}H NMR Spectrum Of DAPT (5.6) In The Presence Of 4 Equivalents Of Acid In CD_3CN

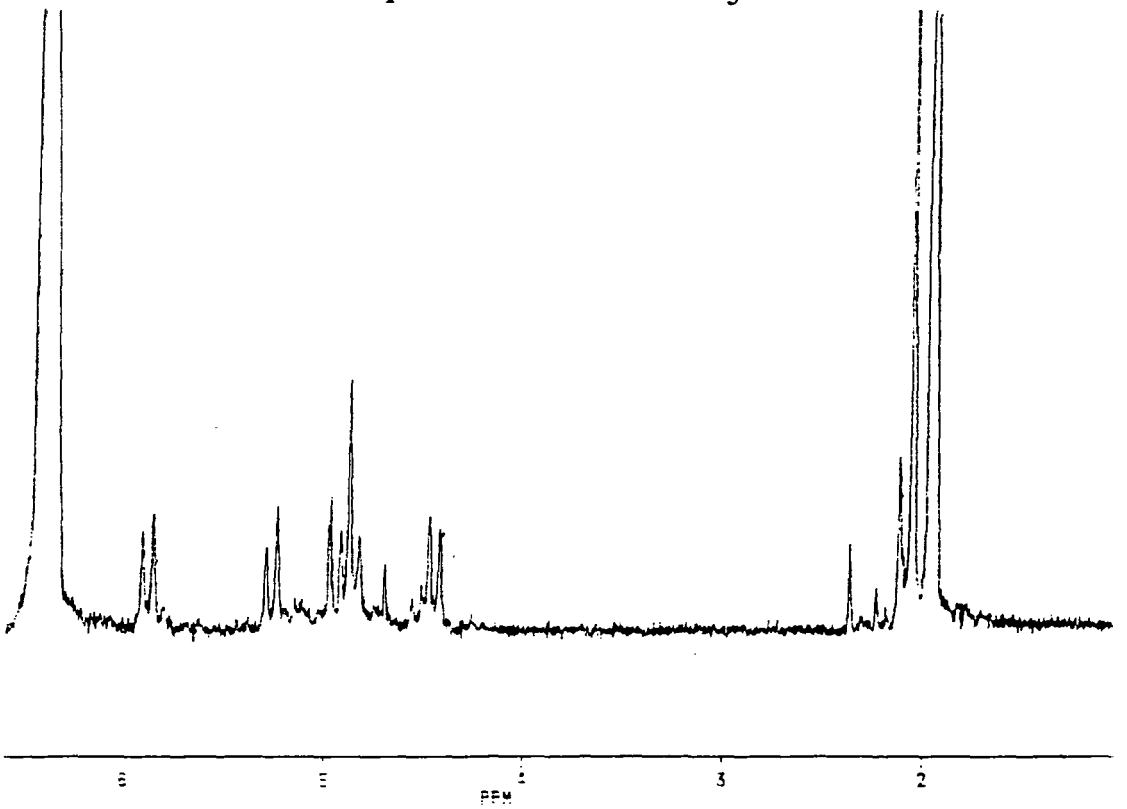

Fig. 5.6

^{1}H NMR Spectrum Of DAPT (5.6) In The Presence Of 6 Equivalents Of Acid In CD_3CN

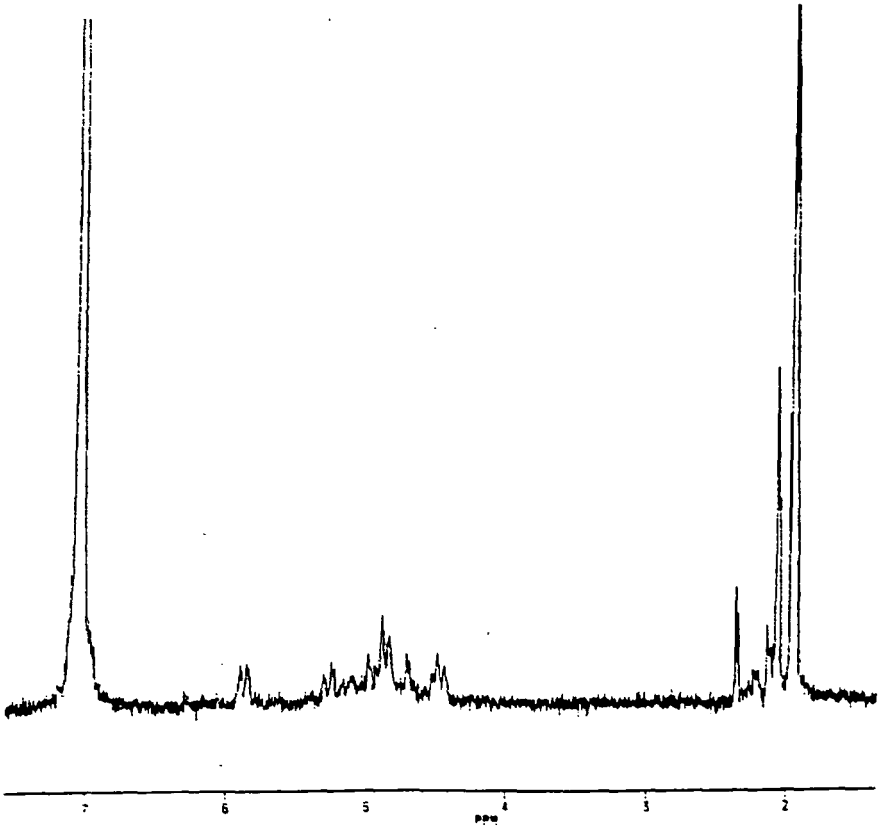

Fig. 5.7

^{1}H NMR Spectrum Of DAPT (5.6) In The Presence Of 2 Equivalents Of Acid In CD_3CN 1 Day Later

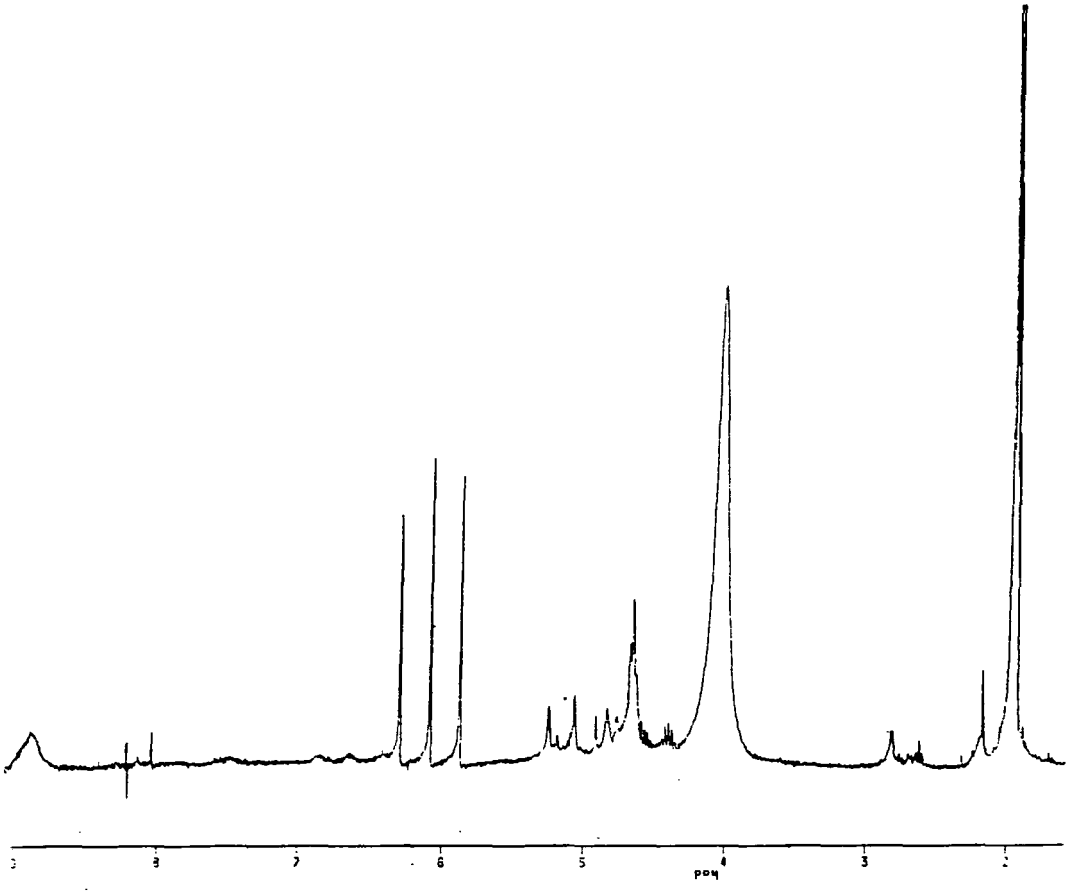

Table 5.2

^{1}H NMR Chemical Shifts For DAPT (0.03M) In CD_3CN Containing Perchloric Acid

	AB Quartets (J = 13Hz)				CH_2 Bridge	Acetyl
DAPT	5.61 5.55	4.94 4.89	4.73 4.68	4.21 4.16	4.20	1.93
1 Equivalent Acid	5.86 5.81	5.22 5.17	4.90 4.85	4.40 4.45	4.76	2.01
2 Equivalents Acid	5.90 5.85	5.27 5.22	4.95 4.89	4.44 4.39	4.85	2.03
4 Equivalents Acid	5.91 5.85	5.29 5.24	4.97 4.92	4.47 4.42	4.87	2.05
6 Equivalents Acid	- -	5.31 5.26	5.00 -	4.49 4.44	4.89	-

After prolonged periods (1 day) a characteristic triplet δ6.0 J=50Hz is observed characteristic of ammonium ions (fig. 5.7). A possible decomposition product, N-acetylamino- ethanol (5.18) was synthesised and found to give NMR bands δ4.5 (CH_2) and δ2.1 (CH_3) in acidic solution.

$$CH_3CONHCH_2OH$$

5.18

This indicates that 5.18 may be a decomposition product of 5.6 as postulated.[8] However, it is thought that 5.18 would not be very stable at these acid concentrations at therefore possibly undergo further decomposition.

5.2.2 Mass Spectrum

The Chemical Ionisation mass spectrum of DAPT shows a prominent M+1 peak corresponding to monoprotonated DAPT (fig 5.8). The theoretical peak intensities agree well with those obtained.

Fig. 5.8
Chemical Ionisation Mass Spectrum Of DAPT (5.6)

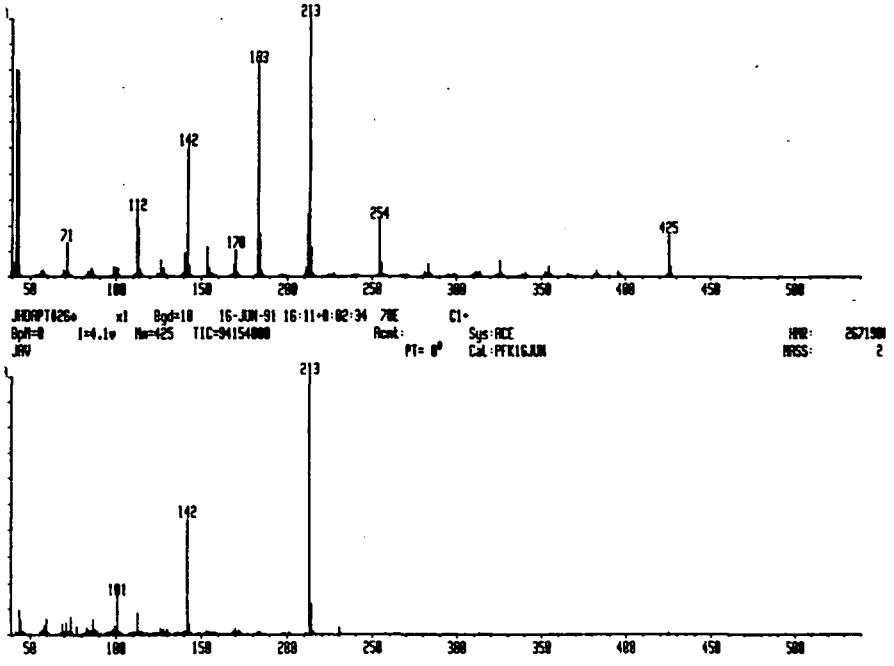

5.2.3 Formaldehyde Determination

It was thought that DAPT (5.6) would produce formaldehyde during its decomposition in acidic media. In a controlled experiment a known amount of DAPT (5.6) was reacted with 1M perchloric acid in 70/30 (v/v) acetonitrile/water. The reaction mixture was left for approximately 15 mins. and then neutralised with aqueous sodium hydroxide before addition of an excess amount of alcoholic dimedone (5.19). The precipitated 1:1 formaldehyde-dimedone adduct[17] was isolated as a pale orange solid which after recrystallisation from 50% aqueous ethanol gave white crystals M.P. 189°C.[18] Approximately 3 moles of formaldehyde were produced per mole of DAPT.

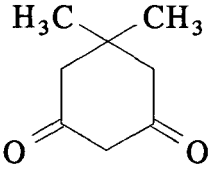

5.19

The combined results of the formaldehyde determination and NMR studies indicate that the decomposition of 5.6 may be written as :-

$$\text{DAPT} \longrightarrow 3CH_2O + 2CH_3CONHCH_2OH + 2NH_3$$

5.2.4 U.V. and Kinetic Studies

5.6 in acetonitrile has λ_{max} 196nm ε=16,000 $dm^3\ mol^{-1}\ cm^{-1}$ (fig. 5.9) and is indefinitely stable. In the presence of acid there is an initial rapid spectral change attributed to protonation.

The data in table 5.3 show that the change in spectrum is >90% complete in a solution of $2x10^{-3}$M acid. Use of equation 5.5 leads to a limit of $K_1 > 4500\ dm^3\ mol^{-1}$, giving a pKa value of > 3.65. The much higher pKa value of DAPT in acetonitrile than in water is in accord with previous results[8,9] noting the acid weakening effect of acetonitrile. The major factor may be the relatively poor solvation of the proton in acetonitrile compared to that in water.

$$DAPT + H^+ \underset{}{\overset{K_1}{\rightleftharpoons}} DAPTH^+ \qquad \text{eqn. 5.4}$$

$$K_1 = \frac{[DAPTH^+]}{[DAPT]\,[H^+]} \qquad \text{eqn. 5.5}$$

Table 5.3
Initial Absorbance Of DAPT ($5x10^{-5}$M) In Acetonitrile Containing Perchloric Acid At 25°C

	Wave length Of Absorbance[a] (nm)		
$10^2[HCLO_4]$ mol dm^{-3}	**200**	**210**	**220**
0	0.7026	0.3484	0.1694
0.2	0.3934	0.1927	0.0687
0.4	0.3878	0.1936	0.0654
0.5	0.3859	0.1943	0.0646
0.8	0.3742	0.1901	0.0628
1.0	0.3556	0.1890	0.0620
2.0	0.3452	0.1891	0.0631
4.0	0.3310	0.1921	0.0637
7.0	0.3025	0.1956	0.0691
10.0	0.2710	0.1998	0.0773
15.0	0.2629	0.2084	0.0887
20.0	0.3011	0.2192	0.1097
30.0	0.3410	0.2570	0.1417
40.0	0.3652	0.2735	0.1576

a) Initial absorbance on addition of acid (using fresh solution of DAPT for each measurement).

The rapid decrease in absorbance due to protonation was followed by a much slower fading reaction which was measured at 220nm. First order kinetics were observed and the rate constants were measured as a function of the acid concentration and water content of the solvent. Results are give in tables 5.4-5.7.

Fig. 5.9

U. V. Spectrum Of DAPT ($7.9x10^{-5}M$) In Acetonitrile/Perchloric Acid

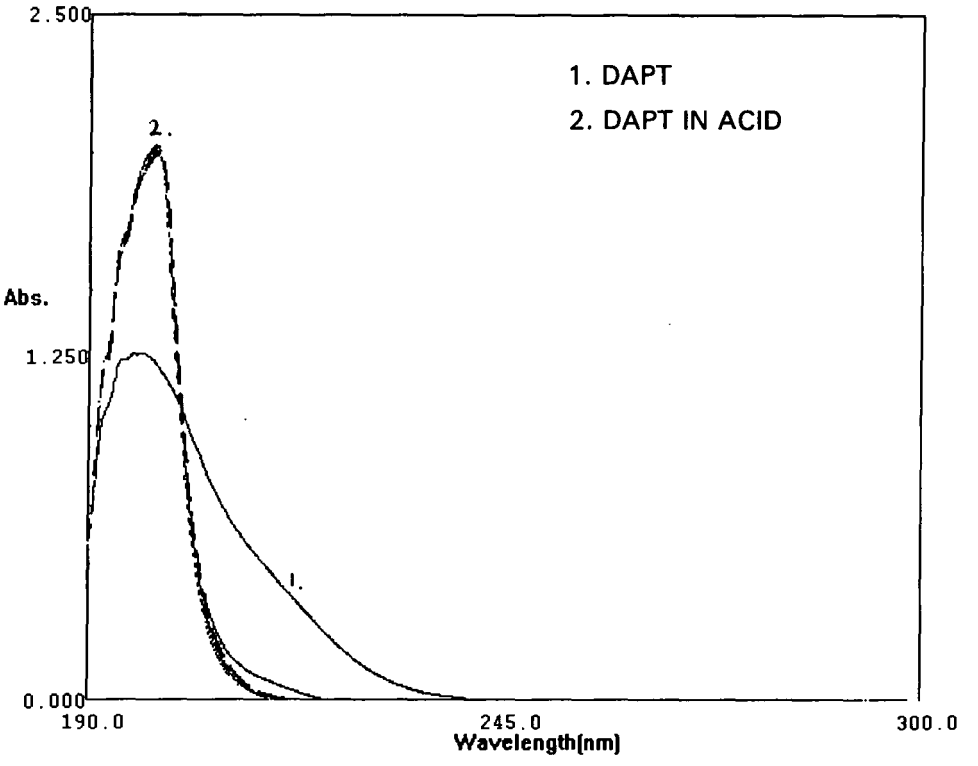

Table 5.4

Rate Constants For The Decomposition Of DAPT ($5x10^{-5}M$) In Acetonitrile/Perchloric Acid

$10^2[HClO_4]$ mol dm^{-3}	Total[a,b] H_2O v/v	k_{obs} 10^{-3} s^{-1}	k_{obs}[c] 10^{-3} s^{-1}	kK_2[d] dm^3 mol^{-1} s^{-1}
0.5	0.07	0.32	0.29	0.050
1	0.09	0.61	0.50	0.050
2	0.13	0.89	0.73	0.037
3	0.17	1.40	1.20	0.040
4	0.21	1.99	1.74	0.043
5	0.25	2.40	2.10	0.042
6	0.29	3.10	2.75	0.046
7	0.33	4.12	3.70	0.053
8	0.37	5.70	5.30	0.066
9	0.41	6.83	6.34	0.070
10	0.45	7.96	7.42	0.074

Table 5.5

Rate Constants For The Decomposition Of DAPT ($5x10^{-5}M$) In Acetonitrile/Perchloric Acid Containing 0.50% Water

$10^2[HClO_4]$ mol dm^{-3}	Total[a,b] H_2O v/v	k_{obs} 10^{-3} s^{-1}	k_{obs}[c] 10^{-3} s^{-1}	kK_2[d] dm^3 mol^{-1} s^{-1}
0.5	0.07	0.46	-	-
1	0.59	1.01	0.30	0.030
2	0.63	1.10	0.34	0.017
3	0.67	1.40	0.60	0.020
4	0.71	1.42	0.57	0.014
5	0.75	1.73	0.83	0.017
6	0.79	2.70	1.75	0.029
7	0.83	2.83	1.82	0.021
8	0.87	2.92	1.88	0.023
9	0.91	4.04	2.95	0.033
10	0.95	4.52	3.38	0.034

Table 5.6

Rate Constants For The Decomposition Of DAPT ($5x10^{-5}M$) In Acetonitrile/Perchloric Acid Containing 0.75% Water

$10^2[HCLO_4]$ mol dm^{-3}	Total[a,b] H_2O v/v	k_{obs} 10^{-3} s^{-1}	k_{obs}[c] 10^{-3} s^{-1}	kK_2[d] dm^3 mol^{-1} s^{-1}
0.5	0.82	0.59	-	-
1	0.84	1.16	0.15	0.015
2	0.88	1.33	0.28	0.014
3	0.92	1.40	-	-
4	0.96	1.45	-	-
5	1.00	1.50	-	-
6	1.04	1.85	0.60	0.010
7	1.08	2.21	0.914	0.013
8	1.12	2.61	1.27	0.016
9	1.16	3.12	1.73	0.019
10	1.20	3.88	2.44	0.024

Table 5.7

Rate Constants For The Decomposition Of DAPT ($5x10^{-5}M$) In Acetonitrile/Perchloric Acid Containing 1.00% Water

$10^2[HClO_4]$ / mol dm^{-3}	Total[a,b] H_2O v/v	k_{obs} / 10^{-3} s^{-1}	k_{obs}[c] / 10^{-3} s^{-1}	kK_2[d] / dm^3 mol^{-1} s^{-1}
0.5	1.07	0.72	-	-
1	1.09	1.30	-	-
2	1.13	1.54	0.189	0.009
3	1.17	1.62	-	-
4	1.21	-	-	-
5	1.25	-	-	-
6	1.29	-	-	-
7	1.33	1.92	0.33	0.005
8	1.37	2.34	0.70	0.009
9	1.41	2.66	0.97	0.011
10	1.45	2.72	0.98	0.010

a) Acetonitrile contains 0.05% water.

b) A solution of 0.01M perchloric acid contains 0.04% water.

c) Corrected k_{obs} using $k_{obs}-k_{H_2O}[H_2O]$. Where $k_{H_2O} = 1.2x10^{-3}$ s^{-1}.

d) $kK_2 = k_{obs}-k_{H_2O}[H_2O] / H^+$

The results are arranged in groups with approximately equal water content. The results show that at a given water concentration k_{obs} increases with increasing acid concentration. However, when the acid concentration is kept constant k_{obs} increases with increasing water content at low acidities $[HClO_4] < 0.03M$ but decreases with increasing water content at higher acidities.

These findings are compatible with competing reaction pathways shown in scheme 5.6. involving :-

i) Reaction of $DAPTH^+$ with water.

ii) Reaction of $DAPTH^+$ with acid.

Scheme 5.6

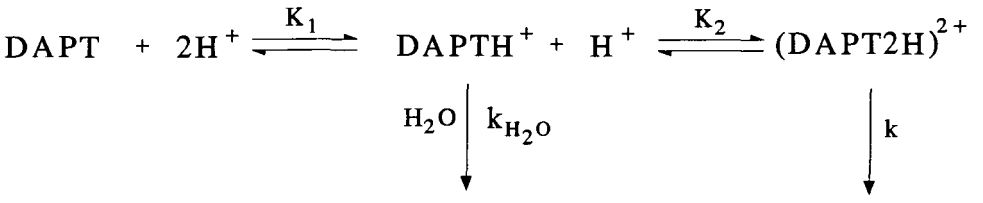

$$k_{obs} = k_{H_2O}[H_2O] + kK_2[H^+] \quad \textbf{eqn. 5.6}$$

The equilibrium results indicate that $K_1\,[H^+] >> 1$, and if $K_2\,[H^+] << 1$ then equation 5.6 follows. The scheme is written in terms of equilibrium protonation (constant K_2) followed by unimolecular reaction of the diprotonated species. However, the results would also be compatible with rate determining attack of acid on the monoprotonated species. The values in tables 5.4-5.7 are compatible with this scheme with a value for k_{H_2O} of 1.2×10^{-3} s^{-1} at 1% (v/v) water. This value may be converted to a second order rate coefficient of 2.2×10^{-3} dm^3 mol^{-1} s^{-1} in terms of the molarity of water.

Although there is some scatter it is shown in fig. 5.10 that the values obtained for kK_2 decrease with increasing water content of the solvent. The values of *ca* 0.05% at 0.1% water content reducing to 0.01 at 0.1% water content. This decrease in the value of kK_2 is explained by the better solvation of the proton as the water content is increased leading to a decrease in the value expected for the protonation constant K_2.

In solutions of low acidity the first term in equation 5.6 will dominate the rate expression so that k_{obs} increases with increasing water content. However, at higher acidities when the second term becomes dominant the decrease in value of kK_2 with increasing water content will result in decrease in the overall value of k_{obs}.

Fig. 5.10

Plot Of kK_2 Values for The Decomposition Of DAPT ($5x10^{-5}M$) In Acetonitrile/Acid Containing Water

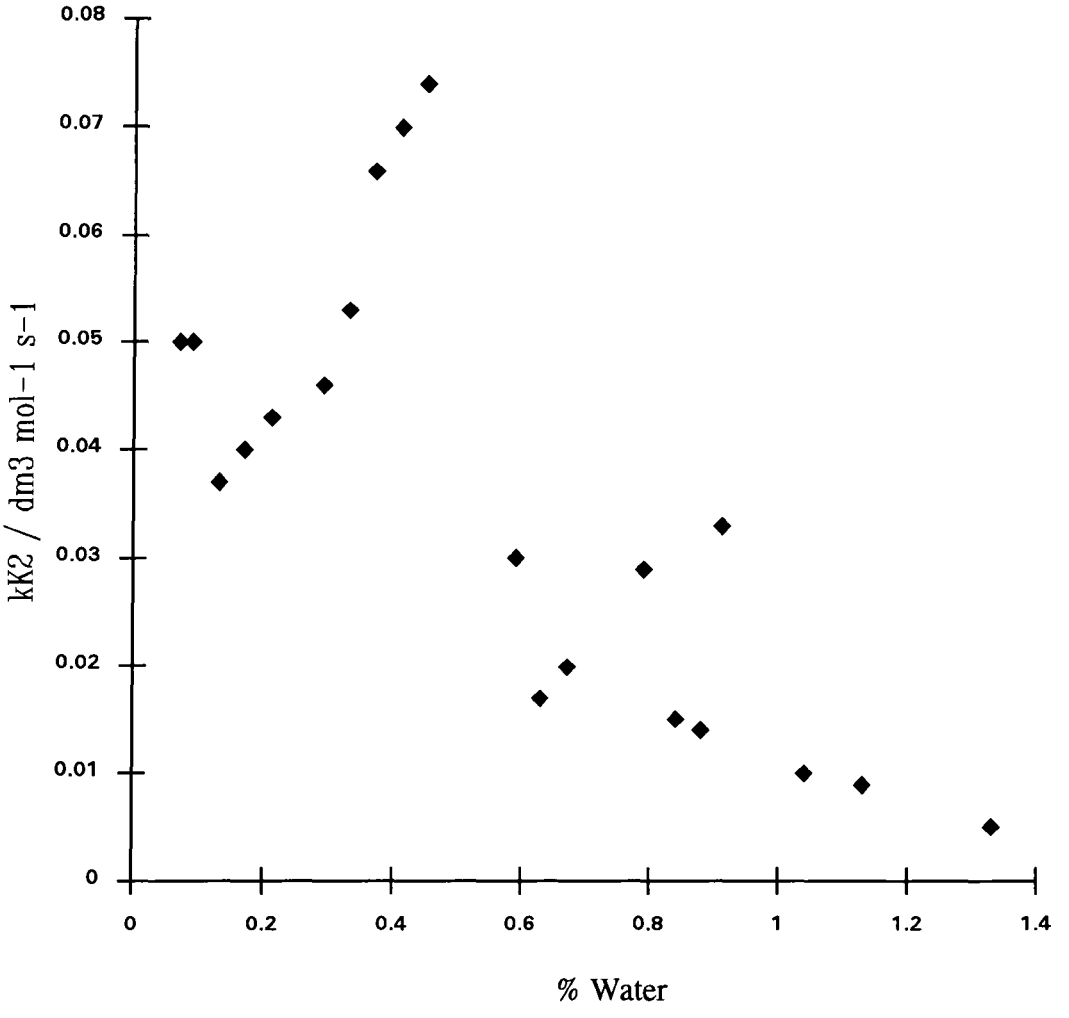

5.3 Dinitropentamethylenetetramine (DPT)

5.3.1 ^{1}H NMR

The ^{1}H NMR spectrum of DPT in deuterioacetonitrile (fig. 5.11) shows bands at δ4.12 (s, CH_2 bridge) and an AB quartet (J=8Hz) due to vicinal coupling of the methylene protons with shifts of δ4.89 and 5.56 respectively.

^{1}H NMR studies reveal that DPT is extensively monoprotonated by one equivalent of acid (fig.5.12). However, on addition of more acid the chemical shifts increase slightly as monoprotonation proceeds to completion (fig. 5.13 and 5.15). By about 4 equivalents of acid there is a further shift of the methylene bridge signal downfield, which may be indicative of diprotonation. The chemical shifts are summarised in table 5.8.

The spectrum in the presence of one equivalent of acid shows essentially monoprotonated DPT which seems to be fairly stable. By 2, 3 and 4 equivalents the spectra show rapid decomposition of the monoprotonated species. However,it is not possible at these high acid concentrations what is actually observed could be conversion of the monoprotonated species into the less stable diprotonated species which rapidly breaks down and therefore may not be observed. Broad bands attributed to NHR type species about δ7 are seen similar to those in DAPT.

Table 5.8
^{1}H NMR Chemical Shifts For DPT (5.9) In CD_3CN Containing Perchloric Acid

	AB Quartets (J=8Hz)		CH_2 Bridge	$\%H_2O$
DPT	5.61 5.56	4.83 4.88	4.13	0.05
1 Equivalent Acid	5.80 5.75	5.01 4.96	4.60	0.21
2 Equivalents Acid	5.86 5.81	5.05 4.99	4.64	0.37
3 Equivalents Acid	- -	5.07 5.01	4.68	0.53
4 Equivalents Acid	5.93 5.88	5.10 5.05	4.78	0.69

Fig. 5.11
^{1}H NMR Spectrum Of DPT (5.9) In CD_3CN

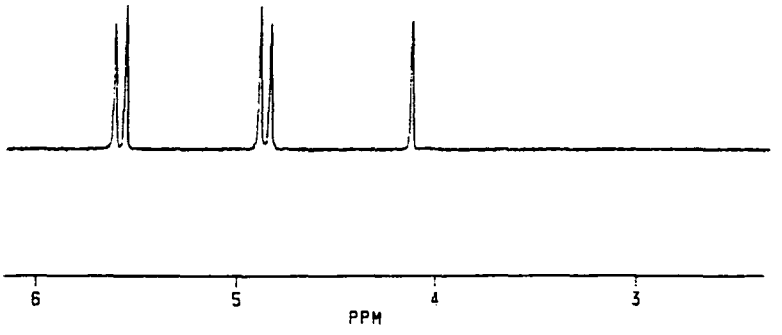

Fig. 5.12
^{1}H NMR Spectrum Of DPT (5.9) In The Presence Of 1 Equivalent Of Acid In CD_3CN

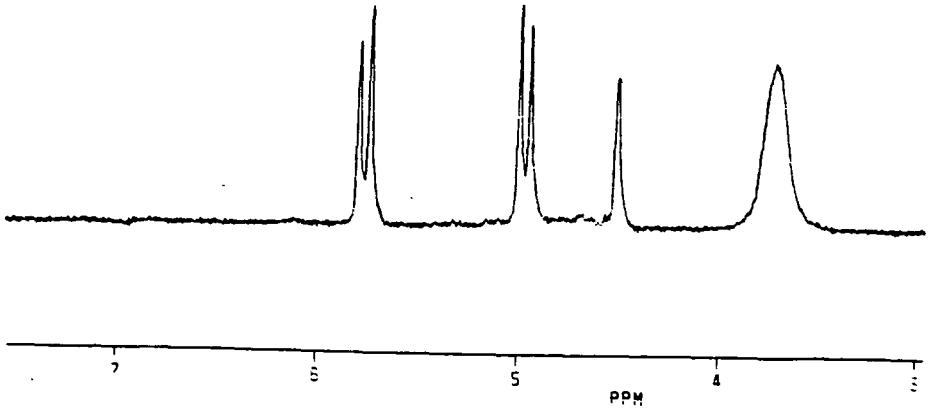

Fig. 5.13

^{1}H NMR Spectrum Of DPT (5.9) In The Presence Of 2 Equivalents Of Acid In CD_3CN

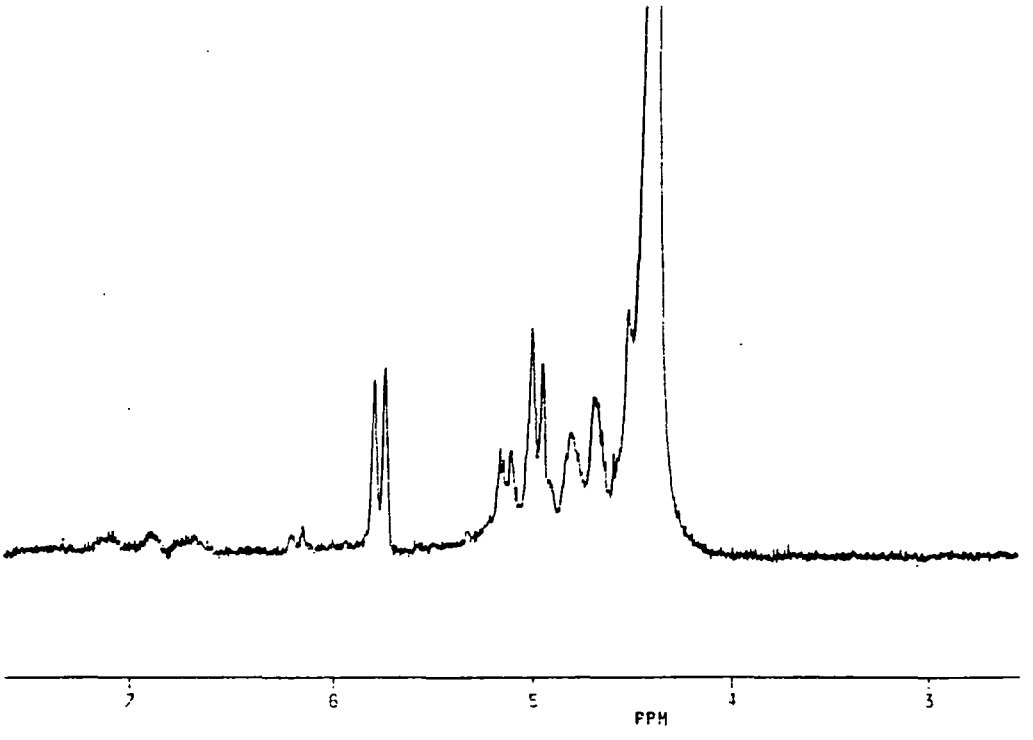

Fig. 5.14

^{1}H NMR Spectrum Of DPT (5.9) In The Presence Of 3 Equivalents Of Acid In CD_3CN

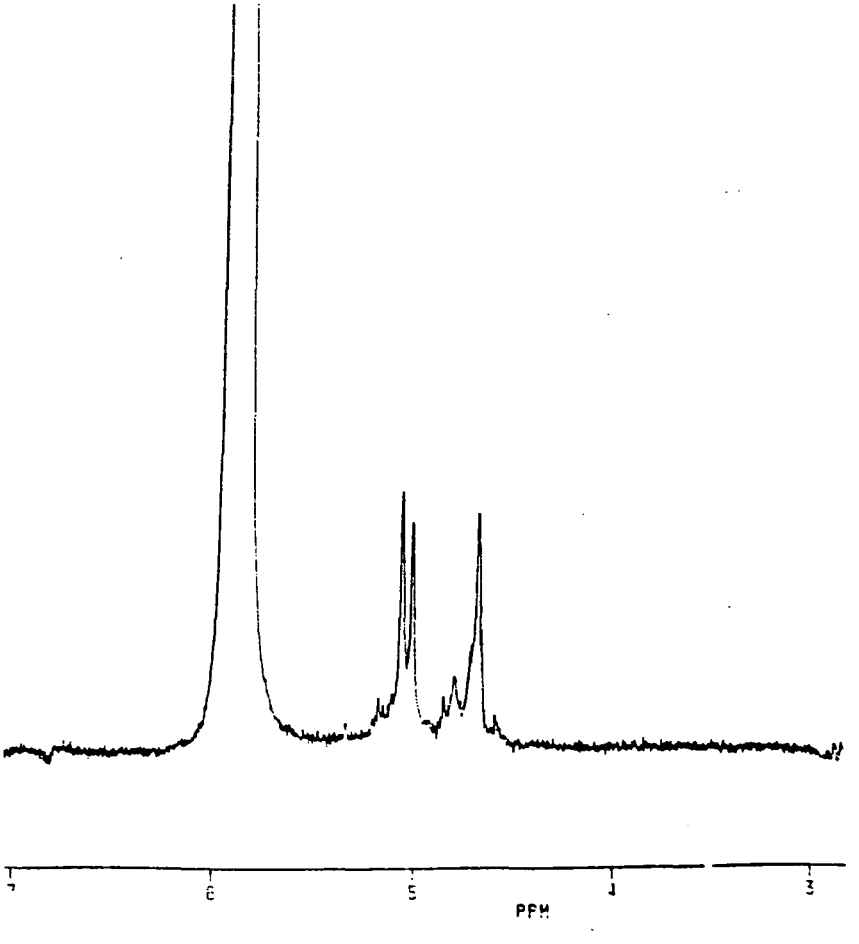

Fig. 5.15

^{1}H NMR Spectrum Of DPT (5.9) In The Presence Of 4 Equivalents Of Acid In CD_3CN

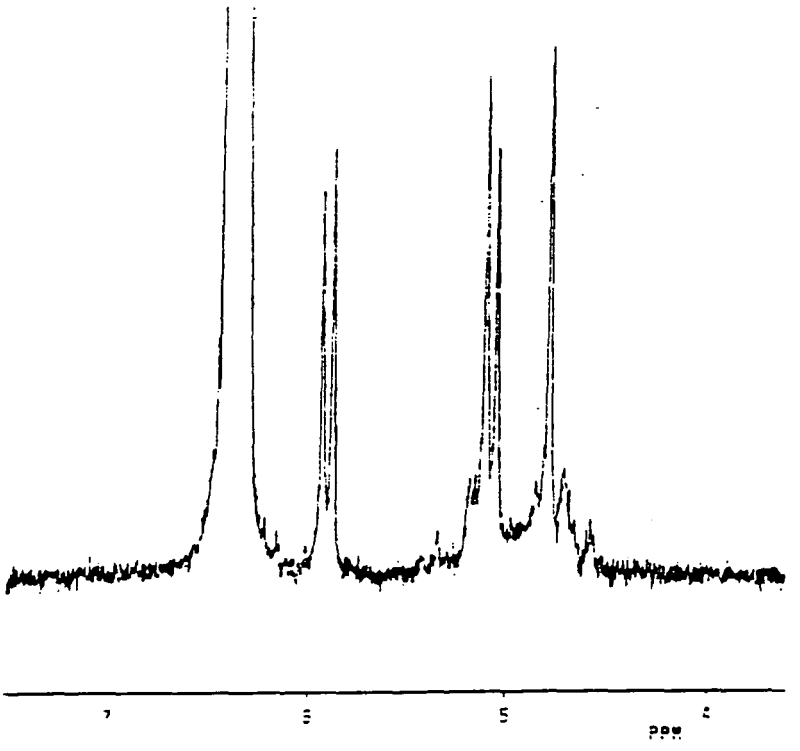

5.9 U. V. And Kinetic Studies

The U. V. spectrum of DPT (5.9) in acetonitrile (fig. 5.15) shows λ_{max} 243nm, $\varepsilon = 10{,}000$ dm^3 mol^{-1} cm^{-1}. In this solvent DPT is stable for several days. However, in the presence of either acid or base changes in spectrum are observed. In acidic solutions there is an instantaneous change indicative of protonation resulting in a hypsochromic shift and a decreased absorbance at 260nm. Measurements at this wavelength are given in table. 5.9.

These results show that at low water content (0.1%) the value of K_1 (eqn. 5.7) is high (>1000) so that protonation is essentially complete at $2x10^{-3}$M acid. However, as the water content increases the extent of conversion to the protonated form decreases, until with 1% water $K_1 \sim 8$ dm^3 mol^{-1}.

$$K_1 = \frac{[DPTH^+]}{[DPT][H^+]} \equiv \frac{(0.48^a - \text{Absorbance}^b)}{(\text{Absorbance}^b - 0.24^c)[H^+]} \quad \textbf{eqn.5.7}$$

a) Initial absorbance of DPT ($8x10^{-5}$M) in acetonitrile

b) Initial absorbance of DPT ($8x10^{-5}$M) in acetonitrile/perchloric acid and water at 260nm

c) Final absorbance of DPT ($8x10^{-5}$M) in acetonitrile/perchloric acid and water at 260nm (at all acid concentrations)

The rapid decrease in absorbance observed on acidification was followed by a slower measureable process. The U. V. spectra in fig. 5.16 indicate an isosbestic at 228nm with decreases in absorbance at higher wavelength and decreases in absorbance at shorter wavelength. The final spectrum shows λ_{max} 210nm and probably represents the formation of nitramide, NH_2NO_2, which is known to absorb at this wavelength[10] and to be stable in acidic solution.

The spectroscopic literature only contains meagre references to aliphatic nitroamines however, certain generalisations can be made. The spectra of primary and secondary nitroamines in ethanol or 1,4-dioxan are relatively simple exhibiting one broad structureless band with λ_{max} in the region 225-240nm.[19]

The work of Thorn and Jones[19] resulted in the following guidelines for use when interpreting the U. V. spectrum of aliphatic nitroamines.

i) **Secondary Nitroamines**

For compounds containing one secondary nitroamine group per molecule , in neutral solution ε_{max} approximates to 5,500 $dm^3\ mol^{-1}\ cm^{-1}$. Observation has indicated that for a molecule containing n secondary nitroamine functions ε_{max} approximates to 5,500 x n $dm^3\ mol^{-1}\ cm^{-1}$.

ii) **Primary Nitroamines**

In neutral solution ε_{max} for the primary nitroamine functions is observed as approximately 7,000 $dm^3\ mol^{-1}\ cm^{-1}$.

iii) **Nitroamines In Alkaline Solution**

The absorbtion maximum of primary nitroamines in alkaline solution shows a shift of λ_{max} to longer wavelength and an increase in λ_{max}. For a molecule containing n primary nitroamine functions ε_{max} approximates to 8,500 x n $dm^3\ mol^{-1}\ cm^{-1}$.

Secondary nitroamines e.g. DPT tend to be unstable in alkaline solution. However, in cases where the compounds are sufficiently stable to enable U. V. spectra to be obtained show no change in λ_{max} from that observed in neutral solution.

The value of ε_{max} of 9,833 $dm^3\ mol^{-1}\ cm^{-1}$ for DPT in acetonitrile (fig. 5.15) agrees quite well with the 5,500 x n formula for secondary nitroamines. The increase in ε_{max} in acidic media to approximately 14,000 $dm^3\ mol^{-1}\ cm^{-1}$ and in basic media to approximately 16,000 $dm^3\ mol^{-1}\ cm^{-1}$ (fig. 5.17) (233nm) agrees quite well with the 7,000 x n and 8,500 x n formulae proposed for primary nitroamines in acidic/neutral and alkaline solution.

It is possible to distinguish between compounds containing primary and secondary nitroamine groups provided that the presence of other functional groups is taken into account. Using the above generalisations it appears that when DPT is put into acidic or basic media the species produced contains 2 primary nitroamine groups. This indicates that the secondary nitroamine groups of DPT are converted by some decomposition pathway into primary nitroamine functions although, this pathway as yet has not been identified. The extinction coefficient of *ca* 14,000 dm^3 mol^{-1} cm^{-1} in acidic media is consistent with the formation of two equivalents of nitramide per mole of DPT.

Fig. 5.15
U. V. Spectrum Of DPT (8.4x10-5M) In Acetonitrile

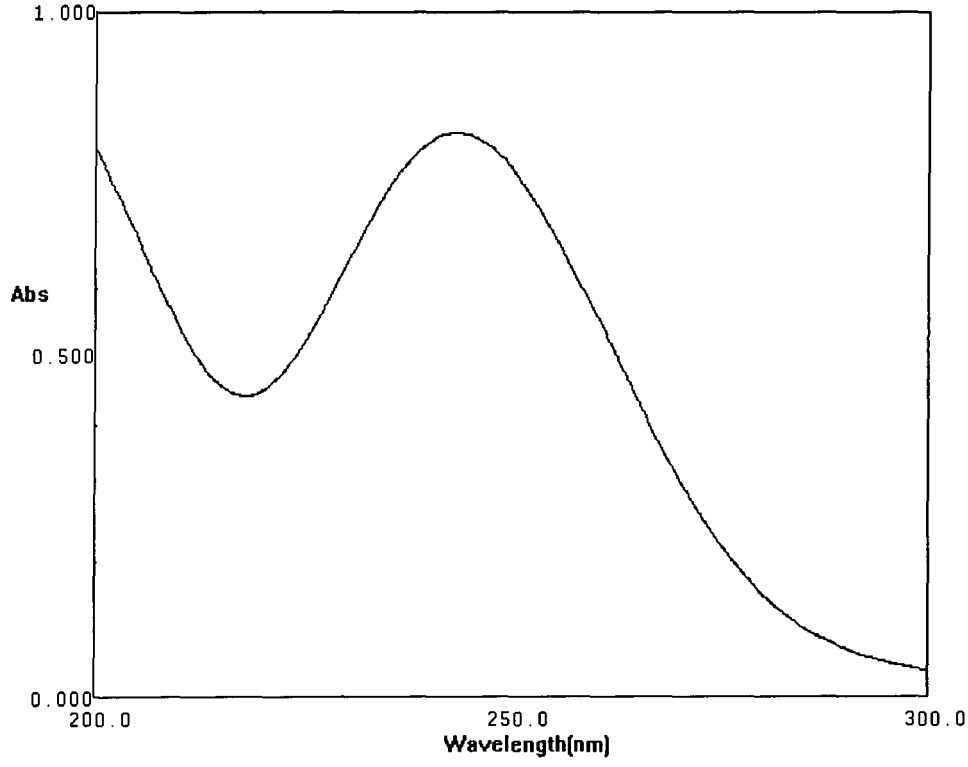

Fig. 5.16

U. V. Spectrum Of DPT In The Presence Of Acid In Acetonitrile

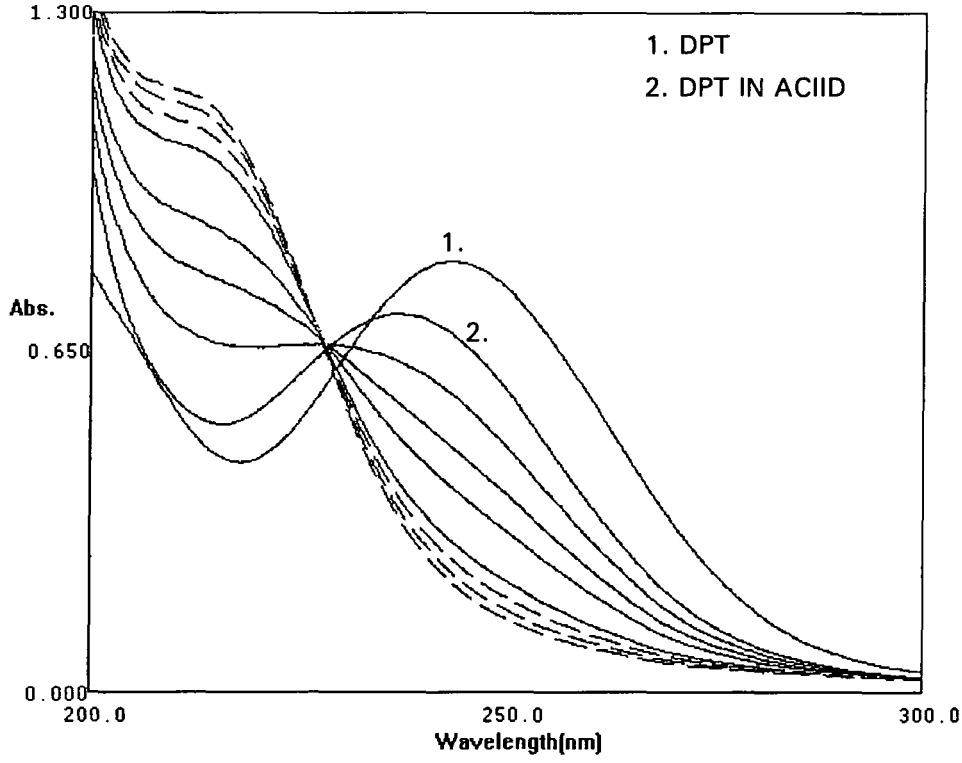

Fig. 5.17

U. V. Spectrum Of DPT ($8.4x10^{-5}$M) In Alkali In Acetonitrile

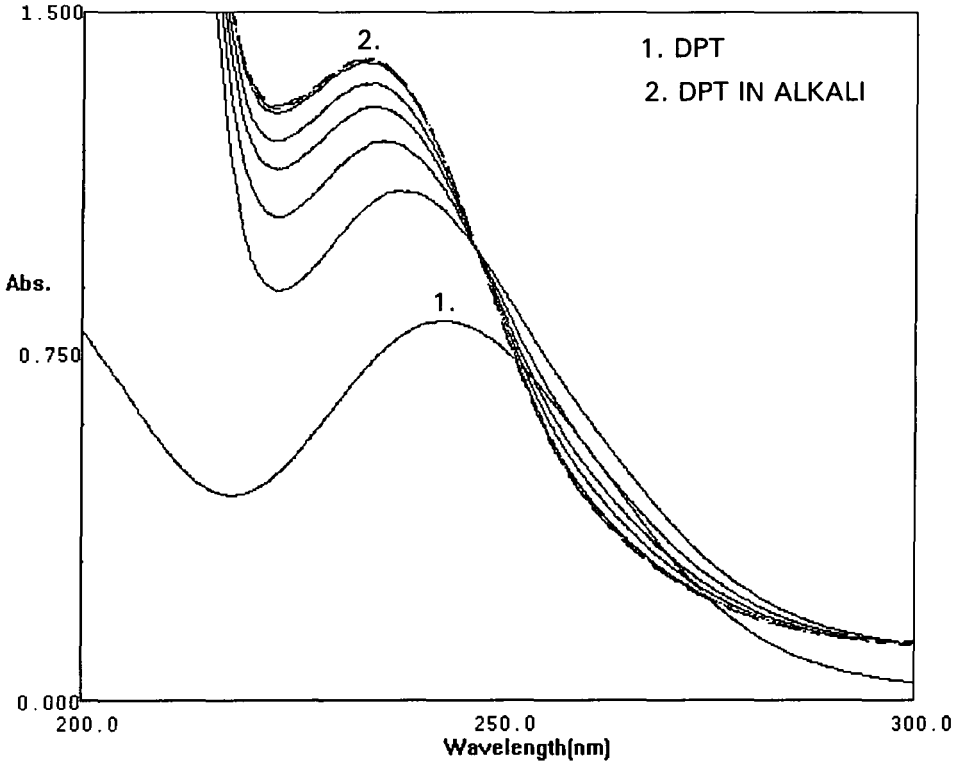

Table 5.9

Absorbance Data For The Initial Protonation Of DPT In Acetonitrile

$10^2[HCLO_4]$ / mol dm^{-3}	Total Water % v/v	Absorbance[a] 260nm	K_1[b]/dm^3 mol^{-1}
0	0.05	0.48	>1000
0.2	0.06	0.24	>1000
0.4	0.07	0.23	>1000
0.6	0.07	0.22	>1000
0.8	0.08	0.24	>1000
1.0	0.09	0.24	>1000
10	0.45	0.24	-
2.0	0.33	0.31	120
2.0	0.53	0.43	26
1.0	0.60	0.43	13
2.0	0.73	0.45	-
2.0	0.93	0.47	-
6.0	1.05	0.40	8
8.0	1.05	0.35	15
10.0	1.05	0.38	7
0.4	1.05	0.47	-
1.0	1.10	0.47	26
1.0	2.10	0.48	-
2.0	1.10	0.45	-
5.0	1.25	0.41	7
			9

a) Initial Absorbance

b) $K_1 = \dfrac{[DPTH^+]}{[DPT][H^+]} \equiv \dfrac{(0.48 - \text{Absorbance})}{(\text{Absorbance} - 0.24)[H^+]}$ (see **eqn.5.7)**

Table 5.10

Approximate values Of K_1 With Increasing Water

% Water	K_1 / dm^3 mol^{-1}
0.10	> 1000
0.33	120
0.60	26
1.00	8

Rate coefficients at low water content are in table 5.11 and in solutions where $[H_2O]$ = 1% in table 5.12. As with DAPT the results are compatible with two decomposition pathways (scheme 5.7) involving reaction of the monoprotonated species with water and with acid respectively.

Scheme 5.7

$$DPT + H^+ \overset{K_1}{\rightleftharpoons} DPTH^+ + H^+ \overset{K_2}{\rightleftharpoons} (DPTH2H)^{2+}$$

$$\downarrow H_2O\ k_{H_2O} \qquad\qquad \downarrow k$$

At low water content k_{H2O} $[H_2O]$ is very small and the pathway involving reaction with water is relatively unimportant. Therefore it follows that

$$k_{obs} = kK_2[H^+]$$

and values in table 5.11 give a value for kK_2 of 0.10 ± 0.01 dm^3 mol^{-1} s^{-1}. (Value of kK_2 can be obtained by plotting k_{obs} vs. $[H^+]$ (without added water) (table 5.11) giving a straight line graph of gradient kK_2 (fig. 5.18)).

Fig. 5.18

Decomposition Of DPT In Acetonitrile/Perchloric Acid Without Added Water

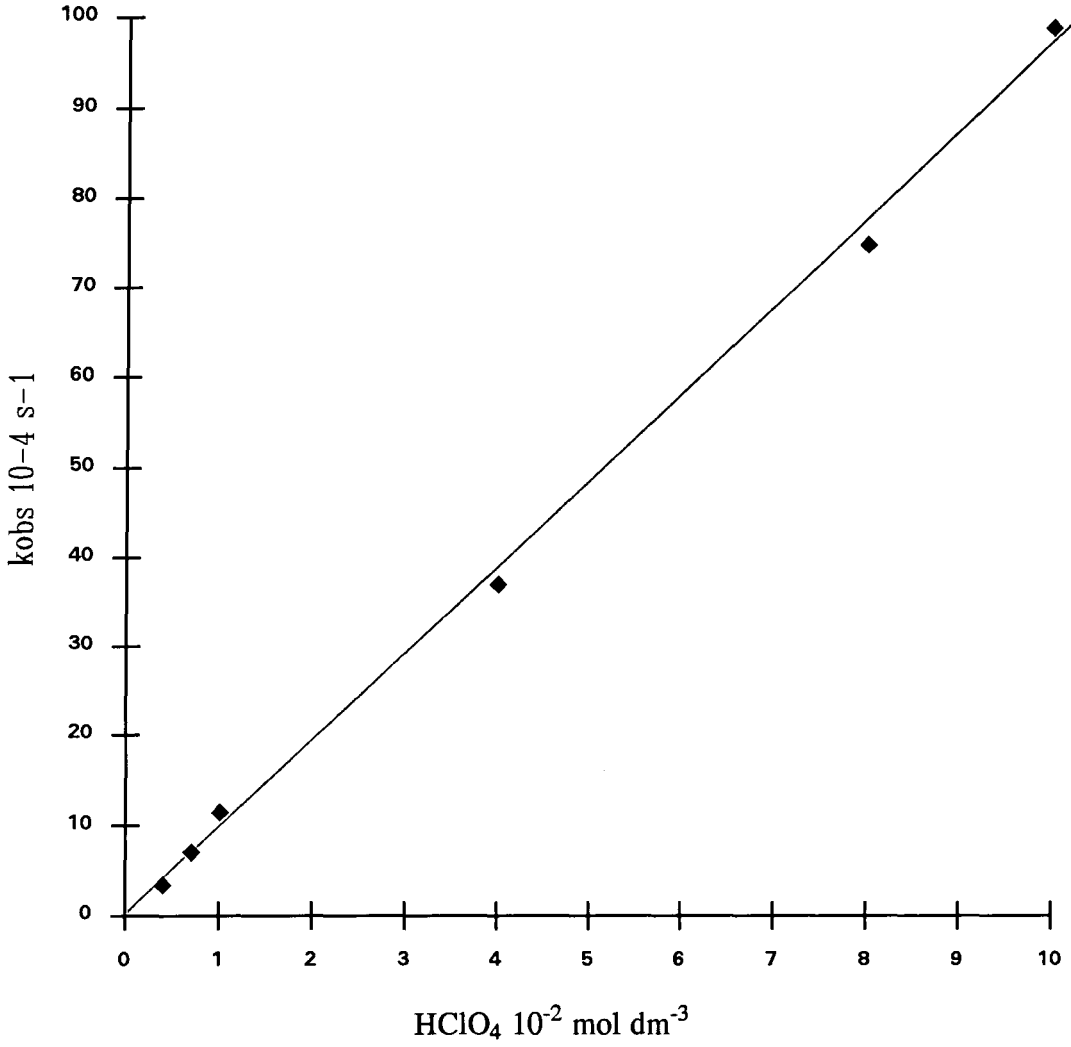

Table 5.11

Rate Constants For Decomposition Of DPT In Acetonitrile/Perchloric Acid At 260nm Without Added Water

10^2 $HClO_4$ mol dm^{-3}	k_{obs} 10^{-4} s^{-1}	kK_2[a] dm^3 mol^{-1} s^{-1}	Total % Water[b] v/v
0.4	3.3	0.082	0.066
0.7	7.1	0.102	0.078
1	11.5	0.115	0.09
4	37	0.093	0.21
8	75	0.094	0.37
10	99	0.099	0.45

Table 5.12

Rate Constants For Decomposition Of DPT In Acetonitrile/Perchloric Acid At 260nm With 1% Added Water

10^2 $HClO_4$ mol dm^{-3}	Total % Water[b] v/v	k_{obs} $10^{-4}s^{-1}$	$K_1[H^+]$ / $1+K_1[H^+]$[c]	$k_{obs}/(K_1[H^+]$ / $1+K_1[H^+])$ / 10^{-4}
0.4	1.05	1.4	0.031	45
1	1.10	3.7	0.074	50
2	1.10	9.0	0.138	65
5	1.25	30	0.286	105
6	1.05	41	0.324	130
8	1.10	63	0.390	160
10	1.05	91.5	0.444	206

a) $kK_2 = k_{obs} / [H^+]$

b) Acetonitrile contains 0.05% water.

c) $K_1 = 8$ mol^{-1} dm^3 for 1% water.

In solutions containing 1% water, the pathway involving reaction with water must be included. Therefore :-

$$\text{velocity} = k_{H_2O}[DPTH^+] + k[DPT2H]^{2+}$$

It can be shown that equation 5.8 holds

$$k_{obs} = (k_{H_2O} + kK_2[H^+]) \frac{K_1[H^+]}{1 + K_1[H^+]} \quad \textbf{eqn. 5.8}$$

Using the value at 1% water for K_1 of 8 $dm^3\ mol^{-1}$ values of the quantity $k_{obs}.(1+K_1[H^+]) / K_1[H^+]$ were plotted against acid concentration. The resulting straight line graph (fig. 5.19) gives values for k_{H2O}, at 1% water, of $4x10^{-3}\ s^{-1}$ and for kK_2 of 0.16 $dm^3\ mol^{-1}\ s^{-1}$. The value obtained for k_{H2O} may be converted to a second order rate constant of $7.3x10^{-3}\ dm^3\ mol^{-1}\ s^{-1}$. Surprisingly, the value of kK_2 at 1% water is larger than the value obtained at lower water concentration. This is unexpected since the value of K_2 will be expected to decrease with increasing water content as the proton activity decreases.

Although most measurements were made in acidic solutions it was found that in basic media the U. V. spectrum of DPT undergoes a hypsochromic shift to give a species with λ_{max} 233nm (fig. 5.17). This species very slowly decomposed. No kinetic measurements were made.

As in aqueous solutions[9] results in acetonitrile are compatible with formation of nitramide as a decomposition product in acidic solutions.

Fig. 5.19
Decomposition Of DPT In Acetonitrile/Perchloric Acid With 1% Added Water

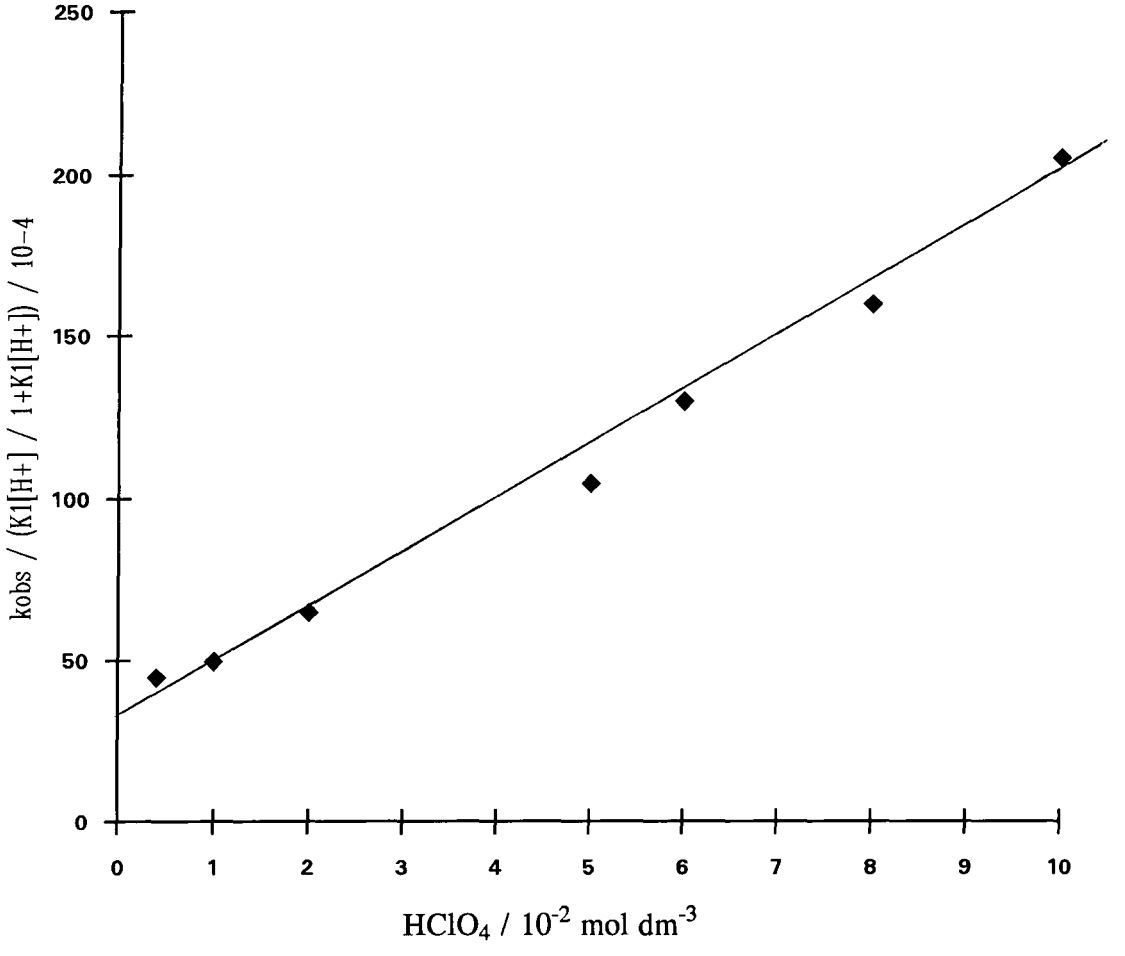

Derivation Of Equation 5.8

$$\text{velocity} = k_{obs}[DPT]_{stoich} \quad \text{eqn. 5.9}$$

for the proposed pathway with 1% water

$$\text{velocity} = k_{H_2O}[DPTH^+] + k[DPT2H]^{2+}$$

$$\text{But } [DPT]_{stoich} = [DPT] + [DPTH^+] + [DPT2H]^{2+}$$

From scheme 5.7

$$K_2 = \frac{[DPT2H]^{2+}}{[DPT][H^+]}$$

$$K_1 = \frac{[DPTH^+]}{[DPT][H^+]}$$

$$[DPT]_{stoich} = [DPTH^+]\left(1 + \frac{1}{K_1[H^+]}\right) + [DPT2H]^{2+}$$

$$= [DPTH^+]\left(\frac{1 + K_1[H^+]}{K_1[H^+]}\right) + [DPT2H]^{2+}$$

$$= [DPT2H]^{2+}\left(1 + \frac{1 + K_1[H^+]}{K_1[H^+]}\right)\frac{1}{K_2[H^+]} + [DPT2H]^{2+}$$

$$= [DPT2H]^{2+}\ \frac{(1 + K_1[H^+] + K_1K_2[H^+]^2)}{K_1K_2[H^+]^2}$$

$$\therefore \text{ velocity} = k_{H_2O}[DPTH^+] + \frac{kK_1K_2[H^+]^2[DPT]_{stoich}}{1 + K_1[H^+] + K_1K_2[H^+]^2}$$

But the extent of diprotonation is expected to be small

$$\therefore K_2[H^+] << 1$$

Then

$$\text{velocity} = k_{H_2O}[DPTH^+] + \frac{kK_1K_2[H^+]^2[DPT]_{stoich}}{1 + K_1[H^+]}$$

and also

$$[DPTH^+] = [DPT]_{stoich} \frac{K_1[H^+]}{1 + K_1[H^+]}$$

$$\therefore \text{velocity} = k_{H_2O} \frac{K_1[H^+][DPT]_{stoich}}{1 + K_1[H^+]} + \frac{kK_1K_2[H^+]^2[DPT]_{stoich}}{1 + K_1[H^+]}$$

comparing with eqn 5.9

$$k_{obs} = (k_{H_20} + kK_2[H^+]) \frac{K_1[H^+]}{1 + K_1[H^+]}$$

5.4. Dinitrosopentamethylenetetramine (DNPT)

5.4.1 ^{1}H NMR

The ^{1}H NMR spectrum of DNPT in deuterioacetonitrile is consistent with that obtained by Stefaniak[14] complex due to DNPT existing in two isomeric forms, where the nitroso groups are either syn or anti to each other (fig. 5.20).

On addition of two equivalents of acid the spectrum in fig. 5.21 is obtained. This indicates rapid decomposition so that spectra of protonated derivatives are not observed. It is thought that formaldehyde is produced as a decomposition product of DNPT. Any formaldehyde produced would be hydrated in the presence of water and therefore is usually observed as a band about δ4.8.[15] Due to presence of a large water peak in this area it is difficult to assign this band. Also seen in the spectrum are six equally spaced broad bands indicative of NH couplings (J=50Hz)

Fig. 5.22 shows the same reaction mixture after one day. A sharp triplet centred around δ6 (J_{NH}=50 Hz) typical of NH_4^+ species. This gives strong evidence of ammonia gas evolution from the decomposition of DNPT, which in acidic solution consequently forms ammonium ions. The three broad bands *ca* δ7 indicate the presence of species of the type NH-R.

Fig. 5.20

^{1}H NMR Spectrum Of DNPT In CD_3CN

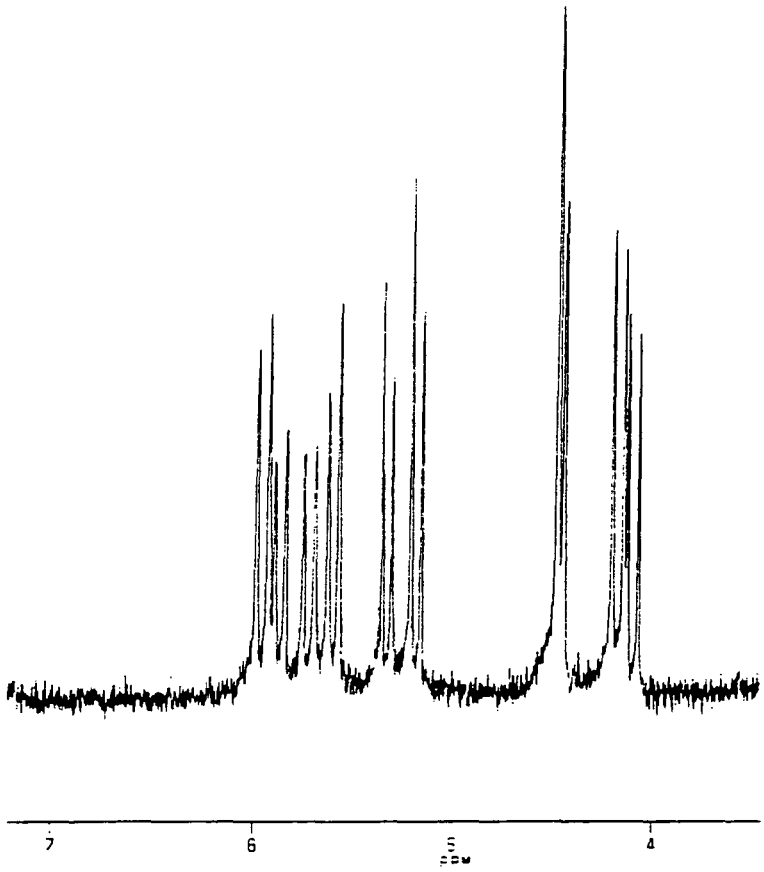

Fig. 5.21

^{1}H NMR Spectrum Of DNPT In The Presence Of 2 Equivalent Of Acid In CD_3CN

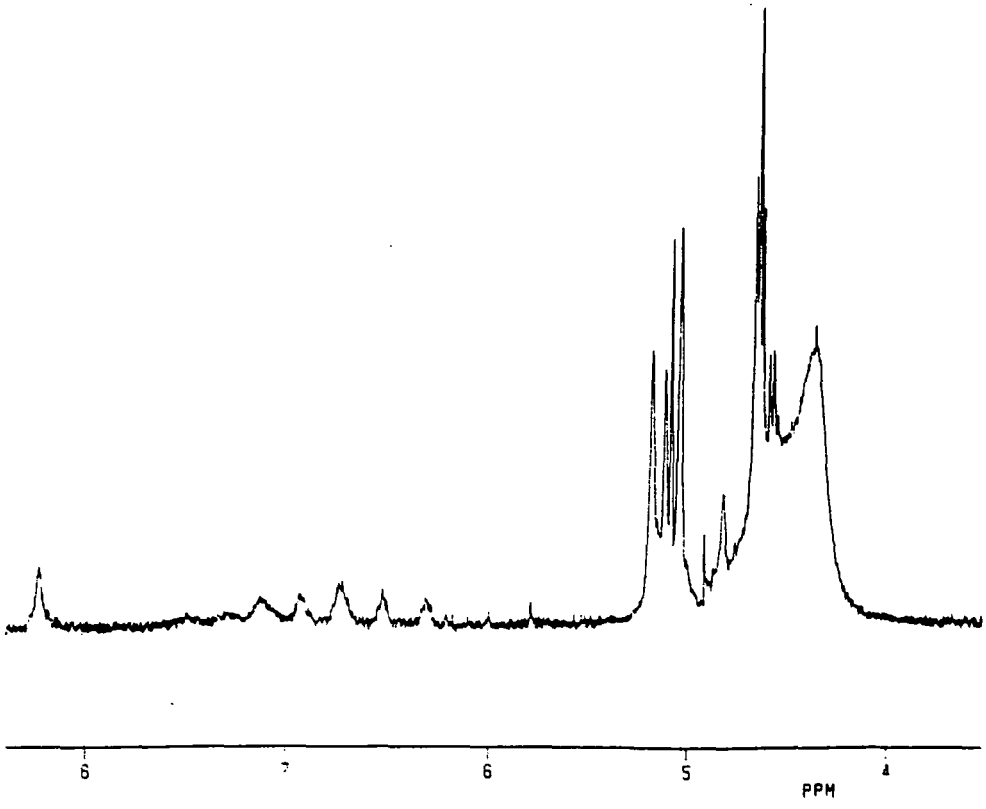

Fig. 5.22
^{1}H NMR Spectrum Of DNPT In The Presence Of 2 Equivalent Of Acid In CD_3CN After 1 Day

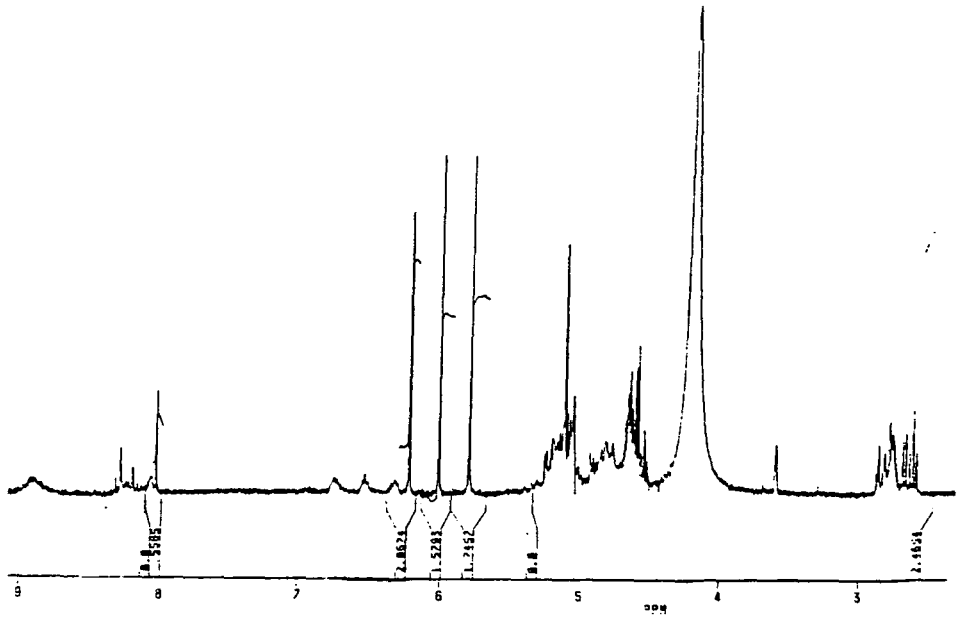

5.4.2 Formaldehyde Determination

It was thought that DNPT would produce formaldehyde during its decomposition in acidic media. In a controlled experiment a known amount of DNPT was reacted with 1M perchloric acid in 70/30 (v/v) acetonitrile/water. Evolution of gas was noted during the addition. The gas was shown to be ammonia (turned moist red litmus blue). The reaction mixture was left for approximately for 15 mins. and then neutralised with aqueous sodium hydroxide before addition of an excess amount of alcoholic dimedone. The precipitated 1:1 formaldehyde-dimedone adduct[17] was isolated as a pale orange solid. As for DAPT 3 moles of the adduct were produced indicating the production of 3 moles of formaldehyde per mole of DNPT.

In the decomposition of DPT it has been shown[9] that nitramide (NH_2NO_2) is an intermediate. Although no intermediate is observed during the decomposition of DNPT it is not possible to rule out the formation of nitrosamine (NH_2NO) as an intermediate, since nitrosamine decomposes very rapidly in acidic media giving nitrogen and water.[20] Coupled with the formaldehyde determination the decomposition is consistent with scheme 5.8.

Scheme 5.8

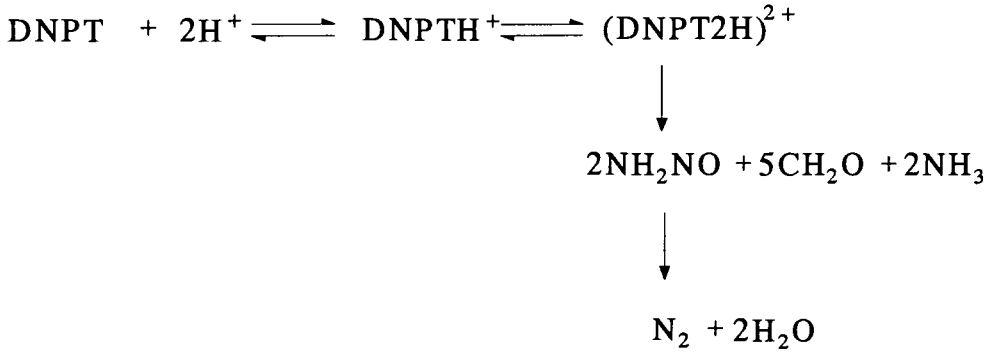

5.4.3 U.V. And Kinetic Studies

The decomposition of DNPT in the presence of acid in acetonitrile was followed by monitoring the fading of U. V. absorbance at 245nm using stopped-flow spectrophotometry. DNPT shows λ_{max} at 228nm ε= 10,000 dm^3 mol^{-1} cm^{-1} in acetonitrile and is found to be stable in neutral and alkaline media for prolonged periods of time (fig. 5.23)

However in acidic solution an accurately first order process is observed resulting in the fading of U. V. absorbance to zero.

The variation of the observed rate coefficient k_{obs} with increasing acidity and water content was measured in acetonitrile. Fig. 5.24 shows the change in spectral shape of DNPT on addition of acid. It was found that only a single process was observable in the decomposition and there was no evidence for the formation of an intermediate.

Fig. 5.23

U. V. Spectrum Of DNPT In Acetonitrile

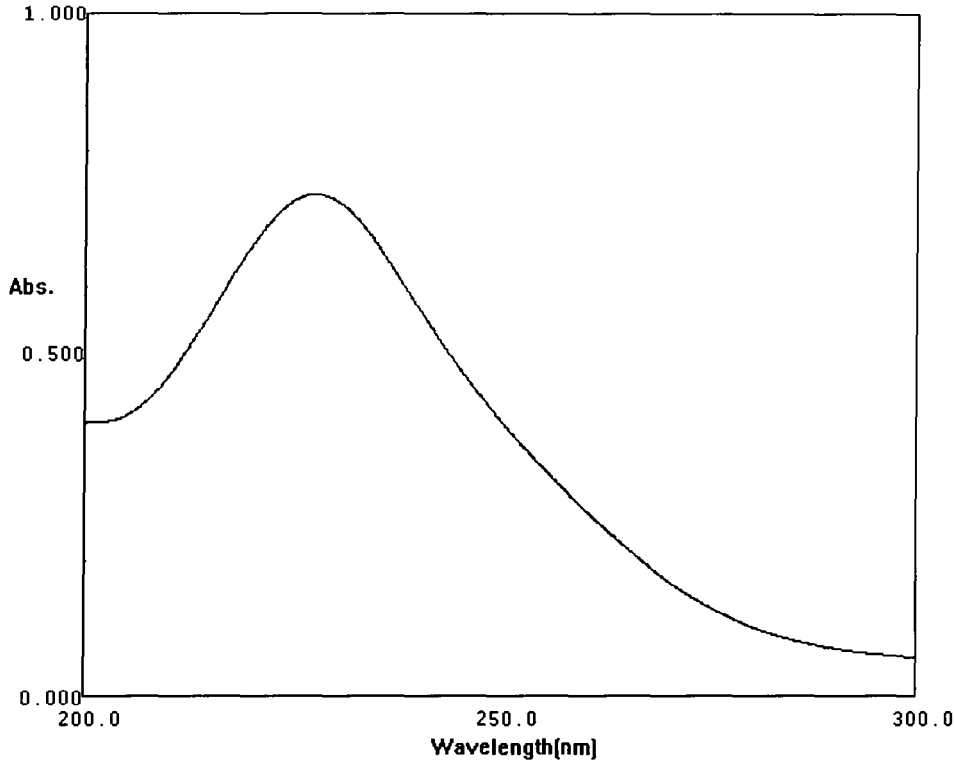

Fig. 5.24

U. V. Spectrum Of DNPT In The Presence Of Acid In Acetonitrile

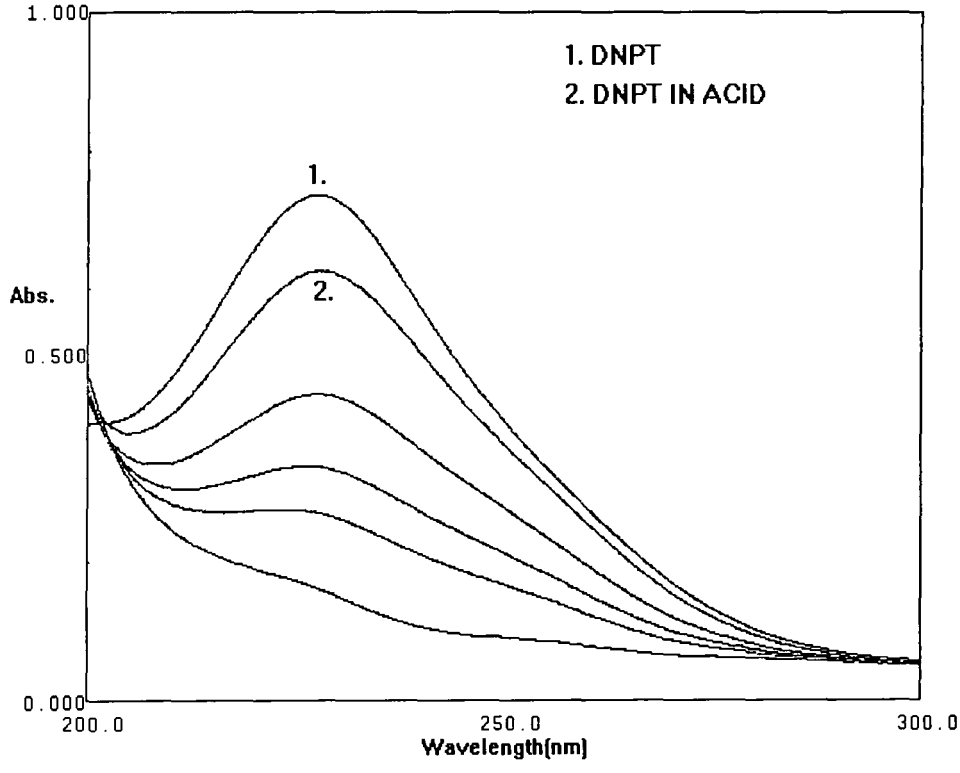

A notable feature of the decomposition was its rapidity compared with DAPT and DPT, so that stopped-flow technique was required. It is seen that the value of k_{obs}, the observed rate coefficient increases with increasing acid concentration (fig. 5.25) In the presence of added water the observed rate coefficient is found to decrease with increasing water concentration. The results are consistent with a scheme involving protonation of DNPT to give the diprotonated species which then subsequently decomposes (scheme 5.9).

Scheme 5.9

$$DNPT + 2H^+ \overset{K_1}{\rightleftharpoons} DNPTH^+ + H^+ \overset{K_2}{\rightleftharpoons} (DNPT2H)^{2+} \xrightarrow{k}$$

Assuming monoprotonation is complete:-

$$k_{obs} = \frac{kK_2[H^+]}{1+K_2[H^+]} \quad \textbf{eqn. 5.10}$$

The results are compatible with a single decomposition pathway involving reaction of the monoprotonated species with acid. The rate of decomposition by this pathway is very much more rapid than the corresponding reactions of DAPT and DPT. This may explain the failure to observe, in the case of DNPT, a pathway involving spontaneous reaction of the monoprotonated species with water. It appears that this pathway becomes insignificant compared with the acid catalysed pathway.

The results indicate that the monoprotonated species does not undergo spontaneous reaction with water. In the presence of water, the equilibrium constant for diprotonation will be expected to decrease and thus values of kK_2 will vary with water content of the solvent (tables 5.13-5.17).

If we assume that at low acid concentration $1 >> K_2[H^+]$ then

$$k_{obs} = kK_2[H^+]$$

i.e. plots of k_{obs} vs. $[H^+]$ at constant water concentration should be linear with slope of kK_2 (fig. 5.26) Table 5.18 gives values of kK_2 calculated at constant water concentration. Alternatively values of kK_2 can be obtained at a single acid concentration with varying water content in the region where $1 >> K_2[H^+]$ (table 5.17). However, at higher acid concentration the denominator in eqn. 5.10 has a greater value than 1 and therefore plots of k_{obs} vs. $[H^+]$ will begin to show curvature

(fig. 5.25). Fig. 5.26 shows gives a straight line graph as expected if the water contribution from the acid is taken into account and the data corrected to 0.1% water (which is the average % water for the range of acid concentrations between 1 x 10^{-3}-0.02M) (table 5.19). A plot of $1/k_{obs}$ vs. $1/[H^+]$ (eqn.5.11) is linear with values of k and K_2 (fig. 5.27) which are in good agreement with those calculated (k=3.9 and kK_2=23 mol^{-1} dm^3 s^{-1}) (table 5.19).

$$\frac{1}{k_{obs}} = \frac{1}{kK_2[H^+]} + \frac{1}{k} \quad \textbf{eqn.5.11}$$

Fig.5.25
Decomposition OF DNPT IN Acetonitrile/Perchloric Acid Without Added Water

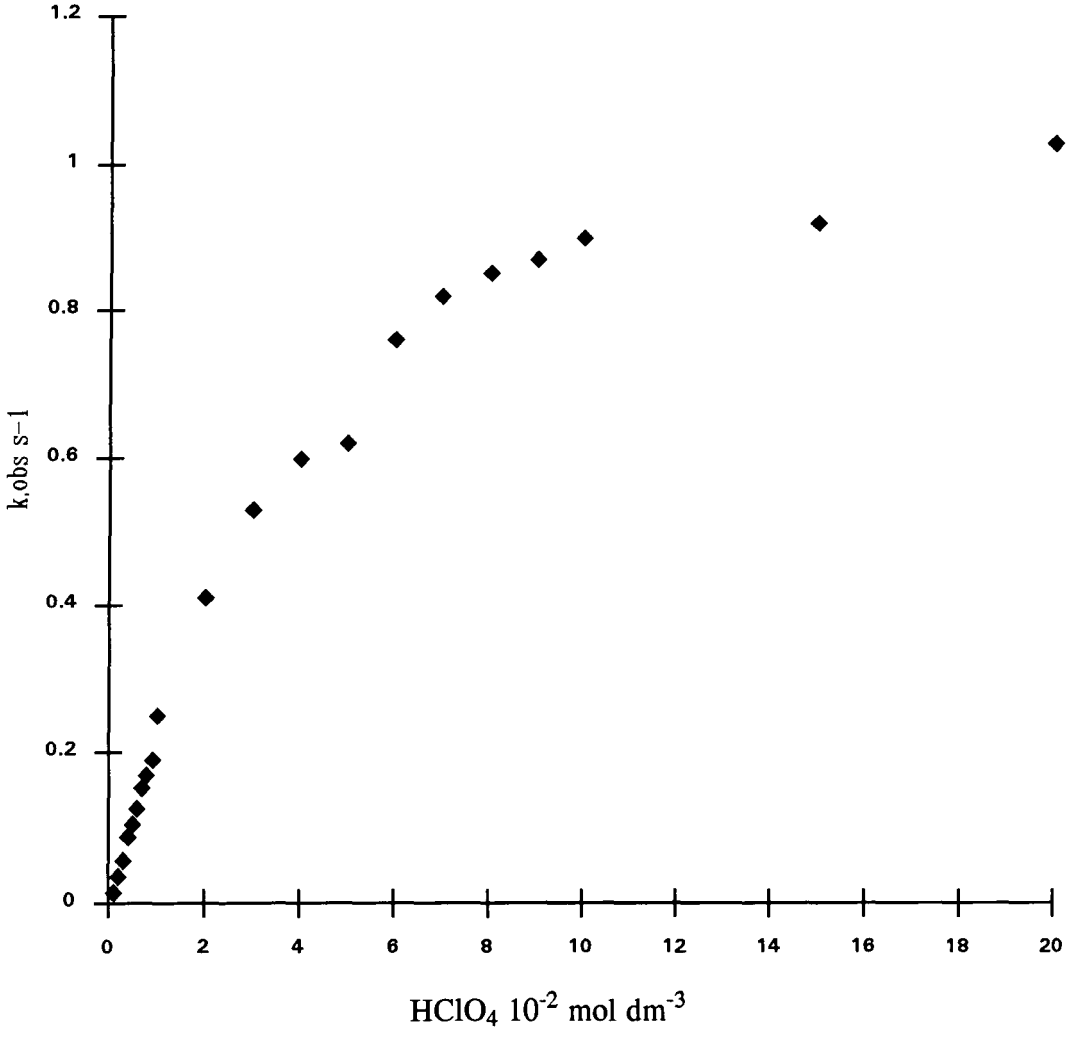

Table 5.13

Rate Constants For The Decomposition Of DNPT ($2.8x10^{-5}M$) In Acetonitrile/Perchloric Acid Without Added Water

10^2HClO_4 mol dm^{-3}	Total % Water[a,b] v/v	k_{obs} s^{-1}	kK_2[c] dm^3 mol^{-1} s^{-1}	kK_2[d] dm^3 mol^{-1} s^{-1}
0.1	0.054	0.014	14	-
0.2	0.058	0.036	18	18
0.3	0.062	0.056	19	19
0.4	0.066	0.088	22	22
0.5	0.070	0.105	21	21
0.6	0.074	0.126	21	21
0.7	0.078	0.153	22	22
0.8	0.082	0.170	21	21
0.9	0.086	0.190	21	21
1.0	0.090	0.250	25	25
2.0	0.130	0.410	20.5	21
3.0	0.170	0.530	18	20
4.0	0.210	0.600	15	18
5.0	0.250	0.620	12.4	17
6.0	0.290	0.760	12.7	17
7.0	0.330	0.820	11.7	17
8.0	0.370	0.850	10.6	16
9.0	0.410	0.870	9.7	15
10.0	0.450	0.900	9	15
15.0	0.650	0.920	6.1	12
20.0	0.850	1.030	5.2	12

a) Acetonitrile contains 0.05% water.

b) 0.01M perchloric acid in acetonitrile contains 0.04% water.

c) k_{obs} / $[H^+]$.

d) Corrected for water contribution from acid/acetonitrile to 0.1% water (average kK_2=21 dm^3 mol^{-1} s^{-1}).

Table 5.14

Rate Constants For The Decomposition Of DNPT (2.8×10^{-5}M) In Acetonitrile/Perchloric Acid Containing 0.25% Water

$10^2 HClO_4$ mol dm^{-3}	Total % Water[a,b] v/v	k_{obs} s^{-1}	kK_2[c] dm^3 mol^{-1} s^{-1}
0.1	-	-	-
0.2	0.31	0.031	15.5
0.3	0.31	0.043	14.3
0.4	0.32	0.053	13.2
0.5	0.32	0.076	15.2
0.6	0.32	0.093	15.5
0.7	0.33	0.105	15
0.8	0.33	0.124	15.5
0.9	0.34	0.140	15.6
1.0	0.34	0.150	15
2.0	0.38	0.210	10.5
3.0	0.42	0.270	9
4.0	0.46	0.350	8.7
5.0	0.50	0.380	7.6
6.0	0.54	0.430	7.2
7.0	0.58	0.440	6.3
8.0	0.62	0.540	6.7
9.0	0.66	0.590	6.6
10.0	0.70	0.620	6.2

Table 5.15

Rate Constants For The Decomposition Of DNPT (2.8×10^{-5}M) In Acetonitrile/Perchloric Acid Containing 0.75% Water

$10^3 HClO_4$ mol dm^{-3}	Total % Water[a,b] v/v	k_{obs} s^{-1}	kK_2[c] dm^3 mol^{-1} s^{-1}
1	0.81	0.011	5.5
2	0.81	0.022	7.3
3	0.82	0.033	8.2
4	0.82	0.039	7.8
5	0.82	0.060	10
6	0.83	0.065	9.3
7	0.83	0.074	9.3
8	0.84	0.090	10
9	0.84	0.098	9.8

Table 5.16

Rate Constants For The Decomposition Of DNPT (2.8×10^{-5}M) In Acetonitrile/Perchloric Acid Containing 1.00 % Water

$10^2 HClO_4$ mol dm^{-3}	Total % Water[a,b] v/v	k_{obs} s^{-1}	kK_2[c] dm^3 mol^{-1} s^{-1}
0.1	-	-	-
0.2	1.06	0.014	5
0.3	1.06	0.019	6.3
0.4	1.06	0.035	8.8
0.5	1.07	0.042	8.4
0.6	1.07	0.037	6
0.7	1.07	0.049	7
0.8	1.08	0.055	7
0.9	1.08	0.067	7
1.0	1.09	0.085	8.5
2.0	1.13	0.107	5.4
3.0	1.17	0.120	4.0
4.0	1.21	0.184	4.6
5.0	1.25	0.225	4.5
6.0	1.29	0.280	4.7
7.0	1.33	0.320	4.6
8.0	1.37	0.370	4.6
9.0	1.41	0.410	4.6
10.0	1.45	0.450	4.5

Table 5.17

Rate Constants For The Decomposition Of DNPT (2.8×10^{-5}M) In 0.01M Perchloric Acid/Acetonitrile

k_{obs} s^{-1}	Total % Water[a,b] v/v	kK_2[c] / dm^3 mol^{-1} s^{-1}
0.261	0.09	26.0
0.179	0.29	17.9
0.134	0.49	13.4
0.115	0.69	11.5
0.098	0.89	9.8
0.090	1.09	9.0

a) Acetonitrile contains 0.05% water.

b) 0.01M perchloric acid in acetonitrile contains 0.04% water.

c) k_{obs} / $[H^+]$.

Table 5.18

Rate Constants For The Decomposition Of DNPT (2.8×10^{-5}M) In Perchloric Acid/Acetonitrile

kK_2[a] / dm^3 mol^{-1} s^{-1}	% Water[b] v/v
21	0.07
15	0.32
9.5	0.82
7.3	1.06

a) Average kK_2 obtained from tables 5.13-5.16.

b) Average value of total % water obtained from tables 5.13-5.16.

Fig. 5.26

Decomposition Of DNPT (2.8x10-5M) In Acetonitrile/Perchloric Acid (Data corrected to 0.1% Water)

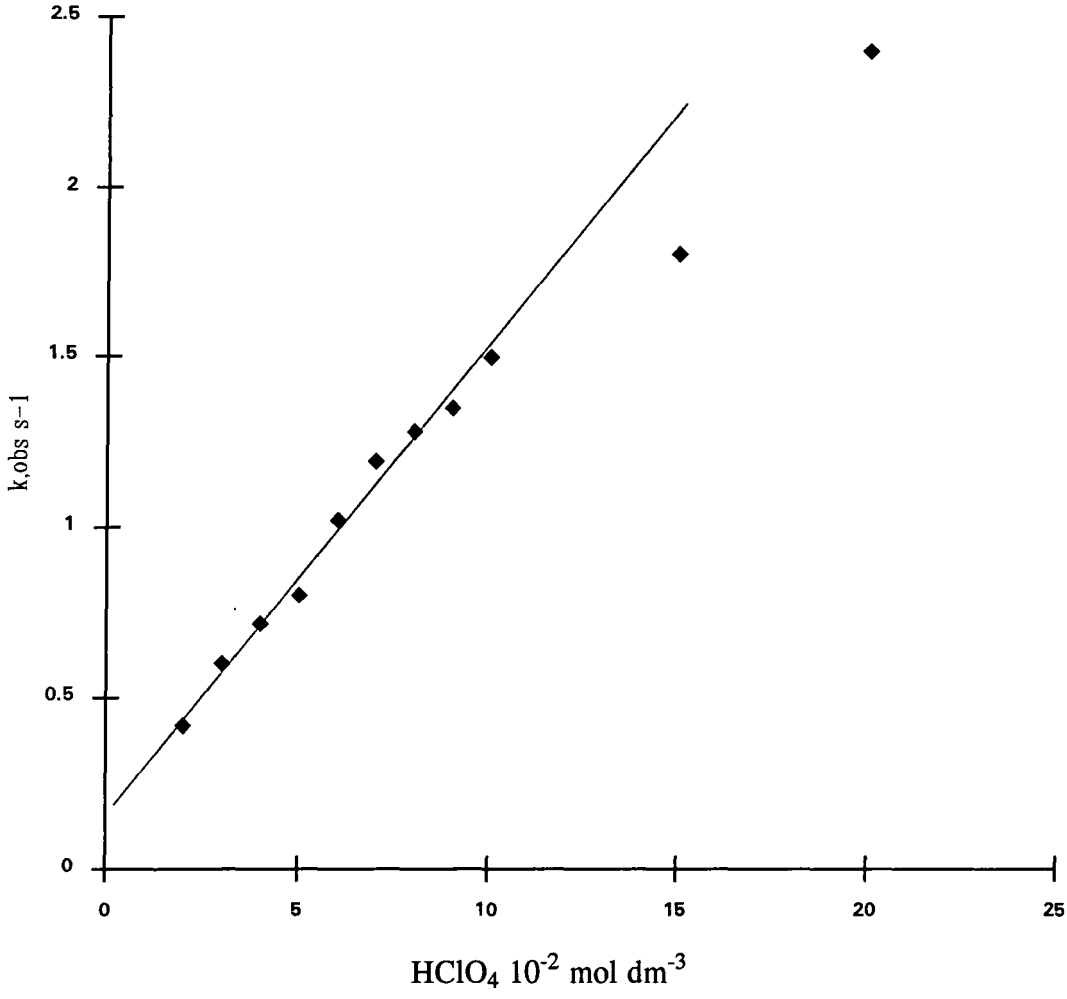

Table 5.19

Rate Constants For The Decomposition Of DNPT (2.8×10^{-5}M) Acetonitrile/Perchloric Acid Corrected To 0.1% Water

$10^2 HClO_4$ mol dm^{-3}	k_{obs} [a] s^{-1}	k_{obs} [b] s^{-1}
1	-	-
2	0.42	0.39
3	0.60	0.56
4	0.72	0.72
5	0.80	0.87
6	1.02	1.02
7	1.19	1.15
8	1.28	1.27
9	1.35	1.39
10	1.50	1.50
15	1.80	2.00
20	2.40	2.30

a) Corrected to 0.1% water using $[H^+]$ x corrected kK_2.

b) Calculated using 21 x $[H^+]$ / $1+K[H^+]$ (eqn. 5.10) (where K=4).

Fig. 5.27

Decomposition Of DNPT (2.8x10-5M) In Acetonitrile/Perchloric Acid (Data corrected to 0.1% Water)

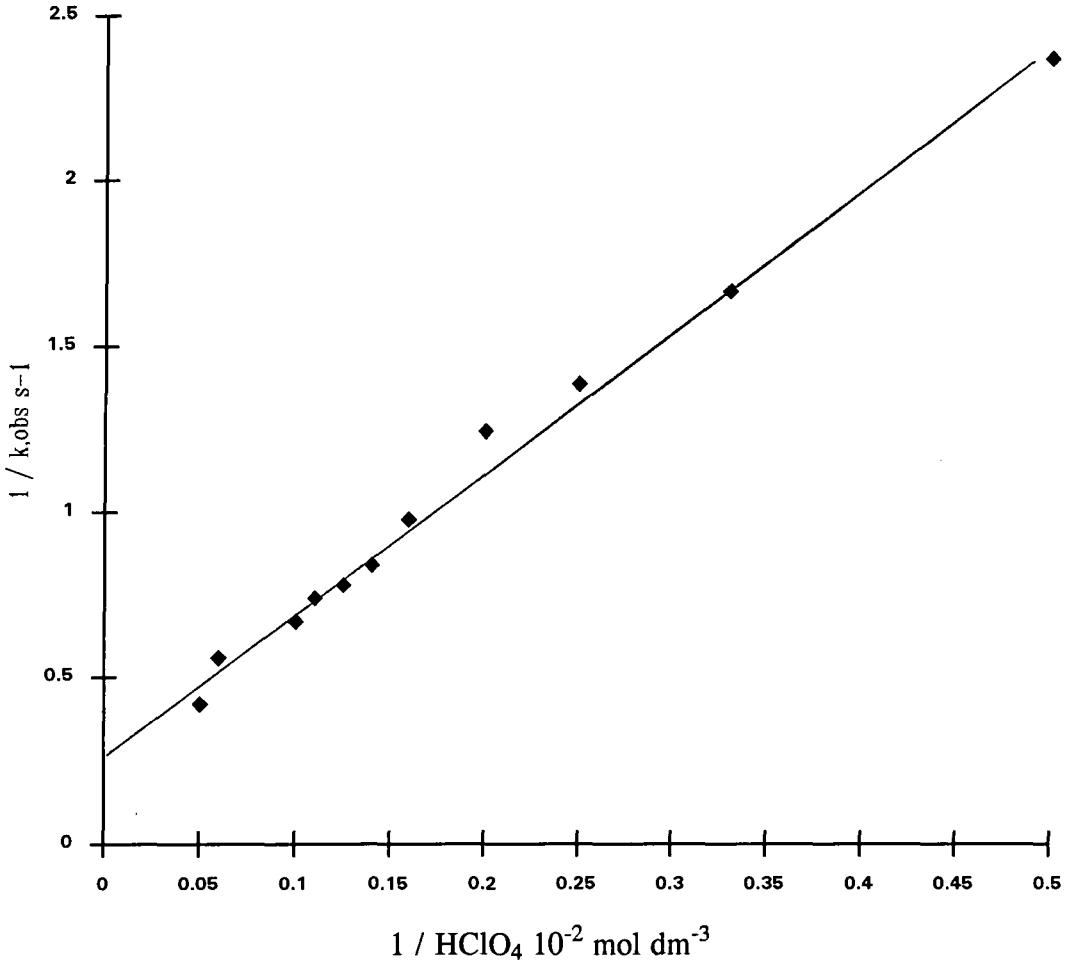

5.5 Comparisons

Rate coefficients for reactions of DAPT, DPT and DNPT in acid solutions in acetonitrile are compared in table 5.20.

Table 5.20

	k_{H2O} dm^3 mol^{-1} s^{-1}	kK_2 dm^3 mol^{-1} s^{-1} (At 0.1% Water)
DAPT	$2.2x10^{-3}$	0.07
DPT	$7.3x10^{-3}$	0.10
DNPT	-	20

It must be noted that compared to water protonation is much more extensive in acetonitrile.[21,22] Thus in water reaction is thought to involve reaction of the unprotonated species with acid whereas in acetonitrile reaction may involve spontaneous reaction of the monoprotonated species with water or reaction via a diprotonated species. A point worthy of mention is the very rapid decomposition of DNPT, compared to DAPT and DPT, in acetonitrile. It is useful to speculate as to the cause of this difference.

A possible decomposition pathway for DAPT, and also DPT is shown in scheme 5.10. Here monoprotonation occurs on a ring nitrogen atom, but there may be a low concentration of an isomeric form X involving cleavage of a C-N bond. Reaction of the iminium ion so formed with water may provide the water catalysed pathway while further protonation on a ring nitrogen atom gives the acid catalysed pathway.

DNPT differs in that there is a possibility of diprotonation involving the nitroso function. The intermediate (Y) may be a very low concentration intermediate produced on monoprotonation. It has been shown by ^1H NMR that protonation of nitrosamines occurs on the nitroso oxygen[23]. Attack by acid at this position enables the elimination of water and nitrogen to occur as shown in scheme 5.11. This, of course, is very speculative but might explain the enormous, 200 fold increase in reactivity of DNPT compared to DAPT and DPT.

It is worth mentioning that even in water a pathway involving a diprotonated species was recognised in the case of DNPT but not for DPT and DAPT. However in water the extent of diprotonation is expected to be very small compared to acetonitrile as solvent.

Scheme 5.10

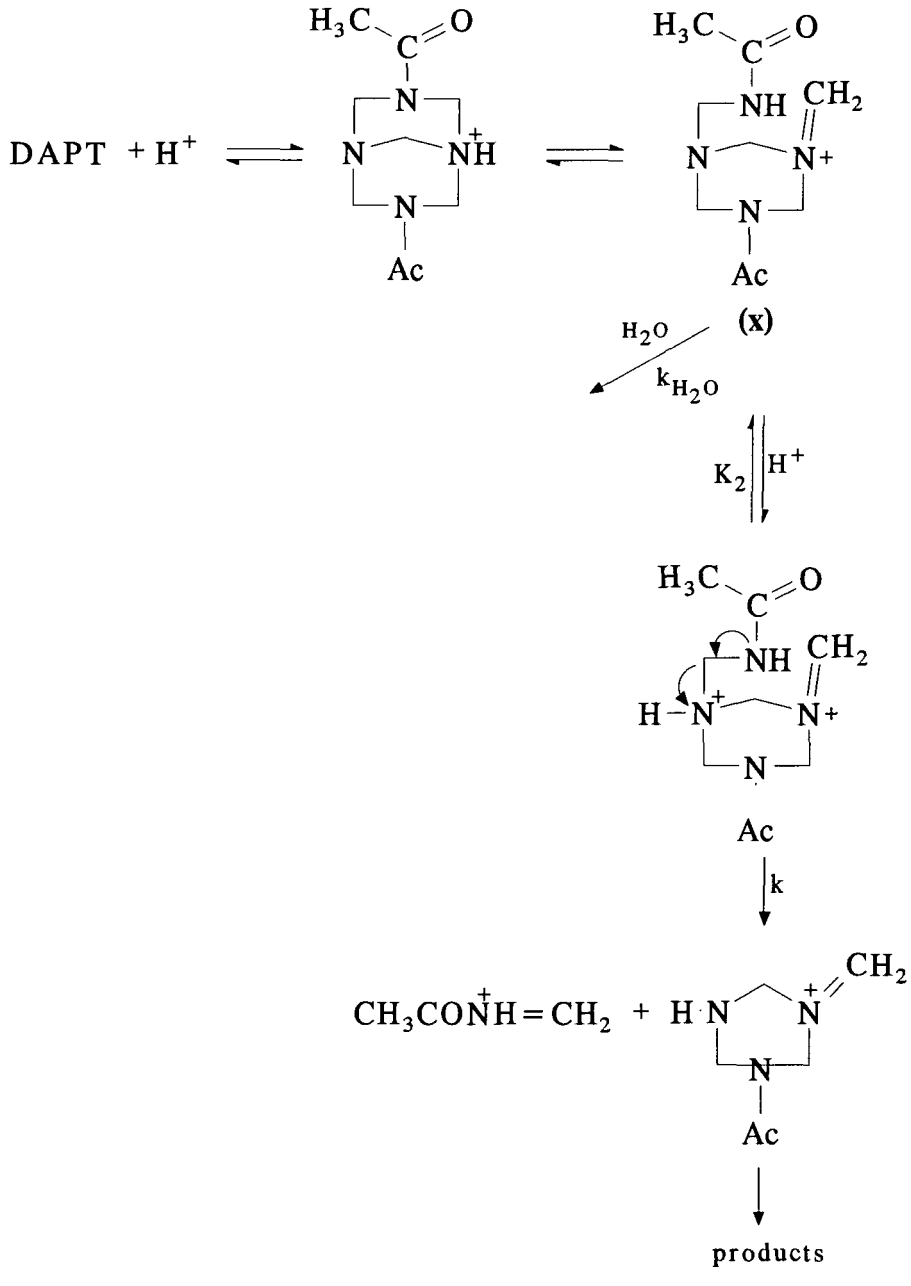

Scheme 5.11

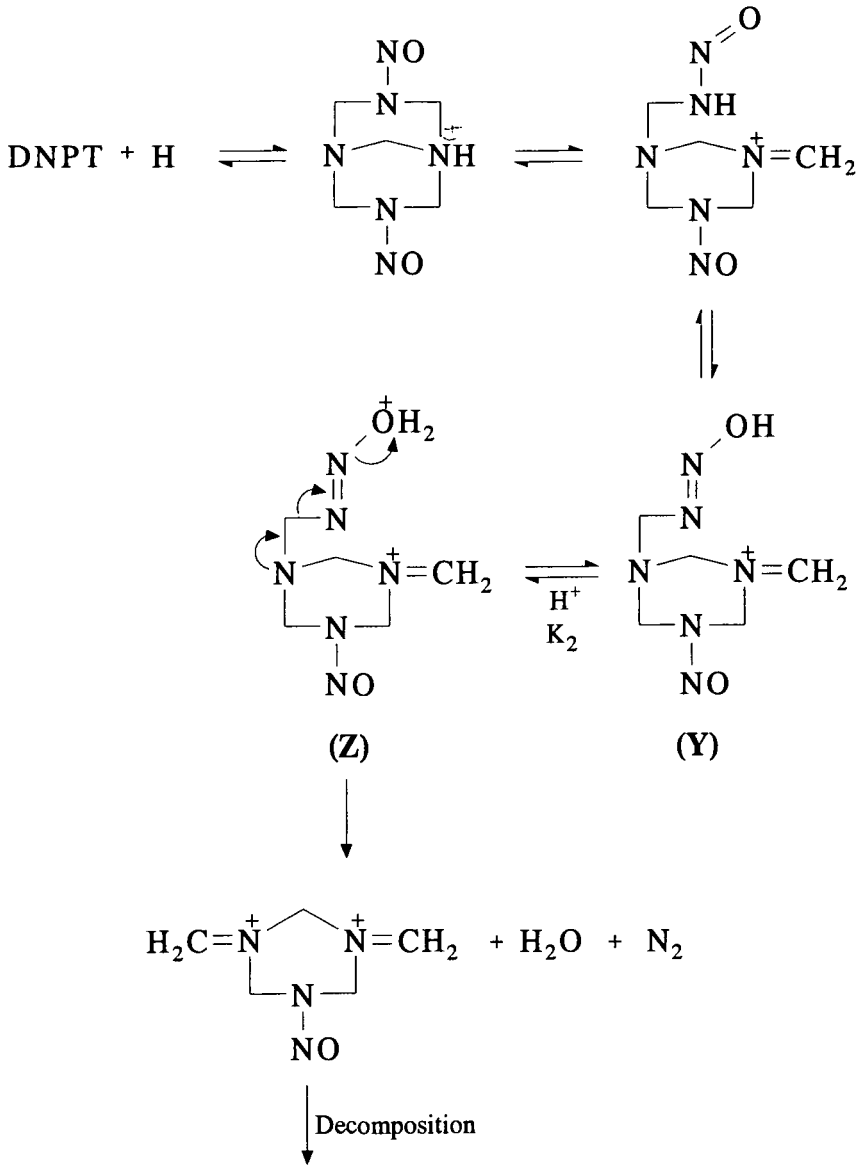
DNPT + H
NO
N
NH
O
N
NH
N
N
CH2
NO
OH2
OH
H+
K2
(Z)
(Y)
H2C=N
N=CH2
+ H2O + N2
Decomposition

References

1. W. E. Bachmann and N. C. Deno, *J. Am. Chem. Soc.*, 1951, 73, 2777.
2. P. Griess and G. Harrow, *Ber.*, 1888, 21, 2737.
3. V. I. Seale, M. Warman and E. E. Gilbert, *J. Heterocyclic Chem.*, 1973, 10, 97.
4. P. Golding, Ministry Of Defence, private communication.
5. G. F. Wright, W. J. Chute, D. C. Downing, A. F. McKay and G. S. Meyers, *Can. J. Res.*, 1949, 27B, 218.
6. G. C. Hale, *J. Am. Chem. Soc.*, 1925, 47, 2754.
7. G. F. Wright and W. J. Chute U. S. Patent 2,678,927.
8. A. P. Cooney, M. R. Crampton and P. Golding *J. Chem. Soc. Perkin Trans (ii)*, 1986, 835.
9. A. P. Cooney, M. R. Crampton, J. K. Scranage and P. Golding *J. Chem. Soc. Perkin Trans (ii)*, 1989, 77.
10. M. R. Crampton J. K. Scranage and P. Golding *J. Chem. Res.*, 1989, 72.
11. M. R. Crampton J. K. Scranage and Peter Golding *J. Chem. Res.*, 1990, 182-183.
12. A. H. Lamberton, C. Lindley and J. Speakman, *J. Chem. Soc.*, 1949, 1650.
13. J. K. Scranage Ph. D. thesis 1989.
14. L. Stefaniak, T. Urbanski and M. Witanowski, *Tetrahedron*, 1974, 30, 3775-3779.
15. M. J. Ridley and J. K. M. Sanders, *J. Pharm. Pharmacol.*, 1983, 35, 712.
16. A. T. Nielson, D. W. Moore, M. D. Ogan and R. L. Atkins, *J. Org. Chem.*, 1979, 44, 1678.
17. A. I. Vogel, " A Textbook Of Practical Organic Chemistry", 3rd edition Longmans, London 1962, p. 332.
18. H. T. Openshaw, " A Laboratory Manual Of Qualitative Organic. Analysis", Camdridge University Press, Cambridge, 1978, p.49.
19. R. N. Jones and G. D. Thorn, *Can. J. Res.*, 1949, 27B, 828.
20. G. A. Olah, R. Herges, J. D. Felberg and G. K. S. Prakash, *J. Am. Chem. Soc.*, 1985, 107, 5282.
21. I. M. Kolthoff, S. Bruckenstein and M. K. Chantooni Jr., *J. Am. Chem. Soc.*, 1961, 83, 3927.
22. J. F. Coetzee *Prog. Phys. Org. Chem.*, 1967, 4, 45.
23. S. J. Kuhn and J.S. McIntyre, *Can. J. Chem.*, 1966, 44, 105. G. A. Olah, D. J. Donovan and L. K. Keefer, *J. Nat. Cancer Inst.*, 1975, 54, 465.

CHAPTER 6

Reaction of 2-Aminobenzylamine With Aqueous Glyoxal To Produce 2,2'-Bis (1,2,3,4-tetrahydroquinoxaline)

6.1 Introduction

The condensation reactions of benzylamine and certain ring substituted benzylamines with aqueous glyoxal were found to give hexabenzylhexa azaisowurtzitane cage structures (chapter 3). These reactions are thought to involve diimine intermediates which subsequently trimerise to give the isowurtzitane cage structures. Other aromatic amines have been found to give 1,2-diimines.[1-3] In this chapter it is reported that the reaction of 2-aminobenzylamine (6.1) with aqueous glyoxal in acetonitrile containing a catalytic amount of acid did not give the expected isowurtzitane structure, but a novel cyclisation product 2,2'-bis (1,2,3,4-tetrahydroquinaxoline), (6.3). It seems likely that 6.3 results from the intramolecular cyclisation of the initially formed diimine intermediate 6.2. (scheme 6.1).

Scheme 6.1

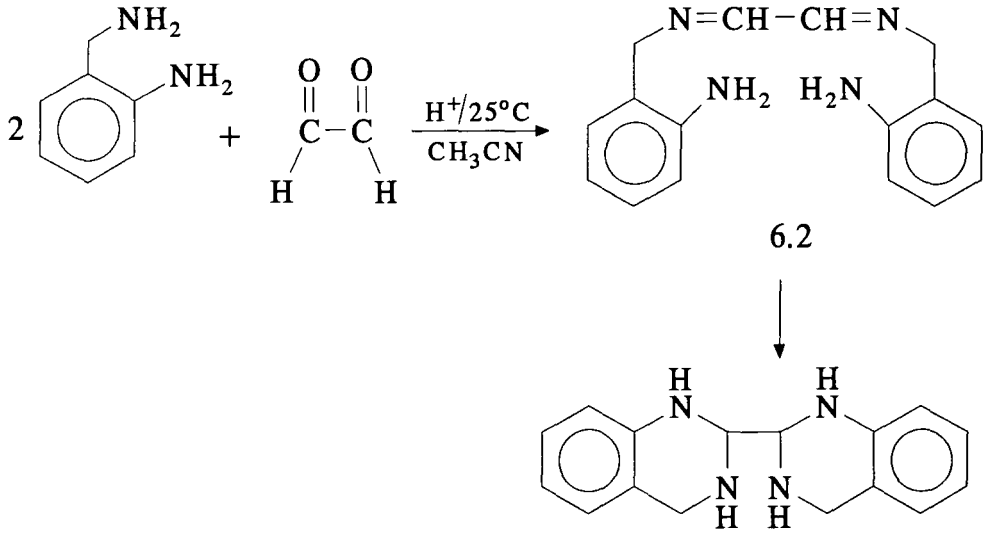

No reports in the literature of this reaction have been found, although Kliegman and Barnes[4] have shown that reaction of aqueous glyoxal with *o*-amino benzoic acid (6.4) gave a 45% yield of 2,2'-bis (1,2-dihydro-4-oxo-3,1-benzoxazine) (6.5), which is also a similar cyclisation product in which self-incorporation of the hydroxylic moiety takes place (scheme 6.2).

Kehrmann[5] also reported that condensation of *o*-aminophenol with diacetyl (2,4-butanedione) gave an eight-membered ring structure containing a diphenyl ether bond thought to be 6.6.

Scheme 6.2

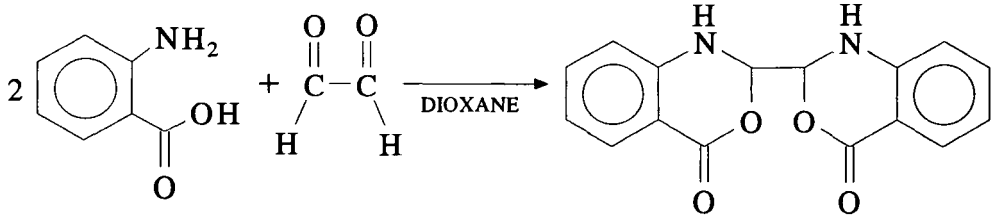

6.4 6.5

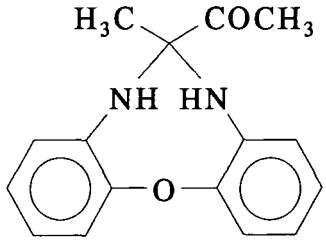

6.6

Recently Bayer[6] assigned Schiff base structures to the compounds obtained by the condensation of aqueous glyoxal and diacetyl (2,3-butanedione) with *o*-aminophenol. However, Murase[7] demonstrated that these were actually cyclisation products. The bibenzooxazoline (6.7) structure was assigned to these products.

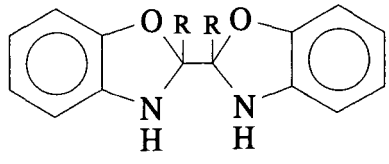

6.7

R=H

R=CH_3

It was also found that acetylation of 6.3 with acetic anhydride gave the tetra-acetylated derivative 6.8.

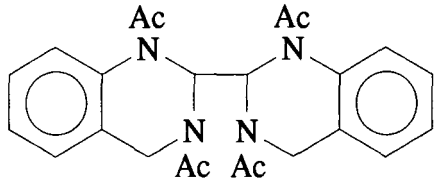

6.8

6.2 X-Ray Crystal Structure

The x-ray crystal structure of 6.3 was determined and is shown in fig.6.1.

Fig. 6.1

X-Ray Crystal Structure Of 2,2'-Bis (1,2,3,4-tetrahydroquinoxaline)

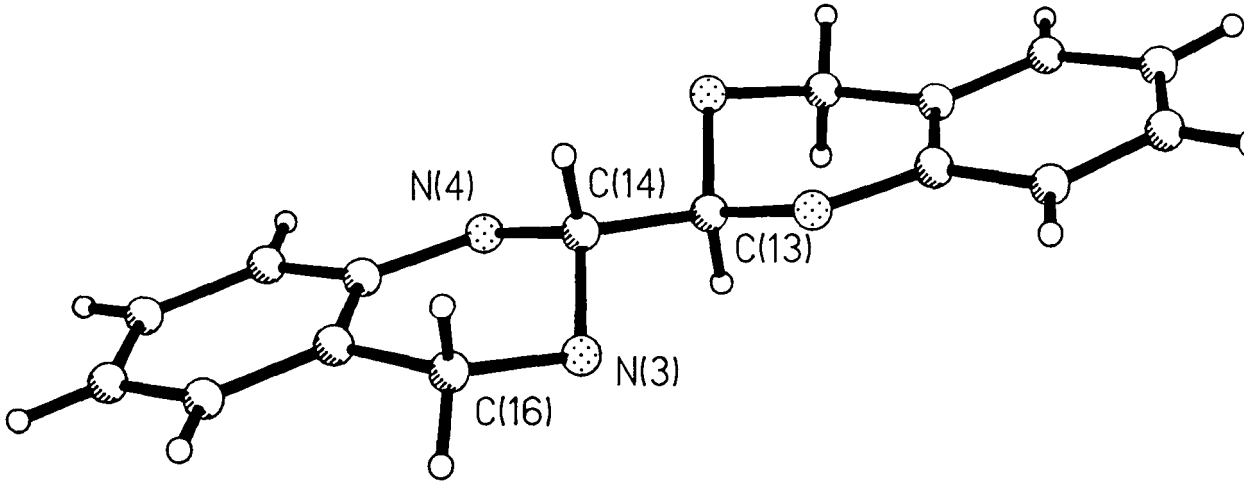

6.3 NMR

6.3.1 ^{1}H NMR Of 6.3

The ^{1}H NMR of 6.3 in deuteriodimethylsulphoxide (fig.6.2) shows an AB quartet (J=18Hz) (4H) due to geminal coupling of the axial and equatorial protons of the two methylene groups with shifts of δ3.81 and 3.91. The methine hydrogens give a single band at δ4.0 (2H). The aromatic protons give a multiplet between δ6.49-6.91 (8H). Also seen is an NH band due to two amino protons adjacent to the aromatic rings at δ5.58 which is found to disappear on addition of D_2O. The singlet at δ3.31 is due to the two aliphatic type amino protons, possibly combined with traces of water in the solvent.

6.3.2 ^{13}C NMR Of 6.3

The ^{13}C proton decoupled NMR spectrum of 6.3 in deuteriodimethylsulphoxide is shown in fig.6.3. The band due to the methine carbons is found at δ70.01 and that of the benzyl methylene carbons at δ47.23. The aromatic carbons are found to appear between δ116-146. The shifts are found to be very similar to those of the isowurtzitane derivatives described in chapter 3. The assignments were confirmed by decoupling/coupling experiments.

Fig. 6.2
^{1}H NMR Spectrum Of 6.3 In DMSO-d_6

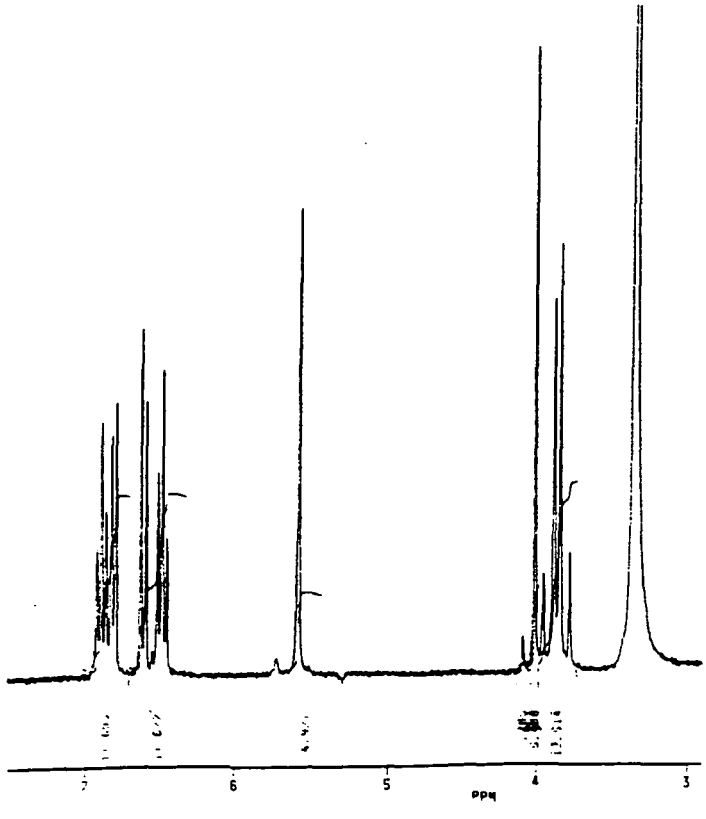

Fig. 6.3

^{13}C Proton Decoupled NMR Spectrum Of 6.3 In DMSO-d_6

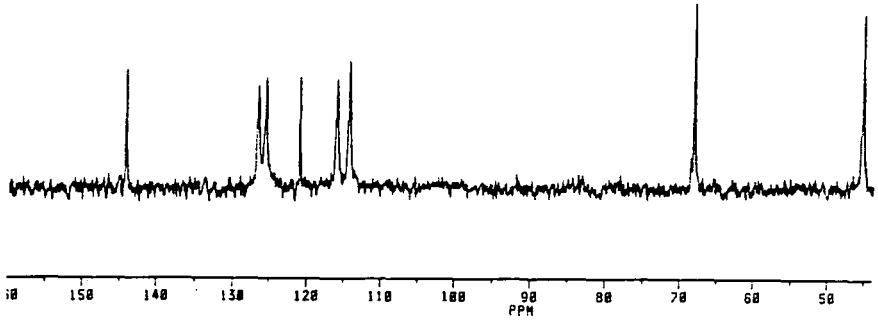

6.3.3 ^1H NMR Of 6.8

The ^1H NMR spectrum of 6.8 in deuteriochloroform is shown in fig.6.4. The spectrum indicates the presence of more than one isomer of 6.8 almost certainly due to restricted rotation about N-acetyl bonds. The methylene signals appear as an AB quartet (J=13Hz) (4H) exhibiting geminal coupling. The methine hydrogen signal is found to have been shifted downfield due to deshielding of the protons by the four surrounding N-acetyl groups and now appears at δ6.79 (2H). The aromatic protons are also shifted slightly downfield and appear between δ7.15-7.38. The acetyl groups appear as two bands at δ2.28 and 1.44 (12H). Bands due to the methylene protons of the isomer of 6.8 are found to appear as 2 AB quartets as a result of the different orientations of the N-acetyl groups in the molecule at δ4.75 and 4.94 and at δ4.42 and 5.34 respectively. The methine and aromatic bands of this minor isomer seem to be overlapping with the major isomer and therefore difficult to assign. But two types of acetyl signals are seen at δ2.12 and 1.28. However, it is not possible at this stage to identify which isomer is actually present.

6.3.4 ^{13}C NMR Of 6.8

The ^{13}C proton decoupled spectrum of the tetraacetylated derivative in deuteriochloroform (fig.6.6) show bands at δ61.64 and δ41.71 attributed to the methine and benzyl carbons respectively. The methyl carbons of acetyl groups appear at δ19.94 and 23.91. The aromatic carbons appear between δ124.98-134.66 and those of the two types of carbonyl groups are found at δ170.18 and 170.97. Also observed in the spectrum are very much smaller bands which almost overlap with the bands of the major compound and are believed to be those of the minor isomer which was also observed in the proton spectrum of 6.8.

Fig. 6.4
^{1}H NMR Spectrum Of 6.8 In $CDCl_3$

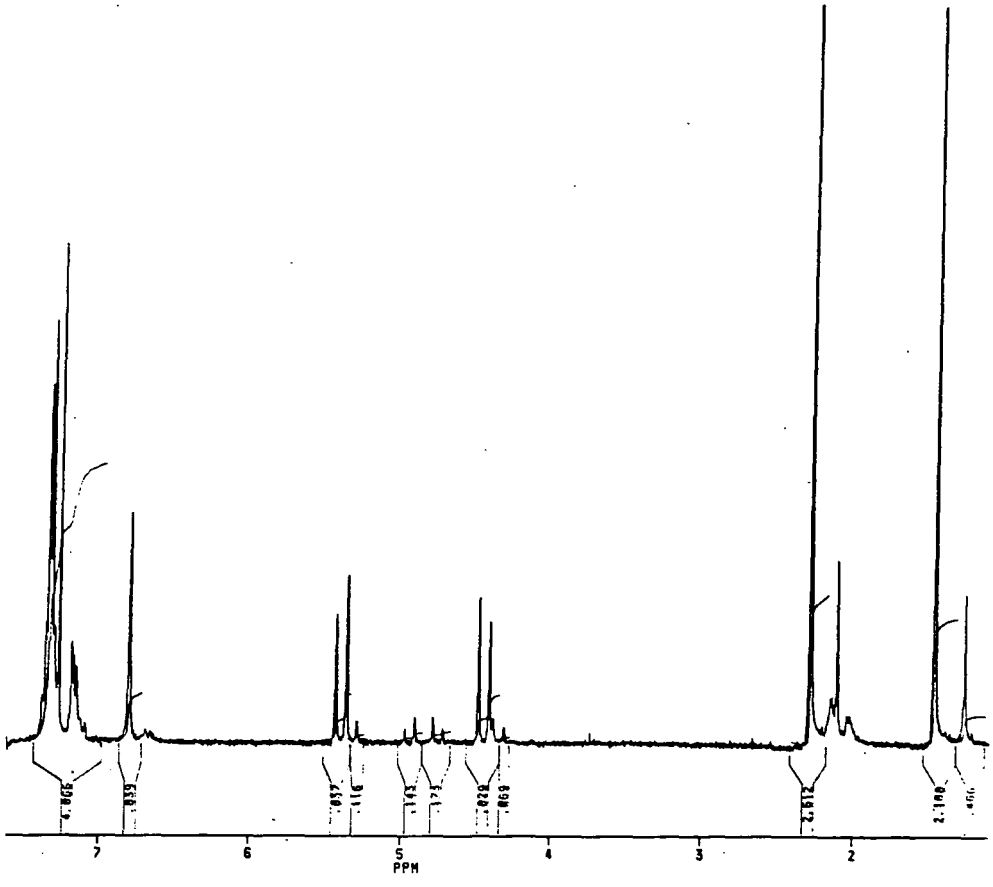

Fig. 6.5

^{13}C Proton Decoupled Spectrum Of 6.8 In $CDCl_3$

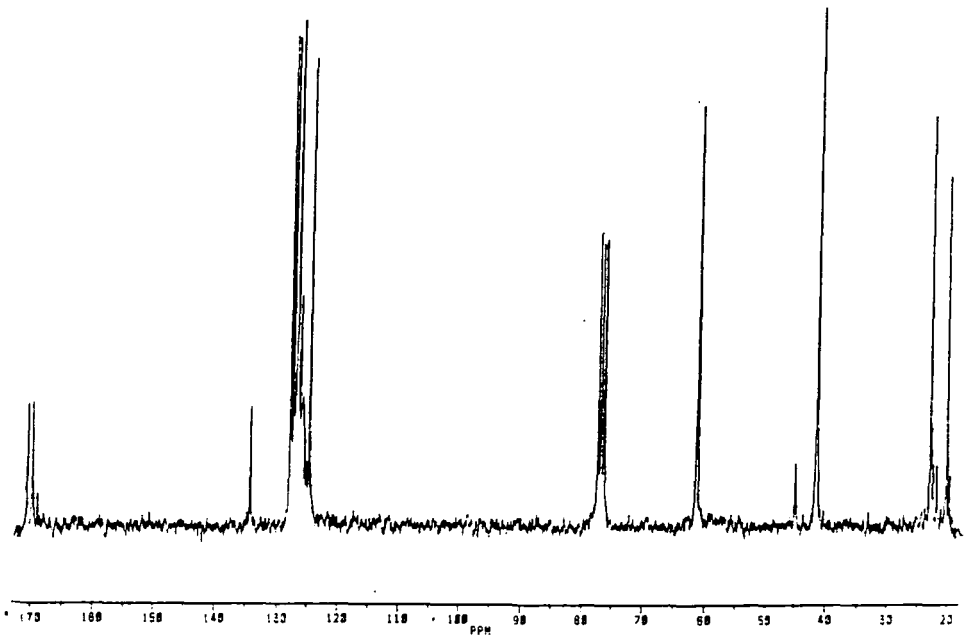

6.4 Infra-Red

6.4.1 I.R. Spectrum Of 6.3

The I.R. spectrum of 6.3 in KBr (fig.6.6) is shown to be quite distinct from that of the HBIW (fig.6.7) indicating that this is not a cage compound as expected. The broad band around 3400cm^{-1} is indicative of an NH stretch which is absent in HBIW and is the main difference in their spectra. Bands at 1600 and 1500cm^{-1} are characteristic aromatic C=C stretches of the phenyl ring. Several bands in the region between 1240 to 1340cm^{-1} are probably due to C-N stretches of the aryl ring nitrogen and those between 1000-1200cm^{-1} are characteristic of C-N stretches of aliphatic C-N groups. However, it must be noted that due to the wide range of values it is difficult for confirmatory purposes as other bands such as C-H stretching and bending vibrations also occur in this region. The band at 740cm^{-1} is a C-H vibration which is useful for indicating the substitution pattern of the benzene ring, in this case 1,2-disubstituted.

In the cage compound the spectrum is much simpler indicating C-H aromatic and aliphatic vibrational bands at 3020 and 2800cm^{-1} respectively, with similar C=C stretches around 1600, 1500 and 1450cm^{-1}. Also possible bands due to C-N stretches in aliphatic amines are observed between 1000-1200cm^{-1}.

Fig. 6.6

I.R. Spectrum Of 6.3 (KBr disc)

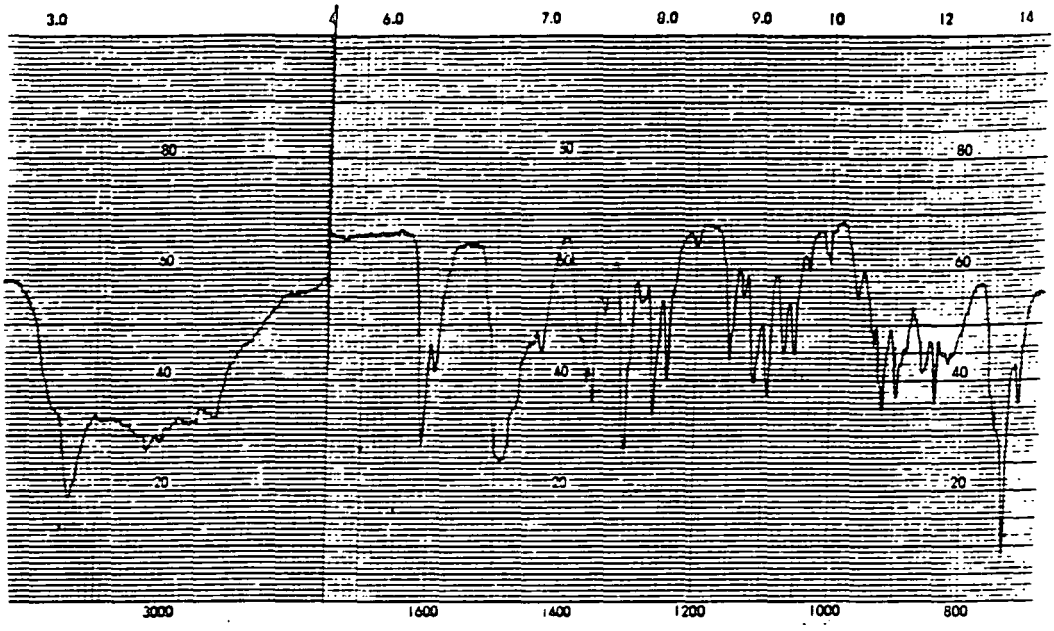

Fig. 6.7

I.R. Spectrum Of HBIW (KBr disc)

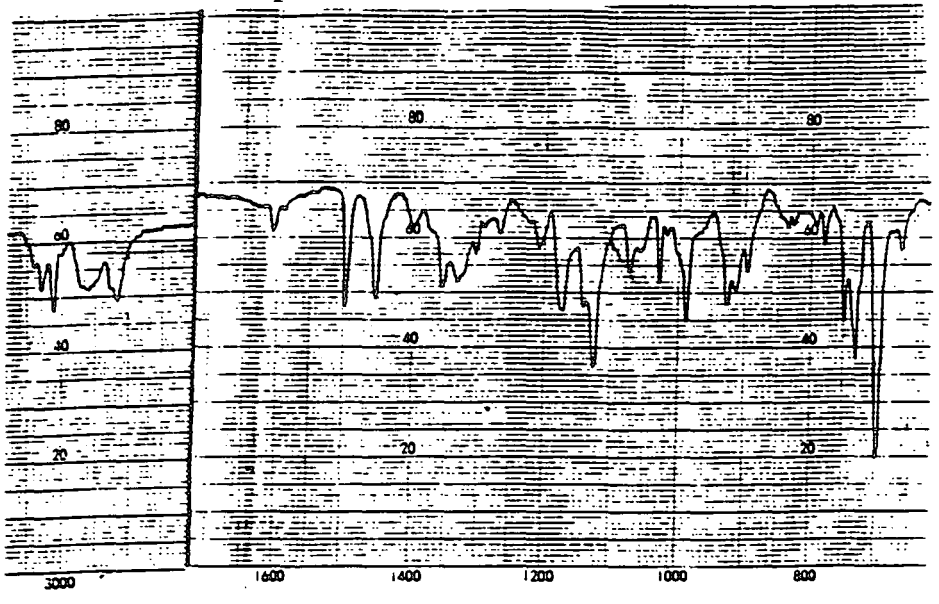

6.4.2 I.R. Spectrum Of 6.8

The I.R. spectrum of 6.8 (fig.6.8) exhibits a large broad band at 1650cm^{-1} characteristic of the carbonyl group and the absence of the large broad NH band around 3400cm^{-1}, although a small broad band is observed around 3500cm^{-1} which is most likely due to some water in the sample.

Fig. 6.8

I.R. Spectrum Of 6.8 (KBr disc)

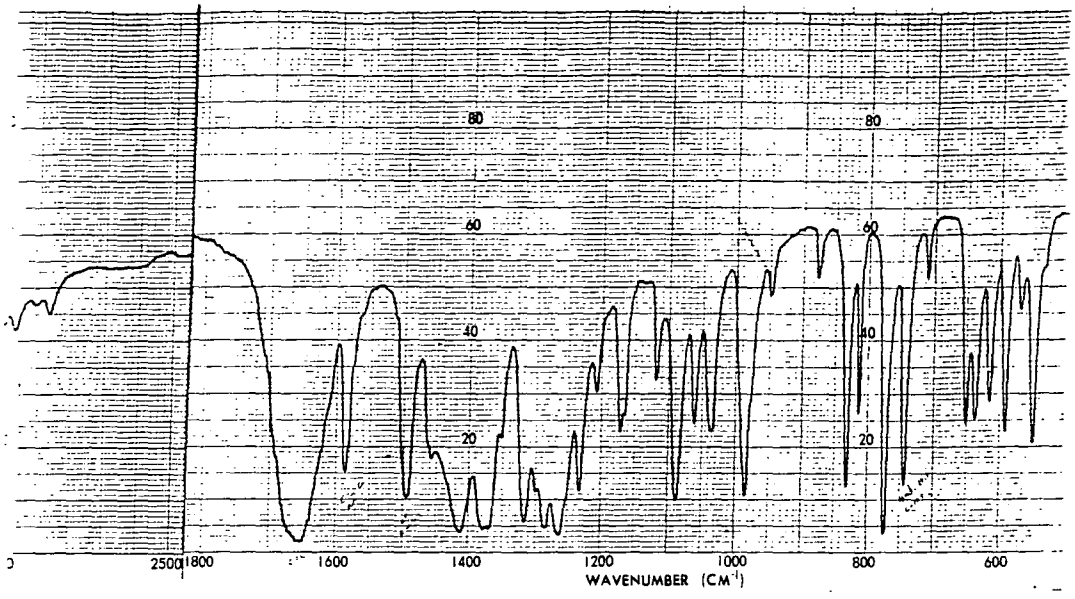

6.5 Mass Spectrum

The chemical ionisation mass spectrum of 6.3 was inconclusive, and revealed that the compound fragmented very easily. However, the chemical ionisation mass spectrum of 6.8 was much more useful giving a large M+1 peak at m/e 435 consistent with the formation of the M+1 cation of 6.8 (fig. 6.9).

Fig. 6.9

C.I. Mass Spectrum Of 6.8

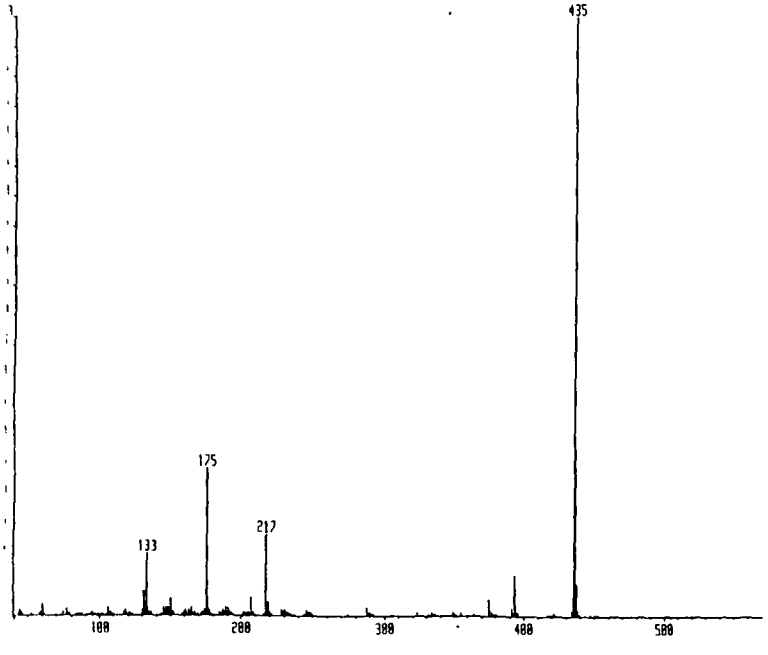

6.6 U.V. Spectrum Of 6.3

The U.V. spectrum of 6.3 in acetonitrile gives a λ_{max}253nm, ε=17,000 $dm^3mol^{-1}cm^{-1}$ and λ_{max}298nm, ε=4,000 $dm^3mol^{-1}cm^{-1}$. However, in the presence of perchloric acid in acetonitrile 6.3 is found to decompose as shown in fig. 6.10. 6.3 shows a hypsochromic shift on addition of acid attributed to protonation to 240nm followed by a slower secondary reaction resulting in the fading of the U.V. absorbance. The final spectrum having a λ_{max} at 251nm.

Although no kinetic studies were undertaken it was shown there was a slight increase in the rate of decomposition with increasing acid concentration. Absorbance vs. time plots did not give true 1st order plots indicating possibly more than one reaction taking place.

The decomposition pathway was not identified although it may be similar to that of bibenzooxazoline[7] (6.7) which was found to be hydrolysed by heating with 6N hydrochloric acid. The decomposition product obtained was *o*-aminophenol hydrochloride. The U.V. spectrum of the final product did not resemble that of 2-aminobenzylamine hydroperchlorate. It is possible other decomposition products are produced which may absorb more strongly than 2-aminobenzylamine hydro-perchlorate and therefore cannot be detected.

Fig. 6.10
U.V. Spectrum Of 6.3 In Acid

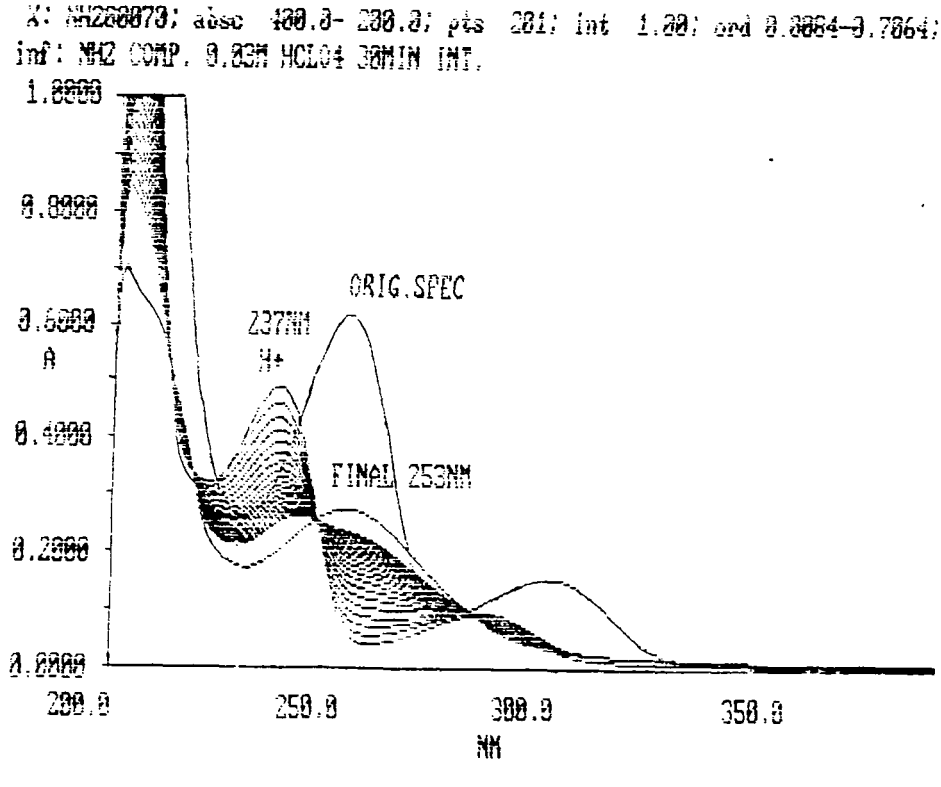

6.7 Reaction Of 4-Aminobenzylamine

Reaction of 4-aminobenzylamine with aqueous glyoxal was carried out as outlined for 2-aminobenzylamine in 6.8.1. A yellow gummy solid was obtained which was suspended in methanol ($50cm^3$) and stirred for an hour to give a fine yellow precipitate which was subsequently dried under vacuum to give a fine yellow powder M.P. 192-197°C (25% yield). The material was insoluble in all the solvents tried and therefore a ^1H NMR could not be obtained for characterisation. The mass spectrum was inconclusive and only revealed a total breakdown of the compound. Elemental analysis gave a compound having an empirical formula identical to that of 6.3 of $C_8H_9N_2$.

The I.R. spectrum under optimum conditions gave no information of functional groups (fig.6.10) but did show bands in the region expected for C-N stretches. It is possible we may have formed a polymeric compound but this is just speculation. The U.V. spectrum in acetonitrile did show a similarity to that of 6.3 (fig.6.11).

An attempted preparation of the diimine intermediate (if one was initially formed) was carried out as outlined in 6.8.2. A white unstable solid was initially formed which very rapidly turned yellow as it was being filtered. The resultant compound was found to be identical to that mentioned in the reaction of 4-amino benzylamine with aqueous glyoxal. From this evidence it is possible to say that the compound formed is not likely to be an isowurtzitane derivative.

Fig. 6.10

I. R. Spectrum Of Yellow Solid

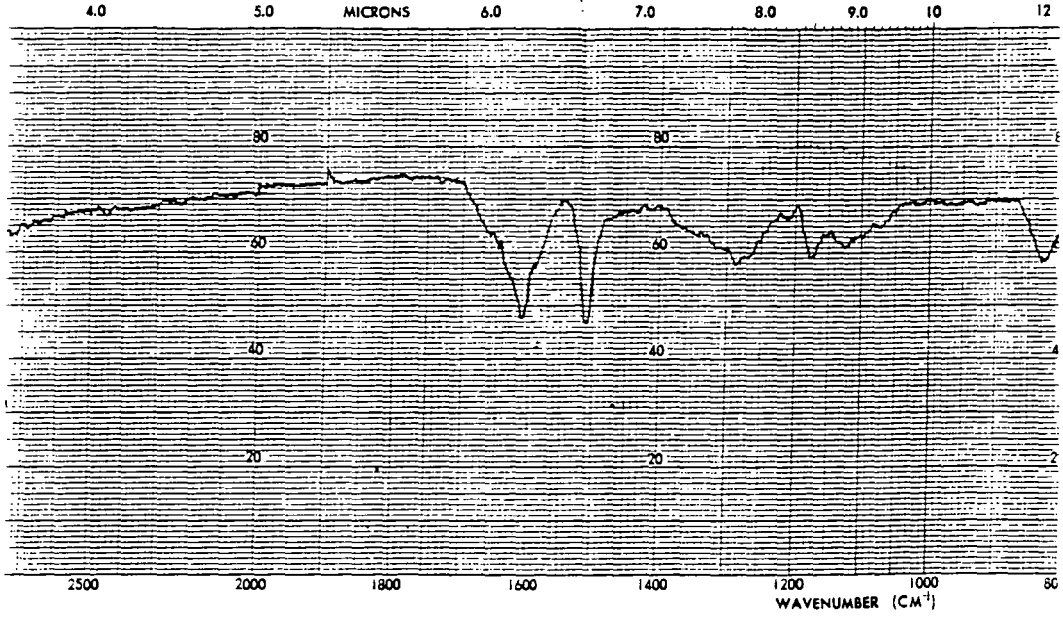

Fig. 6.11

U. V. Spectrum Of Yellow Solid

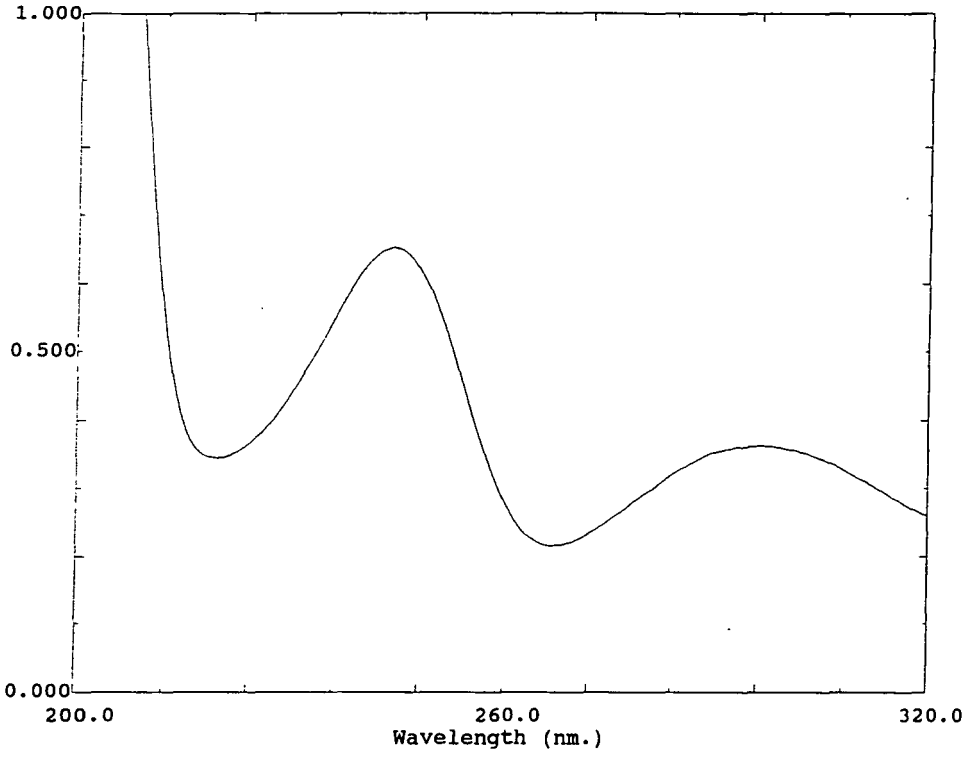

6.8 Experimental

6.8.1 Preparation of 6.3

2-Aminobenzylamine (10g, 0.082mol) was dissolved in acetonitrile (200cm^3) containing 70% nitric acid (0.30cm^3). 40% Aqueous glyoxal (5.95g, 0.041mol) was added dropwise over 45 mins. at room temperature (25°C). Precipitation of 6.3 occurred during the addition of glyoxal. Once all the glyoxal had been added the reaction mixture was left to stir for a further 24 hours. The crude product was filtered by suction filtration and isolated as a white powder which was subsequently washed with acetonitrile (50cm^3) before finally being dried under vacuum to give a fine white powder M.P 157-161°C (69% Yield). Due to the insolubility of 6.3 in most common solvents pure 6.3 could only be obtained by an exhaustive recrystallisation procedure under vacuum[8] (similar to a soxhlet extraction under vacuum). The pure product was obtained as colourless needles M.P. 180-182°C. Elemental analysis gave C=72.09%, H=6.70%, N=21.00%. Calculated for $C_{16}H_{18}N_4$ C=72.18%, H=6.76%, N=21.05%.

It is thought that formation of 6.3 involves intramolecular cyclisation of the diimine 6.2 intermediate. Diimines of benzylamines and ring substituted benzylamines can easily be isolated prior to their self condensation to give iso-wurtzitane cage structures. Similarly it was thought of interest to try to isolate the diimine intermediate (6.2) in the condensation of 2-aminobenzylamine with aqueous glyoxal.

6.8.2 Attempted Preparation Of 6.2

The procedure for the formation of 6.2 was similar to that used for 6.3, except that aqueous ethanol was substituted for acetonitrile solvent and the aqueous glyoxal was added over a 10 minute period while keeping the temperature at 0°C.

Within 5 minutes a gummy white solid was obtained which was filtered immediately and stored in dry ice . The solid was found to be very reactive. Dissolution of the solid in acetonitrile resulted in precipitation of a white solid within a few seconds. This on investigation was found to be 6.3. Due to the very reactive nature of the initially formed solid it was not possible to characterise this compound. However, due to its similar characteristics when compared to the dibenzyl diimines indicates that this may be the diimine intermediate 6.2.

6.8.3 Acetylation Of 6.2

Due to the insolubility of 6.3 in most solvents it was thought that acetylation of 6.3 would give an acetylated derivative which would be more soluble and therefore easier to characterise.

Acetylation of 6.3 involved gentle heating of 6.3 (4g, 0.015mol) in acetic anhydride ($50cm^3$) for 1-2 hours. Cubic off-white crystals of the acetylated derivative 6.8 separated out and were isolated by filtration. The dark brown mother liquor was evaporated under vacuum (50°C) to give a dark brown sticky residue. Addition of the brown solid to an ice/water mixture ($100cm^3$) gave a fine brown precipitate on standing for an hour. Boiling the residue with decolourising charcoal in 50:50 v/v aqueous ethanol and subsequent filtration gave a colourless filtrate which deposited crystals of pure 6.8 M.P. >300°C. The overall yield of 6.8 is 74%.

6.9 References

1. J. M. Kliegman and R. K. Barnes, *Tetrahedron,* 1970, 26, 255.
2. J. M. Kliegman and R. K. Barnes, *Tetrahedron,* 1970, 26, 255.
3. J. M. Kliegman and R. K. Barnes, United States Patent no. 3,652,672 1972.
4. J. M. Kliegman and R. K. Barnes, *J. Org. Chem.,* 1970,35, 3140.
5. F. Kehrmann, *Ber.,* 1895, 28, 343.
6. E. Bayer, *Ber.,* 1957, 90, 2325.
7. I. Murase, *Bull. Chem. Soc. Jap.,* 1959, 32, 827.
8. R. W. H. Small, A. J. Banister and Z.V. Hauptman, *J. Chem. Soc. Dalton Trans.,* 1984, 1377.

CHAPTER 7

EXPERIMENTAL

7.1 Materials

7.1.1 Solvents

Acetone:	General purpose reagent was used for washing apparatus. For synthetic work analytical grade was used without further treatment.
Acetonitrile:	"HiperSolv Far U. V." grade for HPLC was used for all U. V. and synthetic work without further treatment.
Acetic Anhydride:	Analytical reagent. Redistilled prior to use.
Acetic Acid:	Glacial, analytical grade, used as supplied.
Acetyl Bromide:	Commercial grade, used as supplied.
Ammonia:	32% Aqueous solution, commercial grade, used as supplied.
Benzene:	Analytical grade, used without further treatment.
Chloroform:	Analytical grade, used without further treatment.
Cyclohexane:	Analytical grade, used without further treatment.
Dichloromethane:	Analytical grade, used without further treatment.
Diethyl Ether:	Analytical grade. Where necessary distilled over sodium and stored over sodium wire.
Ethanol:	Analytical reagent, used as supplied.
Ethylene Glycol:	Commercial grade, used as supplied.
Formaldehyde:	37% Aqueous solution, analytical grade, used as supplied.
Formic Acid:	98% Analytical grade, used as supplied.
Glyoxal:	40% Aqueous solution, commercial grade, used as supplied.
Hydrazine Hydrate:	Commercial grade, used as supplied.
Hydrobromic Acid:	48% Aqueous solution, analytical grade, used as supplied.
Hydrochloric Acid:	37% Aqueous solution, analytical grade, used as supplied.
Methanol:	Analytical reagent, used as supplied.
Nitric Acid:	95% Fuming, commercial grade, used as supplied.
Nitric Acid:	70% Analytical grade, used as supplied.
Perchloric Acid:	70% Aqueous solution, analytical grade, used as supplied.
Sulphuric Acid:	98% Analytical grade, used as supplied.
Tetrahydrofuran:	Analytical grade, used as supplied.
Water:	Distilled. Where necessary boiled or sonicated under reduced pressure to expel dissolved gases and filtered.
Deuterium Oxide:	99.8% D-atom, commercial grade, used as supplied.
Deuterioacetone:	99.8% D-atom, commercial grade, used as supplied.
Deuteriochloroform:	99.8% D-atom, commercial grade, used as supplied.
Deuterioacetonitrile:	99.8% D-atom, commercial grade, used as supplied.

Deuteriodimethylsulphoxide: 99.8% D-atom, commercial grade, used as supplied.
Deuterionitromethane: 99.8% D-atom, commercial grade, used as supplied.

7.1.2 Salts

Ammonium acetate:	Commercial grade, used as supplied.
Lithium Aluminium Hydride:	Commercial grade, used as supplied.
Lithium Aluminium Deuteride:	98+% D-atom, commercial grade, used as supplied.
Magnesium sulphate:	Anhydrous, commercial grade, used as supplied.
Palladium Hydroxide:	Commercial grade, used as supplied.
Phosphorus Pentoxide:	Commercial grade, used as supplied.
Platinum (iv) Oxide:	Commercial grade, used as supplied.
Potassium Phthalimide:	Commercial grade, used as supplied.
Silica Gel:	60-120 mesh, commercial grade, used as supplied.
Sodium Deuteroxide:	30wt.% Solution in D_2O 99+% D-atom. Commercial grade, used as supplied.
Sodium Hydroxide:	Analytical grade pellets, used as supplied.
Sodium Nitrite:	Commercial grade, used as supplied.
Sodium Sulphate:	Anhydrous, commercial grade, used as supplied.

7.1.3 Substrates

Acetamide:	Commercial grade, used as supplied.
Hexamine:	Commercial grade, used as supplied.
Benzonitrile:	Commercial grade, used as supplied.
4-Chlorobenzonitrile:	Commercial grade, used as supplied.
Paraformaldehyde:	Commercial grade, used as supplied.
Para-Nitrobenzyl Bromide:	Commercial grade, used as supplied.

DPT:

DPT was prepared using a method[1] developed from the Hale[2] Process. This involved gradually adding hexamine (10g, 0.071mol), with stirring to 95% fuming nitric acid (35g) at 0-10°C. On dilution of the reaction mixture with iced-water ($100cm^3$), RDX separated out as a white solid, was filtered off and destroyed by placing in aqueous sulphuric acid immediately. The filtrate was neutralised with ammonia solution while keeping the temperature at 0°C. DPT precipitated out as a white solid, was washed with water and recrystallised from acetone. M.P. 212°C (lit.[3] 213°C).

DNPT:

DNPT was prepared by the method of Bachmann and Deno.[4] This involved addition of an ice-cold solution of sodium nitrite (3g 0.043mol) in water (7.2cm^3) was added to an ice cold solution of hexamine (1g, 0.007mol) in acetic acid (2.8cm^3) in water (64cm^3). The resultant solution was stirred for 1 hour, after which time the precipitated DNPT was filtered off, washed with distilled water, and dried to give a pale yellow powder, M.P. 207°C (lit.[4] 206-209°C).

DAPT:

DAPT was prepared by addition of a mixture of hexamine (14g, 0.10mol), ammonium acetate (6.2g, 0.08mol) and water (7cm^3) to acetic anhydride (31g, 0.3mol) dropwise over 60 minutes with stirring and cooling at 5-10°C. The solution was then stirred at 10°C for 30 minutes and evaporated to dryness. The solid was recrystallised from acetone M.P. 193-195°C (lit.[5] 193-198°C).

2,3-Dihydroxy-1,4-Dioxane:

2,3-Dihydroxy-1,4-dioxane was prepared by the method of Venuti.[7] This involved refluxing a mixture of 40% aqueous glyoxal (52.8g, 0.36mol) and ethylene glycol (230g, 0.37mol) in benzene (100cm^3) with efficient stirring and with azeotropic removal of water via a Dean-Stark trap. After 10 hours, removal of water is complete and the reaction mixture is allowed to cool, separating into 2 layers. The supernatant benzene layer is decanted away, the residual amber syrup is thoroughly triturated with cold acetone (250cm^3) and then refrigerated. The solid material was collected by filtration, washed with cold acetone and dried in vacuo over phosphorus pentoxide for 72 hours to give a lumpy solid which is powdered by spinning on a rotary evaporator to give a fine white powder (yield 19.7g 45%) M.P. 100-104°C (lit.[8] 100-103°C).

Benzylamine-α,α-d_2-N,N-d_2

Benzylamine-α,α-d_2-N,N-d_2 was prepared by reduction of benzonitrile with lithium aluminium deuteride[9] according to a modified procedure of Nystrom and Brown[10] which involved adding lithium aluminium deuteride (1.50g, 0.036mol) dissolved in dry diethyl ether (50cm^3) dropwise through a dropping funnel to benzonitrile (3.2g, 0.031mol), dissolved also in dry diethyl ether (50cm^3) in a 250cm^3 round bottomed flask fitted with a reflux condenser and magnetic stirrer. The rate of addition is such that the mixture is kept kept under gentle reflux. All openings to the atmosphere are protected with calcium chloride drying tubes. After addition of all the lithium aluminium deuteride refluxing was continued for a further 30 minutes. D_20 is then added dropwise (exercise great care!) with vigorous stirring and cooling of the mixture in an ice-water mixture to decompose the excess deuteride. The resultant

solution is filtered and the precipitated aluminium salt washed with a little diethyl ether. The total filtrate is dried with anhydrous sodium sulphate before filtration and evaporation of the ether on a rotary evaporator to give benzylamine-α,α-d_2-N,N-d_2 as a slightly yellow coloured liquid (3.44g, 90% yield). The ^{1}H NMR in deuterio-chloroform reveals absence of benzyl and NH signals.

N-Acetylaminoethanol:

Heating paraformaldehyde and acetamide in 1:1 molar ratio at 120°C in an autoclave for 10 hours gave[6] a clear liquid containing n-acetylaminoethanol.

p-Aminobenzylamine:

This involved a three stage synthesis starting from p-nitrobenzyl bromide.

N-(p-Nitrobenzyl)-phthalimide:

p-Nitrobenzyl bromide (200g, 0.92mol) (20% excess) was heated with potassium phthalimide (34g, 0.183mol) according to the method of Ing and Manske[11] in an oil bath under reflux for about 3 hours. The excess p-nitrobenzyl bromide is removed by steam distillation and the residual solid N-(p-nitrobenzyl)-phthalimide filtered, washed with water and recrystallised from acetic acid (46% yield) M.P. 165-166°C (lit.[12] 174-174°C).

N-(p-Aminobenzyl)-phthalimide:

Catalytic reduction of N-(p-nitrobenzyl)-phthalimide was achieved using the procedure of Kornblum and Iffland[13] which involved shaking N-(p-nitrobenzyl)-phthalimide (20g, 0.071mol) and platinum (iv) oxide (0.15g) in glacial acetic acid (120cm^3) with hydrogen at 3 atmospheres until no more hydrogen uptake occurred. The reduction product was diluted with an equal amount of water, filtered and made alkaline with sodium hydroxide. The precipitated N-(p-aminobenzyl)-phthalimide was isolated by filtration and recrystallised from aqueous ethanol (65% yield) M.P. 197-198°C (lit.[14] 187-188°C).

p-Aminobenzylamine:

N-(p-Aminobenzyl)-phthalimide (11g, 0.044mol) was hydrolysed with hydrazine hydrate (2.2g, 0.044mol) as outlined by Ing and Manske[11] in a 1:1 molar ratio by warming in ethanol (50cm^3). A yellow gelatinous precipitate is formed which was decomposed by warming with an excess of hydrochloric acid. The insoluble phthalyl hydrazide produced was filtered and washed with water. The filtrate was concentrated to remove alcohol and the solution cooled. After filtration of the precipitated phthalyl hydrazide again, the solution was made alkaline with sodium

hydroxide and extracted with ether ($3x30cm^3$). The ether solution was dried with potassium hydroxide pellets and then evaporated. The 4-aminobenzylamine obtained was distilled (48% yield) B.P. 142-143°C (10mm) (lit.[15] 268-270°C).

7.2 Measurement Techniques

7.2.1 U.V. / Vis Spectrophotometry

All U.V. / Vis spectra were recorded using fresh solutions in 1cm pathlength quartz cells on either a Perkin-Elmer Lambda 2 or Lambda 3 or Shimadzu 2101-PC instruments. These same instruments were also used for kinetic and equilibrium measurements (made at 25°C), except in case of the fast reactions, in which case the stopped-flow spectrophotometer was used (see later).

All kinetic measurements were made under pseudo first order conditions and observed rate coefficients were determined by following the change in absorbance at an appropriate wavelength. Absorbance values measured on the Lambda 3 instrument were entered into a suitable program running on an Apple IIe microcomputer; those from the Lambda 2 instrument were entered into a suitable program running on an Epsom AX2 personal computer. These programs calculated the observed rate coefficient based on the following derivation (calculation 7.1).

Calculation 7.1

For a 1st order process

where [A] = Concentration of A

$$-\frac{d[A]}{dt} = k[A] \quad \textbf{eqn. 7.1}$$

Integration of eqn. 7.1 gives an expression for the 1st order observed rate constant, eqn. 7.2.

$$k_o = \frac{1}{t}\ln\left\{\frac{[A]_0}{[A]_t}\right\} \quad \textbf{eqn. 7.2}$$

$[A]_o$ and $[A]_t$ are the concentrations of A corresponding to times t=0 and t=t respectively. Substituting absorbance and extinction coefficients derived from the Beer-Lambert Law into equation 7.2 gives :-

$$k_0 = \frac{1}{t}\ln\left\{\frac{A_0 - A_\infty}{A_t - A_\infty}\right\} \quad \textbf{eqn. 7.3}$$

Rearrangement of equation 7.3 gives :-

$$\ln(A_t - A_\infty) = -k_0 t + \ln(A_0 - A_\infty)$$

where $[A]_\infty$ is the absorbance at "infinite" time.

Thus a plot of ln $([A]_t - [A]_\infty)$ vs. time has a gradient of $-k_{obs}$. If following an increase in absorbance a plot of ln $([A]_\infty - [A]_t)$ vs. time has a gradient of $-k_{obs}$.

For measurements of rate coefficients of reactions too fast for conventional machines a Hi-Tech Scientific SF-3L stopped-flow spectrophotometer was used. This is shown schematically in fig. 7.1.

The two solutions A and B, which undergo reaction, are stored in glass reservoirs, and from there enter identical syringes, so that equal volumes of each solution are mixed at point M (halving the concentration of each solution) before passing into a thermostatted 2mm quartz cell at point O. When the plunger of the third syringe hits the stop the flow of reactants stops and the trigger causes monitoring of the reaction at O to begin. This is accomplished by passing a beam of monochromatic light of the appropriate wavelength through the cell. The reaction within the cell causes a decrease or increase in the transmitted light which is fed through a photomultiplier and displayed on an oscilloscope screen, from where the voltage changes can be read. Although the output of the photomultiplier is not linear, for a small percentage change the voltage can be assumed to be proportional to the absorbance of the reaction mixture, and therefore a plot of log $(V_t - V_\infty)$ vs. time gives k_{obs} from the gradient.

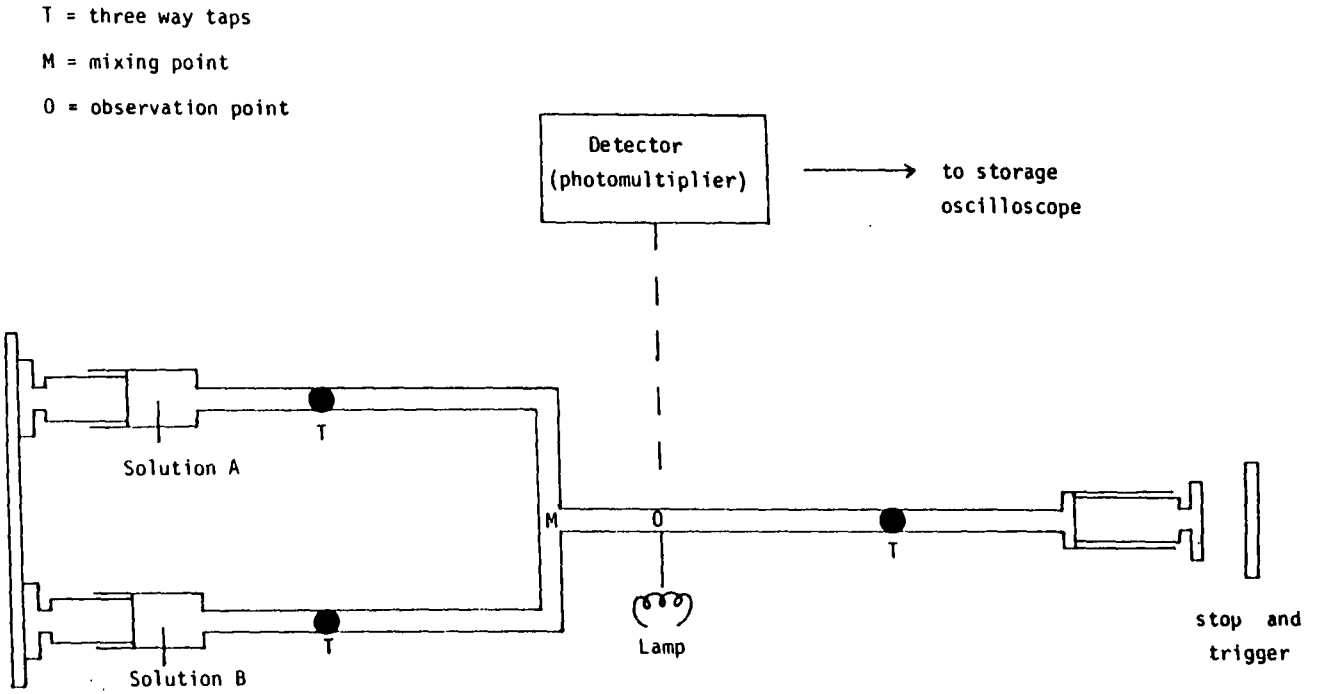
T = three way taps
M = mixing point
O = observation point
Detector
(photomultiplier)
to storage
oscilloscope
T
Solution A
M
O
T
T
Solution B
Lamp
stop and
trigger

Fig. 7.1

7.2.2 Mass Spectrometry

Mass spectrometric measurements were made using a 7070E instrument supplied by V.G. Analytical Limited. Electron ionisation, chemical ionisation or direct current ionisation methods were employed, the most suitable for any compound being determined empirically.

7.2.3 NMR Spectroscopy

^{1}H, ^{13}C and ^{15}N NMR spectra were recorded on either a Bruker AC 250 (250MHz), Varian 400MHz or a Bruker AMX 500 (500MHz) instruments. Chemical shift measurements are quoted as "δ" values relative to tetramethylsilane (TMS).

7.2.4 HPLC Measurements

Reverse-phase HPLC was performed using a Varian 9010 Star System and a Varian 9065 Diode Array Detector with a reverse-phase base deactivated column supplied by Hi-Chrome (HI-RPB-2507). For all HPLC runs an isocratic eluent (30%/65% v/v acetonitrile/water) was used and an observing wavelength of 254nm. Identification was by running known standards prior to the unidentified mixtures and comparison of their U.V. spectra.

7.3.1 X-Ray Crystal Determination For 2-Methyl HBIW (3.1d)

Crystal Data

Empirical Formula	$C_{54}H_{60}N_6$
Colour; Habit	Colourless prism
Crystal size (mm)	0.34 x 0.35 x 0.56
Crystal System	Monoclinic
Space Group	C2 / c
Unit Cell Dimensions	$\underline{a}$ = 16.996 (4) Å
	$\underline{b}$ = 14.201 (3) Å
	$\underline{c}$ = 19.845 (5) Å
	β = 103.11 (2)°
Volume	4665 (2) Å
Z	4
Formula Weight	793.1
Density (calc.)	1.129 Mg/m^3
Absorption Coefficient	0.0067 mm^{-1}
F (000)	1704

Data Collection

Diffractometer Used	Siemens R3m/V
Radiation	Mo Kα (λ = 0.71073 Å)
Temperature (K)	292
Monochromator	Highly orientated graphite crystal
2θ Range	3.0 to 48.0°
Scan Type	Wyckoff
Scan Speed	Variable; 1.50 to 14.65°/min in ω
Scan Range	1.00°
Background Measurement	Stationary crystal and stationary counter at beginning and end of scan, each for 25.0% of total scan time.
Standard Reflections	3 measured every 97 reflections
Index Ranges	$0 \leq h \leq 19$, $0 \leq k \leq 14$
Reflections Collected	3584
Independent Reflections	3129 (R_{int}= 2.17%)
Observed reflections	2090 ($F > 4.0\sigma(F)$)
Absorption Correction	N/A

Solution and Refinement

System Used	Siemens SHELXTL PLUS (VMS)
Solution	Direct Methods
Refinement Method	Full-Matrix Least-Squares
Quantity Minimised	$\Sigma w (F_o-F_c)^2$
Absolute Structure	N/A
Extinction Correction	N/A
Hydrogen Atoms	Riding model, fixed isotropic U
Weighting Scheme	$w^{-1} = \sigma^2 (F) + 0.0003F^2$
Number of Parameters Refined	283
Final R Indices (obs. data)	R = 6.06%, wR = 7.18%
R Indices (all data)	R = 9.31%, wR = 7.62%
Goodness-of-Fit	2.50
Largest and Mean Δ/σ	0.012, 0.002
Data-to-Parameter ratio	7.4:1
Largest Difference Peak	0.21 eA^{-3}
Largest difference Hole	-0.22 eA^{-3}

Table 7.1

Atomic Coordinates (x104) and equivalent Isotropic Displacement Coefficients (Å2 x10^3)

	X	Y	Z	U (eq)
N (1)	5746 (2)	6607 (2)	3281 (1)	41 (1)
N (2)	4097 (2)	6588 (2)	2826 (1)	43 (1)
N (3)	4966 (2)	5142 (2)	3133 (1)	44 (1)
C (1)	5473 (2)	7098 (3)	2619 (2)	41 (1)
C (2)	4241 (2	5601 (3)	2719 (2)	45 (1)
C (3)	5697 (2)	5598 (2)	3060 (2)	41 (1)
C (10)	6591 (2)	6882 (3)	3622 (2)	52 (1)
C (11)	6633 (2)	7839 (3)	3946 (2)	59 (2)
C (12)	6443 (3)	7983 (4)	4585 (2)	78 (2)
C (13)	6504 (4)	8896 (6)	4843 (4)	143(4)
C (14)	6723 (7)	9623 (7)	4502 (7)	196 (6))
C (15)	6929 (6)	9486 (6)	3867 (5)	181 (5)
C (16)	6870 (3)	8592 (4)	3587 (3)	100 (2)
C (17)	6213 (3)	7196 (5)	4993 (2)	110 (3)
C (20)	4077 (3)	6935 (3)	3516 (2)	55 (2)
C (21)	3685 (2)	7896 (3)	3466 (2)	57 (2)
C (22)	2835 (3)	7980 (3)	3276 (2)	68 (2
C (23)	2488 (4)	8843 (5)	3239 (3)	102 (3)
C (24)	2960 (5)	9627(5)	3363 (3)	119 (3)
C (25)	3797 (5)	9588 (4)	3544 (3)	121 (3)
C (26)	4161 (3)	8672 (3)	3612 (3)	81 (2)
C (27)	2286 (3)	7138 (4)	3113 (2)	93 (2)
C (30)	4931 (2)	4917 (3)	3848 (2)	55 (1)
C (31)	5418 (2)	4056 (3)	4113 (2)	56 (2)
C (32)	5179 (3)	3165 (3)	3855 (2)	71 (2)
C (33)	5644 (4)	2389 (3)	4157 (2)	91 (2)
C (34)	6304 (4)	2508 (5)	4683 (3)	97 (3)
C (35)	6554 (3)	3383 (5)	4930 (3)	89 (2)
C (36)	6110 (3)	4152 (3)	4648 (2)	71 (2)
C (37)	4445 (3)	3011 (3)	3294 (2)	97 (2)

* Equivalent isotropic U defined as one third of the trace of the orthogonalised U_{ij} tensor.

Table 7.2

Bond Lenths (Å)

N (1)-C (1)	1.468 (4)	N (1)-C (3)	1.496 (4)
N (1)-C (10)	1.493 (4)	N (2)-C (2)	1.448 (5)
N (2)-C (20)	1.461 (4)	N (2)-C (1A)	1.460 (5)
N (3)-C (2)	1.469 (4)	N (3)-C (3)	1.437 (5)
N (3)-C (30)	1.469 (5)	C (1)-N (2A)	1.460 (5)
C (1)-C (1A)	1.569 (6)	C (2)-C (3A)	1.572 (5)
C (3)-C (2A)	1.572 (5)	C (10)-C(11)	1.498 (5)
C (11)-C (12)	1.392 (7)	C (11)-C (16)	1.395 (7)
C (12)-C (13)	1.390 (10)	C (12)-C (17)	1.485 (8)
C (13)-C (14)	1.332 (14)	C (14)-C (15)	1.397 (18)
C (15)-C (16)	1.380 (10)	C (20)-C (21)	1.512 (6)
C (21)-C (22)	1.413 (6)	C (21)-C (26)	1.360 (6)
C (22)-C (23)	1.354(8)	C (22)-C (27)	1.506 (7)
C (23)-C (24)	1.362 (8)	C (24)-C (25)	1.387 (11)
C (25)-C (26)	1.433 (9)	C (30)-C (31)	1.502 (5)
C (31)-C (32)	1.390 (8)	C (31)-C (36)	1.402 (5)
C (32)-C (33)	1.408 (6)	C (32)-C (37)	1.489 (6)
C (33)-C (34)	1.359 (7)	C (34)-C (35)	1.368 (9)
C (35)-C (36)	1.372 (8)		

Table 7.3

Bond Angles (°)

C (1)-N (1)-C (3)	101.9 (2)	C (1)-N (1)-C (10)	110.9 (3)
C (3)-N (1)-C (10)	111.6 (3)	C (2)-N (2)-C (20)	120.4 (3)
C (2)-N (2)-C (1A)	105.4 (3)	C (20)-N (2)-C (1A)	121.4 (3)
C (2)-N (3)-C (3)	112.2 (3)	C (2)-N (3)-C (30)	115.1 (3)
C (3)-N (3)-C (30)	114.9 (2)	N (1)-C (1)-N (2A)	101.9 (3)
N (1)-C (1)-C (1A)	111.3 (3)	N (2A)-C (1)-C (1A)	116.0 (3)
N (2)-C (2)-N (3)	119.7 (3)	N (2)-C (2)-C (3A)	101.5 (3)
N (3)-C (2)-C (3A)	108.3 (3)	N (1)-C (3)-N (3)	113.2 (3)
N (1)-C (3)-C (2A)	106.0 (3)	N (3)-C (3)-C (2A)	110.7 (3)
N (1)-C (10)-C (11)	112.3 (3)	C (10)-C (11)-C (12)	121.7 (4)
C (10)-C (11)-C (16)	117.9 (4)	C (12)-C (11)-C (16)	120.4 (4)
C (11)-C (12)-C (13)	117.4 (5)	C (11)-C (12)-C (17)	122.0 (5)
C (13)-C (12)-C (17)	120.5 (5)	C (12)-C (13)-C (14)	122.7 (8)
C (13)-C (14)-C (15)	120.5 (9)	C (14)-C (15)-C (16)	118.8 (8)
C (11)-C (16)-C (15)	120.2 (6)	N (2)-C (20)-C (21)	110.3 (3)
C (20)-C (21)-C (22)	120.1 (4)	C (20)-C (21)-C (26)	119.1 (4)
C (22)-C (21)-C (26)	120.8 (4)	C (21)-C (22)-C (23)	119.8 (5)
C (21)-C (22)-C (27)	122.5 (4)	C (23)-C (22)-C (27)	117.8 (4)
C (22)-C (23)-C (24)	120.0 (6)	C (23)-C (24)-C (25)	122.8 (6)
N (24)-C (25)-C (26)	117.1 (6)	C (21)-C (26)-C (25)	119.5 (5)
C (3)-C (30)-C (31)	112.0 (3)	C (30)-C (31)-C (32)	121.3 (3)
C (30)-C (31)-C (36)	119.2 (4)	C (32)-C (31)-C (36)	119.5 (4)
C (31)-C (32)-C (33)	117.8 (4)	C (31)-C (32)-C (37)	122.3 (4)
C (33)-C (32)-C (37)	119.8 (4)	C (32)-C (33)-C (34)	121.1 (5)
C (33)-C (34)-C (35)	121.5 (5)	C (34)-C (35)-C (36)	118.7 (4)
C (31)-C (36)-C (35)	121.4 (4)		

Table 7.4

Anisotropic Displacement Coefficients ($Å^2 x10^3$)

	11		22	U33	U12	U
N(l)	37(2)	44(2)	38(2)	2(1)	4(1)	-1(1)
N(2)	45(2)	45(2)	40(2)	7(1)	12(1)	0(1)
N(3)	38(2)	50(2)	44(2)	3(1)	9(1)	9(1)
C(l)	44(2)	39(2)	38(2)	-2(2)	5(2)	0(2)
C(2)	37(2)	51(3)	46(2)	-2(2)	10(2)	5(2)
C(3)	38(2)	42(2)	42(2)	8(2)	6(2)	2(2)
C(10)	41(2)	64(3)	47(2)	0(2)	-2(2)	-5(2)
C(ll)	55(3)	56(3)	64(2)	-4(2)	-13(2)	-9(2)
C(12)	61(3)	S7(4)	65(3)	10(3)	-6(2)	-34(3)
C(13)	112(3)	153(7)	136(6)	30(5)	-22(4)	-76(6)
C(14)	196(10)	77(6)	263(14)	5(6)	-58(10)	-79(8)
C(15)	204(9)	73(6)	212(9)	-41(5)	-68(8)	0(6)
C(16)	100(4)	81(4)	98(4)	-29(3)	-25(3)	1(3)
C(17)	91(4)	185(6)	56(3)	1(4)	20(3)	-20(4)
C(20)	48(2)	73(3)	46(2)	16(2)	15(2)	0(2)
C(21)	57(3)	69(3)	45(2)	22(2)	14(2)	-5(2)
C(22)	68(3)	78(3)	5S(3)	35(S)	17(2)	-1(2)
C(23)	96(4)	98(4)	110(4)	37(4)	21(3)	-10(4)
C(24)	121(6)	95(5)	141(5)	52(4)	30(4)	-12(4)
C(25)	141(6)	S2(5)	134(3)	-3(4)	42(4)	-49(4)
C(26)	88(3)	70(3)	84(3)	9(3)	18(3)	-24(3)
C(27)	57(3)	128(5)	83(3)	6(3)	13(3)	2(3)
C(30)	58(2)	60(3)	50(2)	10(2)	15(2)	14(2)
C(31)	53(3)	67(3)	50(2)	8(2)	17(2)	20(2)
C(S2)	70(3)	68(3)	78(3)	-5(3)	23(3)	21(3)
C(33)	101(4)	121(4)	109(4)	18(3)	39(4)	24(3)
C(34)	55(4)	115(5)	92(4)	48(4)	41(4)	44(4)
C(35)	70(3)	129(5)	64(3)	32(4)	15(3)	23(3)
C(36)	70(3)	91(4)	54(3)	18(3)	18(2)	16(2)
C(37)	87(4)	82(4)	106(4)	-15(3)	9(3)	6(3)

Table 7.5

H-Atom Coordinates ($x10^4$) and Isotropic Displacement Coefficients ($Å^2 x10^3$)

	x	Y	Z	U
H(l)	5597(17)	7767(23)	2665(14)	43(9)
H(2)	3724(19)	51S3(21)	2775(14)	46(S)
H(3)	6140(18)	5255(20)	3361(15)	39(9)
H(lOA)	6916	6871	3285	80
H(lOB)	6808	6430	3976	80
H(13)	6385	9012	5286	170
H(14)	6752	10245	4696	230
H(15)	70SS	lOOO9	3626	220
H(16)	7004	8482	3149	130
H(17A)	6101	7425	5417	130
H(17B)	5744	6882	4727	130
H(17C)	6657	6761	5096	130
H(20A)	4619	6976	3790	80
H(20B)	3780	6501	3735	80
H(23)	1911	8907	3132	130
H24)	2712	10238	3315	150
H(25)	4125	10144	3734	140
H(26)	4738	8607	3751	110
H(27A)	1733	7340	2997	120
B(27B)	2407	6803	2728	120
H(27C)	2371	6731	3509	120
H(30A)	4379	4815	3870	80
H(30B)	5135	6441	4140	80
H(33)	5490	1769	3984	120
H(34)	6600	1967	4894	130
H(35)	7036	3457	5288	120
H(36)	6273	4770	4820	100
H(37A)	4202	3609	3149	130
H(37B)	4595	2708	2909	130
H(37C)	4066	2623	3459	130

7.3.2 X-Ray Crystal Determination For 4-Chloro HBIW (3.1c)

Crystal Data

Empirical Formula	$C_{48}H_{42}N_6Cl_6$
Colour; Habit	Colourless cube
Crystal size (mm)	0.31 x 0.34 x 0.43
Crystal System	Monoclinic
Space Group	C2 / c
Unit Cell Dimensions	a = 18.916 (4) Å
	b = 11.449 (2) Å
	c = 20.403 (4) Å
	β = 90.72 (2)°
Volume	4418 (2) Å
Z	4
Formula Weight	915.63
Density (calc.)	1.38 Mg/m^3
Radiation	Mo Kα (λ = 0.71073 Å)
μ	4.3 cm^{-1}
F (000)	1896

The setting angles of 25 reflections in the range $7 < \theta < 18^{\circ}$ were measured on a CAD4 diffractometer and analysed. As a check on crystal quality, omega scans of several intense reflections were measured; the width at half-height was 0.30° with a take-off angle of 2.8°, indicating good crystal quality. From the systematic absences of:

$$\begin{array}{ll} hkl & h + k = 2n+1 \\ h01 & 1 = 2n+1 \end{array}$$

and from subsequent least-squares refinement, the space group was determined to be C2/c (#15).

The data collected at a room temperature of $20 \pm 1^{\circ}$ using the ω-2θ scan technique. The scan rate varied from 1 to 7°/min (in omega). The variable scan rate allows rapid data collection for intense reflections where a fast scan rate is used and assures good counting statistics for weak reflections where a range (in deg.) was determined as a function of θ to correct for the separation of the K_{α} doublet; the scan width was calculated as follows:

$$\text{scan width} = 0.6 + 0.350 \tan\theta$$

Moving-crystal moving-counter background counts were made by scanning an additional 25% above and below this range. Thus the ratio of the peak counting time to background counting time was 2:1. The counter aperture was also adjusted as a function of θ. The horizontal aperture width ranged from 2.0 to 2.5mm; the vertical aperture was set at 4.0mm. The diameter of the incident beam collimator was 0.7mm and the crystal to detector distance was 21cm. For intense reflections an attenuator was automatically inserted in front of the detector; the attenuator factor was 17.6.

A total of 5290 reflections were collected of which 2827 were unique and not systematically absent. As a check on the crystal and electronic stability 3 representative reflections were measured every 120 min. The intensities of these standards remained constant within experimental error throughout data collection. No decay correction was applied.

Lorentz and polarisation corrections were applied to the data. the linear absorbtion coefficient is 4.3cm-1 for Mo K_{α} radiation. A numerical absorbtion correction was made. Relative transmission coefficients ranged from 80.955 to 88.530 with an average value of 85.351. A secondary extinction correction was applied. The final coefficient, refined in least-squares, was 1.5×10^{-7} (in absolute units). Intensities of equivalent reflections were averaged. The agreement factors for the averaging of the 170 observed and accepted reflections was 1.4% on intensity and 1.1% based on Fo.

The structure was solved by direct methods. Using 450 reflections (minimum E of 1.20) and 2000 relationships, a total of 54 phase sets were produced. A total of 30 atoms were located from an E-map prepared from the phase set. The remaining atoms were located in succeeding difference Fourier syntheses. Hydrogen atoms were included in the refinement but restrained to ride on the atom to which they are bonded.

The standard deviation on intensities. (Fo), is defined as follows:

$$\sigma(Fo^2) = [S^2 1(C^2 + R^2 B) + (pFo^2)^2]/Lp$$

where S is the scan rate. C is the total integrated peak count, R is the ratio of the scan time to background counting time, B is the total background count, Lp is the Lorentz-polarisation factor, and the parameter p is a factor introduced to downweight intense reflections. Here p was set to 0.038.

Scattering factors were taken from Cromer Waber.[16] Anomalous dispersion effects were included in Fc; the values for f' and f" were those of Cromer. Only the 2827 reflections having intensities greater than 3.0 times their standard deviation were used in the refinements. The final cycle of refinement included 272 variable parameters and converged (largest parameter shift was 0.001 times its esd) with unweighted and weighted agreement factors of:

$$R1 = \Sigma||Fo|-|Fc|| \,/\, \Sigma|Fo| = 0.041$$
$$R2 = (\Sigma w(|Fo|-|Fc|) \,/\, \Sigma w\, Fo)^{1/2} = 0.058$$

The standard deviation of an observation of unit weight was 2.19. The highest peak in the final difference Fourier had a height of 0.23 e/Å^3 with an estimate error[17] based on ΔF of 0.04. Plots of $w(|Fo|-|Fc|)^2$ versus $|Fo|$, reflection order in data collection, $\sin\theta/\lambda$, and various classes of indices showed no unusual trends.

All calculations were performed on a PDP-11 computer using SDP-PLUS.

Table 7.6

Positional and Thermal Parameters and their e.s.d's

Atom	X	Y	Z	B(Å^2)
Cl1	0.17555 (5)	-0.26866 (7)	0.17186 (5)	7.78 (2)
Cl2	-0.22311 (5)	0.51163 (9)	0.07445 (5)	9.14 (2)
Cl3	0.08109 (5)	0.93364 (2)	0.4669 (4)	7.46 (2)
C1	0.0147 (1)	0.2206 (2)	0.2140 (1)	3.90 (5)
N2	0.08066 (9)	0.2846 (2)	0.2046 (1)	3.87 (4)
C3	0.0620 (1)	0.4048 (2)	0.2094 (1)	3.74 (5)
C5'	-0.01511 (1)	0.4070 (2)	0.1811 (1)	3.70 (5)
N6'	-0.03402 (9)	0.2821 (2)	0.16953 (9)	3.91 (4)
N4	0.06179 (9)	0.4633 (2)	0.27362 (9)	3.68 (4)
C11	0.1577 (1)	0.1162 (2)	0.2157 (1)	3.98 (5)
C12	0.1525 (1)	0.0746 (2)	0.1522 (1)	4.89 (6)
C13	0.1573 (1)	-0.0435 (2)	0.1387 (1)	5.24 (6)
C14	0.1683 (1)	-0.1204 (2)	0.1890 (1)	4.87 (6)
C15	0.1736 (1)	-0.0830 (2)	0.2527 (1)	5.1 (6)
C16	0.1676 (1)	0.0351 (2)	0.2654 (1)	4.55 (5)
C17	0.1481 (1)	0.2436 (2)	0.2308 (1)	4.51 (5)
C21	-0.0744 (1)	0.305 (2)	0.0550 (1)	4.44 (5)
C22	-0.1467 (1)	0.2990 (3)	0.0637 (1)	5.55 (6)
C23	-0.1926 (1)	0.3619 (3)	0.0237 (1)	5.98 (7)
C24	-0.1657 (1)	0.42895 (3)	-0.0255 (1)	5.68 (6)
C25	-0.0957 (2)	0.4317 (3)	-0.0638 (1)	6,55 (8)
C26	-0.0503 (1)	0.3693 (3)	0.0036 (1)	5.86 (7)
C27	-0.0238 (1)	0.2444 (2)	0.1012 (1)	4.97 (6)
C31	0.1152 (1)	0.6138 (2)	0.3438 (1)	3.74 (5)
C32	0.1620 (1)	0.6439 (2)	0.03937 (1)	5.12 (6)
C33	0.1523 (1)	0.7412 (2)	0.04319 (1)	5.52 (6)
C34	0.0950 (1)	0.8111 (2)	0.04210 (1)	4.71 (6)
C35	0.0472 (1)	0.7837 (2)	0.3722 (1)	5.29 (6)
C36	0.0574 (1)	0.5858 (2)	0.3345 (1)	4.87 (6)
C37	0.1275 (1)	0.5079 (2)	0.3015 (1)	4.13 (5)

anisotropically refined atoms are given in the form of the isotropic equivalent thermal parameter defined as:

$$4/3[a^2B_{11} + b^2B_{22} + c^2B_{33} + abcos\gamma B_{12} + accos\beta B_{13} + bccos\propto B_{23}]$$

Table 7.7

Bond Lengths (Å)

Cl1	C14	1.739 (3)	C13	C14	1.368 (4)
Cl2	C24	1.748 (3)	C14	C15	1.370 (4)
Cl3	C34	1.742 (3)	C15	C16	1.382 (4)
C1	C1'	1.579 (3)	C21	C22	1.383 (3)
C1	N2	1.461 (3)	C21	C26	1.366 (4)
C1	N6'	1.465 (3)	C21	C27	1.504 (3)
N2	C3	1.460 (3)	C22	C23	1.385 (4)
N2	C17	1.455 (3)	C23	C24	1.365 (4)
C3	C5'	1.561 (3)	C24	C25	1.347 (4)
C3	N4	1.455 (3)	C25	C26	1.382 (4)
C5'	N6'	1.493 (3)	C31	C32	1.383 (3)
C5'	N4	1.438 (3)	C31	C36	1.382 (3)
N6'	C27	1.475 (3)	C31	C37	1.508 (3)
N4	C37	1.453 (3)	C32	C33	1.373 (4)
C11	C12	1.383 (3)	C33	C34	1.363 (4)
C11	C16	1.385 (3)	C34	C35	1.372 (4)
C11	C17	1.503 (3)	C35	C36	1.374 (4)
C11	C13	1.383 (4)			

Table 7.8

Bond Angles (°)

C1'	C1	N2	115.7 (2)	C14	C15	C16	118.6 (2)
C1'	C1	N6'	110.5 (2)	C11	C16	C15	122.0 (2)
N2	C1	N6'	102.1 (2)	N2	C17	C11	110.2 (2)
C1	N2	C3	105.6 (2)	C22	C21	C26	117.8 (2)
C1	N2	C17	122.4 (2)	C22	C21	C27	121.3 (2)
C3	N2	C17	119.9 (2)	C26	C21	C27	120.9 (2)
N2	C3	C5'	101.1 (2)	C21	C22	C23	120.9 (3)
N2	C3	N4	119.1 (2)	C22	C23	C24	119.1 (2)
C5'	C3	N4	108.8 (2)	Cl2	C24	C23	119.3 (2)
C3	C5'	N6'	106.7 (2)	Cl2	C24	C25	119.5 (2)
C3	C5'	N4	109.8 (2)	C23	C24	C25	121.2 (3)
N6'	C5'	N4	112.5 (2)	C24	C25	C26	119.2 (3)
C1	N6'	C5'	102.4 (2)	C21	C26	C25	121.7 (2)
C1	N6'	C27	110.8 (2)	N6'	C27	C21	11.6 (2)
C5'	N6'	C27	113.4 (2)	C32	C31	C36	116.8 (2)
C3	N4	C5'	113.1 (2)	C32	C31	C37	121.3 (2)
C3	N4	C37	119.5 (2)	C36	C31	C37	121.9 (2)
C5'	N4	C37	115.9 (2)	C31	C32	C33	122.1 (2)
C12	C11	C16	117.6 (2)	C32	C33	C34	119.6 (2)
C12	C11	C17	121.2 (2)	Cl3	C34	C33	120.3 (2)
C16	C11	C17	121.1 (2)	Cl3	C34	C35	119.7 (2)
C11	C12	C13	121.3 (2)	C33	C34	C35	120.0 (2)
C12	C13	C14	119.3 (2)	C34	C35	C36	119.8 (2)
Cl1	C14	C13	119.3 (2)	C31	C36	C35	121.7 (2)
Cl1	C14	C15	119.4 (2)	N4	C37	C31	111.7 (2)
C13	C14	C15	121.3 (2)				

7.4 References

1. G. C. Hale *J. Am. Chem. Soc.*, 1925, 47, 2754.
2. P. Golding, Ministry of Defence, private communication.
3. H. Yoshida, G. Sen and B. S. Thyagarajan, *J. Heterocycl. Chem.*, 1973, 10, 725
4. W. E. Bachmann and N. C. Deno, *J. Am. Chem. Soc.*, 1951, 73, 2777.
5. V. I. Seale, M. Warman and E. E. Gilbert, *J. Heterocyclic Chem.*, 1974, 11, 237.
6. H. Bohme, R. Broese, A. Dick, F. Eiden and D. Schunemann, *Chem. Ber.*, 1959, 92, 1599; H. Bohem, A. Dick and G. Driesen, *Chem. Ber.*, 1961, 94, 1879.
7. M. C. Venuti, *Synthesis,* 1982, 61.
8. F. S. H. Head, *J. Am. Chem. Soc.*, 1955, 1036.
9. E. A. Halevi, M. Nussin and A. Ron, *J. Am. Chem. Soc.* 1963, 866.
10. R. F. Nystrom and W.G. Brown, *J. Am. Chem. Soc.*, 1948, 70, 3738.
11. H. R. Ing and H. F. Manske, *J. Am. Chem. Soc.*, 1926, 2348.
12. Salkowski, *Ber.*, 1889, 22, 2142.
13. N. Kornblum and D.C. Iffland, *J. Am. Chem. Soc.*, 1949, 71, 2137.
14. Hafner, *Ber.*, 1890, 23, 341.
15. Amsel and Hofmann, *Ber.*, 1886, 19, 1288.
16. D. T. Cromer and J. T. Waber, "International Tables for X-ray Crystallography", Vol. IV, The Kynoch. Press, birmingham, 1974, Table 2.2B.
17. D. J. Cruickshank, *Acta Crystallogr.*, 1949, 2, 154.

Appendix I

Research Colloquia, Seminars, Lectures And Conferences

AI.1 Colloquia, Lectures And Seminars Given By Invited Speakers At The University Of Durham

AI.1.1 1st August 1989 To 31st July 1990

BADYAL, Dr. J. P. S. (Durham University), Breakthroughs in Heterogenous Catalysis	1st Nov., 1989
BECHER, Dr. J. (Odense University) Synthesis of New Macrocyclic Systems Using Heterocyclic Building Blocks	13th Nov., 1989
BERCAW, Prof. J. E. (California Institute of Technology) Synthetic and Mechanistic Approaches to Ziegler-Natta Polymerisation of Olefins	10th Nov., 1989
BLEASDALE, Dr. C. (Newcastle University) The Mode of Action of some Anti-tumour Agents	21st Feb., 1990
BOWMAN, Prof. J. M. (Emory University) Fitting Experiment with Theory in Ar-OH	23rd March, 1990
*BUTLER, Dr. A. (St. Andrews University) The Discovery of Penicillin: Facts and Fancies	7th Dec., 1989
*CHEETHAM, Dr. A. K. (Oxford University) Chemistry of Zeolite Cages	8th March, 1990
CLARK, Prof. D. T. (ICI Wilton) Spatially Resolved Chemistry (Using Nature's Paradigm in the Advanced Materials Arena)	22nd Feb., 1990
COLE-HAMILTON, Prof. D. J. (St. Andrews University) New Polymers from Homogenous Catalysis	29th Nov., 1989
*CROMBIE, Prof. L. (Nottingham University) The Chemistry of Cannabis and Khat	15th Feb., 1990
DYER, Dr. U. (Glaxo) Synthesis and Conformation of C-Glycosides	31st Jan., 1990
FLORIANI, Prof. C. (University of Lausanne, Switzerland) Molecular Aggregates-A Bridge between Homogenous and Heterogenous Systems	25th Oct., 1989

GERMAN, Prof. L. S. (USSR Academy of Sciences-Moscow) New Synthesis in Fluoroaliphatic Chemistry: Recent Advances in the Chemistry of Fluorinated Oxiranes	9th July, 1990
GRAHAM, Dr. D. (B. P. Research Centre) How Proteins Absorb to Interfaces	4th Dec., 1989
GREENWOOD, Prof. N. N. (University of Leeds) Novel Cluster Geometries in Metalloborane Chemistry	9th Nov., 1989
*HOLLOWAY, Prof. J. H. (University of Leicester) Noble Gas Chemistry	1st Feb., 1990
HUGHES, Dr. M. N. (King's College London) A Bug's Eye View of the Periodic Table	30th Nov., 1989
HUISGEN, Prof. R. (Universität München) Recent Mechanistic Studies of [2+2] Additions	15th Dec., 1989
KLINOWSKI, Dr. J. (Cambridge University) Solid State NMR Studies of Zeolite Catalysts	13th Dec., 1989
*LANCASTER, Rev. R. (Kimbolton Fireworks) Fireworks-Principles and Practice	8th Feb., 1990
LUNAZZI, Prof. L. (University of Bologna) Application of Dynamic NMR to the Study of Conformational Enantiomerism	12th Feb., 1990
*PALMER, Dr. F. (Nottingham University) Thunder and Lightening	17th Oct., 1989
*PARKER, Dr. D. (Durham University) Macrocycles, Drugs and Rock 'n' roll	16th Nov., 1989
PERUTZ, Dr. R. N. (York University) Plotting the Course of C-H Activations with Organometallics	24th Jan., 1990
PLATONOV, Prof. V. E. (USSR Academy of Sciences-Novosibirsk) Polyfluoroindanes: Synthesis and Transformation	9th July, 1990
POWELL, Dr. R. L. (ICI) The Development of CFC Replacements	6th Dec., 1989
POWIS, Dr. I. (Nottingham University) Spinning off in a Huff: Photodissociation of Methyl Iodide	21st March, 1990

ROZHKOV, Prof. I. N. (USSR Academy of Sciences-Moscow) — 9th July, 1990
Reactivity of Perfluoroalkyl Bromides

STODDART, Dr. J. F. (Sheffield University) — 1st March, 1990
Molecular Lego

SUTTON, Prof. D. (Simon Fraser University, Vancouver B. C.) — 14th Feb., 1990
Synthesis and Applications of Dinitrogen and Diazo Compounds of Rhenium and Iridium

THOMAS, Dr. R. K. (Oxford University) — 28th Feb., 1990
Neutron Reflectrometry from Surfaces

THOMPSON, Dr. D. P. (Newcastle University) — 7th Feb., 1990
The Role of Nitrogen in Extending Silicate Crystal Chemistry

AI.1.2 1st August 1990 To 31st July 1991

ALDER, Dr. B. J. (Lawrence Livermore Labs., California) — 15th Jan., 1991
Hydrogen in all its Glory

BELL, Prof. T. (SUNY, Stoney Brook, U.S.A) — 14th Nov., 1990
Functional Molecular Architecture and Molecular Recognition

BOCHMANN, Dr. M. (University of East Anglia) — 24th Oct., 1990
Synthesis, Reactions and Catalytic Activity of Cationic Titaniun Alkyls

BRIMBLE, Dr. M. A. (Massey University, New Zealand) — 29th July, 1991
Synthetic Studies Towards the Antibiotic Griseusin-A

BROOKHART, Prof. M. S. (University of N. Carolina) — 20th June, 1991
Olefin Polymerisations, Oligomerisations and Dimerisations Using Electrophilic Late Transition Metal Catalysts

BROWN, Dr. J. (Oxford University) — 28th Feb., 1991
Can Chemistry Provide Catalysts Superior to Enzymes

BUSHBY, Dr. R. (Leeds University) — 6th Feb., 1991
Biradicals and Organic Magnets

COWLEY, Prof. A. H. (University of Texas) — 13th Dec., 1990
New Organometallic Routes to Electronic Materials

CROUT, Prof. D. (Warwick University) — 29th Nov., 1990
Enzymes in Organic Synthesis

DOBSON, Dr. C. M. (Oxford University) — 6th March, 1991
NMR Studies of Dynamics in Molecular Crystals

*GERRARD, Dr. D. (British Petroleum) — 7th Nov., 1990
Raman Spectroscopy for Industrial Analysis

HUDLICKY, Prof. T. (Virginia Polytechnic Institute) — 25th April, 1991
Biocatalysis and symmetry Based Approaches to the Efficient Synthesis of Complex Natural Products

JACKSON, Dr. R. (Newcastle University) — 31st Oct., 1990
New Synthetic Methods: α-Amino Acids and Small Rings

KOCOVSKY, Dr. P. (Uppsala University) — 6th Nov., 1990
Stereo-Controlled Reactions Mediated by Transition and Non-Transition Metals

*LACEY, Dr. D. (Hull University) — 31st Jan., 1991
Liquid Crystals

*LOGAN, Dr. N. (Nottingham University) — 1st Nov., 1990
Rocket Propellants

*MACDONALD, Dr. W. A. (ICI Wilton) — 11th Oct., 1990
Materials for the Space Age

MARKAM, Dr. J. (ICI Pharmaceuticals) — 7th March, 1991
DNA Fingerprinting

PETTY, Dr. M. C. (Durham University) — 14th Feb., 1991
Molecular Electronics

PRINGLE, Dr. P. G. (Bristol University) — 5th Dec., 1990
Metal Complexes with Functionalised Phosphines

PRITCHARD, Prof. J. (Queen Mary and Westfield College, London University) — 21st Nov., 1990
Copper Surfaces and Catalysts

SADLER, Dr. P. J. (Birbeck College London) — 24th Jan., 1991
Design of Inorganic Drugs: Precious Metals, Hypertension + HIV

SARRE, Dr. P. (Nottingham University) — 17th Jan., 1991
Comet Chemistry

SCHROCK, Prof. R. R. (Massachusetts Institute of Technology) Metal-Ligand Multiple Bonds and Metathesis Initiators	24th April, 1991
*SCOTT, Dr. S. K. (Leeds University) Clocks, Oscillations and Chaos	8th Nov., 1990
SHAW, Prof. B. L. (Ledds University) Syntheses with Coordinated, Unsaturated Phosphine Ligands	20th Feb., 1991
SINN, Prof. E. (Hull University) Coupling of Little Electrons in Big Molecules. Implication for the Active Sites of (Metalloproteins and other) Macromolecules	30th Jan., 1991
SOULEN, Prof. R. (South Western University, Texas) Preparations and Reactions of Bicycloalkenes	26th Oct., 1990
WHITAKER, Dr. B. J. (Leeds University) Two-Dimensional Velocity Imaging of State-Selected Reaction Products	28th Nov., 1990

AI.1.3 1st August 1991 To 31st July 1992

*#BUTLER, Dr. A. R (St. Andrews University) Traditional Chinese Herbal Drugs: A Different Way of Treating Disease	7th Nov., 1991
COOPER, W. D. (Shell Research) Colloid Science, Theory and Practice	11th Dec., 1991
FENTON, Prof. D. E. (Sheffield University) Polynuclear Complexes of Molecular Clefts as Models for Copper Biosites	12th Feb., 1992
*#GANI, Prof. D. (St. Andrews University) The Chemistry Of PLP Dependent Enzymes	13th Nov., 1991
GERHET, Dr. J. C. (Ciba Geigy, Basel) Some Aspects of Industrial Agrochemical Research	13th May, 1992
*#GRIGG, Prof. R. (Leeds University) Palladium Catalysed Cyclisation and Ion Capture Processes	4th Dec., 1991
#HARRIS, Dr. K. D. M. (St. Andrews University) Understanding the Properties of Solid Inclusion Compounds	22nd Jan., 1992

*#HITCHMAN, Prof. M. L. (Strathclyde University) 26th Feb., 1992
Chemical Vapour Deposition

#HOLMES, Dr. A. (Cambridge University) 29th Jan., 1992
Cycloaddition Reactions in the Service of the Synthesis of Piperidine and Indolizidine Natural Products

#JOHNSON, Prof B. F. G. (Edinburgh University) 6th Nov., 1991
Cluster-surface Analogies

KEELEY, Dr. R. (Metropolitan Police Forensic Science) 31st Oct., 1991
Modern Forensic Science

KNIGHT, Prof. D. M. (Philosophy Department, University of Durham) 7th April, 1992
Interpreting Experiments: The Beginning of Electrochemistry

*#MASKILL, Dr. H. (Newcastle University) 18th March, 1992
Concerted or Stepwise Fragmentation in a Deamination-type Reaction

*#MORE O'FERRALL, Dr. R. (University College, Dublin) 20th Nov., 1991
Some Acid -Catalysed Rearrangements in Organic Chemistry

NIXON, Prof. J. F. (University of Sussex) 25th Feb.,1992
The Tilden Lecture: Phosphaalkynes, New Building Blocks in Inorganic and Organometallic Chemistry

*SALTHOUSE, Dr. J. A. (University of Manchester) 17th Oct., 1991
Son et Lumiere- A demonstration lecture

*SMITH, Prof. A. L. (ex Unilever) 5th Dec., 1991
Soaps, Detergents and Black Puddings

#THOMAS, Prof. E. J. (Manchester University) 19th Feb., 1992
Applications of Organostannanes to Organic Synthesis

#THOMAS, Dr. S. E. (Imperial College) 11th March, 1992
Recent Advances in Organoiron Chemistry

WARD, Prof. I. M. (IRC in Polymer Science, University of Leeds) 28th Nov., 1991
The SCI Lecture: The Science and Technology of Orientated Polymers

* Attended

Invited specifically for the postgraduate training programme.

AI.2 Conferences Attended

Winter School on Organic Reactivity II, Bressanone, Italy.
(9-17th Jan., 1992)

Royal Society of Chemistry Organic Reactivity Group Meeting, I.C.I., Blackely, Manchester, poster presented. 1st. Oct. 1990.

AI.3 First Year Induction Course, Oct., 1989

This course consisted of a no. of one hour lectures on the services available in the department.

1. Departmental organisation.
2. Safety matters.
3. Electrical appliances and infra-red spectroscopy.
4. Chromatography and microanalysis.
5. Atomic absorptiometry and inorganic analysis.
6. Library facilities.
7. Mass spectrometry.
8. Nuclear magnetic resonance.
9. Glassblowing technique.

A.I. 4 Sample Kinetic Runs

Absorbance Values For Decomposition Of HBIW (9.7×10^{-5}M) In 0.01M Perchloric Acid At 25°C

Data in acetonitrile at 240nm.

Table A.I. 1.1

T / s	Absorbance	k_{obs} / $x10^{-4}$ s^{-1}
0	0.09	-
120	0.14	8.97
240	0.19	9.51
360	0.23	9.35
480	0.26	8.87
600	0.30	9.32
720	0.32	8.80
840	0.35	9.01
960	0.37	8.83
∞	0.58	-

$k_{obs} = 9.08 \times 10^{-4}\ s^{-1}$ ($\pm$ 5%)

Absorbance Values For The Decomposition Of DPT ($8x10^{-5}M$) In $4x10^{-3}M$ Perchloric Acid At 25°C With 1% Added Water

Data in acetonitrile At 260nm

Table A.I. 1.2

T / s	Absorbance	k_{obs} / $x10^{-4}$ s^{-1}
0	0.025	-
300	0.039	1.43
600	0.052	1.40
900	0.064	1.38
1200	0.075	1.35
1500	0.089	1.42
1800	0.101	1.43
2100	0.113	1.46
2400	0.121	1.41
2700	0.130	1.40
3000	0.142	1.44
3300	0.150	1.42
3600	0.159	1.43
3900	0.167	1.42
∞	0.358	-

$k_{obs} = 1.41 \times 10^{-4}\ s^{-1}$ ($\pm$ 5%)

Absorbance Values For The Decomposition Of DAPT ($5x10^{-5}$M) In 0.01M Perchloric Acid At 25°C

Data in acetonitrile at 215nm

Table A.I. 1.3

T / s	Absorbance	k_{obs} / $x10^{-4}$ s^{-1}
0	0.093	-
300	0.080	5.83
600	0.068	6.15
900	0.058	6.29
1200	0.051	6.09
1500	0.045	5.99
1800	0.040	5.90
2100	0.034	6.21
∞	0.012	-

$k_{obs} = 6.06 \times 10^{-4}\ s^{-1}$ (± 5%)

Values Of k_{obs} For The Decomposition Of DNPT ($2.8x10^{-5}$M) In 0.03M Perchloric Acid At 25°C

Data in acetonitrile at 245nm

Table A.I. 1.4

k_{obs} / s^{-1}	Run
0.5318	1
0.5227	2
0.5388	3
0.5310	4
0.5279	5

$k_{obs} = 0.5304\ s^{-1}$ (± 5%)